

Mass spectrometric analysis of non-enzymatic post-translational modifications introduced by cold plasma-derived reactive species in peptides and proteins

I n a u g u r a l d i s s e r t a t i o n

zur

Erlangung des akademischen Grades eines

Doktors der Naturwissenschaften (Dr. rer. nat.)

der

Mathematisch-Naturwissenschaftlichen Fakultät

der

Universität Greifswald

vorgelegt von

Sebastian Wenske

geboren am 22.08.1989

in Neuruppin, Deutschland

Greifswald, 7th September 2022

Dekan: Prof. Dr. Gerald Kerth

1. Gutachter: Prof. Dr. Michael Lalk

2. Gutachter: Prof. Dr. Jan Benedikt

Tag der Promotion: 07.09.2022

Table of Content

List of Abbreviations	I
Objectives & Outline	II
1. Introduction & Motivation	1
1.1. Current applications and challenges in plasma medicine.....	1
1.2. Reactive species: key actors in cell signaling and oxidative stress.....	4
1.3. Amino acids as a target of bioactive reactive species.....	8
1.4. Mass spectrometric detection of oxidative modifications in proteins and peptides to trace plasma-derived reactive species	11
2. Cold Plasma Effects on Proteins: from Peptides Solutions to Tissue Proteomes	14
2.1. Screening structural changes of peptides in solution.....	14
2.1.1. Biochemical modulation with treatment condition (A1).....	16
2.1.2. Influence of position on amino acids' reactivity (A2)	17
2.1.3. Consequences on protein functioning (A3)	19
2.2. Identification of oxidative modifications in tissue proteomes	21
2.2.1. Human skin wound exudates (A4)	22
2.2.2. Porcine epidermal tissues (A5)	23
3. Conclusions & Outlook	25
3.1. Adjusting cold plasma parameters for biomedical applications	25
3.2. Outlook: enabling CAPs in clinical settings	26
4. Summary	29
5. References	30
6. Original Publications	44
Article A1.....	46
Article A2.....	58
Article A3.....	75
Article A4.....	84
Article A5.....	107
7. Eigenständigkeitserklärung	121
8. Curriculum Vitae	122
9. List of Publications & Conference Contributions	123
10. Acknowledgements	126

List of Abbreviations

CAP	cold atmospheric-pressure plasma
DNPH	2,4-dinitrophenyl hydrazine
Ar	argon
He	helium
EPR.....	electron paramagnetic resonance
ECM	extracellular matrix
HPLC	high-pressure liquid chromatography
ESI.....	electrospray ionization
ELISA.....	enzyme-linked immunosorbent assay
PD.....	proteome discoverer
SILAC.....	stable isotope labeling with amino acids in cell culture
AQUA	absolute quantification
LFQ	label-free quantitation
HR	high resolution
HIF1 α	hypoxia-inducible factor 1-alpha
MALDI.....	matrix-assisted laser desorption ionization
MD.....	molecular dynamic
MMP.....	matrix metalloproteases
MS	mass spectrometry
MS/MS.....	tandem mass spectrometry
oxPTM	non-enzymatic oxidative modifications
PLA ₂	phospholipase A2
RNS	reactive nitrogen species
ROS	reactive oxygen species
RSS	reactive sulfur species
slm.....	standard liter per minute
3-Tyr-NO.....	nitrosotyrosine
VUV	vacuum ultraviolet
VHL.....	von-hippel-lindau
TALIF	two-photon absorption laser-induced fluorescence
3-Tyr-NO ₂	3-nitrotyrosine

In addition to the abbreviations mentioned so far, the one and three-letter codes for proteinogenic amino acids and for the SI units were used.

Objectives & Outline

In the context of newly proposed biomedical tools, the objective of this thesis is to contribute to understand the mechanisms of action and the biological effects of cold atmospheric-pressure plasmas (CAPs). In this work, the applied strategy consisted in characterizing non-enzymatic oxidative modifications, occurring after various plasma treatments in proteins, peptides, and amino acids, developing and applying mass spectrometry-based methods. The main hypothesis is that CAPs can modulate downstream redox signaling pathways by changing the molecular structure of key biomolecules, like proteins and lipids.

The specific objectives are i) to identify all the potential oxidative modifications introduced by cold plasmas in proteins; ii) to compare and characterize the chemistry induced by different plasma sources and treatment parameters; iii) to improve the controllability of the treatments and their effects by identifying main variables; iv) to correlate results obtained from model solutions of peptides and proteins to those obtained treating complex matrices. The thesis contributes to the resolution of these objectives, finally supporting the overall understanding of cold plasmas biological effectiveness, and the possibility to tune plasma sources for targeted biomedical applications in future. In particular, objectives i), ii), and iii) are covered in Section 2.1, while objective iv) is investigated in Section 2.2.

The thesis consists in an introduction, major results obtained from 5 articles published in peer-reviewed journals, a conclusion and outlook section, and a summary. Regarding the results, Articles 1 and 2 (A1 and A2) investigated which type of oxidative modifications can be driven by cold plasmas in model peptides solutions. Articles 3, 4, and 5 (A3, A4, and A5) applied the model systems gained knowledge to plasma treatments of more complex models, such as protein solutions (A3), and epidermal tissues (A4 and A5). **Article 1** examined which modifications could be introduced by plasmas on two peptides (an angiotensin derivate and bradykinin), additionally comparing the produced experimental data with in silico data obtained by previous works. Here, the differential chemistry induced by varying plasma source and treatment conditions have been discussed. **Article 2** deepened and extended this to a library of peptides to compare the amino acids reactivities also based on their position in the peptide primary structure. In both articles, a classification of the reactivity of all proteinogenic amino acids towards plasma sources and the identification of key responsible plasma components, such as reactive species, have been investigated, resulting in a modulation of the effects in relation to variables (e.g., modulating source-design or gas composition).

These findings have been used and applied from model peptide solutions to more complex environments, such as intact protein solutions (**Article 3**), and in the proteome of wound exudates and skin tissues, as investigated respectively in **Article 4** and **Article 5**. An overview of the biological impact on proteins was given also for complex matrices, reflecting the various mechanism of action of plasma components in presence and in absence of a water vehicle. The results were finally discussed in the conclusion and outlook section, where optimized tunable conditions for plasma treatments have been associated to defined proteins effects and proposed for adjusting plasma conditions in relation to the biomedical aim. Finally, still unsolved criticalities in applying cold plasmas in clinical settings have been discussed.

1. Introduction & Motivation

1.1. Current applications and challenges in plasma medicine

Plasma medicine is 25 years since its first application [1, 2], a relatively young medical field. However, the use of cold atmospheric-pressure plasmas has undergone significant progress in recent years. After the realization that this form of plasma could be useful for biological applications, various progress has been made in the field of decontamination [3, 4], dentistry [5, 6], chronic wound healing in both animal model and clinical studies [7-12], and more recently in cancer remediation [13, 14], indicating that cold plasmas can be used in many different research areas. Plasma, which is in the 4th state of matter, is formed when the main gas, for example, the noble gases argon or helium, is provided with energy. Finally, the main gas gets ionized, releasing free electrons, thus forming ions, excited metastable molecules, and other chemical species. In addition to physical components, such as radiation from the vacuum ultraviolet (VUV) to the infrared region, visible light, electromagnetic fields, and thermal radiation, cold atmospheric-pressure plasmas (CAPs) consist of most importantly, a varying type and number of reactive oxygen and nitrogen species, including radicals and neutral or charged species (Figure 1.1) [15]. CAPs differ from thermal plasmas as they are generated by applying electrical fields, resulting in a low ionization degree of the gas, with generation of a rich gas-phase chemistries rather than increase in the amount of hot electrons [16]. Indeed, the temperature of CAPs is between 300 and 370 Kelvin, allowing their usage on mammalian tissues, where temperatures above 310 Kelvin should not be exceeded.

These unique properties make CAPs suitable tools to possibly manipulate biological processes by the exogenous delivery of reactive components, and therefore they are currently proposed for various biomedical applications, such as the treatment of chronic wounds [17] or cancer [14]. In clinical applications, cold plasmas are already used for treating head and neck cancer patients [18, 19]. Here, the bacterial load was reduced due to plasma treatments, in addition to tumor regression and accelerated healing of the wound.

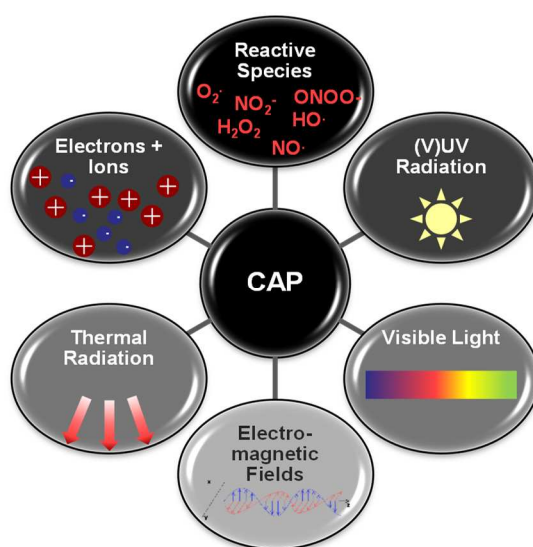


Figure 1.1. Overview of CAP components. CAPs consist of different components, such as reactive species, VUV radiation, visible light, electromagnetic fields, thermal radiation, electrons, ions, radicals, and neutral species.

For the use in medical applications, it is crucial to prove that plasmas do not pose any risk [20, 21] and that the application is beneficial for the patient. One plasma source that has received approval as a certified medical device is the argon-driven plasma jet kINPen MED [22]. This plasma source consists of a pin-type electrode, which is housed in a dielectric ceramic tube (Figure 1.2B). The effluent of the kINPen plasmas forms, among other reactive components, excited argon molecules which can react, due to the turbulent flow, with ambient air molecules (e.g. H_2O , N_2 , and O_2), generating secondary gas species, e.g. short-lived atomic oxygen ($\cdot\text{O}$), singlet oxygen ($^1\text{O}_2$), hydroxyl radicals ($\cdot\text{OH}$) and nitrogen oxide radicals ($\cdot\text{NO}$) [23-25]. Due to the relatively long distance of the kINPen effluent to the target (9-10 mm), more stable long-lived species can be produced, such as ozone (O_3), hydrogen peroxide (H_2O_2), or nitrate (NO_3^-) and nitrite (NO_2^-) in the liquid phase [26-28]. The gaseous chemistry of the kINPen 09 has been investigated by varying conditions related to the gas composition, e.g., in presence of gas admixtures (with a maximum of 1% O_2 and/or N_2). Dominant oxygen chemistry in short (mostly $\cdot\text{O}$ and $^1\text{O}_2$) and long distances (mostly O_3) has been observed by admixing O_2 to the working gas [26, 27, 29]. Typically, this jet is operated with 3 to 5 standard liters per minute (slm). With these parameters, the kINPen is distinguished from the European COST reference micro-plasma MP1101 jet or in short COST-Jet (Figure 1.2A) [30], which has been developed as a standard device to compare other cold physical plasma sources and to allow comparability of results gained by different plasma medicine science groups.

Although this device is not currently certified as a medical tool, it is used as a reference plasma source. In particular, $\cdot\text{O}$ can be produced until the target surface, due to the short distances of the effluent. In contrast to the kINPen, this plasma source is operated with 1.0 slm helium gas and the distance to the target is significantly shorter (2-4 mm). These differences, based on another source design and the use of helium as a driven gas, generate plasmas differentially, leading to a significantly altered plasma chemistry and thus cocktails of plasma components, such as reactive species [23]. The presented plasma sources are those mainly investigated in this thesis.

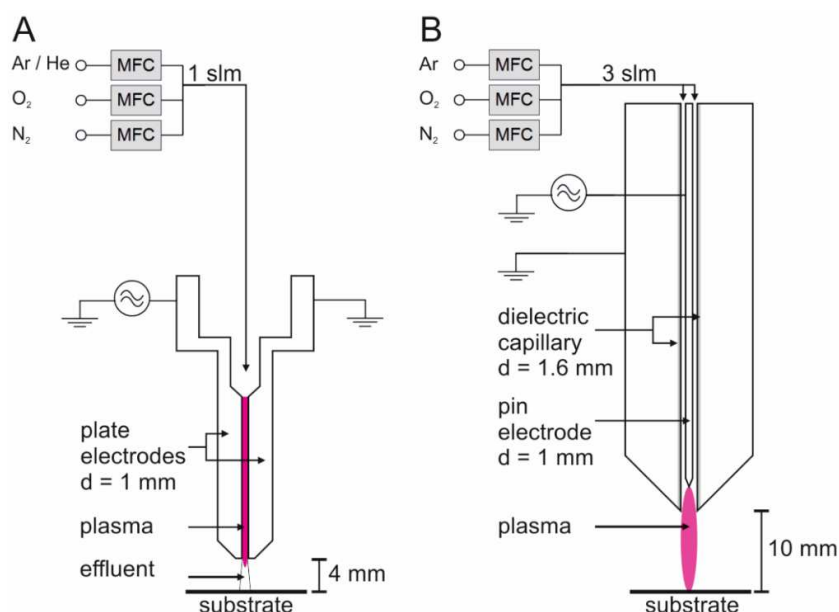


Figure 1.2. Schematics of the COST-Jet (A) and kINPen (B). MFC: mass flow controller, slm: standard liter per minute. Illustration adapted with permission according to [31], <https://creativecommons.org/licenses/by/4.0/>.

These differences may lead to variable medical effects of plasmas, for example in biological modifications occurring on cell proteins. Further studies are required to standardize and optimize the selectivity of biological effects induced by controlled plasma chemistries.

Even though CAP consists of many different components, reactive oxygen (ROS) and nitrogen (RNS) species are probably the most relevant actors, besides H_2O_2 , in plasma medical effects [32-38]. These effects can be potentially a source for several oxidative modifications of cell biomolecules and are therefore presumably involved in modulating redox signaling pathways. To date, the complex gas phase, liquid phase, and interphase chemistry between these two is still under investigation. In particular, it has not been fully characterized, which is the amount and type of short-lived (nanoseconds to milliseconds) or long-lived species (seconds to days) [39] generated especially in liquid compartments surrounding biological cell structures. It becomes even more sophisticated as species that are well studied in the gas phase can differ significantly in the plasma-liquid interphase and in the aqueous phase [40].

Similarly, new species can be formed from gaseous precursor molecules or by following other chemical reaction pathways. As an example, $\cdot\text{NO}$ can be produced in the gas phase, interphase, and liquid phase. In the gas phase, it is formed by the reaction of oxygen (O_2) with a nitrogen radical ($\cdot\text{N}$). In the interphase, it can be generated by the reaction of $\cdot\text{O}$ and $\cdot\text{NO}_2$, while in the liquid phase, among other possible mechanisms, by the reaction of O_3 with $\cdot\text{NO}_2$ [41]. To date, more than 25 different reactive species have been identified in the gas and liquid phase in combination with plasma treatments (e.g. HO_2 , H_2O_2 , OH , O_3 , $^1\text{O}_2$, NO_2^- , NO_3^- , ONOOH , O_2^-) [36], which can potentially react with each other [42], or with target biomolecules, such as proteins and lipids, in a variety of ways [43, 44]. However, the type and amount of these reactive species can also be altered by changing certain plasma parameters, such as treatment time, gas plasma composition [25, 29], solvent, or distance to the treated object [45, 46]. To date, most of the literature focused on the investigation of reactive species in the gas phase due to the detection methods like two-photon absorption laser-induced fluorescence (TALIF) spectroscopy, which allows even absolute quantification of some species like atomic oxygen [26, 47]. Since most processes relevant for biological effects take place in the liquid phase, it is important to gain a deeper knowledge on the characterization of the plasma-stimulated liquid phase and the interphase. Some of these informations have been so far obtained using dynamic simulations [48, 49]. In contrast to short-lived species, long-lived species like H_2O_2 [50], NO_2^- or NO_3^- are relatively easy to measure via colorimetric assays [51].

To detect short-lived species in plasma-stimulated liquids, such as highly reactive radicals, more sophisticated methods are needed. Electron paramagnetic resonance (EPR) spectroscopy is an example [52] which has been used especially to detect ozone, singlet oxygen [53], and nitrogen oxide radicals [41] in treatments with kINPen 09 (a precursor of the kINPen MED) and other plasma sources [54]. However, a direct quantitative detection, especially of extremely short-lived species, is only partially achievable using EPR or other optical spectrometric methods, as they do not produce absolute quantitative results [24].

Different assays exist for the detection of species. As an example, the highly reactive and biologically relevant peroxyxynitrite (ONOO^-) can be detected by using the luminescence of a lanthanide probe [55]. However, knowledge about the mode of action of a set of species for a given condition must be further investigated to standardize biomedical processes, especially in liquid. Therefore, alternative strategies are needed to enable fast and complete detection of the overall chemical reactions and biological effects of plasma sources and treatment

conditions. One possibility to characterize the plasma liquid chemistry of diverse treatment conditions and plasma sources is to investigate the reacting species in liquid by monitoring modifications occurring in proteins, peptides, or amino acids. The detection of these modifications can be carried out by using a wide variety of methods. Spectrophotometric methods are mainly used for the detection of protein carbonylation, using 2,4-dinitrophenylhydrazine (DNPH) as a reagent reacting with the protein in the analysis [56].

Fluorescence measurements of oxidized amino acids have become established in many laboratories, as this is a very robust method with good sensitivity and just small instrumentations are required [57]. However, the disadvantage is that the selectivity of this method is low compared to other methods. Immunochemical methods such as immunoblotting or ELISA represent another large group of techniques for the detection of oxidative modifications using antibodies [58]. However, it is necessary to overcome different problems with these methods.

For example, the exact epitope, which can be bound by the antibody, is often not known; additionally, most antibodies detect more than one oxidation product. Finally, absolute quantifications are difficult to achieve. Thus, the gold standard for the determination of modified amino acids in peptides or proteins is mass spectrometry (MS) [59-61]. This technique can be either coupled with high-pressure liquid chromatography (HPLC) or carried out via direct infusion of the sample. The proteomics MS analysis is generally made by two approaches, called top-down and bottom-up [62, 63]. In the top-down approach, the entire protein of interest gets ionized as a whole and is analyzed and fragmented only in the MS.

In contrast, in the bottom-up approach, the protein of interest is first digested into smaller peptides and examined afterward. The detection of oxidative modifications using HPLC-MS methods in model solutions and tissues is the goal of this work. Main questions addressed in this work are *“How does the impact of various plasma sources and treatment parameters differ on peptides and proteins in form of oxidative modifications, and can these results be used to characterize, foresee, and define the effects of specific treatment conditions?”*

1.2. Reactive species: key actors in cell signaling and oxidative stress

ROS and RNS are generic terms for a large variety of different molecules. It is known for almost 30 years, that a large number of these reactive species is formed in the cell, especially in mitochondria [64], from complex I and III of the electron transport chain [65], as well as from different oxidases [66-68], and that they also have important roles in physiology [69] and disease processes [70]. The principal mechanism of action of reactive species is to lead redox reactions in the cell by inducing non-enzymatic post-translational modifications (PTMs) in proteins, as well as structural modifications of many other biomolecules (e.g., DNA, lipids, sugars). Over the last years, various modifications like acetylation, carbonylation, methylation, and also oxidative modifications like hydroxylation and nitration were found to have a biological impact [71]. Some of the induced modifications are very complex and are present in large numbers in different tissue areas and cell types. These modifications can be reversible (e.g., phosphorylation or hydroxylation) or irreversible (e.g., deamidation).

Smaller chemical groups can be added (e.g., methylation), or even large and complex molecular structures (e.g., ADP-ribosylation) [72]. Many of these modifications play a crucial role in various signaling pathways. One of the most studied modifications is the phosphorylation of proteins, which was already discovered in the 1950s [73]. About 1 to 2/3 proteins in eu-

karyotes [74], thus about 13000 proteins in the entire human proteome, are temporarily phosphorylated. The most common amino acids phosphorylated by protein kinases are serine, threonine, and tyrosine [75]. Through these phospho-modifications, various signaling pathways can be directly activated or inactivated. Interestingly, as described later, the tyrosine kinases themselves can be activated by reactive species, via induction of structural modifications.

This shows how reactive species can change, modulate, and regulate signaling pathways at different levels, being part of a very complex and complicated network. Helmut Sies has done outstanding progress in this field, as he was able to clarify that oxidative stress is not necessarily negative for the organism themselves (Figure 1.3) [76]. Only when uncontrolled reactions occur in presence of very large amounts of reactive species (e.g., exogenously produced), a disturbance of the redox signaling occur and it is possible to speak about the so-called distress [77], or negative stress. However, if the amounts of reactive species are controllable and not in excess, these can induce targeted modifications on specific target molecules, acting on physiological pathways. This phenomenon is referred to as oxidative eustress and could be used to induce beneficial effects by the exogenous introduction of species, e.g., in the case of cold plasmas. The balance between these two oxidative stresses is extremely important for the cell, as many signaling pathways depend on ROS and RNS levels [79-81].

Important signaling pathways, such as the transcription factor NF- κ B, which is responsible for cellular processes like immune response, inflammatory response, cellular adhesion, differentiation, proliferation, autophagy, and apoptosis [82], depend on ROS levels. ROS can stimulate NF- κ B-dependent signaling pathways in the cytoskeleton, and on the other hand, inhibit them in the nucleus. Another example depends on the cellular levels of H₂O₂, which lead to the activation of NF- κ B by alternative phosphorylation of a second factor, I κ B α .

Inhibition of NF- κ B can also be induced when glutathionylation led by ROS action occurs on a cysteine in I κ B α [83]. Other examples of signaling pathways in which ROS plays a regulatory role are the mitogen-activated protein kinase (MAPK) cascades, Keap1-Nrf2-ARE, and phosphoinositide-3-kinase- (PI3K-) Akt [84].

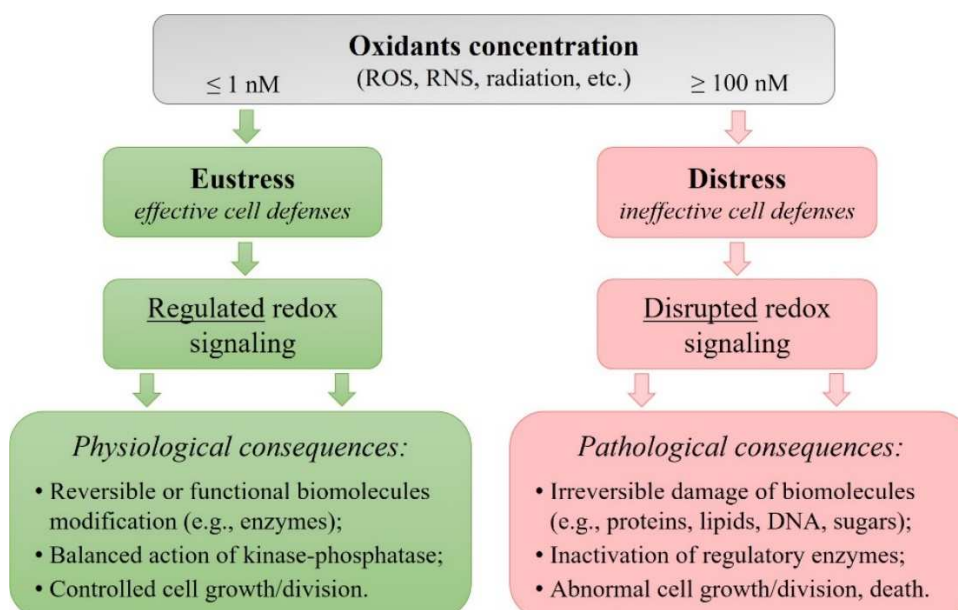


Figure 1.3. Representation of the theory concerning the endogenous homeostasis of reactive species, leading to oxidative eustress and cell stimulation if in small amounts, and to oxidative distress and cell death if highly concentrated. *Illustration redesigned with permission according to [78].*

The direct effect of reactive species as second messengers can be demonstrated also by the example of tyrosine kinases, as shown in Figure 1.4. Endogenous ROS, for example, H_2O_2 , selectively oxidize tyrosine kinases at various cysteine residues, like the apoptosis signal-regulating kinase 1 (ASK1), inducing its activation. This activated kinase can phosphorylate and activate further target enzymes, important in other downstream processes.

Examples are p38 mitogen-activated protein kinase and cJun NH₂-terminal kinase (JNK), which are responsible for apoptosis, cell cycle control, and growth inhibition. Being a regulated process, the oxidized form of kinases can be reduced by the action of thioredoxin reductase (TrxR), which oxidizes thioredoxin-1 (Trx1) in a redox reaction [85]. Hydrogen peroxide (H_2O_2) is one of the most studied reactive species in biological redox reactions [86].

Endogenously, it is formed in the body as a by-product of various biochemical reactions, and it was recognized for a long period only as a harmful species. Sources of H_2O_2 are for example the NAD(P)H oxidases, the mitochondrial respiratory chain, and other oxidases. In total, 31 human intracellular enzymes can form peroxides [87]. The xanthine oxidase, for example, forms hydrogen peroxide during the degradation of hypoxanthine to uric acid [88], which is then converted to water and oxygen by catalase. H_2O_2 was one of the first reactive species to be identified as a messenger molecule [89, 90]. H_2O_2 plays an important role in processes such as cell proliferation and migration. In particular, a model study with injured larvae of a zebrafish was able to show that an H_2O_2 gradient was newly formed after wounding, which then led to increased recruitment of leukocytes [91]. This was an important indication that H_2O_2 plays an important role in wound healing processes, by recruiting cytokines and epidermal growth factors. As anticipated, H_2O_2 mainly acts in signal transduction by adding reversible oxidative modifications to proteins, thus modulating their structure and function [92]. A major mechanism for intracellular signaling pathways is the reversible cysteine oxidation, mediated by H_2O_2 [93]. It must be emphasized that cysteine residues are modified specifically in the cell [94]. Interestingly, between 5 and 12% of all cysteines in the proteome are oxidized under physiological conditions. By adding various oxidative reagents, this value can be increased to over 40% [95]. These oxidations occur on specific cysteine residues.

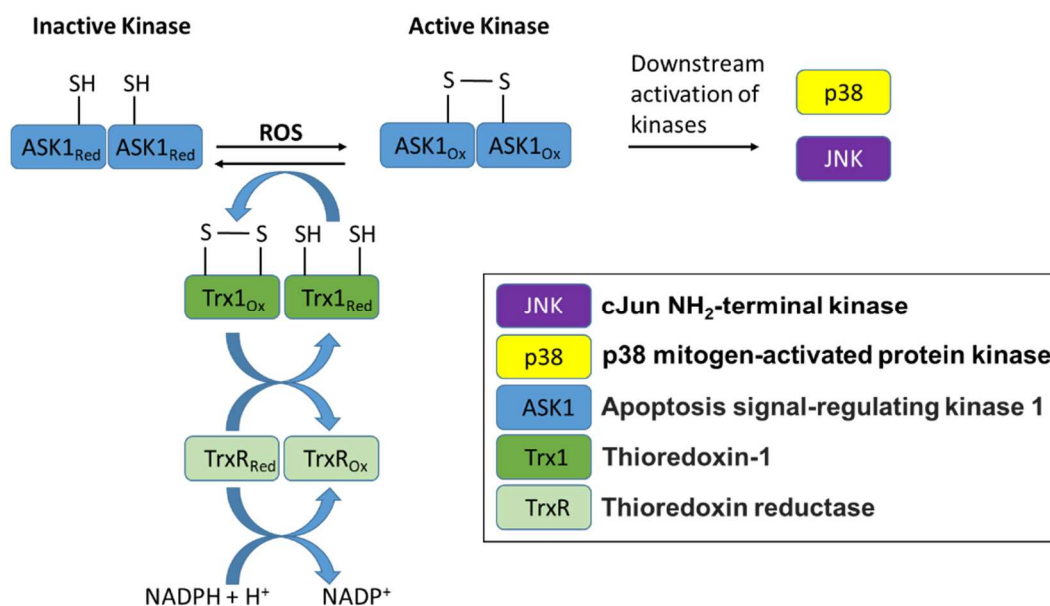


Figure 1.4. Exemplary scheme for the reversible activation of the Apoptosis signal-regulating kinase 1 (ASK1) via cysteine oxidation by reactive oxygen species (ROS).

The local pH, the hydrophobicity of the amino acids close to cysteine residues, and the overall protein structure, influence and regulate oxidative modifications occurring on thiol groups in the cell [96]. Hydrogen peroxide, however, is not the only reactive oxidative messenger molecule. Nitric oxide radical ($\cdot\text{NO}$) is another reactive species released in human cells that can act as a signaling molecule. It has recently been shown that $\cdot\text{NO}$ plays an essential role in embryonic wound healing [97]. This molecule is also known to cause modifications in proteins, mainly S-nitrosylation [98]. $\cdot\text{NO}$ is also a precursor molecule for several other RNS, including nitrogen dioxide radicals ($\cdot\text{NO}_2$), peroxyxynitrite (ONOO^-), nitrite (NO_2^-), nitrate (NO_3^-), nitroxyl (HNO), and dinitrogen trioxide (N_2O_3) [99, 100]. Finally, superoxide anion (O_2^-) and its radical form ($\cdot\text{O}_2^-$) are other reactive compounds that are formed in the cells and act as signal molecules in the redox signaling processes [101].

The relevance of various ROS and RNS, such as hypochlorite anion (ClO^-) [102] and ozone (O_3) [103] in biological processes has also been shown. Although the ROS and RNS lists are not complete, the mode of action is commonly to induce specific structural changes in target molecules, e.g., enzymes or proteins, whose activity or stability gets altered triggering in turn further effects in the cell. Oxidized proteins have reduced activity in most cases [104]. For this reason, these oxidations were often classified as harmful or deleterious in the past. In recent times, however, it has become increasingly apparent that oxidative modifications on proteins can also have beneficial effects for the cell or the organism [105], for example when enzymes have a toxic increase of activity in certain diseases which can be reduced by oxidative modifications. The regulation of the extracellular matrix (ECM) by matrix metalloproteases (MMP) is, for example, important for different types of cancer diseases. This class of enzymes is normally responsible for the extracellular matrix reorganization and angiogenesis [106], but in tumor cells, the activity is increased to the point that malignant cells can spread unhindered and thus form metastases. Inactivation of these enzymes through, for example, oxidative modifications, would therefore mean a better prognosis for the patient.

Today's medicine is already using the effects of targeted ROS and RNS release in different approaches. Cancer-based therapies such as photodynamic therapy, sonodynamic therapy, or chemodynamic therapy, are based on the endogenous production of ROS, e.g., singlet oxygen. Similarly, this mechanism is also used for medical treatments against bacterial infections or cardiovascular and inflammatory diseases [107]. In the same way, CAPs mechanism of action may be based on the introduction of oxidative conditions on the biological target, delivering exogenous reactive species and can lead to mild (e.g., short treatment times, only helium or argon as working gas) or stronger (e.g., long treatments, presence of oxygen in the working gas) oxidation. As observed on biological targets, softer stimulations can increase inflammation, cell proliferation, promoting tissue regeneration and blood coagulation via platelet activation [108]. In contrast, CAPs can also generate a larger amount of highly oxidative reactive species under high oxidative conditions, inducing apoptosis and necrotic cell death reactions on the targeted cells, effects highly beneficial for oncologic treatments [109, 110]. Similarly, strong oxidative conditions have been used in applications involving the antimicrobial effects of plasmas [3, 111], as well as in cancer regression studies *in vitro* and animal models [13, 112-115]. Relevant results have been obtained in controlling the gas-phase chemistry, distance, treatment time, and reaction solution since these are the most important parameters to consider for the production of ROS and RNS in the liquid phase [45]. It has already been shown that plasma treatment can stimulate and promote the Nrf2 signaling pathway [10, 116], which

is relevant for wound healing processes. It was also successfully shown *in vitro* that key tumor suppressor proteins, such as p53 [117], can be modulated by plasmas [118, 119]. Although different physiological effects have been observed, key molecular reaction mechanisms of plasmas are still under investigation. The ability to modify biological structures of the cell and the extracellular matrix (sugars or proteins) was proven as a direct effect of CAPs [36]. Even more importantly, this mode of action, involving the induction of oxidative additions on biomolecules, was also proven *in vitro* and *ex vivo* experiments [120-123]. These modifications, which can occur on proteins, can both lead to a loss or a gain of function, modulating redox signaling pathways [33, 124]. The molecular mechanisms connecting the action of short-lived gaseous species and the long-time scales of the biological effects have been investigated in this thesis. In this context, additional knowledge about the qualitative and quantitative in liquid deposition/formation of species reaching biological targets under defined plasma setups has been clarified. By identifying non-enzymatic oxidative modifications (oxPTMs) in peptides, the present work contributed to the understanding of the nature of molecular biological responses in different amino acids after plasma treatments.

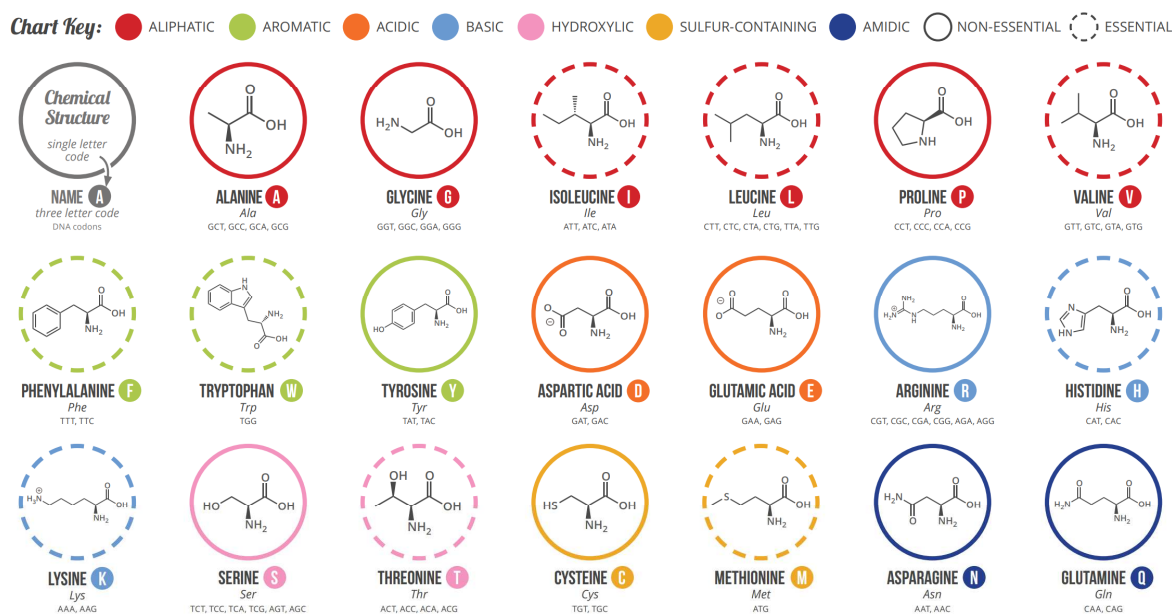
1.3. Amino acids as a target of bioactive reactive species

Proteins and enzymes consist of 22 proteinogenic amino acids, although two non-canonical amino acids, selenocysteine and pyrrolysine, only occur in some bacteria and archaea. The other 20 amino acids (Figure 1.5) form the basic structure of all proteins and enzymes in humans, which are a part of the cell signaling pathways. These alpha-amino acids have an amino group ($-NH_2$), which is located at the second carbon atom (C_α) and is also connected to the carbon atom of the carboxyl group ($-COOH$). In addition, there is a hydrogen atom at the C_α , and a variable side chain ($-R$), which is specific for each amino acid and defines their reactivity. The individual amino acids can be grouped in a variety of ways in relation to the physical-chemical properties, for example in non-polar and polar amino acids, hydrophobic and hydrophilic amino acids, and acidic and basic amino acids. In addition, a distinction can be made based on the side chains, for example in aromatic or aliphatic amino acids, or based on the presence in the side chain of special atoms, such as sulfur or oxygen. The differences in the side chains are the main cause of different amino acids reactivity, which for some amino acids have been already reported towards reactive species [125, 126]. For example, aromatic amino acids like tryptophan have higher reactivity than the simplest and smallest amino acid glycine. Amino acids such as tyrosine, methionine, tryptophan, and phenylalanine are highly reactive towards singlet oxygen [125], while free cysteine and methionine rapidly react with peroxynitrite, as well as tyrosine through a two-step reaction [100].

The complexity increases again significantly if peptides are considered rather than individual amino acids. Peptides consist of a small number (up to 50) of amino acids, linked by a peptide bond ($-OC-NH-$). This bond is formed when the C-atom of the carbonyl group of an amino acid X connects with the N-atom of the amino group of a second amino acid Y, with the elimination of a water molecule. The reactive $-COOH$ and $-NH_2$ groups are then no longer available for a reaction, thus the reactivity of the peptide is defined especially by the different side chains ($-R$). The reactivity of each $-R$ in a peptide, however, is specific towards certain reactive species and is furthermore influenced by neighboring amino acids.

A GUIDE TO THE TWENTY COMMON AMINO ACIDS

AMINO ACIDS ARE THE BUILDING BLOCKS OF PROTEINS IN LIVING ORGANISMS. THERE ARE OVER 500 AMINO ACIDS FOUND IN NATURE - HOWEVER, THE HUMAN GENETIC CODE ONLY DIRECTLY ENCODES 20. 'ESSENTIAL' AMINO ACIDS MUST BE OBTAINED FROM THE DIET, WHILST NON-ESSENTIAL AMINO ACIDS CAN BE SYNTHESISED IN THE BODY.



Note: This chart only shows those amino acids for which the human genetic code directly codes for. Selenocysteine is often referred to as the 21st amino acid, but is encoded in a special manner. In some cases, distinguishing between asparagine/aspartic acid and glutamine/glutamic acid is difficult. In these cases, the codes asx (B) and glx (Z) are respectively used.

© COMPOUND INTEREST 2014 - WWW.COMPOUNDCHEM.COM | Twitter: @compoundchem | Facebook: www.facebook.com/compoundchem
Shared under a Creative Commons Attribution-NonCommercial-NoDerivatives licence.



Figure 1.5. Classification, chemical structure, and codes of the 20 proteogenic amino acids. *Illustration reprinted according to <https://www.compoundchem.com/2014/09/16/aminoacids>, <https://creativecommons.org/licenses/by-nc-nd/4.0/>.*

For example, the reactivity of an amino acid surrounded by aromatic amino acids may be reduced due to the local steric hindrance or increased hydrophobicity. In the same way, the reactivity of an amino acid could be modified by the presence of acidic or basic amino acids, which will modulate the local pH [127]. The complexity and reactivity increase further in proteins and enzymes, where amino acid sequences form highly complex structures (from primary to quaternary), being assembled in variable ways (e.g., hydrophilic or hydrophobic interactions, Van der Waals interactions, ionic or covalent bonds). For various oxidative modifications, the modulation of single amino acid reactivity in peptides or proteins has been not fully investigated. However, these knowledges become essential in medical therapies based on the exogenous delivery of reactive species, as oxidative modifications on amino acids can have a direct influence on signaling pathways. Previous studies have already shown that specific amino acids are targets of plasma-derived reactive species [120, 121, 126, 128].

In biological contexts, cysteine is the most sensitive amino acid to reactive species, together with tyrosine [129-131] and tryptophan [132, 133]. However, amino acids which are modified less often, can have an important physiological influence.

Hypoxia-inducible factor (HIF)-1 α is a master regulator in response to hypoxia and is significantly hydroxylated at proline P564 and P402 under normal conditions. Under pathophysiological conditions, such as stroke and therefore hypoxic conditions, proline becomes dehydroxylated, thus the von Hippel-Lindau (VHL) protein cannot bind (HIF)-1 α . As a result, (HIF)-1 α translocates into the cell nucleus and combines with HIF-1 β . This complex finally binds a DNA region which regulates various processes like erythropoiesis and

angiogenesis. The discovery of this oxidative modification, having such a major physiological impact, was crucial enough to be rewarded with the Nobel Prize in Physiology and Medicine in 2019 [134, 135]. The nitration of tyrosine is also a well-studied oxidative modification. In the 1990s, it was found that peroxynitrite is the main species leading to protein nitration [136, 137]. The ONOO^- dissociates in aqueous solutions with a $\text{pH} < 7.4$ into the radicals $\cdot\text{OH}$ and $\cdot\text{NO}_2$ [138, 139]. The radicalization of tyrosine would then occur in the cell (generating a metastable tyrosyl radical) because of its rapid reaction with $\cdot\text{NO}_2$ and finally generate the nitro-tyrosine [130]. At that time, this modification was considered a damaging outcome of nitrosative stress. Over the last decades, however, it has been recognized that tyrosine is not randomly modified in cell proteins, and that specific nitrated proteins can be used as biomarkers for certain diseases. Firstly it was associated with different cancer types, and nowadays also with neurodegenerative diseases [140], atherosclerosis [141], and systemic lupus erythematosus [142]. In addition, there are other areas in which nitration plays an important role such as the cell signaling cascade or immune response [130]. However, the high abundance of nitrated proteins in biological samples makes it difficult to identify and quantify the exact and specific protein site which is modified [143].

Generally, oxidative modifications can be grouped into reversible and irreversible. Even though nitration is irreversible, and therefore mostly associated with negative impact for a biological system, it has been recently shown that it can occur under normal physiological conditions, such as during pregnancy [144]. Similarly, carbonylation is also an irreversible modification induced by ROS or RNS in proteins under physiological conditions.

Protein carbonylation is produced in various signal transduction pathways [145, 146], being involved in ischemic preconditioning, thus protecting blood flow restoration induced by tissue damage [147]. In addition to these irreversible modifications, there are many reversible ones, such as hydroxylation, acetylation, methylation, glycosylation, and ubiquitylation, influencing cell biology [72, 148]. As anticipated, some of the most relevant oxPTMs are found in proteins cysteines. The sulfur moiety of this amino acid was identified as the most reactive structure towards short-lived reactive species, e.g., $\cdot\text{O}$, $^1\text{O}_2$, $\cdot\text{OH}$, ONOO^- , $\cdot\text{NO}$, $\cdot\text{NO}_2$, also produced from CAPs [126]. Long-lived reactive species, e.g., H_2O_2 , O_3 , react with cysteine especially at higher pH (higher thiolate form) or with the support by cell enzymatic activity.

It was possible to demonstrate that the plasma-driven oxidation of cysteine residues can lead to an inactivation of the RNase A in bacteria [120]. Most cysteine modifications are reversible, allowing a fine regulation of various signaling pathways, such as in the case of S-nitrosothiol (-SNO), and sulfenic acid (-SOH), which can be both induced by ONOO^- for example. Cysteine sulfenic acid can be also produced by reaction with H_2O_2 , $\cdot\text{O}$, $\cdot\text{OH}$, while S-nitrosocysteine can be produced by reaction with a radical (thyl radicals, $-\text{S}^\cdot$) followed by reaction with $\cdot\text{NO}$ or $\cdot\text{NO}_2$ [96]. However, stronger oxidation defined by stronger oxidants (e.g., $^1\text{O}_2$, O_3) or high oxidants amounts leads to the production of sulfinic acid (-SO₂H) and finally the highly oxidized sulfonic acid (-SO₃H), which is an irreversible structural change [149, 150].

Some reversible modifications have a major influence on the regulation of relevant enzymes, e.g., pyruvate kinase M2 [151]. The regulation is possible by preventing the active tetrameric form from nitration and oxidation at specific cysteine residues. The cysteine modifications are also essential in cellular defense mechanisms, where redox signaling cascades counteract stress stimuli [152]. Due to the variety of modifications and their relevance in redox biology, cysteine solutions have been already used to trace the production

of reactive species derived from cold plasma [31, 149, 153]. Finally, further investigations, partially fulfilled in this work, need to be made to underlie which modifications can be introduced by plasma species in peptides and proteins, highlighting the influence that these can have on enzymes reactivities and signaling pathways.

1.4. Mass spectrometric detection of oxidative modifications in proteins and peptides to trace plasma-derived reactive species

Among all plasma components, reactive species, and in part radiation, are responsible of cold plasmas' modulatory effects. As already shown in amino acid solutions, oxidative modifications may be introduced due to the action of reactive species on proteins [126].

Although it is challenging, the precise detection of these modifications in proteins is a key step to investigate the chemistry and the biological mechanisms of action of plasmas. As previously described, the best method for detecting oxidative modifications is mass spectrometry (MS) [154], which is the main technique applied in the present work. MS is used in proteomic studies since the 1980s when electrospray ionization (ESI) and matrix-assisted laser desorption ionization (MALDI) have been developed. The advantages of a proteomics bottom-up MS investigation are various, but mainly, several thousand proteins and corresponding modifications can be identified in a single sample run [155]. Moreover, over being identified precisely, proteins can be also quantified with this technique [156]. Relative quantification can be achieved in a differential proteomic analysis when the abundancies of a protein in a certain condition are compared to the profiles measured in a reference sample.

Typical absolute quantification strategies include the use of stable isotope labeling by amino acids in cell culture (SILAC) [157], using synthetic isotopically labeled peptides (AQUA), or label-free quantification (LFQ) calculations [158]. Due to the low abundances of modified proteins or peptides in comparison to the entire proteome in a cell, different enrichment protocols can be applied to improve their detection. However, this strategy has not been yet implemented for all known oxidative modifications, a reason why this must be further investigated in the future. Currently, only specific oxidative modifications like nitration at tyrosine [159], or oxidation at cysteine [160] can be enriched, e.g., using beads with specific antibodies, or targeting the exact bonds for the $-\text{NO}_2$ or $-\text{O}_x$ groups with specific reagents [96].

Enrichment is an effective way to detect low abundant modifications, having as a downside the potential loss of any other kind of modification from the detected spectra. In an MS analysis, the detection of PTMs occurs on entire or digested proteins (peptides) via the so-called tandem MS (MS/MS or MS^2) [61]. By using an ionization source (e.g., ESI, MALDI), intact proteins or peptides are ionized. At this point, two identification steps based on the biomolecule's mass can take place, one on the MS level, another on the MS/MS level.

The MS spectrum is acquired first, to identify the molecular mass of the entire protein or the peptides (if the protein was digested previously), which is called parent ion. To increase the accuracy of the detection, each protein or peptide can be fragmented via MS/MS by energy impact or transfer with a collisional inert gas. Here, the fragmentation of the peptide bond produces a set of ions (daughter ions) overlapping the sequence of the parent ion in analysis.

If there is a PTM on a certain amino acid, the mass of the modified amino acid will change, and a mass shift (Δm) will be carried in both the parent ion and in one or more daughter ions, as shown in Figure 1.6.

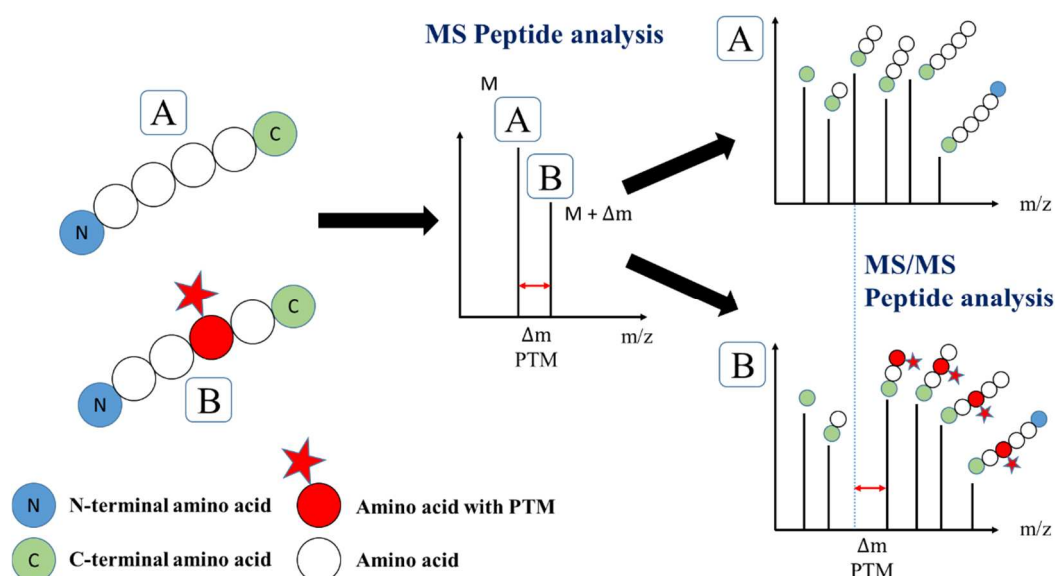


Figure 1.6. Detection of post-translational modifications using tandem mass spectrometry. A peptide (A) consisting of six amino acids produces an MS and an MS/MS fragment spectrum with six peaks. The same peptide with a modification (B) produces shifted MS and MS/MS spectra due to the modified amino acid. The determination of the exact mass shift (Δm) at the MS level allows the identification of the modification, while at the MS/MS level allows the precise localization of the modification on the amino acid level. *Illustration redesigned according to* [61], <https://creativecommons.org/licenses/by/4.0/>.

Analyzing a single peptide manually is possible, but often the proteomics analysis of many complex samples, having tens of thousands of different modified or non-modified proteins, is required (e.g., in case of the analysis of various cancer cell lines). In these cases, the manual data analysis becomes very complicated and time-consuming. Therefore, data are analyzed by using software that can search for several thousand proteins simultaneously, screening additionally for different modifications.

Here, all possible theoretical fragment spectra are generated in the software (in silico) for all identified proteins, and these are compared with the experimentally measured spectra. If the match between the theoretical and experimental spectrum is high enough (score threshold), the protein or peptide is considered to be correctly identified. An example is the software Proteome Discoverer (Thermo Fisher) [161], which is largely used for this purpose in the proteomics field. The software Byonic (Protein Metrics) [162] has been used in the present work as additional software to identify a wide range of oxidative modifications occurring on specific amino acids, overcoming the limits of enrichment techniques.

The latter, indeed, rather focuses on a single modification and requires long and sensitive experimental protocols. Another advantage of Byonic is that an unlimited amount of PTMs can be overall screened, also allowing the identification of more modifications for each single amino acid in a peptide. Furthermore, the so-called Wildcard Search supports the untargeted analysis of all possible modifications found in a sample, without the necessity to plan and focus the study on a previous hypothesis [162].

A relatively small number of studies has been performed on the impact of reactive species in relation to the proteins' structures. Thanks to the described techniques, one of the novelties of the present study include the characterization of the reactivity of amino acids based on the peptide sequence, highlighting competing reactions with other amino acids.

The complex interplay of plasma-induced reactive species, which can also react with each other, and their effects on target molecules, such as proteins, have been also studied in this work, with further focus on modulating plasma jets and conditions to produce a different pattern of plasma components to monitor their biological effects.

For these reasons, the general workflow consisted of 1) a systematic investigation of the biochemical impact of different plasma conditions and sources, 2) the identification of amino acids modifications in peptides via mass spectrometric methods, and 3) the transfer of gained knowledge from model systems to complex molecules and sample-types. Further details about these points are listed below:

- 1) The used plasma sources were the argon-driven kINPen 09, due to the well-characterized gaseous chemistry, and the helium-driven COST-Jet as a reference source (Figure 1.2). Modulated conditions were treatment duration (15 to 60 sec), distance from the jet nozzle to the target surface (from 4 to 9 mm), solvent-type if solutions treated (water, PBS), molecular admixtures in feed gas (0.5% O₂ and/or N₂) (methods applied from A1 to A5).
- 2) The pattern of plasma-induced modifications in every amino acid was identified via nanoliters-flow liquid chromatography (nanoLC) coupled to MS detection, using Orbitrap-type MS systems. The identification of modifications was performed by tandem mass spectrometry (MS/MS). Quantification of the identified modifications was performed via label-free peptide spectrum match counting [163] (methods applied from A1 to A5).
- 3) Modifications occurring in more complex structures were investigated, in particular in i) phospholipase A2 (PLA₂) in aqueous solutions (applied in A3), due to its relevance in lipid metabolism, ii) in patients' wound exudates (applied in A4), and iii) in porcine epidermis skin tissues (applied in A5), due to the application of cold plasmas in wound healing acceleration [7-12].

2. Cold Plasma Effects on Proteins: from Peptides Solutions to Tissue Proteomes

This chapter summarizes the main results of the thesis. First, it focuses on the detection of possible oxidative modifications, induced by cold plasmas in peptides, which have been discussed in **Section 2.1**. Considering a liquid environment surrounding cells, tissues, and molecular structures, the plasma-driven biochemistry induced in aqueous solutions containing peptides has been discussed. The modulation of parameters and sources (kINPen and COST-Jet), which may lead to differences in oxidation potentials of plasmas, are also a part of this chapter.

The generation of plasma species in aqueous solutions has been investigated by screening the resulting oxidative modifications in the peptides. The results obtained from Article A1 have been discussed, where aqueous solutions of two model peptides angiotensin 1-7 and bradykinin have been used. Experimental data were additionally compared with *in silico* data obtained from previous works which applied dynamic simulations, currently widely used in plasma medicine (**Section 2.1.1**). The main findings of Article A2 have been also included to discuss the biochemistry induced on an artificial peptides' library in solutions. Here, an evaluation of the most reactive amino acids in relation to their position in each peptide has been elaborated (**Section 2.1.2**). In **Section 2.1.3**, the knowledge gained in the first part of the work has been applied in aqueous solutions containing the protein phospholipase A2 (PLA₂), as shown in Article A3. Here, the differences in oxidative modifications concerning the treatment of a more complex structure have been discussed and compared with previous results, giving additional insights on how plasma can alter protein functionality. **Section 2.2** finally resumes results obtained on proof-of-concept experiments carried out to verify if plasma-driven modifications occur also in cell proteomes, such as in wound exudates of patients' skin (Article A4, **Section 2.2.1**), and in intact porcine skin (Article A4, **Section 2.2.2**). Due to the relevance of cold plasmas in applications promoting wound healing, the obtained results have been discussed also in terms of clinical safety and effectiveness of plasma treatments.

2.1. Screening structural changes of peptides in solution

Despite the increasing use of plasma in medical applications [164, 165], various questions regarding its mode of action are still unanswered. The effects of CAPs on biological molecules like lipids [123], small molecules [166], and DNA [43, 167] have been previously studied. Still, it is unclear whether plasma can modulate cell signaling pathways through these effects. It is known that reactive species can add a variety of oxidative modifications to proteins and enzymes, but there is no direct link on how CAPs can modify specific amino acids in a peptide or a protein. To investigate these questions, oxidative modifications were characterized after treatment with cold plasmas using mass spectrometry. Firstly on a library consisting of 10 peptides with variable conformations (Fig. 1, A2), then on 2 biologically relevant peptides (angiotensin 1-7 and bradykinin, Fig. 4/5, A1) and finally in aqueous solutions of PLA₂ (A3).

Due to the heterogeneity of plasma sources and their tunable parameters currently proposed for biomedical applications, various conditions (e.g., driven gas composition, treatment duration) and plasma jets (kINPen 09, COST-jet) have been used for these studies.

The results obtained in this thesis support previous works, treating amino acids in aqueous solutions, where it has been shown that different conditions reflect a differential production and generation of plasma components, mainly reactive species [126, 128, 149].

To screen a bigger number of possible modifications on each amino acid, the software Byonic was used to fulfill this task (A1, A2, A3). The software compared real mass shifts (Δm) with theoretical ones calculated *in silico*, finally producing a list of modifications occurring on each amino acid after plasma treatment, as shown in Table 2.1. Each mass shift represents the addition or loss of a certain number in Da, which could be correlated to the addition or loss of a defined molecular group. Due to the high accuracy of the used MS, the monoisotopic mass shift in Da could be calculated, reflecting the precise identification of the functional group added or lost on each amino acid structure. In this thesis, peptides (A1, A2) or a mixture of peptides derived from proteins digestion (A3, A4, A5) have been analyzed via mass spectrometry methods (bottom-up approach).

Spectra of peptides containing each modification on each amino acid were counted and eventually normalized on the number of peptides containing the same unmodified amino acid. After training the software, due to the long calculation times, the presented list of oxidative modifications induced by varying plasma parameters have been applied for target analysis of possible modifications occurring on specific amino acids in Articles A3, A4, and A5, where the analysis of entire proteins or complexes of proteins was performed. More details about the plasma treatment conditions where these modifications occurred, and on which specific amino acids, are discussed in the following sections.

Table 2.1. Main oxidative modifications were detected via nanoLC-MS after treatment with different plasma conditions on peptides amino acids. *Modified and adapted from Articles A1, A2, and A3.*

Δm [Da]	Elemental Composition	Chemical Modification / Potential Product
+ 15.99	+ O	hydroxylation, oxidation
+ 31.98	+ 2O	dihydroxylation, peroxide, dioxidation
+ 47.98	+ 3O	hydroxylation + peroxide, trihydroxylation, trioxidation
+ 28.99	+ N + O - H	Nitrosylation
+ 44.98	+ N + 2O - H	Nitration
+ 60.98	+ N + 3O - H	nitration + oxidation
+ 76.97	+ N + 4O - H	nitration + dioxidation
+ 0.98	- N - H + O	deamidation
- 0.98	+ N + H - O	Amidation
+ 13.98	+ O - 2H	carbonylation (oxo group)
+ 29.97	+ 2O - 2H	oxo group + hydroxylation
+ 45.97	+ 3O - 2H	oxo groups + two hydroxylations or peroxide
- 2.02	- 2H	didehydrogenation (double bond)
- 4.03	- 4H	two didehydrogenation (two double bonds)
+ 4.98	+ 2O - N - C - H	ring cleavage (histidine: formylasparagine)
- 3.05	+ O - 5H - N	oxidative deamination (lysine) [126]
+ 33.96	+ Cl - H	chlorination

2.1.1. Biochemical modulation with treatment condition (A1)

To investigate if and how the modulation of plasma parameters could generate specific protein structural changes, a study has been performed on solutions of peptides in A1. In particular, the impact of CAPs on two peptides, angiotensin 1-7 and bradykinin has been investigated. Indeed, the oxidative modifications induced on these peptides using the COST-jet as a plasma source have been already previously studied using molecular dynamic simulation (MD) [168].

This is a method currently proposed in plasma medicine to contribute to the characterization of molecular mechanisms induced by cold plasmas in aqueous solutions or other biological models [34]. Therefore, in A1 it has been discussed if experimental data would support or correct the mechanisms highlighted by *in silico* simulations. Here, in addition to the COST-jet, the kINPen 09 was used as a plasma source. Differences and similarities in the liquid chemistry of the two plasma sources have been identified, as shown in Figure 2.1.

Tyrosine (Y) was one of the most reactive amino acids in the peptide angiotensin 1-7, being mostly modified when further gases (e.g., N₂, O₂, or both) were added. Another aromatic amino acid, phenylalanine (F), was mostly modified in bradykinin. Regarding Y, this result could be reproduced for both plasma sources. In particular, the addition of -NO₂ (nitration), 1 or 3 -OH groups (hydroxylation) could be observed on the benzene ring on tyrosine (Fig. 3 and 4, A1). The modifications changed qualitatively and quantitatively in relation to the gas composition, reflecting a differential active liquid chemistry. For example, nitration and one hydroxylation occurred mainly with Ar ± N₂/O₂, while a high degree of hydroxylation occurred mainly in Ar + O₂. To support the investigation of bioactive species in liquid, long-lived species (H₂O₂, NO₂⁻, and NO₃⁻) have been quantified in A1 (Fig. 2, A1). H₂O₂ was more significantly produced in Ar plasmas of kINPen 09 compared to the He plasmas of COST-Jet, as the excimers forms of argon in kINPen 09, and the consequential production of VUV radiation [34, 169], may lead to a higher water (H₂O) dissociation into [•]OH and [•]H [170].

The [•]OH can quickly recombine to form H₂O₂. However, in presence of another substrate like tyrosine, [•]OH can react in a direct reaction with Y to hydroxylate it. This mechanism would explain the overall higher production of OH-tyrosine in conditions with Ar-only.

Regarding tyrosine nitration, the presence of both N₂/O₂ produced higher amounts of NO₂⁻ and NO₃⁻, according to previous studies [41, 171]. These RNS are reactive towards tyrosine mainly at low pH (<3) [137], which was not reached after treatment. However, these plasma conditions may produce other species more reactive towards Y, such as gaseous [•]NO and [•]NO₂, or ONOO⁻, whose oxidized forms are NO₂⁻ and NO₃⁻ (Fig. 3, A4) [130, 172].

Although the lowest amount of long-lived species was measured in conditions with O₂, the highest number of modifications was detected (Fig. 3, 6, and 7, A1). To explain this is the fact that gaseous short-lived species like [•]O and ¹O₂ can be formed [26, 166], acting in liquid directly with the amino acids [173, 174] or with water molecules, producing tertiary species such as those resulting from water homolysis and ionization ([•]OH, [•]H, and H₂O₂) [175].

Overall, most amino acids in the model peptides showed strong differences between the two plasma sources, showing ROS-dominated chemistry mostly driven by O₂ or [•]O respectively in kINPen 09 and COST-jet, as shown previously [53, 153, 176, 177]. The reactivity of each amino acid was related to its position in the peptide, as shown for prolines (P) in positions 3 or 7 in bradykinin, or F in positions 5 or 8 in bradykinin (Figure 2.1).

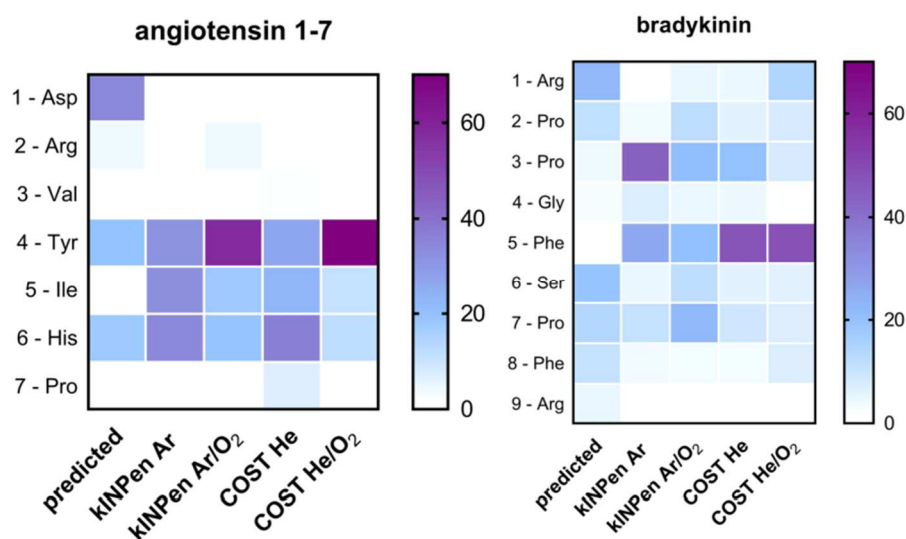


Figure 2.1. Comparison of oxidative modifications (normalized on the untreated control peptide) identified in angiotensin 1-7 and bradykinin after plasma treatments (kINPen 09, Ar \pm O₂; COST-jet, He \pm O₂), and using *in silico* dynamic simulations [168]. Adapted from Article A1.

Further investigations about the influence of the peptide sequence in receiving plasma-driven modifications have been performed in A2, which is resumed in the following section. Finally, differences between experimental and *in silico* data [168] have been identified (Figure 2.1). The major reason for these differences could be connected to the introduction of only \cdot OH in the MD simulation, while real plasma treatments presented a qualitatively and quantitatively different cocktail of plasma-generated reactive species [25, 178].

2.1.2. Influence of position on amino acids' reactivity (A2)

A systematic approach with an artificial peptide library was used to understand how plasmas can differentially modify amino acids, additionally by varying peptide sequences. The library was created to contain all 20 canonic amino acids and included 10 peptides (Fig. 1, Tab. S1, A2) where each amino acid occurred with equal frequency either at the C-terminal, central, or N-terminal of a peptide. A various chemical environment was generated for each amino acid by diversifying the neighboring amino acids. Peptides have been treated in solutions using two plasma sources (kINPen 09 and COST-jet) and modulating various parameters to investigate their influence on the peptides, as in A1. Additionally, the solvent type was modulated in A2, using water-only and PBS solutions and direct vs indirect treatments have been compared.

These conditions were considered as PBS simulates the neutral pH which can be found in physiological applications, and which could be essential in defining the overall chemical dynamics. Indirect treatments, which means treating the solution only, with the following incubation with the peptide in analysis, have been used to simulate the chemistry occurring *in vitro* applications, where cells are incubated with plasma-treated media [179, 180]. The used approach and the follow-up bioinformatic processing of the data enabled specific statements about the reactivity of amino acids in peptides after plasma treatment, in contrast to previous studies focusing on single amino acids solutions and longer treatments [126]. Additionally, in these experiments, the result of competitive reactions possibly occurring also in complex biological systems between different amino acids could be observed. These results supported previously found evidence in A1, extending and completing them for all amino acids.

In particular, sulfur-containing amino acids showed most modifications after plasma treatments, mainly consisting in the addition of oxygen groups to generate highly oxidized forms of sulfenic and sulfonic acid (Fig. 3 and 4, A2), especially in presence of oxygen in the plasma. Also, aromatic amino acids were modified in a higher degree, e.g., nitration or hydroxylation, confirming the results observed in A1. Independently from the applied plasma source, the amino acids cysteine, methionine, tryptophan, tyrosine, and phenylalanine were those overall mostly modified. Other amino acids, quantitatively less modified, showed a bigger difference between sources. Lysine, proline, and serine, for example, were significantly more chlorinated by COST-Jet than kINPen 09 (Fig. 9, A2), and chlorination was the modification overall mainly found with the COST-Jet. This result, which could be observed only due to the presence of sodium chloride (NaCl) in PBS solutions, confirmed the predominant action in this jet of atomic oxygen when oxygen is added to the plasma, according to [181, 182], generating the chlorinating agent hypochlorite (OCl^-) by reaction with chloride ions in water (Fig. 5, A2). Interestingly, in presence of tyrosine close to serine in the peptide chain, a reduction in chlorination was observed in serine in favor of tyrosine chlorination, suggesting a higher reactivity of the aromatic ring in comparison to the aliphatic structure of serine. Nitration, on the other hand, was exclusively found using kINPen 09. The plasma generated by this source is characterized by a turbulent flow with consequent major target liquid admixture and plasma interaction with ambient air molecules (e.g., N_2 , O_2 , H_2O) [166].

The interaction of excited forms of Ar with ambient air is responsible for an increased production of nitrogen chemistry observed in kINPen 09 plasmas. The generation of gaseous $\cdot\text{NO}$, in combination with gaseous $\cdot\text{O}_2$, generated peroxyxynitrite in the liquid target especially in conditions with $\text{Ar} \pm \text{N}_2/\text{O}_2$ [183], as described in A4, which is a strong nitrating reagent (Fig. 8, A2; Figure 2.2) [130]. Interestingly, tryptophan modifications consisted mainly in its cleavage to form kynurenine derivatives (Fig. 6 and 7, A2), which in the cell environment can be produced by the presence of singlet oxygen. Plasmas could induce them when oxygen was present in the driven gas, a condition which was already previously shown to produce gaseous $^1\text{O}_2$ directly acting in the liquid target, especially using kINPen 09 as a source (Fig. 9, A2) [53, 153]. Further results identified the modification pattern for each amino acid under specific conditions, e.g., by varying working gas composition (Fig. 6, A2), treatment time, direct or indirect mode, and solvent type (Fig. 10, A2). This highlights similarities and differences between amino acids also in relation to their position in a peptide structure (Figure 2.2).

This phenomenon could be already observed in A1 (e.g., in Figure 2.1), and has been systematically implemented and discussed in A2 due to the presence of more peptides. The presence of variable neighboring amino acids and the N-, or C-terminal proximity influenced the nitration of tyrosines belonging to different peptides, as shown in Figure 2.2.

In particular, in contrast to solutions with PBS, major nitration has been observed in unbuffered solutions. The presence of chloride anions, indeed, generated rather a major chlorination of amino acids. Possibly, reactive oxygen species are necessary, as previously discussed, to induce both protein chlorination and nitration. The latter modifications could be therefore favored in absence of chloride anions. Furthermore, the terminal position of tyrosine in peptide 1 promoted its nitration, which was quite lower in peptide 6, possibly due to the presence of an aliphatic (valine), and basic (lysine) amino acids. This conformation, indeed, potentially reduced the reaction rate by mechanisms driven by pH modulation and/or steric hindrance.

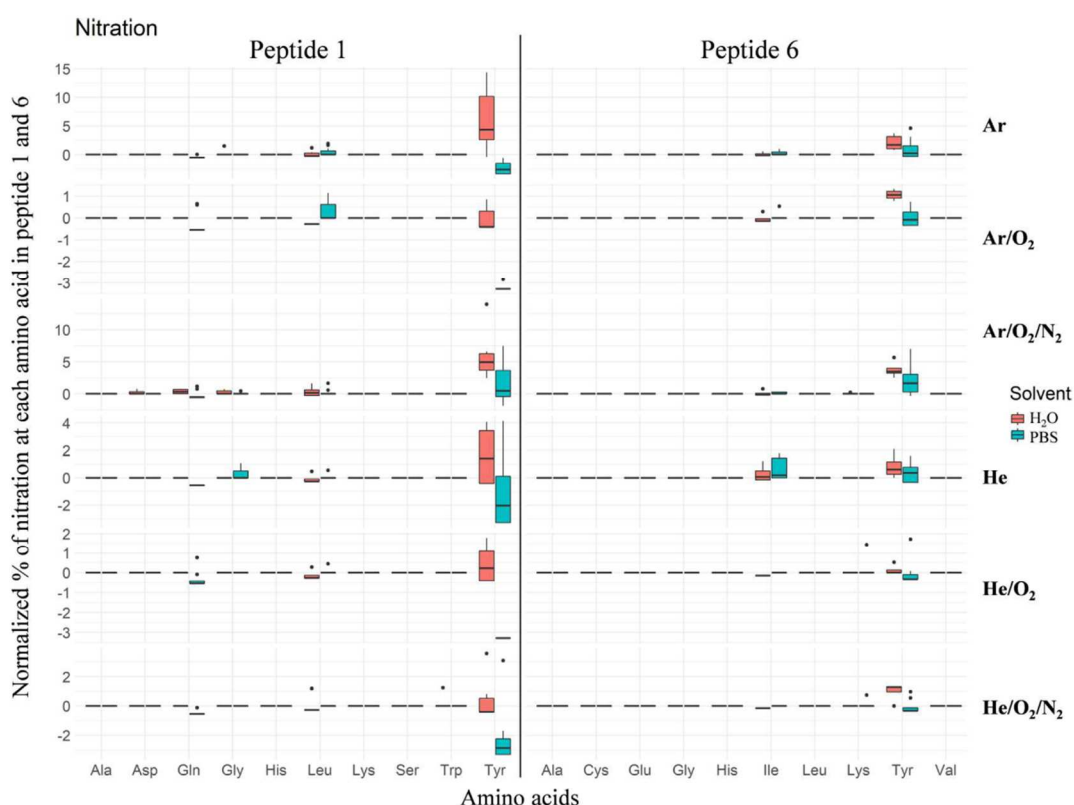


Figure 2.2. Example of differential nitration occurring on tyrosines in having N-terminal position in peptide 1 (left), and internal position in peptide 6 (right). Treatments with kINPen 09 (Ar-driven) or COST-Jet (He-driven). Values in treated peptides normalized on untreated peptides. *Adapted from Article A2.*

It has been shown, indeed, that higher or lower pH may favor tyrosine nitration [137, 172, 184]. Another example involved peptides 3 and 7, having both cysteine (Cys) and tryptophan (Trp) in the chain (Fig. 1, A2). In peptide 7 these two amino acids were separated by only one amino acid, whereas the entire peptide was in between Cys and Trp in peptide 3. While various oxidative modifications (e.g., oxidation, deoxidation; Fig. 7, A2) have been observed at the Trp in peptide 3, treatments with pure argon of peptide 7 solutions showed a definitively lower degree of structural changes in Trp (supporting information in paper A2). In peptide 7, major oxidative modifications have been observed in Cys than Trp, which in this case was the main target of oxidation, dioxidation, and trioxidation mediated by plasmas. Through these results, it was confirmed that cysteine is one of the most sensitive amino acids towards cold plasmas, not only in amino acid solutions but also in peptides and proteins, and could mediate the alteration of redox signaling pathways observed after plasma treatment of cell cultures and other biological samples [11, 12, 118, 180, 185-187]. Through these results, it was confirmed that the peptide structure is an important factor defining the resulting effects of plasma.

Therefore, it can be stated that not only the plasma parameters and the chemistry generated in both the plasma sources must be considered, but also the target must be considered. Finally, deeper studies are necessary to develop targeted applications in plasma medicine.

2.1.3. Consequences on protein functioning (A3)

The identification of oxidized amino acids in different peptides was the initial key step to understanding if and how proteins can be modified by plasmas. From previous results, it was

clear that plasma can interact with amino acids and, in relation to their position in the peptide sequence, induce oxidative modifications. The latter could be introduced based on the used plasma sources and treatment parameters. A further investigation, connecting the hypothesis that plasmas act through biomolecules modifications, was deepened in Article A3. Indeed, the treatment of peptides enriched the information about the reactivity of amino acids in complex biomolecules, however, it must be still clarified whether these structural changes have a demonstrable influence on the activity or stability of a protein and could therefore potentially lead to a modulation of cell signaling pathways mediated by plasmas. For this purpose, an experiment based on the argon plasma treatment with kINPen 09 of buffered aqueous solutions of phospholipase A2 (PLA₂) has been performed and the results have been published in Article A3 and discussed in this section.

PLA₂ is an enzyme capable of cleaving acyl ester bonds from glycerophospholipids, releasing free fatty acids and lysophospholipids. A massive overexpression and thus increased activity of this enzyme occurs in various diseases, such as cancer, asthma, autoimmune disorders, and autism [188-190]. In this context, reducing the activity of this enzyme could be an advantageous strategy to target these diseases. Although the applicability of plasmas in various diseases is still in evolution, the potential of these tools in introducing oxidative modifications able to reduce the functionality of PLA₂ has been tested as an exemplary experiment. After plasma treatment and MS-based analysis of the digested protein, the most frequently modified amino acid was tryptophan (Trp) in position 128 (Figure 2.3). In contrast, another Trp in position 8 did not show modifications at this position. On the other hand, trioxidation at cysteine next to the latter tryptophan was found. As discussed in the previous section, this result may be generated due to the higher reactivity of cysteine in comparison to tryptophan, which results in the preservation of the tryptophan structure in position 8.

Additionally, the two tryptophans were both located at the N- or C-terminal end of the peptide, confirming that, rather than the position, neighboring amino acids, such as cysteine, played a key role in the structural changes of tryptophan. Overall, the presence of PLA₂ in a gold electrode supported lipid bilayer showed that the permeability of the membrane increased in comparison with the lipid bilayer alone (Fig. 2, A3). The tryptophan dioxidation of PLA₂ at position 128 was the most common detected modification. With this knowledge, it was verified via simulations if this structural change could influence the stability and the activity of the protein in the context of a cellular membrane. As a result, it was shown that the modification did not influence the macromolecular folding and structure of the enzyme (Fig. 5, A3), but rather altered the interaction and the stability of the protein in the phospholipid membrane (Fig. 6, A3). In particular, as shown from 2D and 3D simulations of the interaction of PLA₂ with the lipid bilayer, the plasma-induced dioxidation of tryptophan prevented the anchoring of the enzyme on the membrane, which is mediated by the tryptophan carbonyl group connected to the phospholipids via two hydrogen bonds.

The loss of interaction with the membrane may lead to the loss of function of the PLA₂ in biological contexts. Plasmas could finally be applied as a strategy to reduce the activity of similar enzymes having interfacial tryptophan, and therefore exposing this structure to the oxidants generated by plasmas. As an example, tryptophan in enzymes is a locus that many viruses (e.g., Ebola, Influenza) use to stabilize in host cells, confirming the potential target use of plasmas for disinfection purposes [191-194].

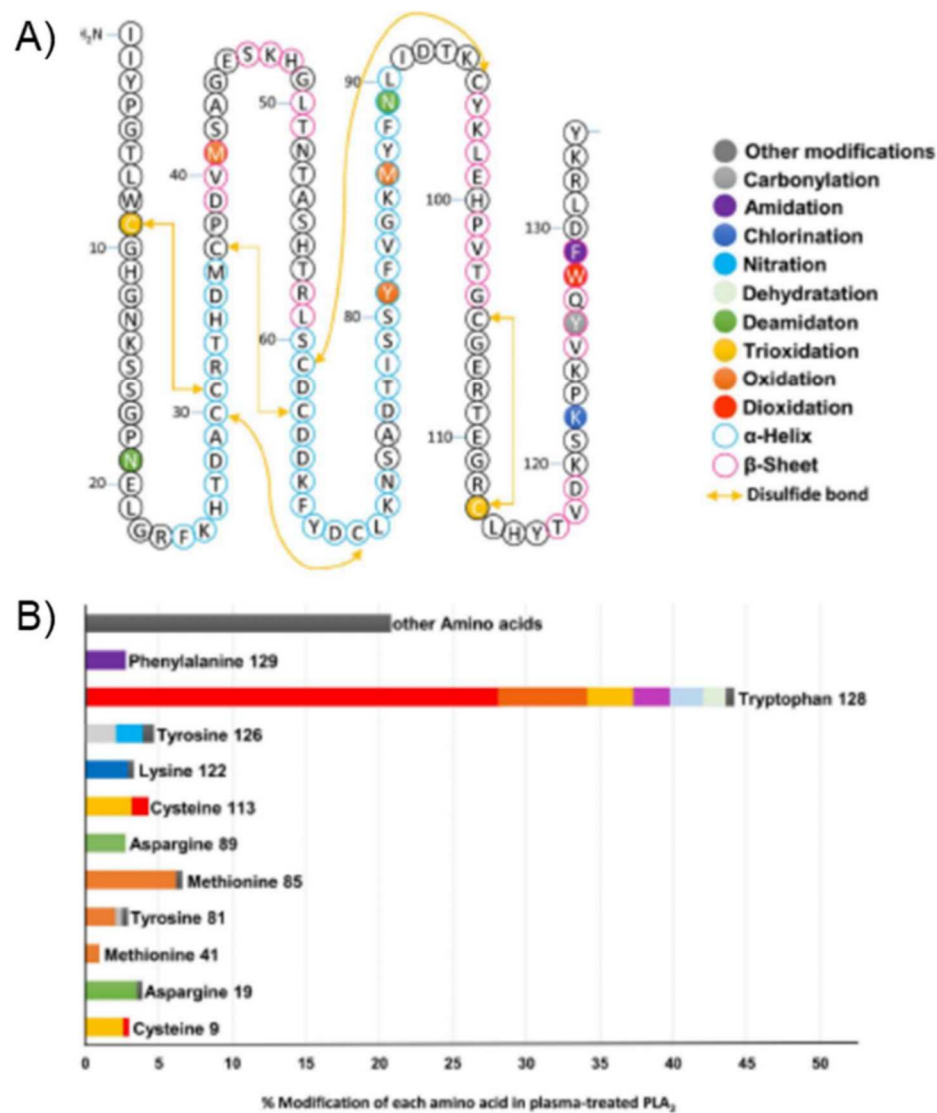


Figure 2.3. The sequence of PLA₂ with location (A) and relative amount (B) of ox-PTMs after plasma treatment (kINPen 09, Ar). Values in treated peptides normalized on untreated peptides. *Adapted from Article A3. The illustration was created in collaboration with Seyedali Memari.*

2.2. Identification of oxidative modifications in tissue proteomes

In the previous sections, it could be shown that plasma treatments can induce very different structural modifications for the analyzed proteins or peptides in liquid solutions, in terms of both amount and type of reactive species, potentially reflecting tunable effects also in cells and tissues. In particular, various variables, such as the used plasma source and gas composition, defined the type of modification, which was also specific in relation to the targeted amino acids and their position in the peptide sequence. The liquid chemistry, generated by a plasma, was similarly differentially modulated with the plasma source and plasma treatment. Further open questions include the verification of the plasma effects in complex matrices rather than model solutions, such as cell cultures or even intact or wounded skin.

Additionally, it must be further investigated if the presence of a water compartment acts as a key amplifier of plasma-induced reactions, or if plasma components present predominantly in the gas phase may also impact dry biological matter, such as intact skin.

This topic is of particular interest considering that, due to the easy accessibility and treatability of human skin, cold plasmas are currently applied in various skin-related diseases (e.g., infections, wound healing, cancer, pigmentation diseases), both in *in vitro* research than in clinical experimental stages [11, 12, 118, 180, 185, 187]. To contribute to the understanding of how plasmas react with complex matrices, results and main conclusions published in Article A4 and Article A5 have been summarized in the following sections. These experiments applied plasma treatments of wounded skin, with consequent oxo-proteomics analysis of the wound exudates (A4), and of intact porcine skin (A5).

2.2.1. Human skin wound exudates (A4)

The deregulation of pathways connected to wound healing following plasma treatments has been already described, showing that the activity and expressions of transcription factors, such NF- κ B or HIPPO [118, 180], could be altered. These alterations have been correlated to the promotion of wound healing induced by plasma treatments using kINPen MED with Ar-only. Although downstream effects such as pathways deregulation and visible acceleration of the healing have been observed, the molecular mechanism of plasma effects is still under investigation. In Article A4 it has been performed a proof-of-concept experiment to verify if cold atmospheric plasma can induce oxidative modifications in human wound proteomes. Oxidative modifications, as for enzymatic modifications, are key pathways regulators, and plasma could trigger a signaling modulation through proteins modifications. Although the effects of plasmas in amino acids, peptides, and proteins solutions have been proven, a screening of oxidative modifications occurring in wound proteomes has been investigated only for the first time in Article A4. Here, patients with diabetic-related complications leading to large wounds have been swabbed before and after plasma treatments (Figure 2.4A), and the wound exudates have been submitted to proteomic analysis as previously described.

A targeted analysis of oxidative modifications on proteins has been performed using Byonic, applying the information previously obtained by screening possible modifications occurring on peptides and proteins in solutions. As a result, 330 proteins have been identified, and by comparing the oxidation state before and after plasma treatments, kINPen MED induced an increase in 63% of oxidation (-OH group addition), 44% more nitration (-NO₂ group addition), and 69% more nitrosylation (-NO group addition), as shown in Figure 2.4B. These results confirmed, those protein modifications may be the first mechanism of action of CAPs, which could justify their visible clinical effects. In particular, blood proteins (e.g., haptoglobin, albumin, hemoglobin) and proteins belonging to the connective tissue (e.g., fibronectins, keratins) were mainly modified, suggesting that external structural proteins could protect deeper skin layers. This aspect must be considered for targeted approaches and further studies must be planned to define how other proteins could transfer the obtained oxidation potential and translate into downstream effects. Interestingly, treatments with plasma not only induced oxidative modifications but also nitrosative modifications, which in the cell environment finely regulate various pathways, in contrast to reactive oxygen species, which generally lead to necrosis or apoptosis pathways. This aspect highlights the potential of cold atmospheric plasma to be finely tuned for targeted aims, which can promote or inhibit different pathways.

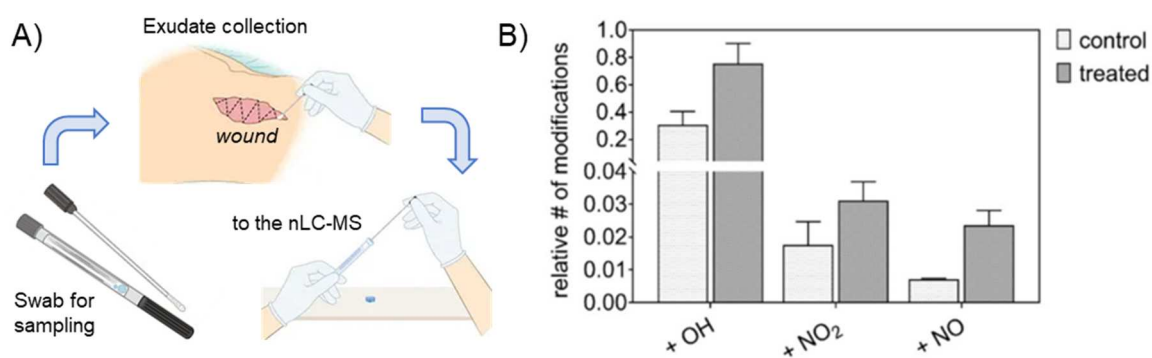


Figure 2.4. Ox-PTMs were identified after plasma treatment (kINPen MED, Ar) of wounds belonging to diabetic patients. Wound exudates were collected and analyzed. Values in treated peptides normalized on untreated peptides. *Modified and adapted from Article A4.*

2.2.2. Porcine epidermal tissues (A5)

The eventuality of changing plasma treatment parameters led to a differential chemistry, and consequentially different biochemical and functional effects on proteins. However, to date, the only certified and clinically approved conditions to be applied using kINPen MED plasmas is the use of Ar-only at 5 slm. The use of other gas compositions is still under investigation, especially in relation to the safety and risks aspects. The eventual change of gas composition will be only possible after reaching some priority milestones, which include the full understanding of which effects Ar-only kINPen MED plasmas can have on human tissues.

In all the studies performed up to date, a major focus has been on the action of plasma-generated reactive species, while the isolated impact on biological structures of plasma radiation has been just studied partially [169]. Additionally, many experiments and studies have been performed in liquid models, an aspect which helped the researcher to highlight that a liquid compartment can be used as a plasma effect amplifier. However, results on how proteins can be modified in dry skin have been not yet elaborated.

To fill this gap, this section includes a summary of the main results shown in Article A5, where porcine skin tissues have been treated with Ar-only kINPen MED. Over treatments with full plasmas, however, which included the impact of reactive species and other plasma-derived particles, the effects of an isolated range of radiation have been evaluated by using various filtering windows between the plasma source and the porcine skin surface. Normally, kINPen MED plasmas can emit from the vacuum UV region (VUV, 100-200 nm) to the infrared region (> 1000 nm), including the UV range (200-400 nm) (Fig. 3, Fig. 4, A5) [169, 195].

As radiation with a shorter wavelength are more ionizing and therefore possibly the most dangerous, the impact of VUV radiation was evaluated by using different windows, such as magnesium fluoride windows (MgF₂), which are permeable to radiation starting from 120 nm, Suprasil-1 windows, permeable from 200 nm, and Borofloat-33 windows, transmitting from 300 nm. In this work, the major focus was centered on the modifications occurring on cysteine, being one of the most sensitive amino acids towards oxidative modifications. Additionally, the effects of plasma in cysteine solutions have been intensely characterized, in previous works and Article A5, and these data allowed a final comparison of effects observed in aqueous or dry models. Additionally, different skin layers have been sampled before and after treatments, allowing the comparison of plasma effects between skin layers.

In comparison to the oxidative modifications observed in cysteine solutions (Fig. 6, A5), where aqueous chemistry was included (Fig. 5, A5), cysteines in the dry tissue proteome were generally less, as reported in Figure 2.5. In particular, the main observed modifications in the tissue proteomes were the addition of another cysteine on a cysteine (forming cystine), cysteine trioxidation (forming sulfonic acids), the breakage of the cysteine C-S bond (forming alanine), the addition of cysteine of a sulfone group ($-\text{SO}_3$, forming cysteine S-sulfonate), and cysteine dehydrogenation (Fig 8, A5). Main effects in terms of modified protein cysteines were observed using the full plasmas Ar-only, especially the formation of S-sulfonate especially in the third layer, and the C-S bond breakage in both the first and third layer. Here, argon metastables and excimers are highly produced in relation to all other conditions and could be therefore responsible for the observed effects [169].

In contrast, Ar + O₂ conditions, which mainly produced gaseous ROS (e.g., $\cdot\text{O}$, $^1\text{O}_2$, O₃) [53, 153], induced mostly cystine formation in the first skin layer, and dehydrogenation in the third layer. These products may be the result of a radical attack to the C-S or C-C bonds, inducing respectively thyl radicals' formation and recombination in cystine, or loss of 2 hydrogens with double bond formation. By filtering only the impact of radiation, dehydrogenation of cysteine was mildly observed in the first and third layer, with a weak increase of S-sulfonate in the third layer. The production of S-sulfonate overall in the third layer suggests that this modification occurs predominantly not for the direct action of reactive species and other gaseous plasma components, but rather as secondary structural changes triggered by plasmas.

This phenomenon may be connected to the excitation and loss of electrons from the thiol moiety induced by radiation [196, 197]. While especially the impact of VUV radiation produced water dissociation in cysteine solutions or solutions without cysteine (monitored by the production of $\cdot\text{OH}$ and H₂O₂, Fig. 5, A5), the effects were minor on dry tissues, as well as for treatments with full plasma. This result suggested that overall, the safety of plasmas can be controlled for various reasons. One reason could be that possibly the scavenging effects of biomolecules could not only mediate the effects of plasmas but also control the negative effects leading to oxidative distress rather than eustress. It could be concluded that the presence of liquid could be used as a compartment to control the further generation of new species, which in turn can be used as an oxidizing cocktail on biological targets. Finally, the effects of VUV radiation could be observed even less in the deeper layers. This shows that although their higher ionization energy, they do not undermine the safety of the plasmas.

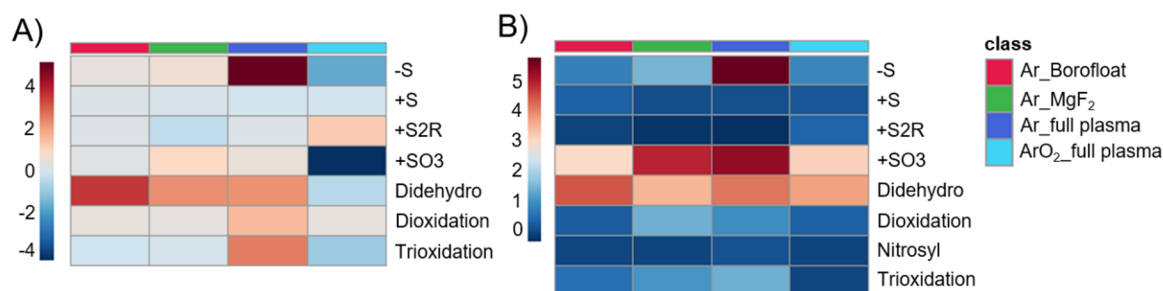


Figure 2.5. Oxidative modifications were identified on the sulfur moieties of the proteome of porcine epidermal skin after plasma treatments (kINPen 09). The first layer (A) and third layer (B) are represented. Values in treated peptides normalized on untreated cysteine-containing peptides. *Adapted from Article A5.*

3. Conclusions & Outlook

Cold atmospheric-pressure plasmas are powerful tools generating oxidative modifications on biomolecules, through the generation in the plasma of bioactive components, especially reactive oxygen and nitrogen species, which production can be further amplified in liquid compartments, generally surrounding cells and tissues. It has been shown that peptides are sensitive structures that can be modified in solutions and biological samples by plasmas.

Oxidative modifications and the consequential structural changes can lead to loss or gain of function of proteins, suggesting that plasmas can be used to modulate complex redox signaling pathways in biomedical applications such as wound healing and cancer treatment. In this work, a screening of possible modifications induced by different CAP sources (kINPen and COST-jet) have been presented and discussed, addressing the objectives i) and ii), regarding the identification of the potential oxidative modifications introduced by cold plasmas in proteins, and the comparison and characterization of the chemistry induced by different plasma sources and treatment parameters. Additionally, different variables, such as gas composition, treatment time, and protein structure, have been identified, and their influence in determining the resulting biochemistry has been presented to improve the controllability of plasma effects in future clinical applications, addressing objective iii). Further conclusions on this objective have been deepened in **Section 3.1**.

In particular, it has been shown that the presence of a liquid vector amplifies the production of species and modifications after plasma treatments, as the water molecules themselves become part of the plasma-chemistry machinery. In contrast, dry biological targets are shown to be modified in a much minor way, supporting the usage of plasma-treated water as a tool itself to be used in various applications (e.g., disinfection). Indeed, in this case, the major target may be rather the open wound, which usually presents a higher level of humification in comparison to the healthy surrounding skin. These results were obtained through the comparison of model solutions containing peptides and proteins with plasma treatments performed on intact porcine skin, in order to address objective iv), regarding the correlation of results obtained from model solutions of peptides and proteins to those obtained treating complex matrices. The present study, finally, enriched the current knowledge in plasma medicine, by connecting in part the translational gap between what is known about plasma chemistry (plasma components produced in the gaseous phase) and plasma biology (deregulated pathways, visible wound improvements).

3.1. Adjusting cold plasma parameters for biomedical applications

A major conclusion supported by this thesis is, that cold plasma can be fine-tuned to affect biological targets differently, inducing specific oxidative modifications in proteins and consequentially, has the potential to regulate in various ways the resulting redox signaling.

Further details about the dependency of peptide modifications on the plasma source and other parameters have been discussed along with all published articles (Articles A1 to A5) and are unified in Figure 3.1. Here, it is possible to assign dependencies from the various parameters for the individual modifications and modified amino acids, in order to be able to predict the influence of a parameter on a certain amino acid for future investigations on other model peptides. In particular, the modulated plasma treatment parameters, as well as different

targets have been used. In Articles A1 and A2, the treatment time, the solvent type, the treatment modality, and the plasma sources have been modulated in treatments of peptide solutions. In Article A3 similar modulations have been applied for treatments of protein solutions. Finally, in Article A4 and A5 plasma parameters have been modulated for the treatment of human wound exudates and porcine skin.

The present work contributed to confirming the results found so far about the analyzed plasma sources in literature and their chemistries (e.g., reactive species on free amino acids) and to assign biological targets in a biological environment, which resulted in the potential biochemical mediator of the visible plasma effectiveness. The results clearly show that not only the treatment time and the distance can influence molecules modification, but also the liquid-type where treatments are performed, the driven gases, and the specific chemistry of target molecules can determine differential plasma effects (see article A2). CAPs are currently used in clinical applications for dentistry and wound healing disorders (e.g., diabetes) and plasma medicine is recently spreading further in cancer treatment, where first successes have been recorded in animal model studies. For the future of plasma medicine and in order to avoid side effects from plasma treatments, it must therefore be ensured that all necessary plasma parameters which affect differently the chemistry and biochemistry of target biomolecules are accurately identified and characterized. Only then it is possible, that these fundamental findings contribute to ensuring, that each pathophysiological problem can eventually receive the optimal plasma treatment condition.

3.2. Outlook: CAPs and clinical applications

As the one focus of the plasma research is to underlie relevant molecular mechanisms of CAPs, the present work intended to fill this knowledge gap regarding CAPs interaction and effects with key biomolecules in the cells, which are proteins. Proteins play a crucial role in many biochemical signaling pathways, especially in the redox signaling. They can stimulate the activation or inactivation of these circuits, being also key reactions accelerators in form of enzymes. Activities and stabilities of proteins can be changed after structural modification, leading to the alteration of relevant pathways. These processes are of interest in various biomedical fields, such as to promote healing processes or induce apoptosis/necrosis pathways in cancer cells. Regarding redox signaling, these modifications can be attached to proteins by chemically reactive species, such ROS and RNS. With the results obtained in the present thesis, it could be concluded that CAPs are a source of ROS and RNS, which pattern can be differentially produced by varying plasma treatments.

Using the modifications induced on protein structures, the liquid chemistry of CAPs was elucidated, proposing a tool to tune plasmas for biomedical applications. To deepen the research connected to the molecular mechanisms of plasmas, a different pattern of oxidative modifications induced in proteins was identified for different conditions, suggesting a potential bridge connecting CAPs with the previously observed physiological effects. Indeed, plasma-modified proteins are candidate biomolecules able to alter the redox signaling and induce defined effects. The results obtained in the model amino acids aqueous solutions have been applied to complex structures, confirming the potential controllability and effectiveness of plasmas in clinical applications. However, the oxidative modifications found are only a first indication of the interaction of plasma and proteins, peptides, and amino acids.

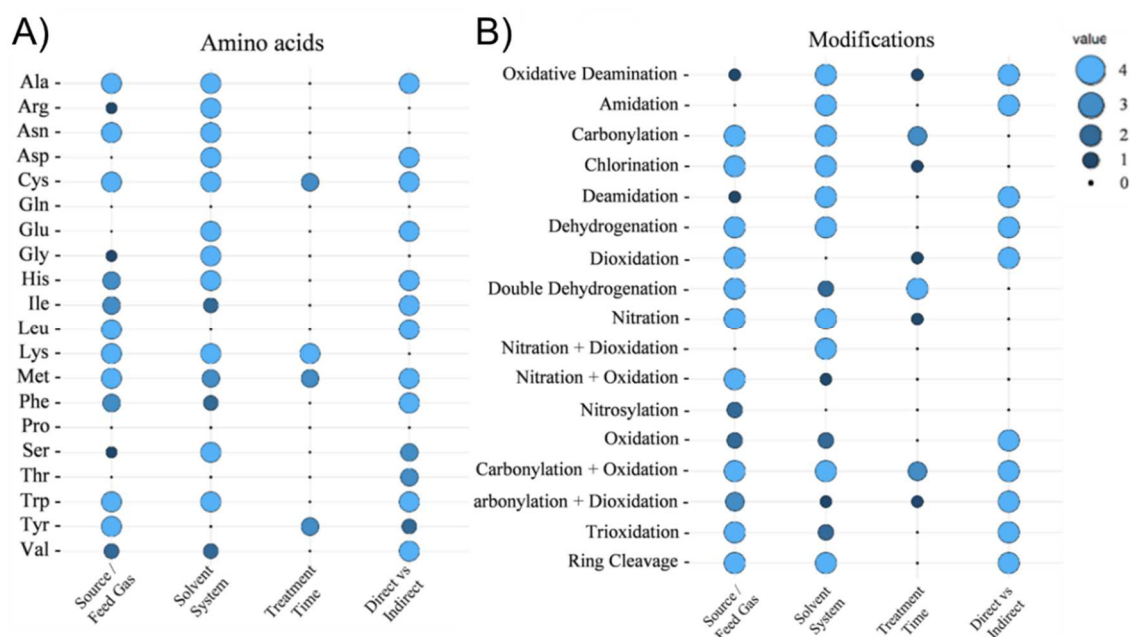


Figure 3.1. Using ANOVA-test calculated dependencies of amino acids (A) and modifications (B) related to the gas composition of the plasma, solvent, treatment time, and treatment conditions (direct or indirect). Significance levels: “4” $p \leq 0.001$; “3” $p \leq 0.01$; “2” $p \leq 0.05$; and “1” $p \leq 0.1$. Adapted from Article A2.

The targeted search for the modifications and their influence on the various biochemical signaling pathways remains an exciting field to be investigated. The open search for modifications at model structures such as known peptides after plasma treatment has been an important tool to screen unknown modifications that CAPs can introduce into proteins. However, this untargeted search could not be expanded in complex biological samples due to long measurement times, reason why in these cases targeted analyses have been performed.

In the future, mass spectrometry will be able to assert itself as the ideal method, since new, faster, and higher-resolution mass spectrometers are constantly being developed. The remaining difficulty will be the correct analysis and interpretation of the obtained data and to do this within a reasonable time period since a wildcard search with a mass range of just 100 Dalton increases the search time approximately 100-fold. The progress of the MS field and connected method must be considered in future also to support a better interpretation of the acquired data, potentially being able to identify isomeric and isobaric structures, and to discriminate the position and the elemental composition of specific functional groups, even when in low amounts. These types of mixed modifications must be considered and accurately defined, due to the complexity of the plasma chemistry, to better optimize and standardize processes and consequences of CAPs, and to finally certify them in clinical applications.

In this context, the present thesis filled a relevant research gap by applying the strategy of carrying out firstly experimental studies on suitable models' solutions of protein structures, which could be transferred to more complex samples. The obtained results, indeed, could be in future used also for the analysis of proteomes after biomedical treatments of patients' skin with plasmas, which could be itself a tool to monitor the progression and the effectiveness after defined treatments in clinical settings.

Of course, there are still several open questions that need to be clarified before then. So far, there is no exact information on how deep the different species can penetrate tissue or cells or up to which layer depth modifications can be detected and thus the impact of plasma.

Various model experiments are already available for this [198-200], but these usually only concern the direct detection of the species and not possible downstream reactions. With the results shown in this thesis it could be shown that plasma-generated reactive species and radiation have not massive effects in dry skin layers, highlighting the importance of the aqueous vehicle to amplifying the gaseous plasma chemistry. However, further studies must be performed to complement these results, as the influence of plasma is often only detectable after days or weeks and thus only long-term changes in the tissue or cell can be detected.

Another important aspect is the influence of the other plasma parameters (for example radiation) on the identified changes (modifications) at proteins and enzymes. The data obtained here provide the basis for the identification of atmospheric plasma-induced oxidative modifications in highly complex samples such as wound samples or whole proteome samples with thousands of proteins per sample. Finally, these results can be helpful for the plasma biomedical community to clarify further the mechanisms of action of CAP. As different conditions have been associated with the production of a specific pattern of reactive species and relative amino acids and protein modifications, these results represent the base to support in future clinicians in the application of specific tuned plasma conditions to achieve desired biological effects. To conclude, part of the gap observed between the knowledge regarding plasma physics/gas chemistry and observed downstream physiological effects of plasmas has been fulfilled with the present work.

4. Summary

This thesis had the stated aim of investigating which oxidative modifications can be found on proteins and peptides after they have been treated with different cold atmospheric plasma conditions, in order to give possible explanations of how these modifications can affect downstream signaling processes. All structural changes induced on two model peptides in solutions were first investigated after treatment with different plasma conditions. Experimental data have been evaluated and compared with existing *in silico* simulations, which are currently the major method applied in the plasma field to study the chemistry in liquids of CAPs (Article A1). In experimental results, plasmas could generate a broad range of modifications at different amino acids, especially different degrees of oxidation, nitration, and nitrosylation.

These results have been complemented with a systematic investigation of ten artificially generated peptide library (Article A2). It could be observed that the general reactivity of an amino acid can be affected by the position or by the neighboring amino acids. Finally, the target chemistry and the amino acids positioning resulted to be relevant aspects influencing plasma-mediated protein oxidation. Cysteine, tyrosine, and tryptophan were the amino acids mostly modified, assuming the potential role in the plasma treated proteome of redox signaling modulators. Additionally, it could be demonstrated that there is unique plasma chemistry in the respective used plasma source and treatment conditions, which can be specifically modulated by different variables (e.g., driven gases, admixture gases, treatment duration, target liquid composition, target chemistry). Therefore, unique modifications, such as carbonylation, chlorination, oxidation, nitration, were detected almost exclusively in certain conditions. The production of specific reactive species cocktails under defined conditions was finally associated with a specific oxidative modification pattern in proteins, potentially leading to controllable biological effects in more complex environment.

The potential of plasmas in inducing oxidative modifications was investigated also in solutions of intact protein (Article A3). PLA₂ was treated with CAPs and examined for oxidative modifications that may explain the reduced activity found after such plasma treatment. It could be shown that one particular amino acid, tryptophan 128, was strongly oxidized, leading to a structural change in the enzyme with reduced functionality.

Therefore, it was shown that the chemical activity of an enzyme could be specifically altered by plasma-induced oxidative modifications, providing an important building block for the elucidation of the mode of action of CAPs on the biological target proteins. In the last part of the work (Articles 4 and 5), the results found so far in model experiments were successfully transferred to real protein samples, respectively analyzing wound exudates and skin proteomes. In particular, modifications identified in model solutions of amino acids were analyzed in the cell proteomes in a targeted manner. Here, it was shown that plasma can induce modifications at defined sites of certain proteins, inducing both nitrosative and oxidative stress in a controllable manner, and inducing downstream pathways modulation. With the studies performed in A5, it has been shown that reactive species mainly influence the modifications of proteins, while plasma radiation play only a minor role, also in dry sample types such skin.

To conclude, specific plasma conditions producing characteristic chemical cocktails have been associated to defined protein modifications, consisting in a further important step for the understanding and controllability of cold atmospheric plasma in medical applications.

5. References

1. Stoffels E, Flikweert AJ, Stoffels WW, Kroesen GMW. Plasma needle: a non-destructive atmospheric plasma source for fine surface treatment of (bio)materials. *Plasma Sources Science & Technology*. 2002;11(4):383-8. doi: 10.1088/0963-0252/11/4/304. PubMed PMID: WOS:000180018500004.
2. Stoffels E, Kieft IE, Sladek REJ. Superficial treatment of mammalian cells using plasma needle. *J Phys D Appl Phys*. 2003;36(23):2908-13. doi: 10.1088/0022-3727/36/23/007. PubMed PMID: WOS:000187842600007.
3. Moreau M, Orange N, Feuilloley MG. Non-thermal plasma technologies: new tools for bio-decontamination. *Biotechnol Adv*. 2008;26(6):610-7. doi: 10.1016/j.biotechadv.2008.08.001. PubMed PMID: 18775485.
4. Fricke K, Tresp H, Bussiahn R, Schroder K, von Woedtke T, Weltmann KD. On the Use of Atmospheric Pressure Plasma for the Bio-Decontamination of Polymers and Its Impact on Their Chemical and Morphological Surface Properties. *Plasma Chemistry and Plasma Processing*. 2012;32(4):801-16. doi: 10.1007/s11090-012-9378-8. PubMed PMID: WOS:000305688700011.
5. Hoffmann C, Berganza C, Zhang J. Cold Atmospheric Plasma: methods of production and application in dentistry and oncology. *Med Gas Res*. 2013;3(1):21. Epub 2013/10/03. doi: 10.1186/2045-9912-3-21. PubMed PMID: 24083477; PubMed Central PMCID: PMC4016545.
6. Jha N, Ryu JJ, Choi EH, Kaushik NK. Generation and Role of Reactive Oxygen and Nitrogen Species Induced by Plasma, Lasers, Chemical Agents, and Other Systems in Dentistry. *Oxid Med Cell Longev*. 2017;2017:7542540. Epub 2017/12/06. doi: 10.1155/2017/7542540. PubMed PMID: 29204250; PubMed Central PMCID: PMC45674515.
7. Bekeschus S, Schmidt A, Weltmann K-D, von Woedtke T. The plasma jet kINPen – A powerful tool for wound healing. *Clinical Plasma Medicine*. 2016;4(1):19-28. doi: 10.1016/j.cpme.2016.01.001.
8. Schmidt A, Bekeschus S, Wende K, Vollmar B, von Woedtke T. A cold plasma jet accelerates wound healing in a murine model of full-thickness skin wounds. *Exp Dermatol*. 2017;26(2):156-62. Epub 2016/08/06. doi: 10.1111/exd.13156. PubMed PMID: 27492871.
9. Arndt S, Unger P, Berneburg M, Bosserhoff AK, Karrer S. Cold atmospheric plasma (CAP) activates angiogenesis-related molecules in skin keratinocytes, fibroblasts and endothelial cells and improves wound angiogenesis in an autocrine and paracrine mode. *J Dermatol Sci*. 2018;89(2):181-90. Epub 2017/12/02. doi: 10.1016/j.jdermsci.2017.11.008. PubMed PMID: 29191392.
10. Schmidt A, Bekeschus S. Redox for Repair: Cold Physical Plasmas and Nrf2 Signaling Promoting Wound Healing. *Antioxidants (Basel)*. 2018;7(10). Epub 2018/10/24. doi: 10.3390/antiox7100146. PubMed PMID: 30347767; PubMed Central PMCID: PMC6210784.
11. Moelleken M, Jockenhofer F, Wiegand C, Buer J, Benson S, Dissemond J. Pilot study on the influence of cold atmospheric plasma on bacterial contamination and healing tendency of chronic wounds. *J Dtsch Dermatol Ges*. 2020. Epub 2020/09/30. doi: 10.1111/ddg.14294. PubMed PMID: 32989866.
12. Stratmann B, Costea TC, Nolte C, Hiller J, Schmidt J, Reindel J, et al. Effect of Cold Atmospheric Plasma Therapy vs Standard Therapy Placebo on Wound Healing in Patients With Diabetic Foot Ulcers: A Randomized Clinical Trial. *JAMA Netw Open*. 2020;3(7):e2010411. Epub 2020/07/17. doi: 10.1001/jamanetworkopen.2020.10411. PubMed PMID: 32672829; PubMed Central PMCID: PMC7366186.
13. Semmler ML, Bekeschus S, Schafer M, Bernhardt T, Fischer T, Witzke K, et al. Molecular Mechanisms of the Efficacy of Cold Atmospheric Pressure Plasma (CAP) in Cancer Treatment. *Cancers (Basel)*. 2020;12(2). Epub 2020/01/26. doi: 10.3390/cancers12020269. PubMed PMID: 31979114.

14. Privat-Maldonado A, Bengtson C, Razzokov J, Smits E, Bogaerts A. Modifying the Tumour Microenvironment: Challenges and Future Perspectives for Anticancer Plasma Treatments. *Cancers*. 2019;11(12):34. doi: 10.3390/cancers11121920. PubMed PMID: WOS:000507382100097.
15. Bruggeman P, Brandenburg R. Atmospheric pressure discharge filaments and microplasmas: physics, chemistry and diagnostics. *J Phys D Appl Phys*. 2013;46(46):464001. doi: Artn 464001 10.1088/0022-3727/46/46/464001. PubMed PMID: WOS:000326956800002.
16. Laroussi M, Akan T. Arc-free atmospheric pressure cold plasma jets: A review. *Plasma Processes and Polymers*. 2007;4(9):777-88. doi: 10.1002/ppap.200700066. PubMed PMID: WOS:000251354100002.
17. Rezaei F, Vanraes P, Nikiforov A, Morent R, De Geyter N. Applications of Plasma-Liquid Systems: A Review. *Materials (Basel)*. 2019;12(17). Epub 2019/08/30. doi: 10.3390/ma12172751. PubMed PMID: 31461960; PubMed Central PMCID: PMC6747786.
18. Metelmann H-R, Seebauer C, Miller V, Fridman A, Bauer G, Graves DB, et al. Clinical experience with cold plasma in the treatment of locally advanced head and neck cancer. *Clinical Plasma Medicine*. 2018;9:6-13. doi: 10.1016/j.cpme.2017.09.001.
19. Metelmann H-R, Nedrelov DS, Seebauer C, Schuster M, von Woedtke T, Weltmann K-D, et al. Head and neck cancer treatment and physical plasma. *Clinical Plasma Medicine*. 2015;3(1):17-23. doi: 10.1016/j.cpme.2015.02.001.
20. Boehm D, Bourke P. Safety implications of plasma-induced effects in living cells - a review of in vitro and in vivo findings. *Biol Chem*. 2018;400(1):3-17. Epub 2018/07/26. doi: 10.1515/hsz-2018-0222. PubMed PMID: 30044756.
21. Bekeschus S, Freund E, Spadola C, Privat-Maldonado A, Hackbarth C, Bogaerts A, et al. Risk Assessment of kINPen Plasma Treatment of Four Human Pancreatic Cancer Cell Lines with Respect to Metastasis. *Cancers (Basel)*. 2019;11(9). Epub 2019/08/28. doi: 10.3390/cancers11091237. PubMed PMID: 31450811; PubMed Central PMCID: PMC6769931.
22. Reuter S, von Woedtke T, Weltmann KD. The kINPen-a review on physics and chemistry of the atmospheric pressure plasma jet and its applications. *J Phys D Appl Phys*. 2018;51(23). doi: 10.1088/1361-6463/aab3ad. PubMed PMID: WOS:000432426400001.
23. Gorbanev Y, Verlackt CCW, Tinck S, Tuenter E, Foubert K, Cos P, et al. Combining experimental and modelling approaches to study the sources of reactive species induced in water by the COST RF plasma jet. *Phys Chem Chem Phys*. 2018;20(4):2797-808. Epub 2018/01/13. doi: 10.1039/c7cp07616a. PubMed PMID: 29323371.
24. Gorbanev Y, Privat-Maldonado A, Bogaerts A. Analysis of Short-Lived Reactive Species in Plasma-Air-Water Systems: The Dos and the Do Nots. *Anal Chem*. 2018;90(22):13151-8. Epub 2018/10/06. doi: 10.1021/acs.analchem.8b03336. PubMed PMID: 30289686.
25. Gaens WV, Iseni S, Schmidt-Bleker A, Weltmann KD, Reuter S, Bogaerts A. Numerical analysis of the effect of nitrogen and oxygen admixtures on the chemistry of an argon plasma jet operating at atmospheric pressure. *New Journal of Physics*. 2015;17(3):033003. doi: 10.1088/1367-2630/17/3/033003.
26. Reuter S, Winter J, Schmidt-Bleker A, Schroeder D, Lange H, Knake N, et al. Atomic oxygen in a cold argon plasma jet: TALIF spectroscopy in ambient air with modelling and measurements of ambient species diffusion. *Plasma Sources Science & Technology*. 2012;21(2):024005. doi: 10.1088/0963-0252/21/2/024005. PubMed PMID: WOS:000302779400008.
27. Reuter S, Winter J, Iseni S, Peters S, Schmidt-Bleker A, Dunnbier M, et al. Detection of ozone in a MHz argon plasma bullet jet. *Plasma Sources Science & Technology*. 2012;21(3):034015. doi: Artn 034015 10.1088/0963-0252/21/3/034015. PubMed PMID: WOS:000304781800018.
28. Iseni S, Zhang S, van Gessel AFH, Hofmann S, van Ham BTJ, Reuter S, et al. Nitric oxide density distributions in the effluent of an RF argon APPJ: effect of gas flow rate and

- substrate. *New Journal of Physics*. 2014;16(12):123011. doi: 10.1088/1367-2630/16/12/123011. PubMed PMID: WOS:000346821400011.
29. Schmidt-Bleker A, Winter J, Bosel A, Reuter S, Weltmann KD. On the plasma chemistry of a cold atmospheric argon plasma jet with shielding gas device. *Plasma Sources Science & Technology*. 2016;25(1):015005. doi: 10.1088/0963-0252/25/1/015005. PubMed PMID: WOS:000370974800012.
 30. Golda J, Held J, Redeker B, Konkowski M, Beijer P, Sobota A, et al. Concepts and characteristics of the 'COST Reference Microplasma Jet'. *Journal of Physics D: Applied Physics*. 2016;49(8):084003. doi: 10.1088/0022-3727/49/8/084003. PubMed PMID: WOS:000369480800006.
 31. Lackmann JW, Wende K, Verlackt C, Golda J, Volzke J, Kogelheide F, et al. Chemical fingerprints of cold physical plasmas - an experimental and computational study using cysteine as tracer compound. *Sci Rep*. 2018;8(1):7736. Epub 2018/05/18. doi: 10.1038/s41598-018-25937-0. PubMed PMID: 29769633; PubMed Central PMCID: PMC5955931.
 32. Graves DB. The emerging role of reactive oxygen and nitrogen species in redox biology and some implications for plasma applications to medicine and biology. *Journal of Physics D: Applied Physics*. 2012;45(26):263001. doi: 10.1088/0022-3727/45/26/263001. PubMed PMID: ISI:000305418900001.
 33. Privat-Maldonado A, Schmidt A, Lin A, Weltmann KD, Wende K, Bogaerts A, et al. ROS from Physical Plasmas: Redox Chemistry for Biomedical Therapy. *Oxid Med Cell Longev*. 2019;2019:9062098. Epub 2019/11/07. doi: 10.1155/2019/9062098. PubMed PMID: 31687089; PubMed Central PMCID: PMC6800937 publication of this paper.
 34. Bruggeman PJ, Kushner MJ, Locke BR, Gardeniers JGE, Graham WG, Graves DB, et al. Plasma-liquid interactions: a review and roadmap. *Plasma Sources Science & Technology*. 2016;25(5):053002. doi: 10.1088/0963-0252/25/5/053002. PubMed PMID: WOS:000384715400001.
 35. Jablonowski H, von Woedtke T. Research on plasma medicine-relevant plasma-liquid interaction: What happened in the past five years? *Clinical Plasma Medicine*. 2015;3(2):42-52. Epub 23.11.2015. doi: 10.1016/j.cpme.2015.11.003.
 36. Wende K, von Woedtke T, Weltmann KD, Bekeschus S. Chemistry and biochemistry of cold physical plasma derived reactive species in liquids. *Biol Chem*. 2018;400(1):19-38. Epub 2018/11/08. doi: 10.1515/hsz-2018-0242. PubMed PMID: 30403650.
 37. Moldgy A, Nayak G, Aboubakr HA, Goyal SM, Bruggeman PJ. Inactivation of virus and bacteria using cold atmospheric pressure air plasmas and the role of reactive nitrogen species. *J Phys D Appl Phys*. 2020;53(43). doi: ARTN 434004 10.1088/1361-6463/aba066. PubMed PMID: WOS:000561590400001.
 38. Shen J, Zhang H, Xu ZM, Zhang ZL, Cheng C, Ni GH, et al. Preferential production of reactive species and bactericidal efficacy of gas-liquid plasma discharge. *Chemical Engineering Journal*. 2019;362:402-12. doi: 10.1016/j.cej.2019.01.018. PubMed PMID: WOS:000457863500042.
 39. Kondeti V, Phan CQ, Wende K, Jablonowski H, Gangal U, Granick JL, et al. Long-lived and short-lived reactive species produced by a cold atmospheric pressure plasma jet for the inactivation of *Pseudomonas aeruginosa* and *Staphylococcus aureus*. *Free Radic Biol Med*. 2018;124:275-87. Epub 2018/06/05. doi: 10.1016/j.freeradbiomed.2018.05.083. PubMed PMID: 29864482.
 40. Morabit Y, Hasan MI, Whalley RD, Robert E, Modic M, Walsh JL. A review of the gas and liquid phase interactions in low-temperature plasma jets used for biomedical applications. *The European Physical Journal D*. 2021;75(1). doi: 10.1140/epjd/s10053-020-00004-4.
 41. Jablonowski H, Schmidt-Bleker A, Weltmann KD, von Woedtke T, Wende K. Non-touching plasma-liquid interaction - where is aqueous nitric oxide generated? *Phys Chem Chem Phys*. 2018;20(39):25387-98. Epub 2018/09/29. doi: 10.1039/c8cp02412j. PubMed PMID: 30264836.

42. Schmidt-Bleker A, Winter J, Iseni S, Dunnbier M, Weltmann KD, Reuter S. Reactive species output of a plasma jet with a shielding gas device-combination of FTIR absorption spectroscopy and gas phase modelling. *J Phys D Appl Phys.* 2014;47(14):145201. doi: Artn 145201 10.1088/0022-3727/47/14/145201. PubMed PMID: WOS:000333332600003.
43. Szili EJ, Gaur N, Hong SH, Kurita H, Oh JS, Ito M, et al. The assessment of cold atmospheric plasma treatment of DNA in synthetic models of tissue fluid, tissue and cells. *J Phys D Appl Phys.* 2017;50(27):274001. doi: ARTN 274001 10.1088/1361-6463/aa7501. PubMed PMID: WOS:000403824400001.
44. Hirst AM, Simms MS, Mann VM, Maitland NJ, O'Connell D, Frame FM. Low-temperature plasma treatment induces DNA damage leading to necrotic cell death in primary prostate epithelial cells. *Br J Cancer.* 2015;112(9):1536-45. Epub 2015/04/04. doi: 10.1038/bjc.2015.113. PubMed PMID: 25839988; PubMed Central PMCID: PMC4454887.
45. Khlyustova A, Labay C, Machala Z, Ginebra MP, Canal C. Important parameters in plasma jets for the production of RONS in liquids for plasma medicine: A brief review. *Frontiers of Chemical Science and Engineering.* 2019;13(2):238-52. doi: 10.1007/s11705-019-1801-8. PubMed PMID: WOS:000468848400003.
46. Weltmann KD, Kindel E, Brandenburg R, Meyer C, Bussiahn R, Wilke C, et al. Atmospheric Pressure Plasma Jet for Medical Therapy: Plasma Parameters and Risk Estimation. *Contrib Plasm Phys.* 2009;49(9):631-40. doi: 10.1002/ctpp.200910067. PubMed PMID: WOS:000272204200004.
47. van Gessel AFH, van Grootel SC, Bruggeman PJ. Atomic oxygen TALIF measurements in an atmospheric-pressure microwave plasma jet within situxenon calibration. *Plasma Sources Sci T.* 2013;22(5). doi: 10.1088/0963-0252/22/5/055010.
48. Verlackt CCW, Van Boxem W, Bogaerts A. Transport and accumulation of plasma generated species in aqueous solution. *Phys Chem Chem Phys.* 2018;20(10):6845-59. Epub 2018/02/21. doi: 10.1039/c7cp07593f. PubMed PMID: 29460930.
49. Van Boxem W, Van der Paal J, Deben C, Verlackt CCW, Smits E, Bogaerts A. Gaining Insight In The Selectivity And Plasma-Liquid Chemistry For Plasma Treatment Of Cancer. *Clinical Plasma Medicine.* 2018;9:30. doi: 10.1016/j.cpme.2017.12.048.
50. Boehm D, Curtin J, Cullen PJ, Bourke P. Hydrogen peroxide and beyond - the potential of high-voltage plasma-activated liquids against cancerous cells. *Anticancer Agents Med Chem.* 2017. Epub 2017/08/02. doi: 10.2174/1871520617666170801110517. PubMed PMID: 28762316.
51. Girard PM, Arbabian A, Fleury M, Bauville G, Puech V, Dutreix M, et al. Synergistic Effect of H₂O₂ and NO₂ in Cell Death Induced by Cold Atmospheric He Plasma. *Sci Rep.* 2016;6:29098. Epub 2016/07/02. doi: 10.1038/srep29098. PubMed PMID: 27364563; PubMed Central PMCID: PMC4929573.
52. Yamazaki I, Piette LH. Epr Spin-Trapping Study on the Oxidizing Species Formed in the Reaction of the Ferrous Ion with Hydrogen-Peroxide. *Journal of the American Chemical Society.* 1991;113(20):7588-93. doi: 10.1021/ja00020a021. PubMed PMID: WOS:A1991GH05800021.
53. Jablonowski H, Santos Sousa J, Weltmann KD, Wende K, Reuter S. Quantification of the ozone and singlet delta oxygen produced in gas and liquid phases by a non-thermal atmospheric plasma with relevance for medical treatment. *Sci Rep.* 2018;8(1):12195. Epub 2018/08/17. doi: 10.1038/s41598-018-30483-w. PubMed PMID: 30111826; PubMed Central PMCID: PMC6093894.
54. Gorbanev Y, O'Connell D, Chechik V. Non-Thermal Plasma in Contact with Water: The Origin of Species. *Chemistry.* 2016;22(10):3496-505. Epub 2016/02/03. doi: 10.1002/chem.201503771. PubMed PMID: 26833560; PubMed Central PMCID: PMC4797710.
55. Breen C, Pal R, Elsegood MRJ, Teat SJ, Iza F, Wende K, et al. Time-resolved luminescence detection of peroxynitrite using a reactivity-based lanthanide probe. *Chemical Science.* 2020;11(12):3164-70. doi: 10.1039/c9sc06053g.

56. Weber D, Davies MJ, Grune T. Determination of protein carbonyls in plasma, cell extracts, tissue homogenates, isolated proteins: Focus on sample preparation and derivatization conditions. *Redox Biol.* 2015;5:367-80. Epub 2015/07/05. doi: 10.1016/j.redox.2015.06.005. PubMed PMID: 26141921; PubMed Central PMCID: PMC4506980.
57. Kehm R, Baldensperger T, Raupbach J, Hohn A. Protein oxidation - Formation mechanisms, detection and relevance as biomarkers in human diseases. *Redox Biol.* 2021:101901. Epub 2021/03/22. doi: 10.1016/j.redox.2021.101901. PubMed PMID: 33744200.
58. Buss H, Chan TP, Sluis KB, Domigan NM, Winterbourn CC. Protein carbonyl measurement by a sensitive ELISA method. *Free Radic Biol Med.* 1997;23(3):361-6. Epub 1997/01/01. doi: 10.1016/s0891-5849(97)00104-4. PubMed PMID: 9214571.
59. Sickmann A, Mreyen M, Meyer HE. Identification of modified proteins by mass spectrometry. *IUBMB Life.* 2002;54(2):51-7. Epub 2002/11/21. doi: 10.1080/15216540214314. PubMed PMID: 12440519.
60. Meng F, Forbes AJ, Miller LM, Kelleher NL. Detection and localization of protein modifications by high resolution tandem mass spectrometry. *Mass Spectrom Rev.* 2005;24(2):126-34. Epub 2004/09/25. doi: 10.1002/mas.20009. PubMed PMID: 15389861.
61. Larsen MR, Trelle MB, Thingholm TE, Jensen ON. Analysis of posttranslational modifications of proteins by tandem mass spectrometry. *Biotechniques.* 2006;40(6):790-8. Epub 2006/06/16. doi: 10.2144/000112201. PubMed PMID: 16774123.
62. Gundry RL, White MY, Murray CI, Kane LA, Fu Q, Stanley BA, et al. Preparation of proteins and peptides for mass spectrometry analysis in a bottom-up proteomics workflow. *Curr Protoc Mol Biol.* 2009;Chapter 10:Unit10 25. Epub 2009/10/10. doi: 10.1002/0471142727.mb1025s88. PubMed PMID: 19816929; PubMed Central PMCID: PMC2905857.
63. Amunugama R, Jones R, Ford M, Allen D. Bottom-Up Mass Spectrometry-Based Proteomics as an Investigative Analytical Tool for Discovery and Quantification of Proteins in Biological Samples. *Adv Wound Care (New Rochelle).* 2013;2(9):549-57. Epub 2014/04/25. doi: 10.1089/wound.2012.0384. PubMed PMID: 24761338; PubMed Central PMCID: PMC3842888.
64. Bolisetty S, Jaimes EA. Mitochondria and reactive oxygen species: physiology and pathophysiology. *Int J Mol Sci.* 2013;14(3):6306-44. Epub 2013/03/27. doi: 10.3390/ijms14036306. PubMed PMID: 23528859; PubMed Central PMCID: PMC3634422.
65. Droese S, Brandt U. Molecular mechanisms of superoxide production by the mitochondrial respiratory chain. *Adv Exp Med Biol.* 2012;748:145-69. Epub 2012/06/26. doi: 10.1007/978-1-4614-3573-0_6. PubMed PMID: 22729857.
66. Maghzal GJ, Krause KH, Stocker R, Jaquet V. Detection of reactive oxygen species derived from the family of NOX NADPH oxidases. *Free Radic Biol Med.* 2012;53(10):1903-18. Epub 2012/09/18. doi: 10.1016/j.freeradbiomed.2012.09.002. PubMed PMID: 22982596.
67. Kalyanaraman B, Hardy M, Zielonka J. A Critical Review of Methodologies to Detect Reactive Oxygen and Nitrogen Species Stimulated by NADPH Oxidase Enzymes: Implications in Pesticide Toxicity. *Current Pharmacology Reports.* 2016;2(4):193-201. doi: 10.1007/s40495-016-0063-0.
68. Schmidt HM, Kelley EE, Straub AC. The impact of xanthine oxidase (XO) on hemolytic diseases. *Redox Biol.* 2019;21:101072. Epub 2018/12/24. doi: 10.1016/j.redox.2018.101072. PubMed PMID: 30580157; PubMed Central PMCID: PMC6305892.
69. Khan AU, Wilson T. Reactive Oxygen Species as Cellular Messengers. *Chemistry & Biology.* 1995;2(7):437-45. doi: 10.1016/1074-5521(95)90259-7. PubMed PMID: WOS:A1995RM82000003.
70. Halliwell B. Free Radicals and Other Reactive Species in Disease. *Encyclopedia of Life Sciences: John Wiley & Sons, Ltd; 2005.*

71. Karve TM, Cheema AK. Small changes huge impact: the role of protein posttranslational modifications in cellular homeostasis and disease. *J Amino Acids*. 2011;2011:207691. Epub 2012/02/09. doi: 10.4061/2011/207691. PubMed PMID: 22312457; PubMed Central PMCID: PMC3268018.
72. Ribet D, Cossart P. Post-translational modifications in host cells during bacterial infection. *FEBS Lett*. 2010;584(13):2748-58. Epub 2010/05/25. doi: 10.1016/j.febslet.2010.05.012. PubMed PMID: 20493189.
73. Burnett G, Kennedy EP. The enzymatic phosphorylation of proteins. *J Biol Chem*. 1954;211(2):969-80. Epub 1954/12/01. doi: 10.1016/s0021-9258(18)71184-8. PubMed PMID: 13221602.
74. Vlastaridis P, Kyriakidou P, Chaliotis A, Van de Peer Y, Oliver SG, Amoutzias GD. Estimating the total number of phosphoproteins and phosphorylation sites in eukaryotic proteomes. *Gigascience*. 2017;6(2):1-11. Epub 2017/03/23. doi: 10.1093/gigascience/giw015. PubMed PMID: 28327990; PubMed Central PMCID: PMC5466708.
75. Tarrant MK, Cole PA. The chemical biology of protein phosphorylation. *Annu Rev Biochem*. 2009;78:797-825. Epub 2009/06/06. doi: 10.1146/annurev.biochem.78.070907.103047. PubMed PMID: 19489734; PubMed Central PMCID: PMC3074175.
76. Sies H, Berndt C, Jones DP. Oxidative Stress. *Annu Rev Biochem*. 2017. doi: 10.1146/annurev-biochem-061516-045037. PubMed PMID: 28441057.
77. Sies H. Oxidative Stress. *Stress: Physiology, Biochemistry, and Pathology* 2019. p. 153-63.
78. Go YM, Jones DP. Redox theory of aging: implications for health and disease. *Clin Sci (Lond)*. 2017;131(14):1669-88. Epub 2017/07/02. doi: 10.1042/CS20160897. PubMed PMID: 28667066; PubMed Central PMCID: PMC5773128.
79. Sies H. Hydrogen peroxide as a central redox signaling molecule in physiological oxidative stress: Oxidative eustress. *Redox Biology*. 2017;11:613-9. doi: 10.1016/j.redox.2016.12.035. PubMed PMID: WOS:000398212000060.
80. Sies H, Jones DP. Reactive oxygen species (ROS) as pleiotropic physiological signalling agents. *Nat Rev Mol Cell Biol*. 2020;21(7):363-83. Epub 2020/04/02. doi: 10.1038/s41580-020-0230-3. PubMed PMID: 32231263.
81. Moldogazieva NT, Mokhosoev IM, Feldman NB, Lutsenko SV. ROS and RNS signalling: adaptive redox switches through oxidative/nitrosative protein modifications. *Free Radic Res*. 2018;52(5):507-43. Epub 2018/03/29. doi: 10.1080/10715762.2018.1457217. PubMed PMID: 29589770.
82. Bonizzi G, Karin M. The two NF-kappaB activation pathways and their role in innate and adaptive immunity. *Trends Immunol*. 2004;25(6):280-8. Epub 2004/05/18. doi: 10.1016/j.it.2004.03.008. PubMed PMID: 15145317.
83. Morgan MJ, Liu ZG. Crosstalk of reactive oxygen species and NF-kappaB signaling. *Cell Res*. 2011;21(1):103-15. Epub 2010/12/29. doi: 10.1038/cr.2010.178. PubMed PMID: 21187859; PubMed Central PMCID: PMC3193400.
84. Zhang J, Wang X, Vikash V, Ye Q, Wu D, Liu Y, et al. ROS and ROS-Mediated Cellular Signaling. *Oxid Med Cell Longev*. 2016;2016:4350965. Epub 2016/03/22. doi: 10.1155/2016/4350965. PubMed PMID: 26998193; PubMed Central PMCID: PMC4779832.
85. Truong TH, Carroll KS. Redox regulation of protein kinases. *Crit Rev Biochem Mol Biol*. 2013;48(4):332-56. Epub 2013/05/04. doi: 10.3109/10409238.2013.790873. PubMed PMID: 23639002; PubMed Central PMCID: PMC34358782.
86. Sies H. Findings in redox biology: From H₂O₂ to oxidative stress. *J Biol Chem*. 2020;295(39):13458-73. Epub 2020/09/27. doi: 10.1074/jbc.X120.015651. PubMed PMID: 32978328; PubMed Central PMCID: PMC7521638.
87. Jones DP, Eklöw L, Thor H, Orrenius S. Metabolism of Hydrogen Peroxide in Isolated Hepatocytes: Relative Contributions of Catalase and Glutathione Peroxidase in

- Decomposition of Endogenously Generated H₂O₂. *Arch Biochem Biophys.* 1981;210(2):505-16.
88. McCord JM, Fridovich I. The reduction of cytochrome c by milk xanthine oxidase. *J Biol Chem.* 1968;243(21):5753-60. Epub 1968/11/10. doi: 10.1016/s0021-9258(18)91929-0. PubMed PMID: 4972775.
 89. Rhee SG. Cell signaling. H₂O₂, a necessary evil for cell signaling. *Science.* 2006;312(5782):1882-3. Epub 2006/07/01. doi: 10.1126/science.1130481. PubMed PMID: 16809515.
 90. Rhee SG, Kang SW, Jeong W, Chang TS, Yang KS, Woo HA. Intracellular messenger function of hydrogen peroxide and its regulation by peroxiredoxins. *Curr Opin Cell Biol.* 2005;17(2):183-9. Epub 2005/03/23. doi: 10.1016/j.ceb.2005.02.004. PubMed PMID: 15780595.
 91. Niethammer P, Grabher C, Look AT, Mitchison TJ. A tissue-scale gradient of hydrogen peroxide mediates rapid wound detection in zebrafish. *Nature.* 2009;459(7249):996-9. doi: 10.1038/nature08119. PubMed PMID: 19494811; PubMed Central PMCID: PMCPMC2803098.
 92. D'Autreaux B, Toledano MB. ROS as signalling molecules: mechanisms that generate specificity in ROS homeostasis. *Nat Rev Mol Cell Bio.* 2007;8(10):813-24. doi: 10.1038/Nrm2256. PubMed PMID: ISI:000249642900014.
 93. Garcia-Santamarina S, Boronat S, Hidalgo E. Reversible cysteine oxidation in hydrogen peroxide sensing and signal transduction. *Biochemistry.* 2014;53(16):2560-80. Epub 2014/04/18. doi: 10.1021/bi401700f. PubMed PMID: 24738931.
 94. Le Moan N, Clement G, Le Maout S, Tacnet F, Toledano MB. The *Saccharomyces cerevisiae* proteome of oxidized protein thiols: contrasted functions for the thioredoxin and glutathione pathways. *J Biol Chem.* 2006;281(15):10420-30. Epub 2006/01/19. doi: 10.1074/jbc.M513346200. PubMed PMID: 16418165.
 95. Go YM, Jones DP. The redox proteome. *J Biol Chem.* 2013;288(37):26512-20. Epub 2013/07/19. doi: 10.1074/jbc.R113.464131. PubMed PMID: 23861437; PubMed Central PMCID: PMCPMC3772199.
 96. Paulsen CE, Carroll KS. Cysteine-mediated redox signaling: chemistry, biology, and tools for discovery. *Chem Rev.* 2013;113(7):4633-79. Epub 2013/03/22. doi: 10.1021/cr300163e. PubMed PMID: 23514336; PubMed Central PMCID: PMCPMC4303468.
 97. Abaffy P, Tomankova S, Naraine R, Kubista M, Sindelka R. The role of nitric oxide during embryonic wound healing. *BMC Genomics.* 2019;20(1):815. Epub 2019/11/07. doi: 10.1186/s12864-019-6147-6. PubMed PMID: 31694542; PubMed Central PMCID: PMCPMC6836512.
 98. Kovacs I, Lindermayr C. Nitric oxide-based protein modification: formation and site-specificity of protein S-nitrosylation. *Front Plant Sci.* 2013;4(137):137. Epub 2013/05/30. doi: 10.3389/fpls.2013.00137. PubMed PMID: 23717319; PubMed Central PMCID: PMCPMC3653056.
 99. Moller MN, Rios N, Trujillo M, Radi R, Denicola A, Alvarez B. Detection and quantification of nitric oxide-derived oxidants in biological systems. *J Biol Chem.* 2019;294(40):14776-802. Epub 2019/08/15. doi: 10.1074/jbc.REV119.006136. PubMed PMID: 31409645; PubMed Central PMCID: PMCPMC6779446.
 100. Alvarez B, Radi R. Peroxynitrite reactivity with amino acids and proteins. *Amino Acids.* 2003;25(3-4):295-311. Epub 2003/12/09. doi: 10.1007/s00726-003-0018-8. PubMed PMID: 14661092.
 101. Thannickal VJ, Fanburg BL. Reactive oxygen species in cell signaling. *Am J Physiol Lung Cell Mol Physiol.* 2000;279(6):L1005-28. Epub 2000/11/15. doi: 10.1152/ajplung.2000.279.6.L1005. PubMed PMID: 11076791.
 102. Hawkins CL, Davies MJ. Reaction of HOCl with amino acids and peptides: EPR evidence for rapid rearrangement and fragmentation reactions of nitrogen-centred radicals. *Journal of the Chemical Society, Perkin Transactions 2.* 1998;(9):1937-46. doi: 10.1039/a802949k.

103. Kotiaho T, Eberlin MN, Vainiotalo P, Kostianen R. Electrospray mass and tandem mass spectrometry identification of ozone oxidation products of amino acids and small peptides. *J Am Soc Mass Spectrom.* 2000;11(6):526-35. Epub 2000/06/01. doi: 10.1016/s1044-0305(00)00116-1. PubMed PMID: 10833026.
104. Hawkins CL, Davies MJ. Detection, identification, and quantification of oxidative protein modifications. *J Biol Chem.* 2019;294(51):19683-708. Epub 2019/11/02. doi: 10.1074/jbc.REV119.006217. PubMed PMID: 31672919; PubMed Central PMCID: PMC6926449.
105. Cai Z, Yan LJ. Protein Oxidative Modifications: Beneficial Roles in Disease and Health. *J Biochem Pharmacol Res.* 2013;1(1):15-26. Epub 2013/05/11. PubMed PMID: 23662248; PubMed Central PMCID: PMC6926449.
106. Quintero-Fabian S, Arreola R, Becerril-Villanueva E, Torres-Romero JC, Arana-Argaez V, Lara-Riegos J, et al. Role of Matrix Metalloproteinases in Angiogenesis and Cancer. *Front Oncol.* 2019;9:1370. Epub 2020/01/11. doi: 10.3389/fonc.2019.01370. PubMed PMID: 31921634; PubMed Central PMCID: PMC6915110.
107. Yang B, Chen Y, Shi J. Reactive Oxygen Species (ROS)-Based Nanomedicine. *Chem Rev.* 2019;119(8):4881-985. Epub 2019/04/12. doi: 10.1021/acs.chemrev.8b00626. PubMed PMID: 30973011.
108. Bekeschus S, Brüggemeier J, Hackbarth C, von Woedtke T, Partecke L-I, van der Linde J. Platelets are key in cold physical plasma-facilitated blood coagulation in mice. *Clinical Plasma Medicine.* 2017;7-8(Supplement C):58-65. doi: 10.1016/j.cpme.2017.10.001.
109. Virard F, Cousty S, Cambus JP, Valentin A, Kemoun P, Clement F. Cold Atmospheric Plasma Induces a Predominantly Necrotic Cell Death via the Microenvironment. *PLoS One.* 2015;10(8):e0133120. Epub 2015/08/15. doi: 10.1371/journal.pone.0133120. PubMed PMID: 26275141; PubMed Central PMCID: PMC4537210.
110. Dubuc A, Monsarrat P, Virard F, Merbahi N, Sarrette J-P, Laurencin-Dalieux S, et al. Use of cold-atmospheric plasma in oncology: a concise systematic review. *Therapeutic Advances in Medical Oncology.* 2018;10:1758835918786475. doi: 10.1177/1758835918786475. PubMed PMID: 30046358.
111. Matthes R, Hubner NO, Bender C, Koban I, Horn S, Bekeschus S, et al. Efficacy of different carrier gases for barrier discharge plasma generation compared to chlorhexidine on the survival of *Pseudomonas aeruginosa* embedded in biofilm in vitro. *Skin pharmacology and physiology.* 2014;27(3):148-57. Epub 2014/01/18. doi: 10.1159/000353861. PubMed PMID: 24434726.
112. Bekeschus S, Moritz J, Helfrich I, Boeckmann L, Weltmann K-D, Emmert S, et al. Ex Vivo Exposure of Human Melanoma Tissue to Cold Physical Plasma Elicits Apoptosis and Modulates Inflammation. *Applied Sciences.* 2020;10(6):1971. PubMed PMID: doi:10.3390/app10061971.
113. Bauer G, Sersenová D, Graves DB, Machala Z. Cold Atmospheric Plasma and Plasma-Activated Medium Trigger RONS-Based Tumor Cell Apoptosis. *Scientific Reports.* 2019;9(1):14210. doi: 10.1038/s41598-019-50291-0.
114. Liedtke KR, Bekeschus S, Kaeding A, Hackbarth C, Kuehn JP, Heidecke CD, et al. Non-thermal plasma-treated solution demonstrates antitumor activity against pancreatic cancer cells in vitro and in vivo. *Sci Rep.* 2017;7(1):8319. Epub 2017/08/18. doi: 10.1038/s41598-017-08560-3. PubMed PMID: 28814809; PubMed Central PMCID: PMC6926449.
115. Bekeschus S, Lippert M, Diepold K, Chiosis G, Seufferlein T, Azoitei N. Physical plasma-triggered ROS induces tumor cell death upon cleavage of HSP90 chaperone. *Sci Rep.* 2019;9(1):4112. Epub 2019/03/13. doi: 10.1038/s41598-019-38580-0. PubMed PMID: 30858416; PubMed Central PMCID: PMC6926449.
116. Schmidt A, von Woedtke T, Vollmar B, Hasse S, Bekeschus S. Nrf2 signaling and inflammation are key events in physical plasma-spurred wound healing. *Theranostics.* 2019;9(4):1066-84. Epub 2019/03/15. doi: 10.7150/thno.29754. PubMed PMID: 30867816; PubMed Central PMCID: PMC6926449.

117. Suzuki K, Matsubara H. Recent advances in p53 research and cancer treatment. *J Biomed Biotechnol.* 2011;2011:978312. Epub 2011/07/19. doi: 10.1155/2011/978312. PubMed PMID: 21765642; PubMed Central PMCID: PMC3134396.
118. Schmidt A, Bekeschus S, Jarick K, Hasse S, von Woedtke T, Wende K. Cold Physical Plasma Modulates p53 and Mitogen-Activated Protein Kinase Signaling in Keratinocytes. *Oxid Med Cell Longev.* 2019;2019:7017363. Epub 2019/02/09. doi: 10.1155/2019/7017363. PubMed PMID: 30733851; PubMed Central PMCID: PMC6348845.
119. Ma Y, Ha CS, Hwang SW, Lee HJ, Kim GC, Lee KW, et al. Non-thermal atmospheric pressure plasma preferentially induces apoptosis in p53-mutated cancer cells by activating ROS stress-response pathways. *PLoS One.* 2014;9(4):e91947. doi: 10.1371/journal.pone.0091947. PubMed PMID: 24759730; PubMed Central PMCID: PMC3997341.
120. Lackmann JW, Baldus S, Steinborn E, Edengeiser E, Kogelheide F, Langklotz S, et al. A dielectric barrier discharge terminally inactivates RNase A by oxidizing sulfur-containing amino acids and breaking structural disulfide bonds. *J Phys D Appl Phys.* 2015;48(49). doi: Artn 494003 10.1088/0022-3727/48/49/494003. PubMed PMID: WOS:000368442600003.
121. Lackmann J-W, Edengeiser E, Schneider S, Benedikt J, Havenith M, Bandow JE. Effects of the Effluent of a Microscale Atmospheric Pressure Plasma-jet Operated with He/O₂ Gas on Bovine Serum Albumin. *Plasma Medicine.* 2013;3(1-2):115-24. doi: 10.1615/PlasmaMed.2014008858.
122. Lackmann JW, Bandow JE. Inactivation of microbes and macromolecules by atmospheric-pressure plasma jets. *Appl Microbiol Biotechnol.* 2014;98(14):6205-13. Epub 2014/05/21. doi: 10.1007/s00253-014-5781-9. PubMed PMID: 24841116.
123. Striesow J, Lackmann JW, Ni Z, Wenske S, Weltmann KD, Fedorova M, et al. Oxidative modification of skin lipids by cold atmospheric plasma (CAP): A standardizable approach using RP-LC/MS(2) and DI-ESI/MS(2). *Chem Phys Lipids.* 2020;226:104786. Epub 2019/06/24. doi: 10.1016/j.chemphyslip.2019.104786. PubMed PMID: 31229410.
124. Clemen R, Bekeschus S. Oxidatively Modified Proteins: Cause and Control of Diseases. *Applied Sciences.* 2020;10(18). doi: 10.3390/app10186419.
125. Michaeli A, Feitelson J. Reactivity of singlet oxygen toward amino acids and peptides. *Photochem Photobiol.* 1994;59(3):284-9. doi: 10.1111/j.1751-1097.1994.tb05035.x. PubMed PMID: 8016206.
126. Takai E, Kitamura T, Kuwabara J, Ikawa S, Yoshizawa S, Shiraki K, et al. Chemical modification of amino acids by atmospheric-pressure cold plasma in aqueous solution. *J Phys D Appl Phys.* 2014;47(28):285403. doi: 10.1088/0022-3727/47/28/285403. PubMed PMID: WOS:000338721900012.
127. Berger MT, Hemmler D, Walker A, Rychlik M, Marshall JW, Schmitt-Kopplin P. Molecular characterization of sequence-driven peptide glycation. *Sci Rep.* 2021;11(1):13294. Epub 2021/06/26. doi: 10.1038/s41598-021-92413-7. PubMed PMID: 34168180; PubMed Central PMCID: PMC8225897.
128. Zhou R, Zhou R, Zhuang J, Zong Z, Zhang X, Liu D, et al. Interaction of Atmospheric-Pressure Air Microplasmas with Amino Acids as Fundamental Processes in Aqueous Solution. *PLoS One.* 2016;11(5):e0155584. doi: 10.1371/journal.pone.0155584. PubMed PMID: 27183129; PubMed Central PMCID: PMC4868320.
129. Leinisch F, Mariotti M, Hagglund P, Davies MJ. Structural and functional changes in RNase A originating from tyrosine and histidine cross-linking and oxidation induced by singlet oxygen and peroxy radicals. *Free Radic Biol Med.* 2018;126:73-86. Epub 2018/07/22. doi: 10.1016/j.freeradbiomed.2018.07.008. PubMed PMID: 30031072.
130. Ferrer-Sueta G, Campolo N, Trujillo M, Bartesaghi S, Carballal S, Romero N, et al. Biochemistry of Peroxynitrite and Protein Tyrosine Nitration. *Chem Rev.* 2018;118(3):1338-408. Epub 2018/02/06. doi: 10.1021/acs.chemrev.7b00568. PubMed PMID: 29400454.
131. Radi R. Protein tyrosine nitration: biochemical mechanisms and structural basis of functional effects. *Acc Chem Res.* 2013;46(2):550-9. Epub 2012/11/20. doi:

- 10.1021/ar300234c. PubMed PMID: 23157446; PubMed Central PMCID: PMCPMC3577981.
132. Ehrenshaft M, Deterding LJ, Mason RP. Tripping up Trp: Modification of protein tryptophan residues by reactive oxygen species, modes of detection, and biological consequences. *Free Radic Biol Med.* 2015;89:220-8. Epub 2015/09/24. doi: 10.1016/j.freeradbiomed.2015.08.003. PubMed PMID: 26393422; PubMed Central PMCID: PMCPMC4684788.
133. Triquigneaux MM, Ehrenshaft M, Roth E, Silman I, Ashani Y, Mason RP, et al. Targeted oxidation of Torpedo californica acetylcholinesterase by singlet oxygen: identification of N-formylkynurenine tryptophan derivatives within the active-site gorge of its complex with the photosensitizer methylene blue. *Biochem J.* 2012;448(1):83-91. Epub 2012/08/15. doi: 10.1042/bj20120992. PubMed PMID: 22888904; PubMed Central PMCID: PMCPMC3613852.
134. Semenza GL. Hydroxylation of HIF-1: Oxygen sensing at the molecular level. *Physiology.* 2004;19(4):176-82. doi: 10.1152/physiol.00001.2004. PubMed PMID: WOS:000224298700002.
135. Metzzen E, Ratcliffe PJ. HIF hydroxylation and cellular oxygen sensing. *Biol Chem.* 2004;385(3-4):223-30. Epub 2004/05/12. doi: 10.1515/bc.2004.016. PubMed PMID: 15134335.
136. Beckman JS. Oxidative damage and tyrosine nitration from peroxynitrite. *Chem Res Toxicol.* 1996;9(5):836-44. Epub 1996/07/01. doi: 10.1021/tx9501445. PubMed PMID: 8828918.
137. Ramezani MS, Padmaja S, Koppenol WH. Nitration and hydroxylation of phenolic compounds by peroxynitrite. *Chem Res Toxicol.* 1996;9(1):232-40. Epub 1996/01/01. doi: 10.1021/tx950135w. PubMed PMID: 8924596.
138. Ischiropoulos H. Biological selectivity and functional aspects of protein tyrosine nitration. *Biochem Biophys Res Commun.* 2003;305(3):776-83. Epub 2003/05/24. doi: 10.1016/s0006-291x(03)00814-3. PubMed PMID: 12763060.
139. Rubbo H, Radi R. Protein and lipid nitration: role in redox signaling and injury. *Biochim Biophys Acta.* 2008;1780(11):1318-24. Epub 2008/04/09. doi: 10.1016/j.bbagen.2008.03.007. PubMed PMID: 18395525.
140. Bandoowala M, Sengupta P. 3-Nitrotyrosine: a versatile oxidative stress biomarker for major neurodegenerative diseases. *Int J Neurosci.* 2020;130(10):1047-62. Epub 2020/01/09. doi: 10.1080/00207454.2020.1713776. PubMed PMID: 31914343.
141. Thomson L. 3-nitrotyrosine modified proteins in atherosclerosis. *Dis Markers.* 2015;2015:708282. Epub 2015/03/31. doi: 10.1155/2015/708282. PubMed PMID: 25814781; PubMed Central PMCID: PMCPMC4359869.
142. Khan F, Siddiqui AA, Ali R. Measurement and significance of 3-nitrotyrosine in systemic lupus erythematosus. *Scand J Immunol.* 2006;64(5):507-14. Epub 2006/10/13. doi: 10.1111/j.1365-3083.2006.01794.x. PubMed PMID: 17032243.
143. Dekker F, Abello N, Wisastra R, Bischoff R. Enrichment and detection of tyrosine-nitrated proteins. *Curr Protoc Protein Sci.* 2012;Chapter 14:Unit 14 3. Epub 2012/08/02. doi: 10.1002/0471140864.ps1413s69. PubMed PMID: 22851496.
144. Webster RP, Roberts VH, Myatt L. Protein nitration in placenta - functional significance. *Placenta.* 2008;29(12):985-94. Epub 2008/10/15. doi: 10.1016/j.placenta.2008.09.003. PubMed PMID: 18851882; PubMed Central PMCID: PMCPMC2630542.
145. Moller IM, Rogowska-Wrzesinska A, Rao RS. Protein carbonylation and metal-catalyzed protein oxidation in a cellular perspective. *J Proteomics.* 2011;74(11):2228-42. Epub 2011/05/24. doi: 10.1016/j.jprot.2011.05.004. PubMed PMID: 21601020.
146. Wong CM, Bansal G, Marcocci L, Suzuki YJ. Proposed role of primary protein carbonylation in cell signaling. *Redox Rep.* 2012;17(2):90-4. Epub 2012/05/09. doi: 10.1179/1351000212y.0000000007. PubMed PMID: 22564352; PubMed Central PMCID: PMCPMC4157310.

147. Serviddio G, Di Venosa N, Federici A, D'Agostino D, Rollo T, Prigigallo F, et al. Brief hypoxia before normoxic reperfusion (postconditioning) protects the heart against ischemia-reperfusion injury by preventing mitochondria peroxyde production and glutathione depletion. *Faseb J.* 2005;19(3):354-61. Epub 2005/03/05. doi: 10.1096/fj.04-2338com. PubMed PMID: 15746178.
148. Audagnotto M, Dal Peraro M. Protein post-translational modifications: In silico prediction tools and molecular modeling. *Comput Struct Biotechnol J.* 2017;15:307-19. Epub 2017/05/02. doi: 10.1016/j.csbj.2017.03.004. PubMed PMID: 28458782; PubMed Central PMCID: PMC5397102.
149. Bruno G, Heusler T, Lackmann J-W, von Woedtke T, Weltmann K-D, Wende K. Cold physical plasma-induced oxidation of cysteine yields reactive sulfur species (RSS). *Clinical Plasma Medicine.* 2019;14:100083. doi: 10.1016/j.cpme.2019.100083.
150. Yang J, Carroll KS, Liebler DC. The Expanding Landscape of the Thiol Redox Proteome. *Mol Cell Proteomics.* 2016;15(1):1-11. Epub 2015/11/01. doi: 10.1074/mcp.O115.056051. PubMed PMID: 26518762; PubMed Central PMCID: PMC4762510.
151. Mitchell AR, Yuan M, Morgan HP, McNae IW, Blackburn EA, Le Bihan T, et al. Redox regulation of pyruvate kinase M2 by cysteine oxidation and S-nitrosation. *Biochem J.* 2018;475(20):3275-91. Epub 2018/09/27. doi: 10.1042/bcj20180556. PubMed PMID: 30254098; PubMed Central PMCID: PMC6208296.
152. Forman HJ, Davies MJ, Kramer AC, Miotto G, Zaccarin M, Zhang H, et al. Protein cysteine oxidation in redox signaling: Caveats on sulfenic acid detection and quantification. *Arch Biochem Biophys.* 2017;617:26-37. Epub 2016/10/04. doi: 10.1016/j.abb.2016.09.013. PubMed PMID: 27693037; PubMed Central PMCID: PMC5318241.
153. Wende K, Bruno G, Lalk M, Weltmann K-D, von Woedtke T, Bekeschus S, et al. On a heavy path – determining cold plasma-derived short-lived species chemistry using isotopic labelling. *Rsc Adv.* 2020;10(20):11598-607. doi: 10.1039/c9ra08745a.
154. Aebersold R, Mann M. Mass spectrometry-based proteomics. *Nature.* 2003;422:198-207. doi: 10.1038/nature01511.
155. Meissner F, Mann M. Quantitative shotgun proteomics: considerations for a high-quality workflow in immunology. *Nat Immunol.* 2014;15(2):112-7. Epub 2014/01/23. doi: 10.1038/ni.2781. PubMed PMID: 24448568.
156. Lindemann C, Thomanek N, Hundt F, Lerari T, Meyer HE, Wolters D, et al. Strategies in relative and absolute quantitative mass spectrometry based proteomics. *Biol Chem.* 2017;398(5-6):687-99. Epub 2017/03/11. doi: 10.1515/hsz-2017-0104. PubMed PMID: 28282288.
157. Ong SE, Mann M. A practical recipe for stable isotope labeling by amino acids in cell culture (SILAC). *Nat Protoc.* 2006;1(6):2650-60. doi: 10.1038/nprot.2006.427. PubMed PMID: 17406521.
158. Nahnsen S, Bielow C, Reinert K, Kohlbacher O. Tools for label-free peptide quantification. *Mol Cell Proteomics.* 2013;12(3):549-56. Epub 2012/12/20. doi: 10.1074/mcp.R112.025163. PubMed PMID: 23250051; PubMed Central PMCID: PMC3591650.
159. Abello N, Barroso B, Kerstjens HA, Postma DS, Bischoff R. Chemical labeling and enrichment of nitrotyrosine-containing peptides. *Talanta.* 2010;80(4):1503-12. Epub 2010/01/20. doi: 10.1016/j.talanta.2009.02.002. PubMed PMID: 20082808.
160. Chang YC, Huang CN, Lin CH, Chang HC, Wu CC. Mapping protein cysteine sulfonic acid modifications with specific enrichment and mass spectrometry: an integrated approach to explore the cysteine oxidation. *Proteomics.* 2010;10(16):2961-71. Epub 2010/07/16. doi: 10.1002/pmic.200900850. PubMed PMID: 20629170.
161. Orsburn BC. Proteome Discoverer-A Community Enhanced Data Processing Suite for Protein Informatics. *Proteomes.* 2021;9(1). Epub 2021/04/04. doi: 10.3390/proteomes9010015. PubMed PMID: 33806881; PubMed Central PMCID: PMC8006021.

162. Bern M, Kil YJ, Becker C. Bionic: advanced peptide and protein identification software. *Curr Protoc Bioinformatics*. 2012;Chapter 13:Unit13 20. Epub 2012/12/21. doi: 10.1002/0471250953.bi1320s40. PubMed PMID: 23255153; PubMed Central PMCID: PMC3545648.
163. Pagel O, Loroach S, Sickmann A, Zahedi RP. Current strategies and findings in clinically relevant post-translational modification-specific proteomics. *Expert Rev Proteomics*. 2015;12(3):235-53. Epub 2015/05/09. doi: 10.1586/14789450.2015.1042867. PubMed PMID: 25955281; PubMed Central PMCID: PMC354487610.
164. Bernhardt T, Semmler ML, Schafer M, Bekeschus S, Emmert S, Boeckmann L. Plasma Medicine: Applications of Cold Atmospheric Pressure Plasma in Dermatology. *Oxid Med Cell Longev*. 2019;2019:3873928. Epub 2019/10/01. doi: 10.1155/2019/3873928. PubMed PMID: 31565150; PubMed Central PMCID: PMC6745145 publication of this paper.
165. von Woedtke T, Schmidt A, Bekeschus S, Wende K, Weltmann KD. Plasma Medicine: A Field of Applied Redox Biology. In vivo (Athens, Greece). 2019;33(4):1011-26. Epub 2019/07/08. doi: 10.21873/in vivo.11570. PubMed PMID: 31280189; PubMed Central PMCID: PMC6689367.
166. Lackmann JW, Bruno G, Jablonowski H, Kogelheide F, Offerhaus B, Held J, et al. Nitrosylation vs. oxidation - How to modulate cold physical plasmas for biological applications. *PLoS One*. 2019;14(5):e0216606. Epub 2019/05/09. doi: 10.1371/journal.pone.0216606. PubMed PMID: 31067274; PubMed Central PMCID: PMC6505927.
167. Privat-Maldonado A, O'Connell D, Welch E, Vann R, van der Woude MW. Spatial Dependence of DNA Damage in Bacteria due to Low-Temperature Plasma Application as Assessed at the Single Cell Level. *Sci Rep*. 2016;6:35646. doi: 10.1038/srep35646. PubMed PMID: 27759098; PubMed Central PMCID: PMC5069486.
168. Verlackt CCW, Van Boxem W, Dewaele D, Lemiere F, Sobott F, Benedikt J, et al. Mechanisms of Peptide Oxidation by Hydroxyl Radicals: Insight at the Molecular Scale. *J Phys Chem C*. 2017;121(10):5787-99. doi: 10.1021/acs.jpcc.6b12278. PubMed PMID: WOS:000396969900037.
169. Jablonowski H, Bussiahn R, Hammer MU, Weltmann KD, von Woedtke T, Reuter S. Impact of plasma jet vacuum ultraviolet radiation on reactive oxygen species generation in bio-relevant liquids. *Physics of Plasmas*. 2015;22(12):122008. doi: Artn 122008 10.1063/1.4934989. PubMed PMID: WOS:000367460400010.
170. Azrague K, Bonnefille E, Pradines V, Pimienta V, Oliveros E, Maurette MT, et al. Hydrogen peroxide evolution during V-UV photolysis of water. *Photochem Photobiol Sci*. 2005;4(5):406-8. Epub 2005/05/06. doi: 10.1039/b500162e. PubMed PMID: 15875072.
171. Hansen L, Schmidt-Bleker A, Bansemer R, Kersten H, Weltmann K-D, Reuter S. Influence of a liquid surface on the NO_x production of a cold atmospheric pressure plasma jet. *Journal of Physics D: Applied Physics*. 2018;51(47):474002. doi: 10.1088/1361-6463/aad6f0.
172. Koppenol WH, Moreno JJ, Pryor WA, Ischiropoulos H, Beckman JS. Peroxynitrite, a cloaked oxidant formed by nitric oxide and superoxide. *Chem Res Toxicol*. 1992;5(6):834-42. Epub 1992/11/01. doi: 10.1021/tx00030a017. PubMed PMID: 1336991.
173. Egli CM, Stravs MA, Janssen EML. Inactivation and Site-specific Oxidation of Aquatic Extracellular Bacterial Leucine Aminopeptidase by Singlet Oxygen. *Environ Sci Technol*. 2020;54(22):14403-12. Epub 2020/11/05. doi: 10.1021/acs.est.0c04696. PubMed PMID: 33146524.
174. Di Mascio P, Martinez GR, Miyamoto S, Ronsein GE, Medeiros MHG, Cadet J. Singlet Molecular Oxygen Reactions with Nucleic Acids, Lipids, and Proteins. *Chem Rev*. 2019;119(3):2043-86. Epub 2019/02/06. doi: 10.1021/acs.chemrev.8b00554. PubMed PMID: 30721030.
175. Waskoenig J, Niemi K, Knake N, Graham LM, Reuter S, Schulz-von der Gathen V, et al. Atomic oxygen formation in a radio-frequency driven micro-atmospheric pressure plasma jet. *Plasma Sources Science & Technology*. 2010;19(4):045018. doi: Artn 045018 Doi 10.1088/0963-0252/19/4/045018. PubMed PMID: ISI:000280407300019.

176. Sgonina K, Bruno G, Wyprich S, Wende K, Benedikt J. Reactions of plasma-generated atomic oxygen at the surface of aqueous phenol solution: Experimental and modeling study. *J Appl Phys.* 2021;130(4):043303. doi: 10.1063/5.0049809.
177. Myers B, Barnat E, Stapelmann K. Atomic oxygen density determination in the effluent of the COST reference source using in situ effective lifetime measurements in the presence of a liquid interface. *Journal of Physics D: Applied Physics.* 2021;54(45). doi: 10.1088/1361-6463/ac1cb5.
178. Xu H, Chen C, Liu DX, Wang WT, Xia WJ, Liu ZJ, et al. The effect of gas additives on reactive species and bacterial inactivation by a helium plasma jet. *Plasma Sci Technol.* 2019;21(11):115502. doi: UNSP 115502 10.1088/2058-6272/ab3938. PubMed PMID: WOS:000484751000001.
179. Terefinko D, Dzimitrowicz A, Bielawska-Pohl A, Klimczak A, Pohl P, Jamroz P. The Influence of Cold Atmospheric Pressure Plasma-Treated Media on the Cell Viability, Motility, and Induction of Apoptosis in Human Non-Metastatic (MCF7) and Metastatic (MDA-MB-231) Breast Cancer Cell Lines. *Int J Mol Sci.* 2021;22(8). Epub 2021/05/01. doi: 10.3390/ijms22083855. PubMed PMID: 33917790; PubMed Central PMCID: PMC8068204.
180. Shome D, von Woedtke T, Riedel K, Masur K. The HIPPO Transducer YAP and Its Targets CTGF and Cyr61 Drive a Paracrine Signalling in Cold Atmospheric Plasma-Mediated Wound Healing. *Oxid Med Cell Longev.* 2020;2020:4910280. Epub 2020/02/28. doi: 10.1155/2020/4910280. PubMed PMID: 32104533; PubMed Central PMCID: PMC7040405 paper.
181. Knake N, Reuter S, Niemi K, Schulz-von der Gathen V, Winter J. Absolute atomic oxygen density distributions in the effluent of a microscale atmospheric pressure plasma jet. *J Phys D Appl Phys.* 2008;41(19):6. doi: 10.1088/0022-3727/41/19/194006. PubMed PMID: WOS:000259441800013.
182. Wende K, Williams P, Dalluge J, Gaens WV, Aboubakr H, Bischof J, et al. Identification of the biologically active liquid chemistry induced by a nonthermal atmospheric pressure plasma jet. *Biointerphases.* 2015;10(2):029518. Epub 2015/05/08. doi: 10.1116/1.4919710. PubMed PMID: 25947392.
183. Zielonka J, Sikora A, Joseph J, Kalyanaraman B. Peroxynitrite Is the Major Species Formed from Different Flux Ratios of Co-generated Nitric Oxide and Superoxide DIRECT REACTION WITH BORONATE-BASED FLUORESCENT PROBE. *Journal of Biological Chemistry.* 2010;285(19):14210-6. doi: 10.1074/jbc.M110.110080. PubMed PMID: WOS:000277299700017.
184. Koppenol WH, Bounds PL, Nauser T, Kissner R, Ruegger H. Peroxynitrous acid: controversy and consensus surrounding an enigmatic oxidant. *Dalton Trans.* 2012;41(45):13779-87. Epub 2012/09/26. doi: 10.1039/c2dt31526b. PubMed PMID: 23007920.
185. Liu DW, Zhang YH, Xu MY, Chen HX, Lu XP, Ostrikov K. Cold atmospheric pressure plasmas in dermatology: Sources, reactive agents, and therapeutic effects. *Plasma Processes and Polymers.* 2020;25. doi: 10.1002/ppap.201900218. PubMed PMID: WOS:000510977700001.
186. Gjika E, Pal-Ghosh S, Kirschner ME, Lin L, Sherman JH, Stepp MA, et al. Combination therapy of cold atmospheric plasma (CAP) with temozolomide in the treatment of U87MG glioblastoma cells. *Sci Rep.* 2020;10(1):16495. Epub 2020/10/07. doi: 10.1038/s41598-020-73457-7. PubMed PMID: 33020527; PubMed Central PMCID: PMC8068204.
187. Assadian O, Ousey KJ, Daeschlein G, Kramer A, Parker C, Tanner J, et al. Effects and safety of atmospheric low-temperature plasma on bacterial reduction in chronic wounds and wound size reduction: A systematic review and meta-analysis. *Int Wound J.* 2019;16(1):103-11. Epub 2018/10/13. doi: 10.1111/iwj.12999. PubMed PMID: 30311743; PubMed Central PMCID: PMC7379569.
188. Qasem H, Al-Ayadhi L, Al Dera H, El-Ansary A. Increase of cytosolic phospholipase A2 as hydrolytic enzyme of phospholipids and autism cognitive, social and sensory dysfunction

- severity. *Lipids in Health and Disease*. 2017;16. doi: 10.1186/s12944-016-0391-4. PubMed PMID: WOS:000415608100001.
189. Trotter A, Anstadt E, Clark RB, Nichols F, Dwivedi A, Aung K, et al. The role of phospholipase A2 in multiple Sclerosis: A systematic review and meta-analysis. *Mult Scler Relat Disord*. 2019;27:206-13. doi: 10.1016/j.msard.2018.10.115. PubMed PMID: WOS:000455500500040.
190. Peng Z, Chang Y, Fan J, Ji W, Su C. Phospholipase A2 superfamily in cancer. *Cancer Lett*. 2021;497:165-77. Epub 2020/10/21. doi: 10.1016/j.canlet.2020.10.021. PubMed PMID: 33080311.
191. Ogata N. Inactivation of influenza virus haemagglutinin by chlorine dioxide: oxidation of the conserved tryptophan 153 residue in the receptor-binding site. *J Gen Virol*. 2012;93(Pt 12):2558-63. Epub 2012/08/31. doi: 10.1099/vir.0.044263-0. PubMed PMID: 22933663.
192. Johnson KA, Pokhrel R, Budicini MR, Gerstman BS, Chapagain PP, Stahelin RV. A Conserved Tryptophan in the Ebola Virus Matrix Protein C-Terminal Domain Is Required for Efficient Virus-Like Particle Formation. *Pathogens*. 2020;9(5):402. doi: ARTN 402 10.3390/pathogens9050402. PubMed PMID: WOS:000541443700085.
193. Ito K, Olsen SL, Qiu W, Deeley RG, Cole SP. Mutation of a single conserved tryptophan in multidrug resistance protein 1 (MRP1/ABCC1) results in loss of drug resistance and selective loss of organic anion transport. *J Biol Chem*. 2001;276(19):15616-24. Epub 2001/03/30. doi: 10.1074/jbc.M011246200. PubMed PMID: 11278867.
194. Reid LO, Thomas AH, Herlax V, Dantola ML. Role of Tryptophan Residues in the Toxicity and Photosensitized Inactivation of *Escherichia coli* alpha-Hemolysin. *Biochemistry*. 2020;59(44):4213-24. Epub 2020/10/29. doi: 10.1021/acs.biochem.0c00660. PubMed PMID: 33108867.
195. Reuter S, von Woedtke T, Weltmann KD. The kINPen-a review on physics and chemistry of the atmospheric pressure plasma jet and its applications. *J Phys D Appl Phys*. 2018;51(23):233001-51. doi: 10.1088/1361-6463/aab3ad. PubMed PMID: WOS:000432426400001.
196. Pattison DI, Rahmanto AS, Davies MJ. Photo-oxidation of proteins. *Photochem Photobiol Sci*. 2012;11(1):38-53. Epub 2011/08/23. doi: 10.1039/c1pp05164d. PubMed PMID: 21858349.
197. Pattison DI, Davies MJ. Actions of ultraviolet light on cellular structures. *EXS*. 2006;(96):131-57. Epub 2005/12/31. doi: https://doi.org/10.1007/3-7643-7378-4_6. PubMed PMID: 16383017.
198. Oh JS, Szili EJ, Hong SH, Gaur N, Ohta T, Hiramatsu M, et al. Mass Spectrometry Analysis of the Real-Time Transport of Plasma-Generated Ionic Species Through an Agarose Tissue Model Target. *J Photopolym Sci Tec*. 2017;30(3):317-23. doi: DOI 10.2494/photopolymer.30.317. PubMed PMID: WOS:000407658300012.
199. Van der Paal J, Hong SH, Yusupov M, Gaur N, Oh JS, Short RD, et al. How membrane lipids influence plasma delivery of reactive oxygen species into cells and subsequent DNA damage: an experimental and computational study. *Phys Chem Chem Phys*. 2019;21(35):19327-41. Epub 2019/08/28. doi: 10.1039/c9cp03520f. PubMed PMID: 31453592.
200. Lu X, Keidar M, Laroussi M, Choi E, Szili EJ, Ostrikov K. Transcutaneous plasma stress: From soft-matter models to living tissues. *Materials Science and Engineering: R: Reports*. 2019;138:36-59. doi: 10.1016/j.msere.2019.04.002.

6. Original Publications

The present work is based on peer-reviewed articles published or submitted in international scientific journal. These are listed below together with the authors' contribution.

Article A1

S. Wenske, J.-W. Lackmann, S. Bekeschus, K.-D. Weltmann, T. von Woedtke and K. Wende. "Nonenzymatic post-translational modifications in peptides by cold plasma derived reactive oxygen and nitrogen species". *Biointerphases*, 15 (6), 061008, 2020.

The experiment was designed by SW, JWL and KW. The measurements, data evaluation and visualization were performed by SW and JWL. The manuscript was written by SW, JWL and KW and edited by all co-authors.

Article A2

S. Wenske, J.-W. Lackmann, L.-M. Busch, S. Bekeschus, T. von Woedtke and K. Wende. "Reactive species driven oxidative modifications of peptides—Tracing physical plasma liquid chemistry". *J. Appl. Phys.*, 129 (19), 193305, 2021.

The experiment was designed by SW, JWL and KW. The measurements, data evaluation and visualization were performed by SW, LMB and KW. The manuscript was written by SW and KW and edited by all co-authors.

Article A3

Z. Nasri, S. Memari, S. Wenske, R. Clemen, U. Martens, M. Delcea, S. Bekeschus, K.-D. Weltmann, T. von Woedtke and K. Wende. "Singlet Oxygen-Induced Phospholipase A2 Inhibition: a Major Role for Interfacial Tryptophan Dioxidation", *Chem. Eur. J.*, 27 (59), 14702, 2021.

The experiment was designed by ZN and KW. The electrochemical experiments and data evaluation were performed by ZN and SM. The mass spectrometric experiments and data evaluation was performed by SW and SM. The manuscript was written by ZN, SM, SW, RM and edited by KW.

Article A4

G. Bruno, S. Wenske, J.-W. Lackmann, M. Lalk, T. von Woedtke, and K. Wende. "On the liquid chemistry of the reactive nitrogen species peroxyxynitrite and nitrogen dioxide generated by physical plasmas". *Biomolecules*, 10 (12), 1687, 2020.

The experiment was designed by GB and KW. The experiments and data evaluation were performed by GB and SW for the proteomics data elaboration. The manuscript was written by GB and edited by SW, JWL and KW.

Article A5

G. Bruno, S. Wenske, H. Mahdikia, T. Gerling, T. von Woedtke, and K. Wende. "Radiation driven chemistry in biomolecules – is (V)UV" involved in the bioactivity of argon jet plasmas?". *Frontiers in Physics*, 9, 759005, 2021.

The experiment was designed by GB and KW. The experiments and data evaluation were performed by GB and SW for the proteomics data elaboration. The manuscript was written by GB and edited by SW and KW.

Approved:

Date

Sebastian Wenske

Date

Prof. Dr. Michael Lalk

Article A1

Nonenzymatic post-translational modifications in peptides by cold plasma-derived reactive oxygen and nitrogen species

S. Wenske, J.-W. Lackmann, S. Bekeschus, K.-D. Weltmann, T. von Woedtke and K. Wende. *Biointerphases*, 15 (6), 061008, 2020.

© 2020 Author(s)

Nonenzymatic post-translational modifications in peptides by cold plasma-derived reactive oxygen and nitrogen species

Cite as: Biointerphases 15, 061008 (2020); <https://doi.org/10.1116/6.0000529>

Submitted: 07 August 2020 • Accepted: 15 October 2020 • Published Online: 25 November 2020

Sebastian Wenske,  Jan-Wilm Lackmann,  Sander Bekeschus, et al.



View Online



Export Citation



CrossMark

ARTICLES YOU MAY BE INTERESTED IN

[Reactive species driven oxidative modifications of peptides—Tracing physical plasma liquid chemistry](#)

Journal of Applied Physics **129**, 193305 (2021); <https://doi.org/10.1063/5.0046685>

[Perspectives on cold atmospheric plasma \(CAP\) applications in medicine](#)

Physics of Plasmas **27**, 070601 (2020); <https://doi.org/10.1063/5.0008093>

[Cold atmospheric plasma for SARS-CoV-2 inactivation](#)

Physics of Fluids **32**, 111702 (2020); <https://doi.org/10.1063/5.0031332>



Biointerphases
A Journal of Biomaterials and Biological Interfaces

Submit Today!

SPECIAL TOPIC

Polymeric Biointerfaces — A Collection
in celebration of Nicholas D. Spencer's career



Nonenzymatic post-translational modifications in peptides by cold plasma-derived reactive oxygen and nitrogen species

Cite as: *Biointerphases* 15, 061008 (2020); doi: 10.1116/6.0000529

Submitted: 7 August 2020 · Accepted: 15 October 2020 ·

Published Online: 25 November 2020



View Online



Export Citation



CrossMark

Sebastian Wenske,¹ Jan-Wilm Lackmann,²  Sander Bekeschus,¹  Klaus-Dieter Weltmann,³  Thomas von Woedtke,³  and Kristian Wende^{1,a)} 

AFFILIATIONS

¹ZIK plasmatis, Leibniz Institute for Plasma Science and Technology (INP Greifswald), Felix-Hausdorff-Straße 2, 17489 Greifswald, Germany

²Cluster of Excellence Cellular Stress Responses in Aging-Associated Diseases, University of Cologne, Joseph-Stelzmann-Straße 26, 50931 Cologne, Germany

³Leibniz Institute for Plasma Science and Technology (INP Greifswald), Felix-Hausdorff-Straße 2, 17489 Greifswald, Germany

^{a)}Author to whom correspondence should be addressed: kristian.wende@inp-greifswald.de

ABSTRACT

Cold physical plasmas are emerging tools for wound care and cancer control that deliver reactive oxygen species (ROS) and nitrogen species (RNS). Alongside direct effects on cellular signaling processes, covalent modification of biomolecules may contribute to the observed physiological consequences. The potential of ROS/RNS generated by two different plasma sources (kINPen and COST-Jet) to introduce post-translational modifications (PTMs) in the peptides angiotensin and bradykinin was explored. While the peptide backbone was kept intact, a significant introduction of oxidative PTMs was observed. The modifications cluster at aromatic (tyrosine, histidine, and phenylalanine) and neutral amino acids (isoleucine and proline) with the introduction of one, two, or three oxygen atoms, ring cleavages of histidine and tryptophan, and nitration/nitrosylation predominantly observed. Alkaline and acidic amino acid (arginine and aspartic acid) residues showed a high resilience, indicating that local charges and the chemical environment at large modulate the attack of the electron-rich ROS/RNS. Previously published simulations, which include only OH radicals as ROS, do not match the experimental results in full, suggesting the contribution of other short-lived species, i.e., atomic oxygen, singlet oxygen, and peroxyxynitrite. The observed PTMs are relevant for the biological activity of peptides and proteins, changing polarity, folding, and function. In conclusion, it can be assumed that an introduction of covalent oxidative modifications at the amino acid chain level occurs during a plasma treatment. The introduced changes, in part, mimic naturally occurring patterns that can be interpreted by the cell, and subsequently, these PTMs allow for prolonged secondary effects on cell physiology.

© 2020 Author(s). All article content, except where otherwise noted, is licensed under a Creative Commons Attribution (CC BY) license (<http://creativecommons.org/licenses/by/4.0/>). <https://doi.org/10.1116/6.0000529>

I. INTRODUCTION

Cold physical plasma is increasingly used for various biomedical applications. Besides decontamination and surface optimization for medical products such as implants,^{1,2} acute and chronic wound management,³ and cancer treatment^{4,5} are major fields of research and (pre)clinical use. Specifically, the controllable mix of short- and long-lived reactive oxygen and nitrogen species (ROS/RNS) in combination with electrical fields and UV radiation allows plasmas

to interfere with cellular signaling processes on different levels.^{6–8} Besides a direct interaction of ROS with cellular signal receptors, e.g., peroxiredoxins (reviewed in Ref. 9), short-lived reactive species such as singlet oxygen [$O_2(^1\Delta_g)$], atomic oxygen O, or peroxyxynitrite (ONOO⁻) may introduce covalent chemical changes in a range of biomolecules, thereby influencing their structure and activity.^{10–13} Assumingly, such covalent modifications contribute to the observed physiological impact of plasma specifically when the resulting

structure resembles biologically active post-translational modifications (PTMs). However, mechanisms and extent remain to be elucidated.

Post-translational modifications are versatile “customizations” of proteins and peptides, controlling their activity, fate, and lifetime.^{14,15} Often, they are enzymatically introduced after protein translation, and more than 200 biologically relevant types of PTMs have been identified,¹⁶ with phosphorylations, ubiquitination, and glycosylations being the most frequent.¹⁷ However, the database Unimod (<http://www.unimod.org/>) contains 1500 entries of protein modifications (May 2020), many of those with unknown impact in biological systems, showing the complexity of the research area. Also, nonenzymatic routes have been described and were found relevant for biological processes,^{18,19} this time focusing on oxidative structures including hydroxylation, carbonylation, and nitration.²⁰ The proteome-wide identification of enzymatic and nonenzymatic PTMs by high-resolution mass spectrometry is a challenging approach receiving increasing attention.^{21,22}

Here, the impact of the cold plasma treatment on two model peptides, angiotensin 1–7 and bradykinin, was investigated. The widely used argon based plasma jet kINPen and the helium based plasma jet COST-Jet were tested for their ability to introduce nonenzymatic post-translational modifications and to infer on the underlying chemical reactions and reactive species, respectively. Both plasma sources vary significantly in design and reactive species output.^{23–26} Bradykinin is a small pro-inflammatory peptide in mammals, which is composed of nine amino acids (Arg-Pro-Pro-Gly-Phe-Ser-Pro-Phe-Arg), and angiotensin 1–7 (Asp-Arg-Val-Tyr-Ile-His-Pro) is the amino-terminal fragment of the angiotensin I/II involved in blood pressure regulation. The amino acids present contain hydrophobic side chains (valine and isoleucine), aromatic side chains (tyrosine and phenylalanine), charged (arginine and histidine) or uncharged side chains (asparagine and serine), and some special cases (glycine and proline) and represent a suitable range of target structures. Of note, no sulfur-containing amino acid is present in both peptides since previous experiments revealed a strong oxidation of thiol groups by reactive species, precluding an unbiased view of the other amino acids’ reactivity.^{27,28}

Recent work by various authors rose awareness to discriminate between interface and bulk reactions in liquids that are in contact with a plasma discharge or the active effluent,^{29–33} indicating that the short-lived species such as hydroxyl radicals dominate the downstream chemistry. This is addressed in a molecular dynamics simulation study on the impact of hydroxyl radicals on bradykinin and angiotensin published by Verlact *et al.*,³⁴ allowing to pre-estimate target structures for the current approach and to identify relevant reactive species by comparison between theoretical and experimental results. Using the peptides as target molecules that preserve the impact of reactive species in a covalent chemical bond allows taking snapshots of the plasma chemistry at the interface and bulk simultaneously, augmenting electron paramagnetic resonance spectroscopy data present for the kINPen.^{35,36}

In conclusion, two different plasma sources are used to tackle the following questions: First, which PTMs are induced nonenzymatically by ROS/RNS and which amino acids are the major targets? Second, which reactive species are responsible for these modifications? And third, are the experimental results congruent

with the simulation results? High-resolution mass spectrometry coupled to nanoflow liquid chromatography (nanoLC-MS/MS) along with bioinformatics tools was applied to identify and quantify the oxidative post-translational modifications resulting from the treatment by the two applied plasma sources. The results confirm the relevance of secondary effects in cold plasma effects.

II. EXPERIMENT

A. Treatment conditions and plasma sources

Angiotensin 1–7 and bradykinin (Sigma-Aldrich-Chemie GmbH, Germany) were dissolved in 500 μ l of double distilled H₂O (Millipore) with a concentration of 0.2 mg/ml. The water was thoroughly degassed by bubbling with argon gas for 30 min to reduce background reactions. For the treatments, we used the kINPen (neoplas tools GmbH, Germany)³⁷ and the COST Reference Microplasma Jet (COST-Jet is the outcome of the European COST action MP 1101 “Biomedical Applications of Atmospheric Pressure Plasma Technology”).³⁸ The kINPen consists of a grounded ring electrode and a ceramic capillary, where a centered rod electrode is located inside (Fig. 1 right). A voltage of 2–6 kV_{pp} is applied to the central electrode with a frequency of 1.1 MHz. Argon gas (purity 99.999%) was used as a working gas with a flow rate of 3 standard liters per minute (sLm).³⁹ For some treatments, 0.5% of the working gas was replaced with N₂, O₂, or with a mixture of both gases (15 SCCM each). The COST-Jet is a device that was developed by the European COST action MP 1101 as a reference device for plasma sources. It consists of two 1 mm thick metal plate electrodes spaced 1 mm apart in between which the plasma is ignited (Fig. 1 left). A Tektronix DPO 4104 Digital Phosphor Oscilloscope was used to measure the time resolved voltage for the plasma. For pure helium experiments, the plasma was sustained to 143 mV, for helium/oxygen to 145 mV, for helium/nitrogen to 159 mV, and for helium/oxygen/nitrogen to 165 mV. The treatments were performed at a sample distance of 4 mm and 1 sLm helium. If desired, 0.5% oxygen, nitrogen, or both gases were added (5 SCCM each). All treatments were done in 24-well plates and placed 4 mm (COST-Jet) or 9 mm (kINPen) away from the liquid surface for 30 or 60 s. After each individual treatment, samples were placed on wet ice and immediately analyzed by nanoLC-MS/MS to minimize postdischarge reactions (see Sec. II B). Three independent experiments were performed.

For further characterization of the two plasma sources, the long-lived species H₂O₂, nitrate (NO₃⁻), and nitrite (NO₂⁻) (Fig. 2) were also determined for the different compositions of gases. The quantification of nitrite and nitrate was performed with ion chromatography (ICS-5000, Thermo Fisher Scientific). For the separation, an IonPac AS23 anion exchange column (2 \times 250 mm, Thermo Fisher Scientific) and an isocratic mobile phase (4.5 mM Na₂CO₃/0.8 mM NaHCO₃) with 250 μ l/min were used. Hydrogen peroxide was quantified via the colorimetric reaction with xylenol orange using a commercially available assay (Pierce Quantitative Peroxide Assay Kit, Thermo Scientific) according to the manufacturer’s protocol.

B. nanoLC-MS/MS acquisition

An UltiMate 3000 RSLCnano system equipped with an Acclaim Pepmap C18 column (150 mm \times 75 μ m, 2.0 μ m particle

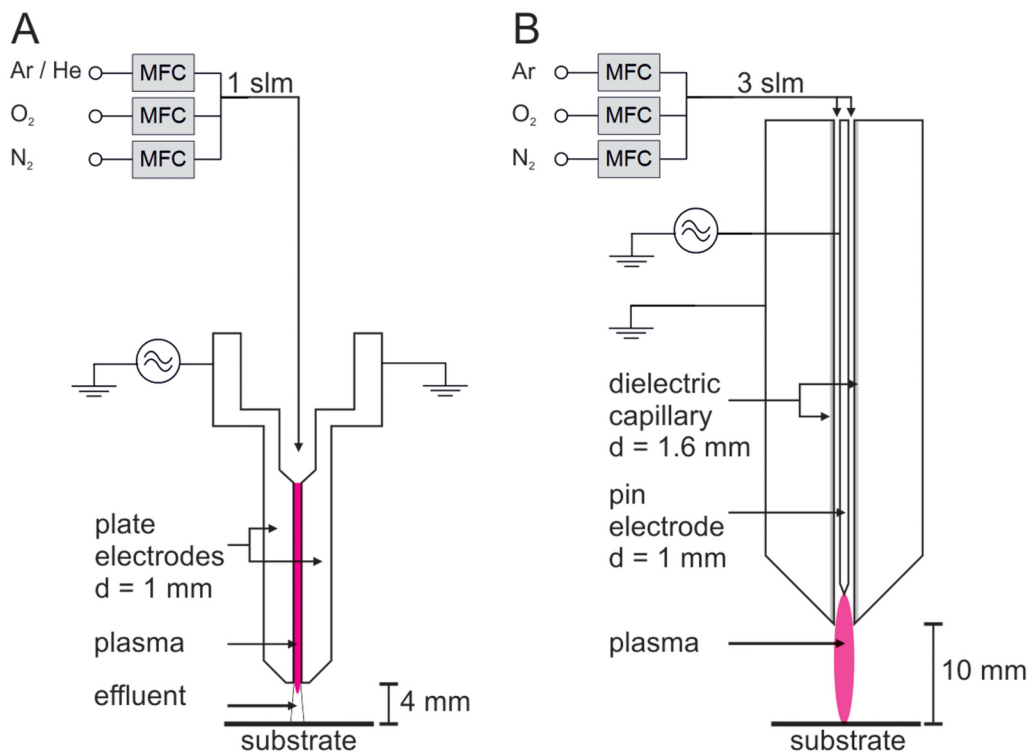


FIG. 1. Schematics of the COST-Jet (a) and kINPen (b). MFC, mass flow controller; sLm, standard liter per minute. Reprinted with permission from Lackmann *et al.*, *Sci. Rep.* 8, 7736 (2018). Copyright 2018 Author(s), licensed under a Creative Commons Attribution (CC BY) License.

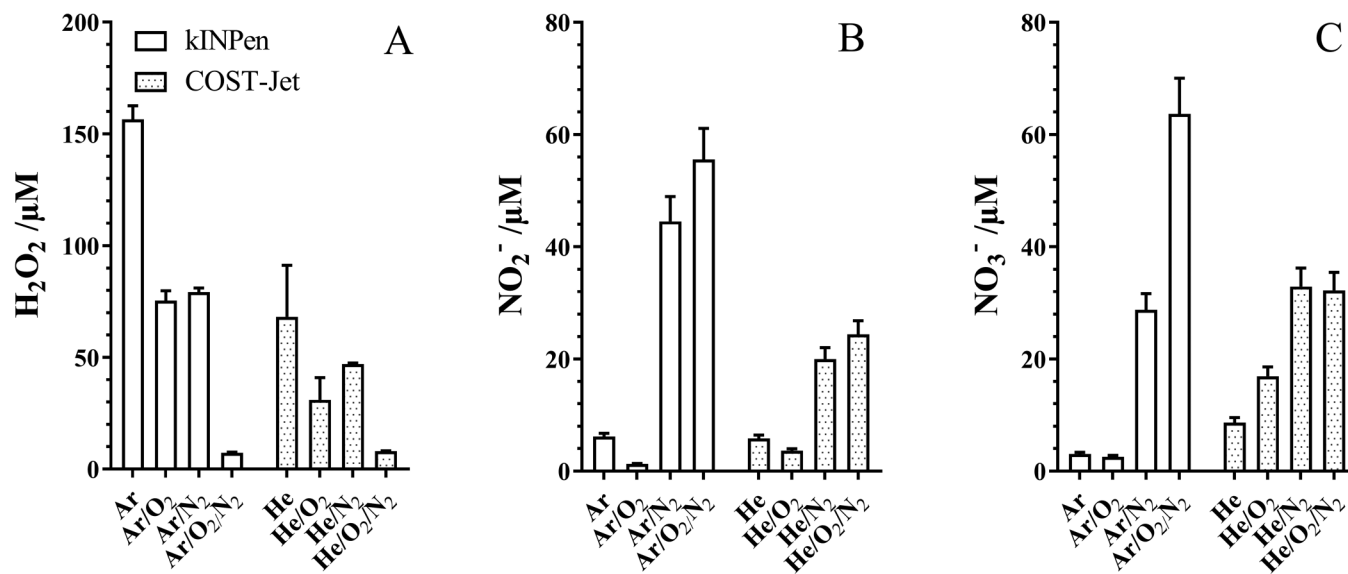


FIG. 2. Measured concentrations of H₂O₂ (a), nitrite (b), and nitrate (c) in ultrapure MS water after 60 s kINPen or COST-Jet treatment for various gas compositions (0.5% of molecular gases added in part). For the exact determination of the concentration, see text. Mean of three replicates + SD.

TABLE I. Flow gradient for LC separation of model peptides.

Eluent B (%)	Time (min)	Flow ($\mu\text{l}/\text{min}$)
12	0	0.400
12	8	0.400
20	10	0.300
22	26	0.400
80	29	0.500
80	31	0.500
12	32	0.400
12	35	0.400

size, Thermo Fisher Scientific) and corresponding precolumn and a QExactive Hybrid-Quadrupol-Orbitrap mass spectrometer from Thermo Fisher was used. The injection volume was $1\ \mu\text{l}$, equaling 200 ng of sample. A step gradient (see Table I) consisting of water/0.1% v/v acetic acid (A) and acetonitrile/0.1% v/v acetic acid (B) was applied to achieve separation of modified peptides. All samples were injected twice.

MS acquisition was performed in a data dependent Top 10 mode (full MS/dd-MS/MS) at resolving powers of 70,000 in MS mode and 17,500 in MS/MS mode. A Nanospray Flex electrospray ion source was used in positive mode, and the spray voltage was set to 2.30 kV using stainless steel emitters. The temperature of the transfer capillary was set to 250 °C. The collision energy in the higher-energy collisional dissociation cell was fixed at 27.5 V (HCD fragmentation). The observed mass shifts allowed identification of the peptide sequence and to pinpoint modified amino acids.

C. Peptide and post-translational modification identification

Raw data analysis was achieved by the Proteome Discoverer 2.2 software (Thermo Fisher Scientific) using Byonic (Protein Metrics),⁴⁰ Version 3.4.1, as a plug-in to identify post-translational modifications. This tool significantly extends search options for peptide modifications. Based on the previous work,^{12,41,42} an inclusion list of expected oxidative modifications was compiled (Table II). In the search, precursor mass tolerance was set to 3 ppm and fragment mass tolerance to 10 ppm. A false discovery rate of 1% was accepted. Due to calculation power restraints, maximum three PTMs were allowed per peptide. The spectra were examined manually to ensure the presence of specified modification. To obtain semiquantitative data, the number of spectra matching a detected modifications summed up (PSM counting).⁴³

III. RESULTS AND DISCUSSION

Previous investigations on isolated amino acids determined a broad range of chemical structures to be susceptible to the impact of plasma-derived reactive species.^{12,29,44} For one, it remained to be clarified whether similar covalent changes occur in a peptide chain, since the competition for targets or species may occur. For another, it should be determined whether these modifications relate to physiological PTMs since they may contribute to the observed physiological consequences of cold plasma.^{8,45}

TABLE II. List of preferred native (oxidative) post-translational modifications searched in angiotensin 1–7 and bradykinin. A given mass shift may reflect different chemical structures depending on the target structure.

Monoisotopic mass shift (Da)	Elemental composition	Name/potential product
+15.994 915	+O	Hydroxy
+31.989 829	+2O	Hydroperoxide/dihydroxy
+47.984 744	+3O	Trihydroxy/sulfonic acid/hydroxyformylkynurenin
+28.990 164	+N + O – H	Nitrosylation
+44.985 078	+N + 2O – H	Nitration
+0.984 016	–N – H + O	Deamidation
–0.984 016	+N + H – O	Amidation
+13.979 265	+O – 2H	Oxo, carbonyl
+29.974 179	+2O – 2H	Dione (quinone)
+ 45.969 094	+3O – 2H	Dione (quinone) + hydroxy
–2.015 65	–2H	Didehydro
+4.978 93	+2O – N – C – H	Formylasparagine
+33.961 028	+Cl – H	Chlorination

A. Oxidative PTMs observed for kINPen treatments

The argon-driven kINPen showed a significant impact on the amino acids in both angiotensin 1–7 and bradykinin (Figs. 3 and 4). The reactivity toward the plasma-derived species differs by amino acid, its position within the peptide chain, the gas phase composition, and the plasma source (kINPen or COST-Jet). The highest numbers of post-translational modifications were observed for tyrosine (Y), isoleucine (I), and histidine (H) in the angiotensin 1–7 and phenylalanine (F) and proline (P) in bradykinin. Interestingly, the proline in angiotensin 1–7 (position 7) remains almost unmodified, while at the positions 3 and 7 of bradykinin, it is significantly attacked. In the same molecule, proline at the position 2 remains scarcely attacked by the plasma-generated species. A similar behavior was observed for phenylalanine of bradykinin at positions 5 (center) and 8 (carboxy terminal end). Assumingly, steric hindrances and local variations of the electron densities of heteroatoms or aromatic rings contribute to the observed divergence in reactivity. In Fig. 4, the most commonly observed modifications for angiotensin 1–7 (A) and bradykinin (B) are shown. For pure argon discharge, the most frequent modifications are the oxidation ($\Delta m +15.99\ \text{Da}$) and nitration ($\Delta m +44.99\ \text{Da}$) at the amino acids tyrosine and isoleucine of angiotensin and oxidation of phenylalanine at position 5 of bradykinin. Additionally, dioxidations ($\Delta m +31.99\ \text{Da}$) were found at histidine (angiotensin) and proline (bradykinin, positions 3 and 7). A ring cleavage forming formylasparagine ($\Delta m +4.98\ \text{Da}$) was found for histidine according to the literature driven by singlet oxygen.⁴⁶ Almost no modifications of the arginine moiety were observed. With respect to the positively charged guanidinium group, a significant impact of the electron-rich (and in part negatively) charged reactive oxygen species was assumed. However, in accordance with qualitative

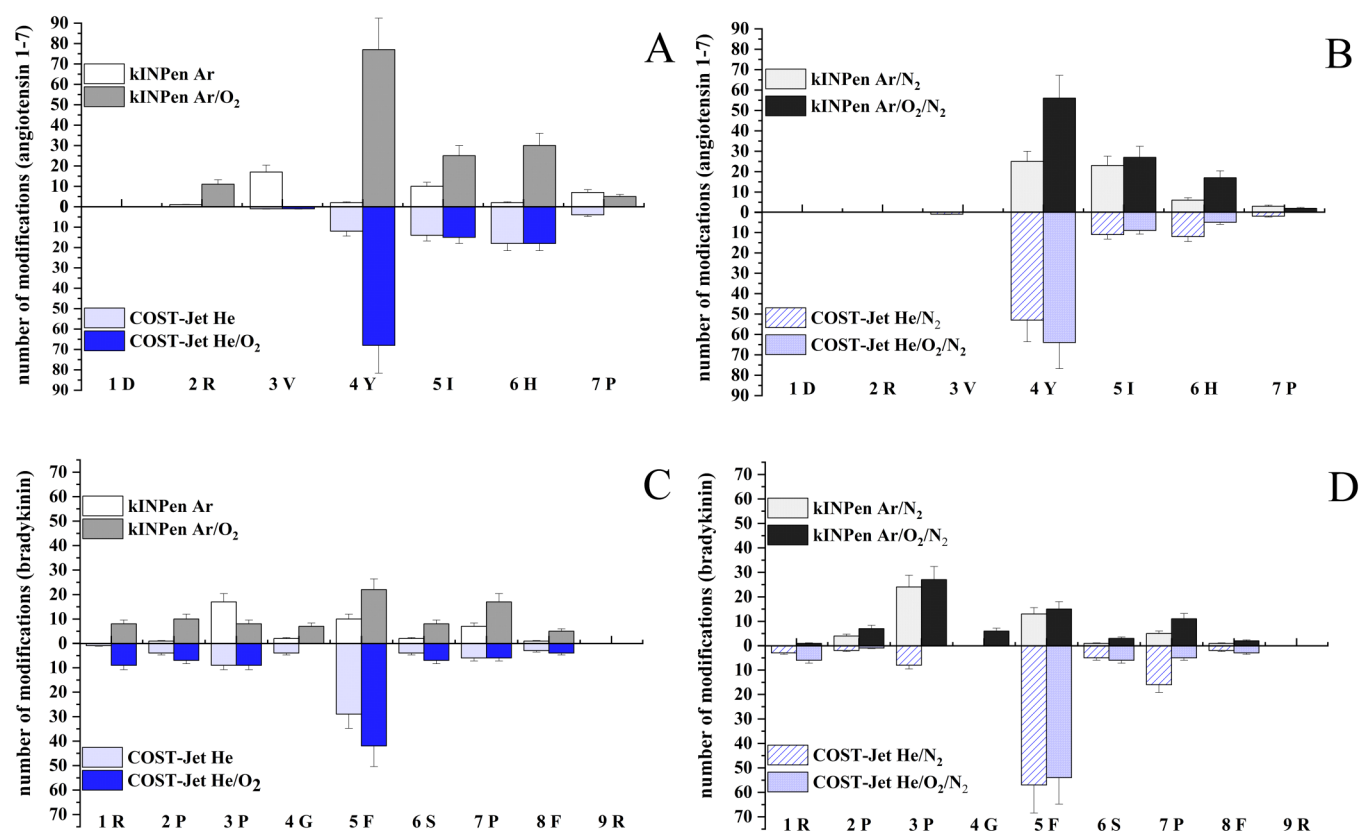


FIG. 3. Observed extent of modifications at angiotensin 1–7 (a) and (b) or bradykinin (c) and (d) after plasma treatment (60 s of kINPen/COST-Jet). Argon/helium was enriched with 0.5% molecular gases where necessary. Mean of three replicates/two injections + SD.

observations,¹² arginine shows a remarkably resilience to reactive species that is lifted to some extent by ROS-rich Ar/O₂ discharges.

If O₂ is added to the working gas, nitrations disappear in favor of oxygen-dominated PTMs, reflecting changes in the gas phase and liquid phase chemistry.^{47,48} Oxygen enriched plasmas are known to produce O₃, [•]O, and ¹O₂,⁴⁹ species that are strong oxidants⁵⁰ with high prevalence in the gas-liquid interface.²⁹ Experimental evidence is the observation of a modification on tyrosine of Δm +47.98 Da with three oxygen atoms and the increase in Δm +31.99 Da mass shifts (e.g., isoleucine hydroperoxide and double oxidized histidine). Interestingly, it is the only condition where arginine is oxidized, implying a role for atomic and singlet oxygen.

When nitrogen was added to the working gas, the aromatic amino acids become the major target. The nitration of phenylalanine occurs only under these conditions in bradykinin, and monohydroxylation of the aromatic rings in either Phe or Tyr was found. The oxidation of proline (Δm +15.99 Da) at position 3 of bradykinin was observed only here, indicating that this modification is destroyed by harsher oxidizing conditions as in Ar/O₂.

For the kINPen argon/O₂/N₂ plasma, nitrogen-containing modifications were frequent, with nitrosylation of phenylalanine as

a marker for the presence of nitric oxide standing out in bradykinin. In the angiotensin 1–7 peptide, nitrotyrosine is formed via reaction with peroxynitrite ONOO⁻,^{51,52} which yields at the gas-liquid interface from the reaction of superoxide (O₂^{•-}) and nitric oxide ([•]NO),⁵³ and it is already shown that this molecule also occurs in physical plasma.⁵⁴ This nitrotyrosine is not formed when oxygen or nitrogen alone is used as an admixture. This supports the notion that nitric oxide is formed at the interphase by the reaction of nitrogen dioxide radicals and atomic oxygen and that it serves as a reactant for the formation of peroxynitrite,⁵⁵ and such requires both ROS and RNS.

B. Oxidative PTMs observed for COST-Jet treatments

For COST-Jet, similar amino acid modifications were observed (Fig. 3). Their overall number is lower than for the kINPen. This is particularly evident for the 60 s helium plasma treatment of angiotensin [Fig. 3(a)]. While the same three amino acids, tyrosine, isoleucine, and histidine, are modified, its total extent is only 25%–30% of the kINPen treatments. The main modifications of tyrosine are quinone formation (Δm +29.97 Da) and monoxidation (Δm +15.99 Da). The structure is shown in Fig. 5(a). In bradykinin,

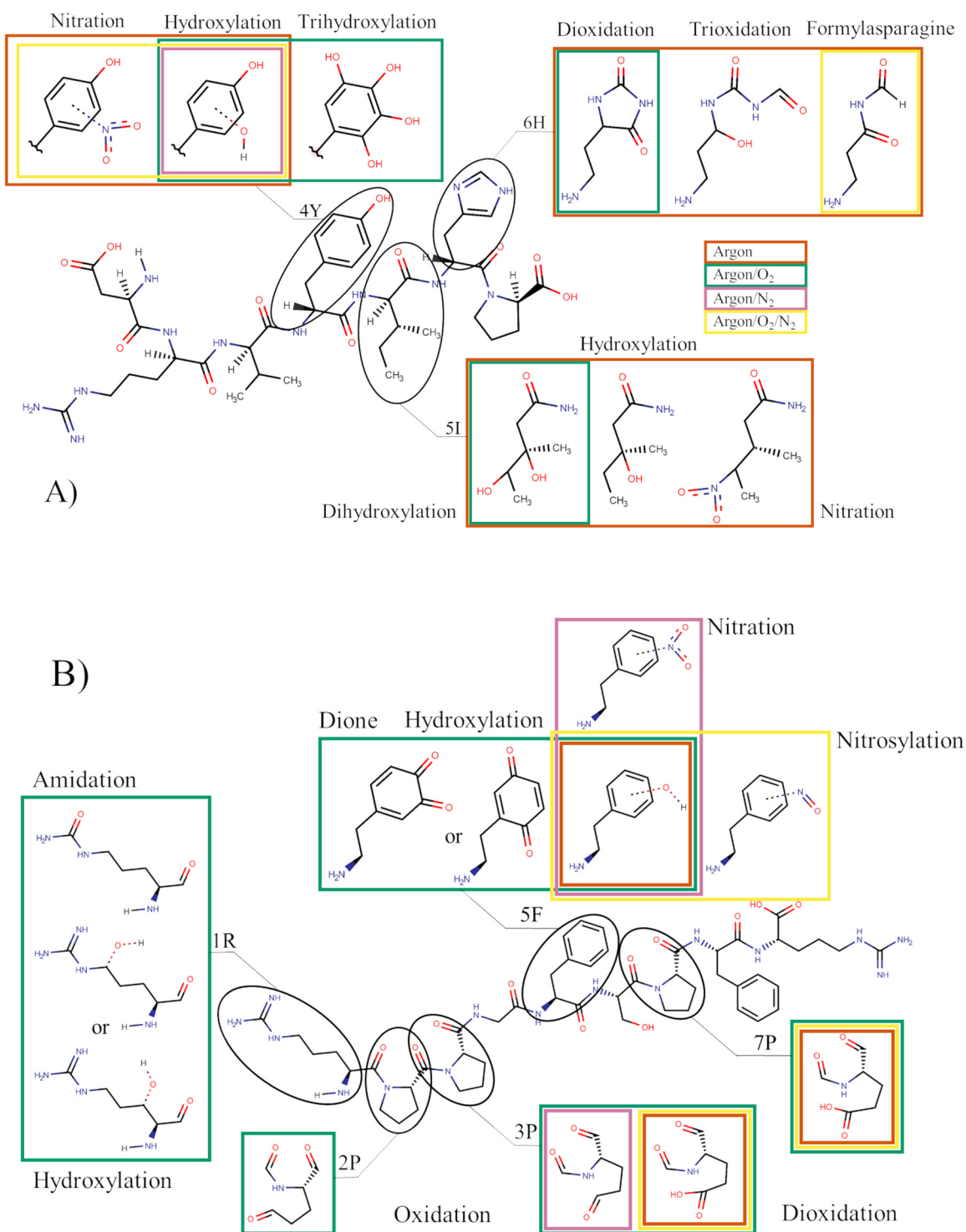


FIG. 4. Most common oxidative modifications for angiotensin 1–7 (a) and bradykinin (b) after 60 s kINPen treatment. The peptides amino acid sequence is drawn in full, the colored rectangles indicate the observed changes to the molecule. The gas phase compositions have a significant impact: argon (orange), Ar/0.5% O₂ (green), Ar/0.5% N₂ (pink), or Ar/0.5% O₂ and 0.5% N₂ (yellow). Not all modifications are present at the same time, see text.

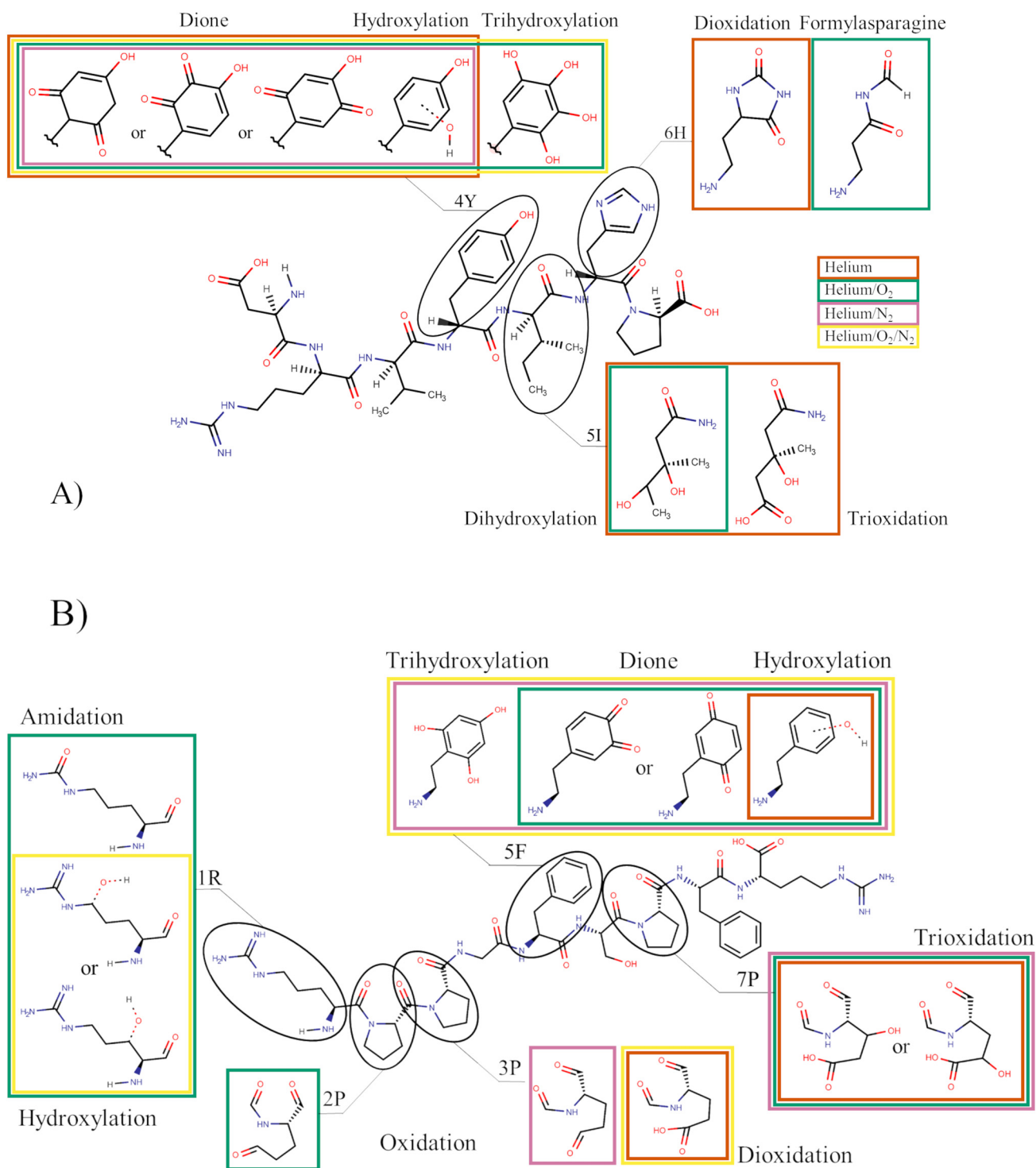


FIG. 5. Most common oxidative modifications for angiotensin 1–7 (a) and bradykinin (b) after 60 s COST-Jet treatment. The peptide amino acid sequence is drawn in full, the colored rectangles indicate the observed changes to the molecule. The gas phase compositions have a significant impact: helium (orange), He/0.5% O₂ (green), He/0.5% N₂ (pink), or He/0.5% O₂ and 0.5% N₂ (yellow). Not all modifications are present at the same time, see text.

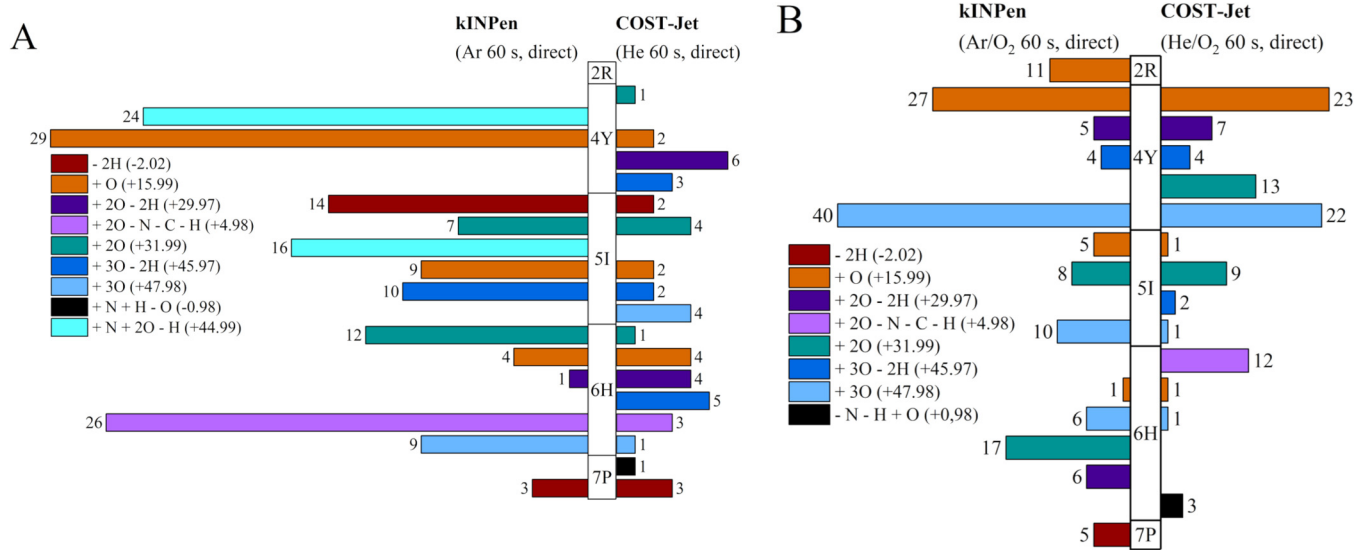


FIG. 6. Angiotensin 1–7: Absolute number and type of modifications observed as peptide spectrum matches in five of the seven amino acids that differ by a plasma source. (a) For kINPen, hydroxylation (+O) and nitration (+N + 2O – H) of tyrosine (4Y) and ring cleavage (+2O – N – C – H) of histidine (6H) dominate. The COST-Jet was less effective but more versatile. (b) Oxygen admixture increased the effectivity of the COST-Jet, reduced impact of RNS (no +N + 2O – H), and yielded in one (+O), two (+2O), or three (+3O) added oxygen as dominant products. Error bars are not shown for the sake of clarity, and the experimental error is ≈20% (see Fig. 3).

phenylalanine at position 5 is the major target [Figs. 3(c) and 3(d)]. With the pure helium discharge, hydroxylations (+O, Δm +15.99 Da) dominate by far (Fig. 7). Two proline residues at positions 3 and 7 are modified to carry two or three oxygen atoms (Δm +31.99 or Δm +47.98 Da). The oxygen admixture to the feed gas led in a massive increase of tyrosine oxidation (one to three oxygen atoms added) in angiotensin. This result mirrors observations using phenol as a target molecule³² assumingly due to atomic oxygen and/or singlet oxygen that are produced in high levels by COST-Jet in these conditions.²⁶ Of note, a modification of the arginine residue at position 1 occurs in the same kind and amount as with the kINPen. Phenylalanine was oxidized to a 1,2- or 2,5-quinone [Δm +29.97 Da, Fig. 5(b)].

By adding nitrogen to COST-Jet, the modification of phenylalanine is further increased, yielding, especially, trihydroxylation (+3O, Δm +47.98 Da). However, under these conditions, RNS were expected, yet no nitration or nitrosylation was observed for any

COST-Jet conditions. This is in accordance to the literature, with oxygen species dominating in the discharge. If both molecular gases were added, tyrosine at position 4 of angiotensin 1–7 and phenylalanine at position 5 of bradykinin remain the main targets for the ROS/RNS in the plasma [Figs. 3(b) and 3(d)].

C. Similarities and differences between the plasma sources

In general, the treatment of a peptide by COST-Jet led to a significantly lower total number of PTMs than the kINPen (Fig. 3). This is due to a lower gas flow rate and the significantly lower specific density of helium. The combination of heavy argon and a higher gas flow rate create an entirely different gas dynamics and mechanical impact of the kINPen,⁵⁶ yielding a richer interface chemistry. Both plasma sources yielded different modification patterns at the two model peptides (Figs. 6 and 7) reflecting their

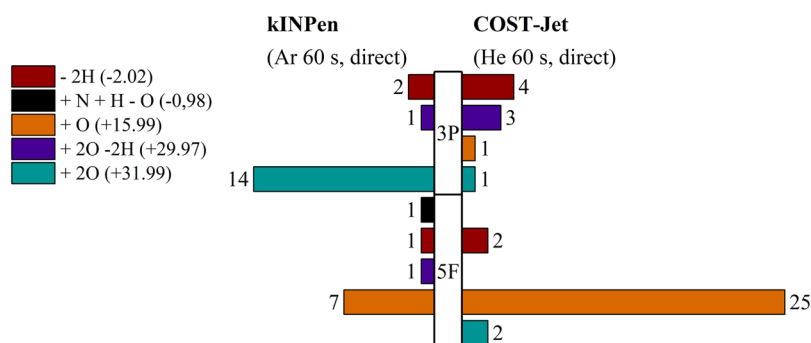


FIG. 7. Bradykinin: Absolute number and type of modifications observed at the amino acids phenylalanine (5P) and proline (3P) after kINPen (Ar) or COST-Jet (He) treatment (60 s). The differences reflect distinct species production by each source, see text. Error bars are not shown for the sake of clarity, and the experimental error is ≈20% (see Fig. 3).

different gas-phase and liquid-phase chemistries that were observed for cysteine and glutathione model systems.^{27,28}

Nitration and nitrosylations were found for conditions rich in RNS deposition as reported for kINPen (Ar, Ar/N₂/O₂).^{55,57,58} When atomic oxygen was a major species (COST-Jet), quinone formation at tyrosine or histidine was observed. As well, the dioxidation of tyrosine does occur predominantly for variants rich in atomic oxygen [Figs. 4(a), 5(a), and 6]^{32,59} but not in the singlet oxygen rich kINPen that favored the formylasparagine modification (+2O – H – C – H) at histidine [ninefold higher than COST-Jet, Fig. 6(a)]. Other modifications attributed to hydroxyl radicals were found in both plasma sources in the same extent as the monoxidation of histidine or the didehydration of proline ($\Delta m -2.02$ Da). A strong variation in the modification rate of the same amino acids at a different position (=a different chemical environment) was observed at the bradykinin's phenylalanine residue at position 5. For COST-Jet, this amino acid was oxidized particularly strong (Figs. 3 and 7). When treated with He/N₂, 5 F modification by the COST-Jet exceeded that of the kINPen by a factor of 5. In contrast, the phenylalanine residue at position 8 remained without detected modifications. Bradykinin's proline (3P) is the main target for the kINPen derived reactive species with dioxidation as the most common modification. The same amino acid loses two hydrogen atoms (didehydration) by the COST-Jet treatment, assumingly via an addition-subtraction reaction mechanism driven by hydroxyl radicals. These observations fit to previous results,²⁹ showing that the kINPen liquid chemistry is influenced by singlet oxygen O₂(¹Δ_g), leading to the dioxidation of thiols. On the other hand, the role of atomic oxygen in case of COST-Jet³⁸ leads to hydroxyl radical driven oxidations such as hydroxylations (+O) or H abstractions (-2H). Besides the short-lived species, both plasma sources deposit long-lived species in liquids (see Fig. 2). Hydrogen peroxide is a major product in kINPen and COST-Jet for argon or helium only discharges while nitrite and nitrate dominate conditions with

N₂ and N₂/O₂ admixtures. Despite the significant concentrations (up to 150 μM), only a very limited impact on the peptides could be attributed to their presence. In indirect treatments (peptides were added after the plasma was switched off), only a negligible number of PTMs was observed. This is in accordance with previous results using cysteine as a tracer.^{27,42,44}

D. Comparing MD simulations with experiment data

Verlacket *et al.* published in 2017 a study investigating the oxidation of bradykinin and angiotensin 1–7 by OH radicals³⁴ using a combined approach of reactive and nonreactive long time scale molecular dynamics simulation. In angiotensin, the four amino acids, asparagine, tyrosine, histidine, and proline, were identified as major targets; for bradykinin, the corresponding targets were arginine, serine, and proline. Predominantly, an H-atom abstraction was predicted as an initial step. Only for bradykinin, a minor 3% of the reactions were OH additions at phenylalanine 8, yielding predominantly tyrosine or positional isomer thereof. The current experimental data, comparing kINPen and COST-Jet, revealed both similarities and differences with the model (Fig. 8). For angiotensin 1–7, a good agreement between expected and observed chemical reactivity toward kINPen (Ar-) and COST-Jet (He-) derived reactive species was found for the amino acids valine, tyrosine, and histidine. The aromatic amino acids tyrosine and histidine are electron-rich and intermediates stabilize via electron delocalization, accordingly the model and the experiment coaligned on their intense modification. In the simulation, valine and isoleucine are inert to the OH attack in the tested time frame (10 ps), while experimentally, valine and, especially, isoleucine were oxidized by both plasma sources. This is in agreement with Takai *et al.* who reported the formation of hydroxylated dicarbonic acids.¹² The longer side chain of isoleucine protruding from the peptide backbone and the presence of an additional secondary C-atom discriminate it from

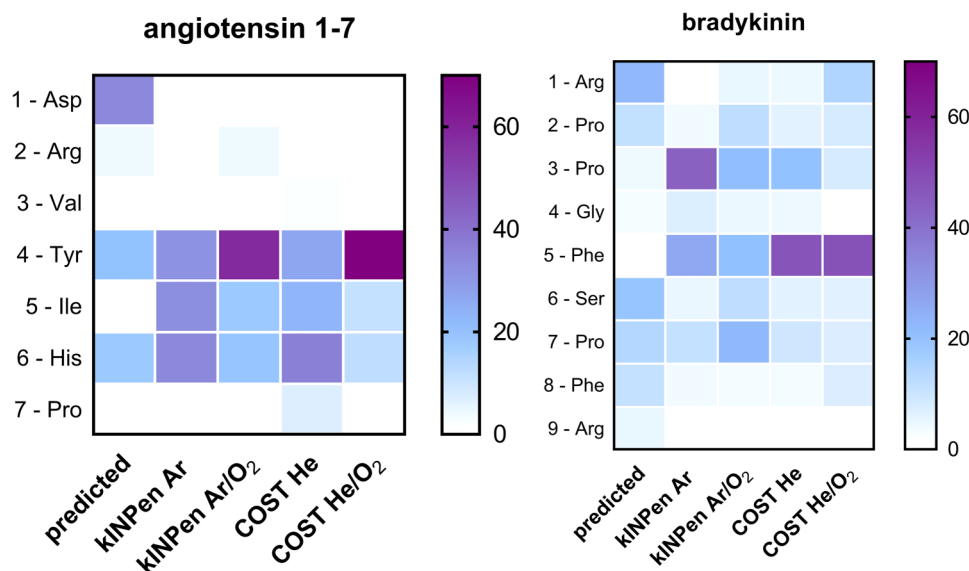


FIG. 8. Comparison of the extent of modifications found in angiotensin (left) and bradykinin (right) with simulations by Verlacket *et al.*³⁴ kINPen Ar or Ar/O₂ and COST He or He/O₂ were considered, and relative values (%) are shown. Significant differences between the model and the experiment and between plasma sources/discharge conditions are obvious, see text.

the less modified valine. Presumably, time scales >10 ps or reactive species not considered in the simulation are relevant in the attack. Atomic oxygen, the major species produced by COST-Jet in the He/O₂ regime, did not yield to a stronger isoleucine oxidation than singlet oxygen rich kINPen. A discord between the model and the experiment was also observed for aspartic acid: in contrast to predictions, no modifications were detected, which is again in agreement with Takai *et al.* It may be concluded that the assumed abstraction of an H-atom at the side chain carbonic acid moiety is not relevant for subsequent covalent modifications since the resulting radical is resonance stabilized at low energy. Additionally, with a pKa of 3.9, the β -COOH moiety is quite acidic and deprotonates in near neutral solutions. The resulting electron-rich COO⁻ moiety deters electron-rich and negatively charged reactive species and thereby protecting the carbon backbone from modification. A similar observation was made for Pro at carboxy terminus position 7 in angiotensin. With a pKa value of 1.99, the COOH moiety deprotonates under the experimental conditions, deterring the attack of electron-rich reactive species. In contrast, for bradykinin, where proline's carboxyl group is masked as an amide, modifications (dioxidations/ring cleavages) were frequent. Finally, arginine (Arg) was expected to be a major target, but neither source led to observed modifications, in good agreement with Takei *et al.* In the model, bradykinin's phenylalanine at position 5 was expected to be inert, yet the experimental observations showed that the amino acid is indeed a good target due to its large and resonance stabilized aromatic moiety. The discrepancy with simulation can be explained by technical restraints in the model and, additionally, by the relevant reactive species (assumably atomic oxygen) that the model did not consider. Regarding the comparison of the experimental data obtained for the oxygen admixture with the models' prediction, a gradual improvement could be observed. Specifically, for COST-Jet He/O₂ and peptide bradykinin, a good correlation between the prediction and the observation—with the exception of phenylalanine—can be stated. Under this condition, the COST-Jet is known to produce reactive oxygen species, with atomic oxygen as major species. In contrast, reactive nitrogen species have low abundance. Such model, taking OH radicals into account that easily yield from the reaction of atomic oxygen with water molecules, has a higher prediction power for this source. The kINPen, with its significant production of reactive nitrogen species, highlights the limits of the simulation.

In conclusion, the observed divergence between the model and the experiment is multifaceted: beyond OH radicals, further species such as atomic oxygen, singlet oxygen, and the triad nitric oxide/superoxide/peroxynitrite contribute to liquid chemistry.^{35,44,55,60–62} Technical constraints of simulation studies limit the ability to address, e.g., local electron density changes or the degree of solvation. Experimental limitations include that natural occurring PTMs were focused, limiting the detection of unexpected modifications. However, the significant overlap with the plasma treatment of isolated amino acids suggests their extent to be minor.

E. Implications for cold plasma effectivity in biomedicine

Despite the known efficacy of cold plasma in biological systems *in vitro* and *in vivo*, a gap between the ns/ μ s time scales of the

gaseous plasma chemistry and the short lifetime of the reactive species involved compared to the substantial longer time scales of cellular processes (seconds to hours) must be acknowledged. In addition to direct effects of long-lived species (e.g., hydrogen peroxide), secondary processes resulting from the modifications of biomolecules by the short-lived species may modulate cell response and signaling processes. It was observed that the cold plasma treatment interferes with the protein structure and subsequently its function.^{11,63–67} More recently, oxidative modifications to proteins have been connected to changes in the immune response, possibly attenuating cancer cell immunoeediting. The current results reveal parts of the underlying molecular basis showing that cold plasma can introduce nonenzymatically post-translational modifications in a number of amino acids and that most of these PTMs belong to the natural subset that can be interpreted by the cellular machinery. Heavy oxidation directs a protein toward protein ubiquitinylation and subsequent degradation, or activates chaperons-like heat shock proteins to regain its normal function. Along with the significant oxidation of cysteine, seminal processes like the unfolded protein response that control cell fate and function can be triggered.⁶⁸ Less extensive modifications like nitrations or nitrosylations at tyrosine can be involved in kinase signaling cascades, influencing phosphorylation events as has been observed in the nitric oxide research community for the human aldolase A.⁶⁹ In this light, a strong link between the short-lived species in the discharge and the cells prolonged response can be found in the covalent modifications of proteins and peptides.

IV. SUMMARY AND CONCLUSION

Utilizing the model peptides bradykinin and angiotensin 1–7, nine different post-translational modifications (PTMs) were observed after cold plasma treatment (kINPen and COST-Jet). Major targets were the amino acids tyrosine, tryptophan, histidine, and phenylalanine as well as the aliphatic amino acids proline and isoleucine. In contrast, the amino acids valine, arginine, and aspartic acid remained mostly unchanged. The observed PTM patterns indicate the activity of the short-lived species hydroxyl radicals, atomic and singlet oxygen, and peroxynitrite. Frequent observed PTMs were nitration, oxidation (plus one/two oxygen atoms), and ring cleavage (e.g., histidine). Experimental data only in part overlap with a previously published molecular dynamics simulation, indicating that hydroxyl radicals are not the only—or major—oxidant. The chemical environment and steric restriction within the peptide chain significantly influenced the amino acids' reactivity, a fact requesting consideration when analyzing complex 3D structures like proteins. Since the observed PTMs belong to naturally occurring modifications, it can be assumed that CPPs derive their impact on biological systems in part via protein modification. The presented data pave the way for further studies to evaluate their impact on cellular signaling pathways in inflammatory processes in cancer and wound biology in full.

ACKNOWLEDGMENT

Funding from the German Federal Ministry of Education and Research [Grant Nos. 03Z22DN11 (S.B.) and 03Z22DN12 (K.W.)] supported this work.

REFERENCES

¹U. Schnabel, R. Niquet, U. Krohmann, J. Winter, O. Schluter, K. D. Weltmann, and J. Ehlbeck, *Plasma Process. Polym.* **9**, 569 (2012).

²M. Polak, J. Winter, U. Schnabel, J. Ehlbeck, and K.-D. Weltmann, *Plasma Process. Polym.* **9**, 67 (2012).

³A. Schmidt, S. Bekeschus, K. Wende, B. Vollmar, and T. von Woedtke, *Exp. Dermatol.* **26**, 156 (2017).

⁴H.-R. Metelmann, C. Seebauer, R. Rutkowski, M. Schuster, S. Bekeschus, and P. Metelmann, *Contrib. Plasma Phys.* **58**, 415–419 (2018).

⁵K. D. Weltmann, H. R. Metelmann, and T. von Woedtke, *Europhys. News* **47**, 39 (2016).

⁶P. J. Bruggeman *et al.*, *Plasma Sources Sci. Technol.* **25**, 053002 (2016).

⁷M. L. Semmler *et al.*, *Cancers* **12**, 269 (2020).

⁸A. Privat-Maldonado, A. Schmidt, A. Lin, K. D. Weltmann, K. Wende, A. Bogaerts, and S. Bekeschus, *Oxid. Med. Cell Longevity* **2019**, 9062098.

⁹J. Egea *et al.*, *Redox Biol.* **13**, 94 (2017).

¹⁰K. Wende, T. von Woedtke, K. D. Weltmann, and S. Bekeschus, *Biol. Chem.* **400**, 19 (2018).

¹¹J. W. Lackmann *et al.*, *J. Phys. D Appl. Phys.* **48**, 494003 (2015).

¹²E. Takai *et al.*, *J. Phys. D Appl. Phys.* **47**, 285403 (2014).

¹³T. Nybo *et al.*, *Redox Biol.* **20**, 496 (2019).

¹⁴Y. L. Deribe, T. Pawson, and I. Dikic, *Nat. Struct. Mol. Biol.* **17**, 666 (2010).

¹⁵G. Duan and D. Walther, *PLoS Comput. Biol.* **11**, e1004049 (2015).

¹⁶C. T. Lu *et al.*, *Nucleic Acids Res.* **41**, D295 (2013).

¹⁷S. Doll and A. L. Burlingame, *ACS Chem. Biol.* **10**, 63 (2015).

¹⁸R. Harmel and D. Fiedler, *Nat. Chem. Biol.* **14**, 244 (2018).

¹⁹R. Bischoff and H. Schluter, *J. Proteomics* **75**, 2275 (2012).

²⁰T. M. Karve and A. K. Cheema, *J. Amino Acids* **2011**, 207691.

²¹C. L. Hawkins and M. J. Davies, *J. Biol. Chem.* **294**, 19683 (2019).

²²M. Rykaer, B. Svensson, M. J. Davies, and P. Hagglund, *J. Proteome Res.* **16**, 3978 (2017).

²³K. D. Weltmann, E. Kindel, R. Brandenburg, C. Meyer, R. Bussiahn, C. Wilke, and T. von Woedtke, *Contrib. Plasma Phys.* **49**, 631 (2009).

²⁴S. Bekeschus, A. Schmidt, K.-D. Weltmann, and T. von Woedtke, *Clin. Plas. Med.* **4**, 19 (2016).

²⁵N. Knake, S. Reuter, K. Niemi, V. Schulz-von der Gathen, and J. Winter, *J. Phys. D Appl. Phys.* **41**, 6 (2008).

²⁶S. Schroter *et al.*, *Phys. Chem. Chem. Phys.* **20**, 24263 (2018).

²⁷J. W. Lackmann *et al.*, *Sci. Rep.* **8**, 7736 (2018).

²⁸C. Klinkhammer *et al.*, *Sci. Rep.* **7**, 13828 (2017).

²⁹K. Wende, G. Bruno, M. Lalk, K.-D. Weltmann, T. von Woedtke, S. Bekeschus, and J.-W. Lackmann, *RSC Adv.* **10**, 11598 (2020).

³⁰A. Stancampiano, T. Galligani, M. Gherardi, Z. Machala, P. Maguire, V. Colombo, J. M. Povesle, and E. Robert, *Appl. Sci. Basel* **9**, 3861 (2019).

³¹E. Simoncelli, A. Stancampiano, M. Boselli, M. Gherardi, and V. Colombo, *Plasma* **2**, 369 (2019).

³²J. Benedikt, M. Mokhtar Hefny, A. Shaw, B. R. Buckley, F. Iza, S. Schakermann, and J. E. Bandow, *Phys. Chem. Chem. Phys.* **20**, 12037 (2018).

³³Y. Gorbanev, J. Van der Paal, W. Van Boxem, S. Dewilde, and A. Bogaerts, *Phys. Chem. Chem. Phys.* **21**, 4117 (2019).

³⁴C. C. W. Verlact, W. Van Boxem, D. Dewaele, F. Lemiere, F. Sobott, J. Benedikt, E. C. Neyts, and A. Bogaerts, *J. Phys. Chem. C* **121**, 5787 (2017).

³⁵H. Jablonowski, J. Santos Sousa, K. D. Weltmann, K. Wende, and S. Reuter, *Sci. Rep.* **8**, 12195 (2018).

³⁶H. Tresp, M. U. Hammer, J. Winter, K. D. Weltmann, and S. Reuter, *J. Phys. D Appl. Phys.* **46**, 435401 (2013).

³⁷S. Reuter, T. von Woedtke, and K.-D. Weltmann, *J. Phys. D Appl. Phys.* **51**, 233001 (2018).

³⁸J. Golda *et al.*, *J. Phys. D Appl. Phys.* **49**, 084003 (2016).

³⁹S. Reuter, J. Winter, A. Schmidt-Bleker, H. Tresp, M. U. Hammer, and K. D. Weltmann, *IEEE Trans. Plasma Sci.* **40**, 2788 (2012).

⁴⁰M. Bern, Y. J. Kil, and C. Becker, *Curr. Protoc. Bioinformatics* **40**, 13.20.1 (2012).

⁴¹J.-W. Lackmann, G. Bruno, H. Jablonowski, F. Kogelheide, B. Offerhaus, J. Held, V. Schulz-von der Gathen, K. Stapelmann, T. von Woedtke, K. Wende, *PLoS One* **14**, e0216606 (2019).

⁴²G. Bruno, T. Heusler, J.-W. Lackmann, T. von Woedtke, K.-D. Weltmann, and K. Wende, *Clin. Plasma Med.* **14**, 100083 (2019).

⁴³O. Pagel, S. Lorocho, A. Sickmann, and R. P. Zahedi, *Expert Rev. Proteomics* **12**, 235 (2015).

⁴⁴J. W. Lackmann *et al.*, *PLoS One* **14**, e0216606 (2019).

⁴⁵T. von Woedtke, A. Schmidt, S. Bekeschus, K. Wende, and K. D. Weltmann, *In Vivo* **33**, 1011 (2019).

⁴⁶A. Michaeli and J. Feitelson, *Photochem. Photobiol.* **59**, 284 (1994).

⁴⁷K. Wende *et al.*, *Biointerphases* **10**, 029518 (2015).

⁴⁸A. Schmidt-Bleker, J. Winter, S. Iseni, M. Dunnbier, K. D. Weltmann, and S. Reuter, *J. Phys. D Appl. Phys.* **47**, 145201 (2014).

⁴⁹B. T. J. van Ham, S. Hofmann, R. Brandenburg, and P. J. Bruggeman, *J. Phys. D Appl. Phys.* **47**, 224013 (2014).

⁵⁰M. J. Davies, *Biochem. J.* **473**, 805 (2016).

⁵¹J. E. Plowman, S. Deb-Choudhury, A. J. Grosvenor, and J. M. Dyer, *Photochem. Photobiol. Sci.* **12**, 1960 (2013).

⁵²S. Bartesaghi and R. Radi, *Redox Biol.* **14**, 618 (2018).

⁵³R. E. Huie and S. Padmaja, *Free Radical Res. Commun.* **18**, 195 (1993).

⁵⁴P. Lukes, E. Dolezalova, I. Sisrova, and M. Clupek, *Plasma Sources Sci. Technol.* **23**, 015019 (2014).

⁵⁵H. Jablonowski, A. Schmidt-Bleker, K. D. Weltmann, T. von Woedtke, and K. Wende, *Phys. Chem. Chem. Phys.* **20**, 25387 (2018).

⁵⁶A. Schmidt-Bleker, J. Winter, A. Bosel, S. Reuter, and K. D. Weltmann, *Plasma Sources Sci. Technol.* **25**, 015005 (2016).

⁵⁷L. Hansen, A. Schmidt-Bleker, R. Bansemmer, H. Kersten, K.-D. Weltmann, and S. Reuter, *J. Phys. D Appl. Phys.* **51**, 474002 (2018).

⁵⁸A. Schmidt-Bleker, R. Bansemmer, S. Reuter, and K.-D. Weltmann, *Plasma Process. Polym.* **13**, 1120 (2016).

⁵⁹S. Bekeschus *et al.*, *Sci. Rep.* **7**, 2791 (2017).

⁶⁰P. Heirman, W. Van Boxem, and A. Bogaerts, *Phys. Chem. Chem. Phys.* **21**, 12881 (2019).

⁶¹V. S. S. K. Kondeti, C. Q. Phan, K. Wende, H. Jablonowski, U. Gangal, J. L. Granick, R. C. Hunter, and P. J. Bruggeman, *Free Radical Biol. Med.* **124**, 275 (2018).

⁶²C. Breen, R. Pal, M. R. J. Elsegood, S. J. Teat, F. Iza, K. Wende, B. R. Buckley, and S. J. Butler, *Chem. Sci.* **11**, 3164 (2020).

⁶³Z. G. Ke and Q. Huang, *Plasma Process. Polym.* **10**, 731 (2013).

⁶⁴E. Takai, K. Kitano, J. Kuwabara, and K. Shiraki, *Plasma Process. Polym.* **9**, 77 (2012).

⁶⁵P. Attri *et al.*, *Sci. Rep.* **5**, 8221 (2015).

⁶⁶G. Nayak, H. A. Aboubakr, S. M. Goyal, and P. J. Bruggeman, *Plasma Process. Polym.* **15**, 1700119 (2018).

⁶⁷J.-W. Lackmann, E. Edengeiser, S. Schneider, J. Benedikt, M. Havenith, and J. E. Bandow, *Plasma Med.* **3**, 115 (2013).

⁶⁸C. Hetz and F. R. Papa, *Mol. Cell* **69**, 169 (2018).

⁶⁹Y. Sekar, T. C. Moon, C. M. Slupsky, and A. D. Befus, *J. Immunol.* **185**, 578 (2010).

Article A2

Reactive species driven oxidative modifications of peptides—Tracing physical plasma liquid chemistry

S. Wenske, J.-W. Lackmann, L.-M. Busch, S. Bekeschus, T. von Woedtke and K. Wende. *J. Appl. Phys.*, 129 (19), 193305, 2021.

© 2021 Author(s)

Reactive species driven oxidative modifications of peptides—Tracing physical plasma liquid chemistry

Cite as: J. Appl. Phys. **129**, 193305 (2021); <https://doi.org/10.1063/5.0046685>

Submitted: 05 February 2021 • Accepted: 28 April 2021 • Published Online: 21 May 2021

Sebastian Wenske,  Jan-Wilm Lackmann, Larissa Milena Busch, et al.

COLLECTIONS

Paper published as part of the special topic on [Plasma-Liquid Interactions](#)



View Online



Export Citation



CrossMark

ARTICLES YOU MAY BE INTERESTED IN

[Plasma-driven solution electrolysis](#)

Journal of Applied Physics **129**, 200902 (2021); <https://doi.org/10.1063/5.0044261>

[The essential role of the plasma sheath in plasma-liquid interaction and its applications—A perspective](#)

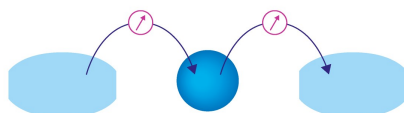
Journal of Applied Physics **129**, 220901 (2021); <https://doi.org/10.1063/5.0044905>

[Nonenzymatic post-translational modifications in peptides by cold plasma-derived reactive oxygen and nitrogen species](#)

Biointerphases **15**, 061008 (2020); <https://doi.org/10.1116/6.0000529>

Webinar

Interfaces: how they make
or break a nanodevice



March 29th – Register now



Zurich
Instruments

Reactive species driven oxidative modifications of peptides—Tracing physical plasma liquid chemistry

Cite as: J. Appl. Phys. 129, 193305 (2021); doi: 10.1063/5.0046685

Submitted: 5 February 2021 · Accepted: 28 April 2021 ·

Published Online: 21 May 2021



Sebastian Wenske,¹ Jan-Wilm Lackmann,²  Larissa Milena Busch,³ Sander Bekeschus,¹ 
Thomas von Woedtke,^{4,5}  and Kristian Wende^{1,a)} 

AFFILIATIONS

¹ZIK plasmatis, Leibniz Institute for Plasma Science and Technology (INP Greifswald), Felix-Hausdorff-Straße 2, 17489 Greifswald, Germany

²Cluster of Excellence Cellular Stress Responses in Aging-Associated Diseases, University of Cologne, Joseph-Stelzmann-Straße 26, 50931 Cologne, Germany

³Interfaculty Institute of Genetics and Functional Genomics, Department of Functional Genomics, University Medicine Greifswald, Felix-Hausdorff-Straße 8, Greifswald, Germany

⁴Leibniz Institute for Plasma Science and Technology (INP Greifswald), Felix-Hausdorff-Straße 2, 17489 Greifswald, Germany

⁵Institute for Hygiene and Environmental Medicine, University Medicine Greifswald, Walther-Rathenau-Str. 48, 17489 Greifswald, Germany

Note: This paper is part of the Special Topic on Plasma-Liquid Interactions.

^{a)}**Author to whom correspondence should be addressed:** kristian.wende@inp-greifswald.de

ABSTRACT

The effluence of physical plasma consists of a significant share of reactive species, which may interact with biomolecules and yield chemical modifications comparable to those of physiological processes, e.g., post-translational protein modifications (oxPTMs). Consequentially, the aim of this work is to understand the role of physical plasma-derived reactive species in the introduction of oxPTM-like modifications in proteins. An artificial peptide library consisting of ten peptides was screened against the impact of two plasma sources, the argon-driven MHz-jet kINPen and the helium-driven RF-jet COST-Jet. Changes in the peptide molecular structure were analyzed by liquid chromatography–mass spectrometry. The amino acids cysteine, methionine, tyrosine, and tryptophan were identified as major targets. The introduction of one, two, or three oxygen atoms was the most common modification observed. Distinct modification patterns were observed for nitration (+N + 2O–H), which occurred in kINPen only (peroxynitrite), and chlorination (+Cl–H) that was exclusive for the COST-Jet in the presence of chloride ions (atomic oxygen/hypochlorite). Predominantly for the kINPen, singlet oxygen-related modifications, e.g., cleavage of tryptophan, were observed. Oxidation, carbonylation, and double oxidations were attributed to the impact of hydroxyl radicals and atomic oxygen. Leading to a significant change in the peptide side chain, most of these oxPTM-like modifications affect the secondary structure of amino acid chains, and amino acid polarity/functionality, ultimately modifying the performance and stability of cellular proteins.

© 2021 Author(s). All article content, except where otherwise noted, is licensed under a Creative Commons Attribution (CC BY) license (<http://creativecommons.org/licenses/by/4.0/>). <https://doi.org/10.1063/5.0046685>

I. INTRODUCTION

The 2019 Nobel Prize in Physiology and Medicine was awarded to the discovery that the degradation of the protein hypoxia-inducible factor 1 α is accelerated by its hydroxylation under normal oxygen levels, while in lack of oxygen—such as stroke—the protein is not hydroxylated and accumulates, launching physiological countermeasures.^{1,2} This example illustrates the important role of (oxidative) post-translational

modifications (oxPTMs) in the regulation, protein functionality, and relevance for most cellular signaling pathways.^{3,4} More than 200 different (ox)PTMs are known, dominated by phosphorylation, acetylation, and ubiquitinylation with a massive impact on a proteins function and lifetime.⁵ Kinase-driven protein phosphorylation⁶ activates or prevents downstream signals⁷ and was found relevant in the response of mammalian cells toward cold physical plasma treatment (CAP).⁸

The role of oxPTMs^{9,10} on cellular signaling is in the focus of research activities, fostered by the improvement of high-resolution mass spectrometry instrumentation and workflows.^{11–13} For a long time, (ox)PTMs had been considered as signs of destruction only, such as aging processes.¹⁴ A complex regulation network is currently being revealed, it has been proven that downregulation (distress) and stimulating effects (eustress) coexist,^{15,16} and the cellular processes are influenced by various modifications at the same time. Apoptosis, for example, is regulated by S-nitrosylation,¹⁷ N-acetylation,¹⁸ and N-myristoylation.¹⁹

Controlled production of reactive oxygen and reactive nitrogen species (ROS/RNS) is also found in cold physical plasma, generating short- and long-lived reactive species, which are capable of reacting with most biomolecules and representing an emerging field of redox therapy. Due to its unique properties, physical plasma serves many applications. For long, it has been used for decontamination²⁰ or the refinement of various surfaces.²¹ Recently, physical plasma treatments have been proven to be useful in medical applications, e.g., the treatment of chronic wounds^{22,23} or cancers.^{24–27} However, the molecular mechanisms are not yet fully understood. It remains elusive, i.e., which species penetrate sufficiently in biological systems and which of those are (chemically) active to trigger downstream signals. While the long-lived plasma-derived species as H₂O₂, nitrite, and nitrate can be easily quantified and used as fundamental markers for CAP treatment, the short-lived species are difficult to access. However, they appear to be of significant importance.^{28–35} Given their high reactivity, a penetration seems unlikely. Alternatively, it may be hypothesized that exposure of biomolecules to short-lived species yields secondary products, which have biological effects on themselves and ultimately modulate the physiological processes in a cell or tissue.

A number of reports indicate that amino acids in proteins are excellent targets for plasma-derived reactive species.^{36–40} In addition, their regulation via physiological (ox)PTMs offers an excellent intersection with physical plasma. The aim of this work is, therefore, to determine the impact of plasma-derived reactive species on model peptides, focusing on the formation of artificial non-enzymatic post-translational modifications. To gain an overview of a variety of gas phase chemistries, the argon-driven kINPen was compared to the helium-driven COST-Jet⁴¹ while modulating the discharge parameters including the gas phase composition. To investigate these modifications, high-resolution mass spectrometry coupled to nanoflow liquid chromatography and subsequent bioinformatical analysis were used.

II. EXPERIMENTAL

A. Development of the artificial peptide library

A peptide library of ten peptides with a length of ten amino acids each was designed and synthesized (ProteoGenix, Schiltigheim, France) in such a way, that the 20 major proteino-genic amino acids occur with equal incidence (Fig. 1 and Table S1 in the [supplementary material](#)). In addition, the peptide sequence was designed to locate each amino acid at the N-terminus, the C-terminus, and the center region and to have as many different neighboring amino acids as possible, exemplified for alanine (A, red) and tryptophan (W, blue) in Fig. 1.

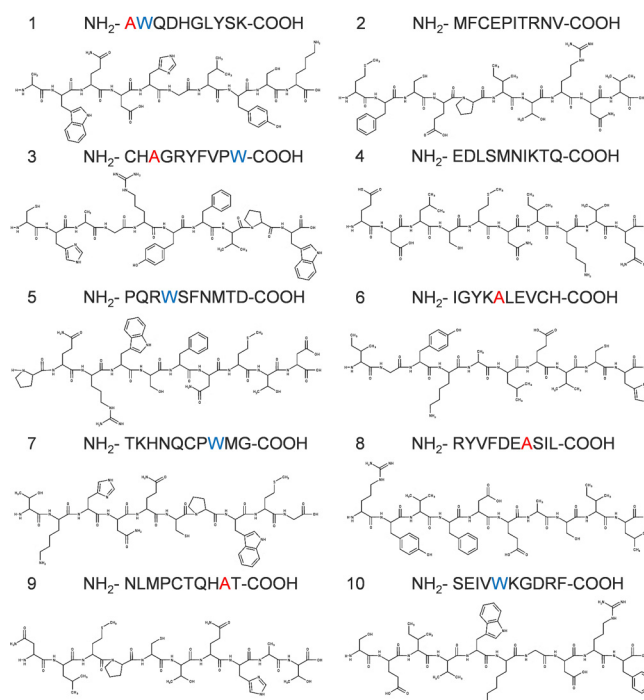


FIG. 1. Expanded peptide sequence of the ten-peptide library challenged with physical plasma-derived reactive species. Alanine (A, red) and tryptophan (W, blue) exemplify the varying positions adopted by each amino acid in the peptides.

B. Treatment conditions and plasma sources

The peptides were dissolved in double distilled water (Merck Millipore, Darmstadt, Germany) or phosphate buffered saline (PBS, Sigma Aldrich, Deisenhofen, Germany) at a concentration of 0.1 mg/ml. Both solvents were degassed by bubbling with argon gas for at least 30 min to reduce background reactions. The treatments with cold atmospheric pressure plasma were performed with an argon plasma jet (kINPen, neoplas tools GmbH, Greifswald, Germany) and a helium plasma jet (COST-Jet, a standard device identified by the European COST action MP 1101 “Biomedical Applications of Atmospheric Pressure Plasma Technology”). The kINPen⁴² [Fig. 2(b)] consists of a grounded ring electrode enclosing a ceramic capillary, where a powered central rod electrode is located inside (2–6 kV_{pp} at 1.1 MHz). A 3000 standard cubic centimeters per minute (SCCM) flow of argon (Air Liquide, 99.999%) served as the main feed gas. For some treatments, 0.5/1% of the feed gas was replaced by oxygen (15 SCCM) or by oxygen + nitrogen (15 sccm each). The COST-Jet [Fig. 2(a)] consists of two 1 mm thick metal plate electrodes leaving a 1 mm gap, where the plasma is ignited. The capacitively coupled electrodes are driven by an AC voltage at 13.56 MHz. The dissipated power was held constant at 330 mW by using a Tektronix DPO 4104 Digital Phosphor Oscilloscope in accordance with Ref. 41. The helium feed gas flow was kept at 1000 SCCM and if desired, enriched with 0.5% oxygen (5 SCCM), or 0.5% oxygen + 0.5% nitrogen (5 SCCM each).

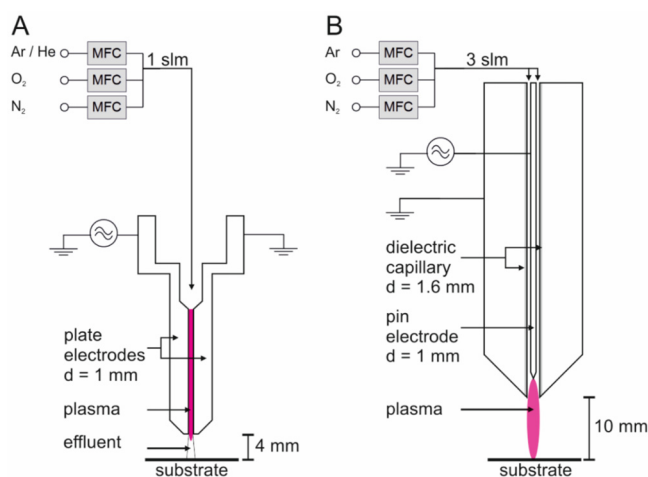


FIG. 2. Schematics of the COST-Jet (a) and kINPen (b). MFC: mass flow controller, sLm: standard liter per minute. For details, see text. Reprinted with permission from Lackmann *et al.*, *Sci. Rep.* **8**, 7736 (2018). Copyright 2018 Author(s), licensed under a Creative Commons Attribution (CC BY) License.

750 μl of each peptide solution (water/PBS) was placed in 24-well plates and treated 15 or 60 s with a nozzle to a liquid distance of 4 mm (COST-Jet) or 9 mm (kINPen) for each gas mix (feed gas + O_2 or O_2/N_2). For indirect treatments, the procedure was adapted: only the solvents were plasma-treated and the peptides were added 1 min after the plasma was switched off as a bolus solution. After each individual treatment, samples were placed on ice, and immediately analyzed by nanoflow liquid chromatography-mass spectrometry (nano-LC-MS/MS), to minimize post-discharge reactions. Three independent experiments and measurements were performed. The long-lived species H_2O_2 , nitrate (NO_3^-) and nitrite (NO_2^-) were determined according to the previously published approach.³⁸

C. Nano-LC-MS/MS acquisition

For nanoflow liquid chromatography mass spectrometry, an UltiMate 3000 RSLCnano (Thermo Scientific, Dreieich Germany) system was used with an Acclaim Pepmap C18 column (150 mm \times 75 μm , 2.0 μm particle size, Thermo Scientific, Dreieich Germany) with the corresponding precolumn (20 mm \times 100 μm , 5.0 μm particle size). The injection volume was 1 μl , equaling 100 ng of the sample. A gradient (see Table I) consisting of water/0.1% v/v acetic acid (A) and acetonitrile/0.1% v/v acetic acid (B) was applied to achieve separation.

Mass spectrometry acquisition was carried out in a data dependent mode with a full scan range of 86.7–1300 m/z (resolution 70 000) and with the fragmentation of the top ten most abundant precursor ions (QExactive Hybrid-Quadrupol-Orbitrap, Thermo Scientific, Dreieich Germany). Precursor ions were fragmented using normalized higher energy collisional dissociation (HCD, 27.5 eV) and detected at a mass resolution of 17 500 at m/z 200. The automatic gain control (AGC) target for full MS was set

TABLE I. Flow gradient for nano-LC separation of peptides on a PepMap100 C18 column. A = water/0.1% v/v acetic acid, B = acetonitrile/0.1% v/v acetic acid.

Eluent B (%)	Time (min)	Flow ($\mu\text{l}/\text{min}$)
15	0	0.700
18	4.5	0.700
22	10.5	0.700
85	11	0.700
85	15	0.700
15	17	0.700
15	20	0.700

to 1×10^6 ions and for MS/MS to 2×10^5 ions with a maximum ion injection time of 120 ms for both modes. Dynamic exclusion was set to 30 s and ions with charge state one or above eight were excluded.

D. Raw data analysis, data handling, and statistics

To identify the peptides and their potential post-translational modifications, the MS raw data were analyzed by the software Proteome Discoverer 2.4 (Thermo Scientific, Dreieich Germany). For the detection of covalent modifications in the amino acid chain, the software Byonic (Protein Metrics), version 3.6.0, was used as a plug-in tool. In contrast to the Proteome Discoverer, this program is able to perform unlimited searches for multiple modifications in a single peptide. The precursor mass tolerance was set to 3 parts per million (ppm) and fragment mass tolerance to 10 ppm. The false discovery rate (FRD) was set to 1%. For technical limitations, the allowed maximum of modifications per peptide was set to three. The dataset was pre-filtered using different scores from Byonic.⁴³ The first filter was the Byonic score with a cut-off of 250 (range 0–1000), and the Delta Mod score was set to 5 (range from 0 to 100). Both scores result from the match of the theoretical fragment spectrum of a peptide and the experimental one. Following vendor recommendations, these cut-offs can be considered significant. To obtain semi-quantitative data, the number of peptide spectra matches (PSMs) that were detected for a specific modification were counted (PSM counting).⁴⁴

In total, 103 497 PSMs were analyzed with R (v4.0.2)⁴⁵ using RStudio (v1.3.1093) and the Tidyverse (v1.3.0)⁴⁶ package. The observation data were normalized on the total number of spectra matches for each peptide to account for variances in the ionization efficiency after background subtraction, yielding the occurrence of *de novo* modifications in percent. Linear models [later referred to as n-way analysis of variance (ANOVA)] were used to analyze the effects of discharge parameters on peptide modification. This statistical method was chosen due to its simplicity, the existence of negative values in the dependent variable (percentage of modifications), and the assumption that in general modification percentages in similar treated samples show a Gaussian distribution. The percentage of one particular PTM was modeled as a result of the categorical effects: (1) amino acid, (2) peptide, (3) solvent, (4) plasma, (5) indirect or direct treatment, and (6) treatment time. To address the issue, that the amino acid sites of the modification (not only the

type of modification) might be dependent on the effects (2) to (6) as well, models were additionally fitted considering those interactions. Fitted models with and without interactions were compared for each modification and the models with interaction were significantly more fitting (F-Test; p -value $< 2.2 \times 10^{-16}$). This indicates an important impact of the “biochemical” background for the occurrence of modifications.

III. RESULTS AND DISCUSSION

A. Sulfur-containing and aromatic amino acids are the major targets of plasma-derived reactive species

The dominant targets within the investigated peptide library were the sulfur-containing amino acids cysteine (Cys) and methionine (Met) and the aromatic amino acids tryptophan, tyrosine, and phenylalanine (see Fig. 3), corroborating previous studies using cold physical plasma (CAP).^{36–39} The thiol group of cysteine and the thioether group of methionine are excellent targets for oxidation, carrying predominantly one oxygen (Met) or even three (Cys), in this case forming the strongly acidic sulfonic acid moiety. This oxidation is irreversible; prohibiting the formation of sulfide bridges and consequently interferes with protein folding and signaling processes. Alongside, modifications containing only one (cysteine sulfenic acid) or two oxygen atoms (cysteine sulfinic acid) are possible and have been found using cysteine as a model compound during CAP treatment.^{28,30} These oxidation states are still reversible in physiologic conditions, e.g., via sulfiredoxin activity, but under CAP impact quickly convert into the stable sulfonic acid form. Further oxidation yielding sulfate and a residual alanine has been found for CAP-driven cysteine oxidation; however, a conversion from cysteine to alanine was not observed in the studied peptide library. Methionine monoxidation is prevalent *in vivo* and is a marker for oxidative stress.⁴⁷ It occurs during sample preparation by oxidation via triplet oxygen as an artifact, indicating the high reaction probability at the thioether. Methionine oxidation is

linked to conformational changes of proteins, modulating their functionality.⁴⁸

From the group of aromatic amino acids, tryptophan (Trp) is the major target. The possible chemical reactions are far more complex than for Cys or Met, with special regards to the heterocyclic nature of one of the two annealed rings.⁴⁹ The position of the nitrogen within the rings increases the electron density in both rings, facilitating electrophile substitution reactions introducing oxygen, nitrogen, or chloride atoms that subsequently allow elimination or oxidation reactions enriching the observable product portfolio. In addition, the N-containing 5-ring substructure is prone to ring cleavages via a variety of reaction pathways (see below). Due to its bulkiness and relative hydrophobicity, Trp is typically found in the inner and/or hydrophobic parts of a protein, impeding access by reactive species from the outside. The impact on protein function is hard to predict due to the diversity of the products.

Next to Trp, tyrosine (Tyr) and phenylalanine (Phe) as hydroxybenzene resp. benzene derivatives of α -amino propionic acid belong to the most relevant targets of CAP-derived reactive species. However, due to the higher electron density in the aromatic ring of Tyr resulting from the hydroxyl group, this amino acid is far more often modified than Phe. Again, electrophile substitution reactions dominate, and downstream reactions yield a variety of products. While one or two additional hydroxyl groups and the corresponding oxidation products (quinones, semi-quinones) dominate, an interesting role can be attributed to nitrogen-derived modifications, especially nitration. Nitrated tyrosine residues are reported as markers for oxidative stress. The presence of the electron-pulling nitro group in the aromatic system decreases the pK_a value of the amino acid hydroxyl group, subsequently increasing the probability for its phosphorylation by regulatory proteins (tyrosine kinases).^{50,51} Therefore, a significant impact on protein functionality can be assumed.

The other 15 amino acids are modified by CAP-derived species to a (far) lesser extent. However, some of the observed modifications are indicative of the presence of specific reactive species and may serve as a diagnostic marker (see below). Ahead of all, lysine (Lys) with its ϵ -positioned primary amino group is sensitive toward hypochlorite, a species that is generated from atomic oxygen when conditions allow. The products comprise simple chlorination, and addition–elimination reactions ultimately yielding multiple bonds in the Lys molecule.

Somewhat unexpectedly, most of the aliphatic amino acids like valine (Val), leucine (Leu), and isoleucine (Iso) were often targeted, indicating a significant role of primary or secondary generated OH radicals. The products were hydroxylated molecules that in the physiologic context may be relevant by increasing the hydrophilicity of the respective amino acid yielding a modulation of protein conformation and interaction with binding partners. The polar amino acids aspartic acid (Asp), asparagine (Asn), glutamic acid (Glu), glutamine (Gln), arginine (Arg), and serine (Ser) rarely bore modifications. Since these amino acids carry electron-rich structures such as hydroxyl and carboxyl groups or a guanidinium moiety, a significant reactivity was expected.⁵² However, most bonds in the respective moieties are resonance stabilized, reducing their reactivity. In addition, they can reform without a permanent change in the chemical composition exemplified in the following reaction (1):

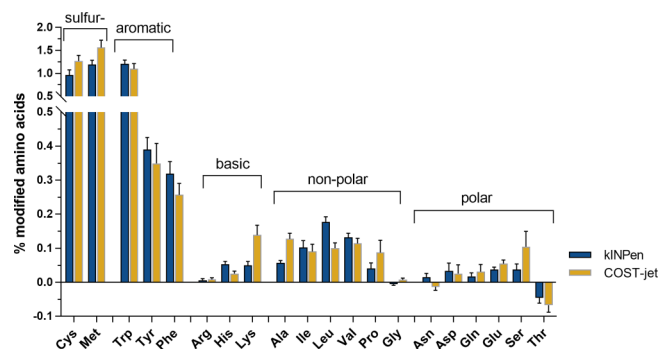
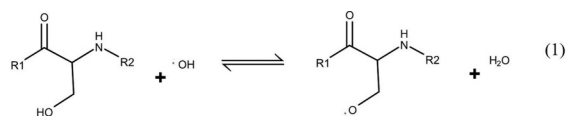
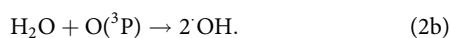
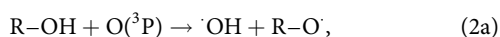


FIG. 3. Occurrence of amino acid modifications in all direct treatment conditions for kINPen (Ar, in part w/ admix, blue) or COST-Jet (He, in part w/ admix, yellow). Amino acids are sorted according to their major chemical characteristics. Data presented relative to the untreated peptide control. Note the split y axis.



The formation of an alkoxy radical via H-atom abstraction, shown in (1) for a serine moiety, is a typical reaction of an OH radical.⁵³ The radical may return to ground state by reaction with water. Alkoxy radicals are not very reactive, yet dimerization forming a peroxide or hydroperoxide can occur.⁵⁴ Since this structure is not stable, the reverse reaction yields to the initial hydroxyl group. Alternatively, atomic oxygen, O(³P), can replace the OH radical, as shown in (2),⁵⁵



When applying the reaction (1) to an aliphatic amino acid, a two-step reaction yields hydroxylated amino acids. The resulting product 3-hydroxy valine (3b) is stable and yields a permanent

change that is annotated as hydroxylation (+15.99 Da),



The annular amino acids histidine (His) and proline (Pro) remain predominantly unchanged (Fig. 3), except when Pro has an exposed amino group in position one in the peptide (peptide 5, NH₂-PQRWSFNMT-COOH). His has a special reactivity toward singlet oxygen, yielding ring-open products (see below).

B. Reactive oxygen-derived modifications dominate in the product profile

In all, 17 different modifications were observed in the investigated peptide library. Assumingly, all of these derived from the attack of reactive species contained a differing number of oxygen atoms. In some cases, oxygen is eliminated during formation or

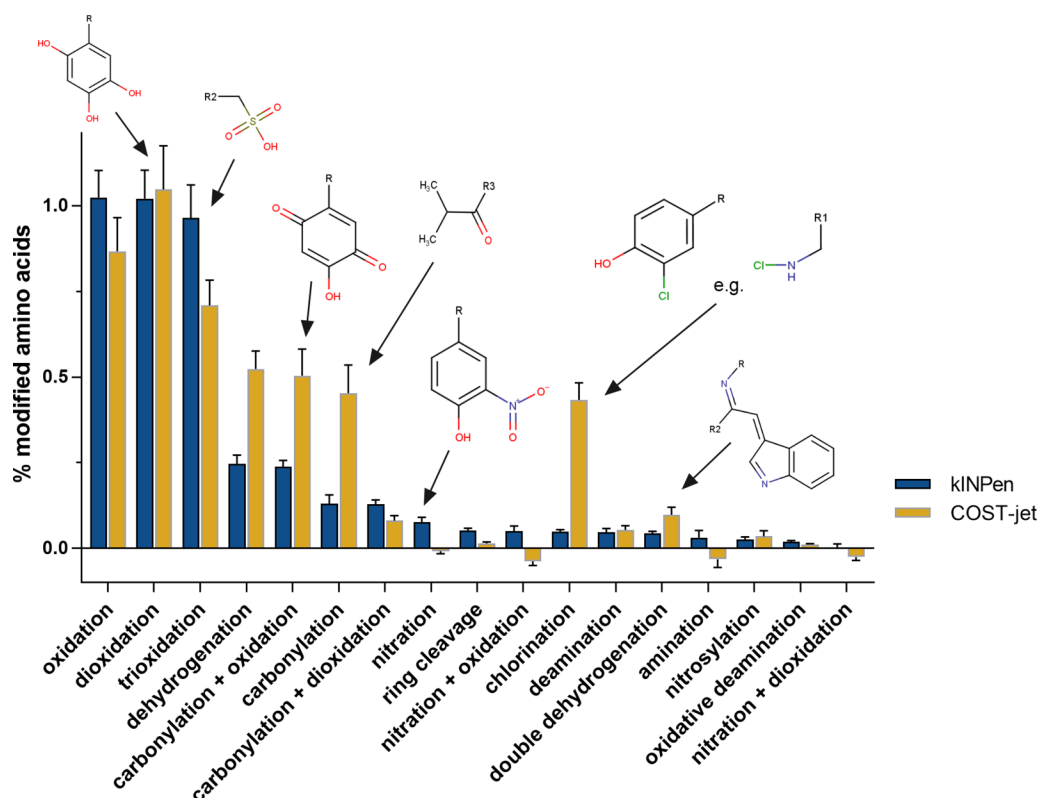


FIG. 4. Most relevant modifications after direct treatment within the peptide library. Data presented relative to the untreated peptide control. Background artifacts were removed. Chemical structures exemplify modifications with high incidence, basing on tyrosine, cysteine, isoleucine, lysine, or tryptophan.

TABLE II. Major amino acid modifications observed within the ten-peptide library after plasma treatment.

Monoisotopic mass shift (Da)	Elemental composition	Chem. mod./(potential product)
+15.99	+O	Oxidation (e.g., hydroxyl group)
+31.98	+2O	Dioxidation (two hydroxyl groups, peroxide)
+47.98	+3O	Trioxidation (hydroxyl group + peroxide, three hydroxyl groups, sulfonic acid)
+28.99	+N + O–H	Nitrosylation (nitroso group)
+44.98	+N + 2O–H	Nitration (nitro group)
+60.98	+N + 3O–H	Nitration + oxidation
+76.97	+N + 4OH	Nitration + dioxidation
+0.98	–N–H + O	Deamination (loss of amino group)
–0.98	+N + H–O	Amination (amino group)
+13.98	+O–2H	Carbonylation (oxo group)
+29.97	+2O–2H	carbonylation + oxidation (oxo group + hydroxyl group)
+45.97	+ 3O–2H	Carbonylation + dioxidation (oxo group + two hydroxyl groups or peroxide)
–2.02	–2H	Dehydrogenation (loss of two hydrogen atoms, creating a double bond)
–4.03	–4H	Double dehydrogenation (two double bonds)
+4.98	+2O–N–C–H	Ring cleavage (histidine: formylasparagine)
–3.05	+O–5H–N	Oxidative deamination (lysine) ³⁶
+33.96	+Cl–H	Chlorination (chlorine atom replaces hydrogen)

downstream reactions. Of the detected modifications, 13 contained oxygen atoms, up to three (Fig. 4 and Table II). Two modifications (dehydrogenation/double dehydrogenation) were solely characterized by a loss of atoms, forming multiple bonds. In one modification (chlorination), chlorine apparently replaces one hydrogen atom in the initial molecule. Nitrogen, as the second most relevant contributor to the CAP-derived reactive species, contributed to five modifications. However, the abundance of such modifications is significantly lower than that for the oxygen counterparts. Besides a lower prevalence of reactive nitrogen species in the investigated discharges, subsequent elimination reactions further reduce their presence as indicated by the deamination of free amino groups that are observed under some conditions. Some of these modifications are created by enzymatic processes during physiological post-translational processing and via redox-controlled signaling events,^{3,18,56} pointing at the potential to interfere with protein and ultimately cell functionality via CAP-derived reactive species. The major modifications base on the introduction of gas phase derived hydroxyl radicals or atomic oxygen as shown for the aliphatic amino acids [reaction (3)].^{30,32} The hydroxylation observed in the aliphatic amino acids, according to (3a) and (3b), may be driven by hydroxyl radicals. However, due to the slow reaction of atomic oxygen with water ($2.2 \times 10^{-23} \text{ m}^3 \text{ s}^{-1}$), yielding to hydroxyl radicals [reaction (2)],⁵⁷ their role may be limited while the direct attack of atomic oxygen at the peptide amino acid moieties is in favor ($1.1 \times 10^{-17} \text{ m}^3 \text{ s}^{-1}$).³² This is in contrast to experiments using Fenton's reaction to generate hydroxyl radicals in liquids, indicating that this model suffers limitations when used to mimic plasma-derived reactive species.⁵⁸ A significant role of singlet oxygen is indicated by the fact that by far the insertion of two oxygen atoms, yielding a dihydroxylation or peroxidation, prevails over monooxidation (hydroxylation) or triple hydroxylation. Since the peroxides are unstable during sample preparation and analysis, two hydroxyl groups are the oxidative modification observed.⁵⁹

In addition, ring cleavage reactions in histidine and tryptophan (see below) are indicative for 2 + 2 or 4 + 2 cycloaddition reactions known for singlet oxygen. In the presence of chloride ions, CAP-derived atomic oxygen leads to the formation of hypochlorite (OCl^-).^{31,33} The OCl^- ion is unstable; it acts as a chlorination agent and an oxidant, yielding a number of prominent modifications, above all chlorination, carbonylation, and dehydrogenation. The molecule is reactive and reacts both with primary amines, yielding *N*-chloro- or *N,N*-dichloro compounds (chloramines)⁶⁰ and with aromatic systems,⁶¹ yielding mono-, di-, or trichloro derivatives (electrophilic substitution). Accordingly, lysine and tyrosine were the main targets observed (Fig. 5 and Fig. S2 in the supplementary material). Surprisingly, no significant chlorination could be found at phenylalanine; although its aromatic ring is similar to Tyr, it lacks the electron-pushing hydroxyl group. Further modifications related to the presence of atomic oxygen are dehydrogenations and the formation of oxo groups (carbonylation). In both cases, addition–elimination reaction occurs. The peptide backbone (amide bonds) was insensitive toward hypochlorite and no fragments have been detected. Since chloride ions are ubiquitous in biological systems, hypochlorite and its downstream products (ClO_2^- , ClO_3^-)⁶² and described peptide modifications must be considered for all plasma discharges creating atomic oxygen.

C. The type of plasma source and the working gas composition determine the introduction of peptide modifications

While it was already shown that the feed gas composition of a given plasma source influences the presence of modifications for some amino acids bound in a peptide,^{37–39} the current approach using a peptide library should provide a more general insight. Despite a general concordance in the main target amino acids and

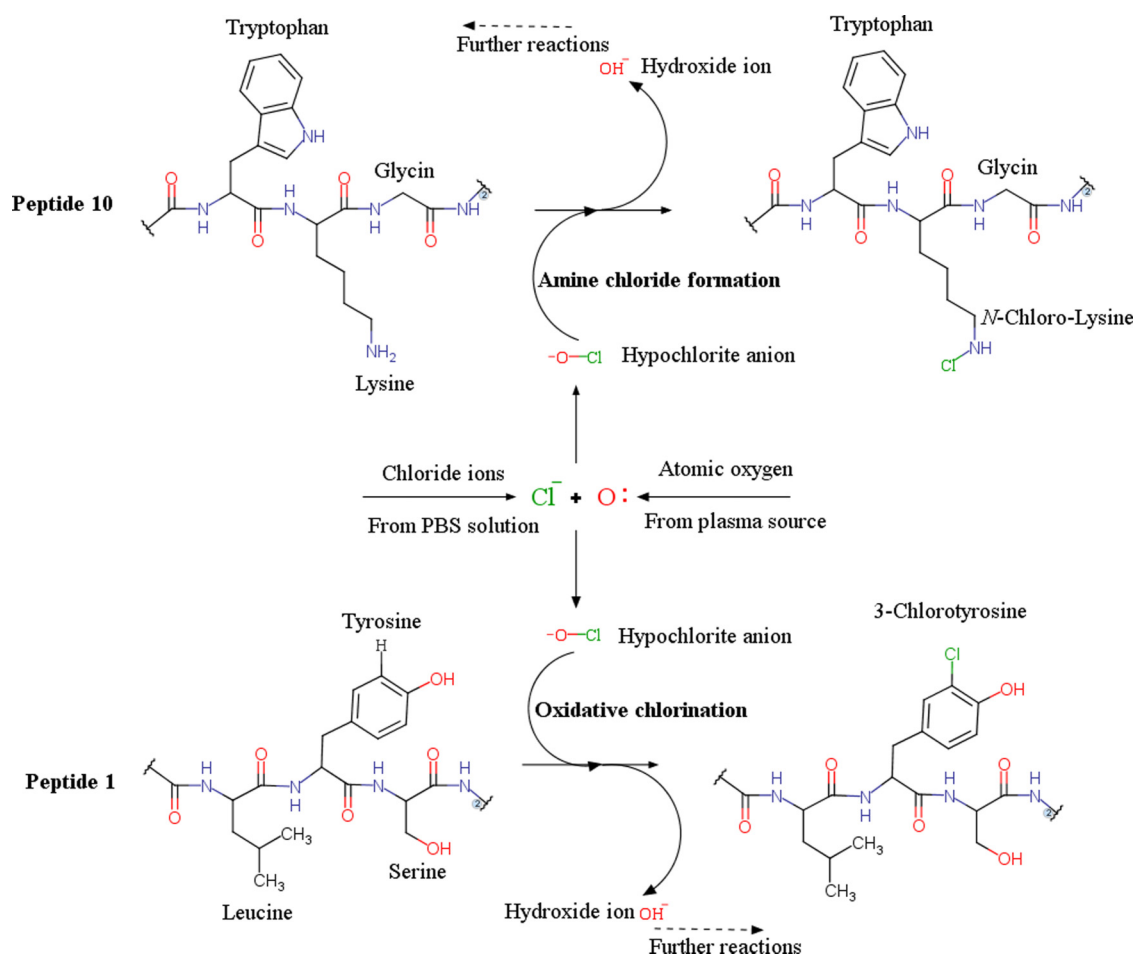


FIG. 5. Suggested reaction mechanism for the generation of *N*-chloro-lysine in peptide 10 ($\text{NH}_2\text{-SEIWWKGDRF-COOH}$) and 3-chlorotyrosine in peptide 1 ($\text{NH}_2\text{-AWQDHGLYSK-COOH}$). Shown is the structure of lysine and tyrosine and the two respective neighboring amino acids tryptophan and glycine as well as leucine and serine. Hypochlorite is formed by the atomic oxygen from the plasma source and chloric ions in solution from PBS. The amine chloride formation and oxidative chlorination take place with the elimination of a hydroxyl anion for further reactions like carbonylation.

the type of introduced modifications (Figs. 3 and 4), explicit differences can be found for a number of specific gas plasma conditions [Figs. 6(a) and 6(b)]. The most obvious difference between the two plasma sources is the introduction of chlorination, carbonylation, and additional double bonds (one/two dehydrogenations) that were observed for the COST-Jet (He/O_2) mainly and are related to the prominent generation of atomic oxygen by this device. For example, the amino acid lysine that was not attacked by kINPen was chlorinated extensively. However, when the COST-jet is driven in the He-only mode, the reactivity is almost completely lost. Instead, kINPen treatment yielded trioxidation (e.g., three hydroxyl groups) and the cleavage of heterocyclic rings that are related to the reactivity of singlet oxygen. In contrast to the COST-Jet, the kINPen also introduced nitrogen-containing modifications, especially nitration, in part combined with oxidation. Both plasma sources did not differ in the total number of the most common

modification, the simple hydroxylation (+16 Da). Some amino acids were modified by the COST-Jet modified to a larger extent, e.g., serine, methionine, and cysteine, probably due to the atomic oxygen density of this device. In contrast, phenylalanine was a better target for the kINPen-derived species. Most aliphatic amino acids (e.g., valine and isoleucine) are modified to a similar extent by both plasma sources, and no clear correlation with the working gas composition was found.

The observations reflect the differences of the working gases argon and helium regarding the formation and lifetime of higher energy states and the different electrode configuration/driving power, yielding differences in reactive species formation and dynamics, which is further modulated by the addition of molecular gases.^{63,64} For the helium-only COST-Jet, an almost complete absence of any modifications was noticed, indicating the inability of He higher energy states to reach the surface of the target and a

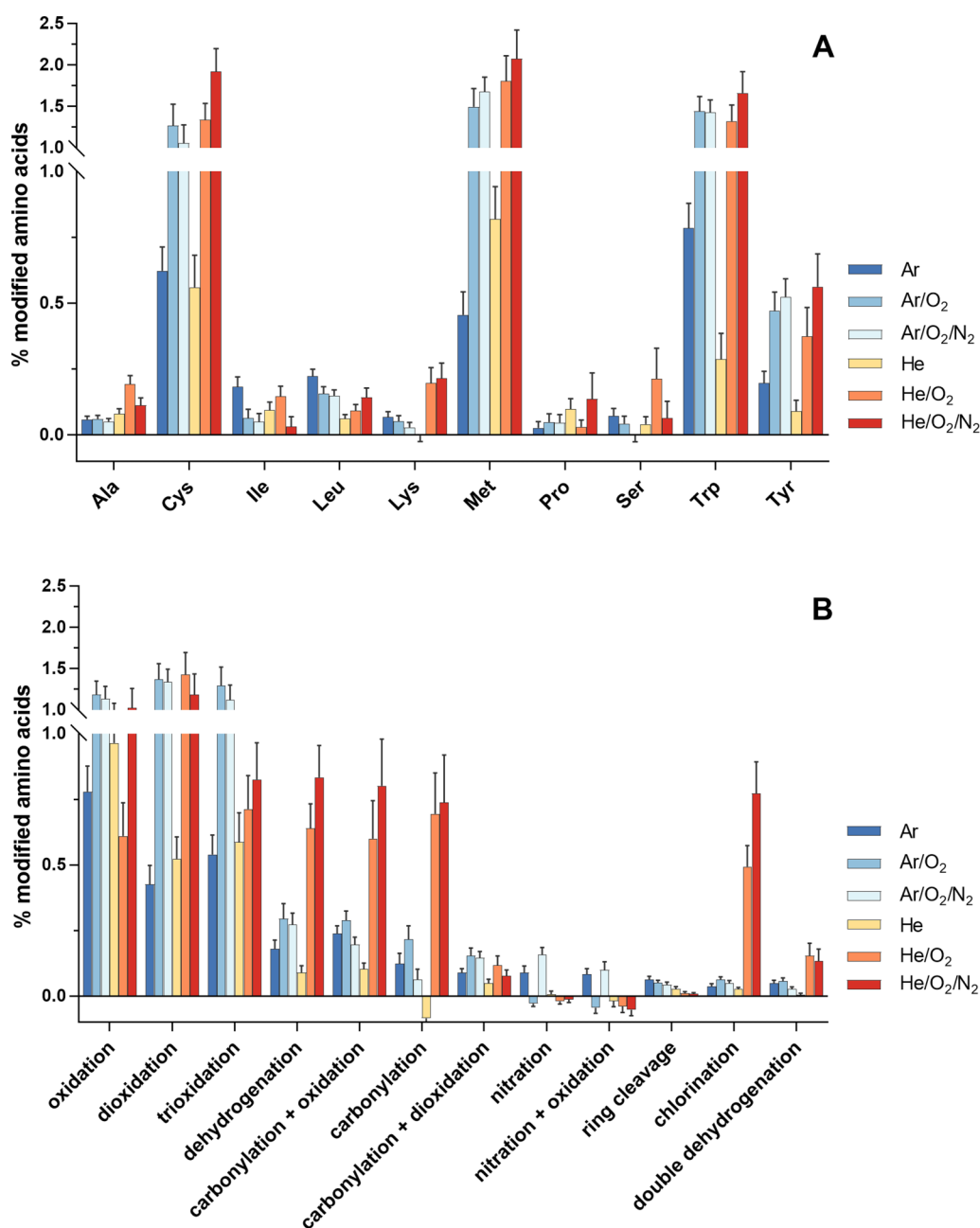


FIG. 6. Most frequently modified amino acids (a, in alphabetical order) and major modifications (b) for kINPen (blue, Ar) or COST-Jet (yellow-red, He) when modulating the working gas composition (+0.5% oxygen or +0.5% oxygen and +0.5% nitrogen). The occurrence relative to the untreated peptide control is given.

very limited impact of ambient air species due to a laminar gas flow leading to a minimum of reactive species.

kINPen in the Ar-only mode retained a high basal generation of ROS and RNS due to the turbulent effluent and the subsequent interaction with the ambient air, and the higher mobility of argon higher energy states. The device showed an interesting modification

pattern regarding carbonylation, ring cleavage reactions, and nitration. Carbonylation, which is dominant for the COST-jet and induced by atomic oxygen, was detected for Ar/O₂ treatment and decreases again with N₂-admixture. This indicates that kINPen forms atomic oxygen to a limited extent, but the observed chemistry is dominated by singlet oxygen³⁵ and N_xO_y molecules.⁶⁵

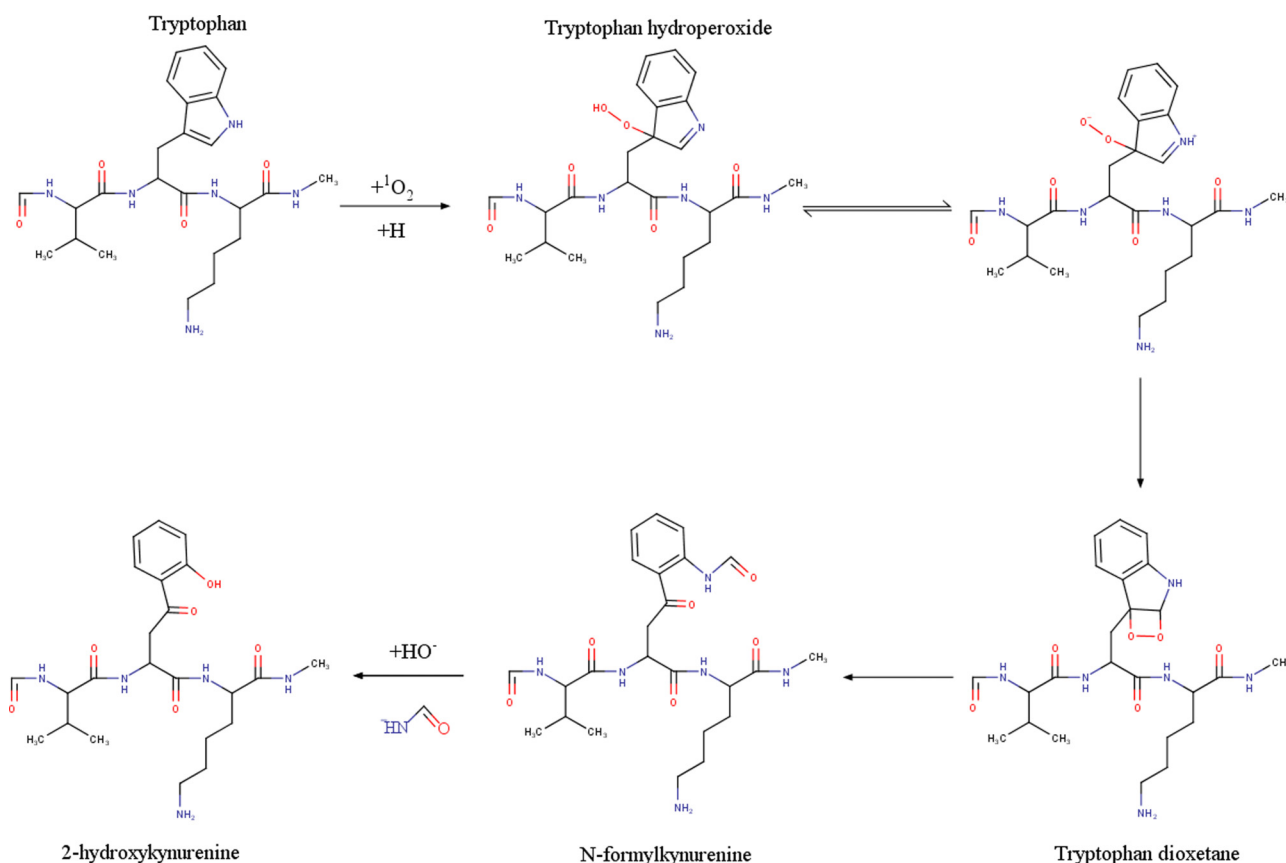


FIG. 7. Tryptophan cleavage by singlet oxygen yielding kynurenine derivatives ($+20\text{-N-C-H}$, $+4.98$ Da). For explanation, see text.

Second, ring cleavage reactions at tryptophan or histidine, which are maximal in argon only conditions and decrease with each additional gas, are exclusively formed after kINPen treatments. The reaction is attributed to singlet oxygen and the potential mechanism for the reaction with tryptophan is shown in Fig. 7.^{49,66} Initially, singlet oxygen attacks the carbon atom and forms tryptophan hydroperoxide, which converts to the tryptophan dioxetane. Alternatively, a $2+2$ cycloaddition yields directly the dioxetan ring. Subsequent rearrangement forms the *N*-formylkynurenine. In the last step, the final product 2-hydroxykynurenine is formed under the attack of a hydroxyl ion. It remains elusive why the addition of oxygen does not favor an increase of Trp cleavage, since the generation of singlet oxygen increases in this condition.³⁵ It may be speculated that either changes in reactive species dynamics at the boundary layer and the liquid bulk reduced the fraction of the chemically active singlet oxygen (e.g., ozone formation) or subsequent secondary reactions after the initial cleavage of the Trp moiety led to non-recognizable modifications. Third, the introduction of nitro groups into aromatic amino acids (nitration, nitration + oxidation), which is exclusive for the kINPen, appears for Ar or Ar/O₂/N₂ admixtures but not in Ar/O₂, supporting the above conclusion. Nitration is mainly found in peptides

1 (NH₂-AWQDHGLYSK-COOH) and 6 (NH₂-IGYKALEVCH-COOH) at tyrosine (Fig. 11). An assumed mechanism for the nitration of the peptide is shown in Fig. 8.

Assumingly, peroxyinitrite is the main responsible reactive species. Its generation by plasmas is well-recognized^{68,69} and production at the interface from nitric oxide and superoxide anion radicals can be assumed.⁷⁰ If only oxygen is available in the discharge, NO[•] can no longer be generated in sufficient quantity and thus ONOO⁻ generation ceases, yielding a reduced number of nitrations [Fig. 6(b)]. Additionally, secondary reactions remove the bulky nitro groups in favor of hydroxyl groups or quinones.⁷¹ In Fig. 9, the amino acids Cys, Lys, Pro, Ser, Trp, and Tyr are compared, displaying strong differences in type and amount of modifications in dependence on the used plasma source and between the different amino acids. This is specifically obvious for amino acids that can be modified by chlorination (Tyr, Lys), or singlet oxygen (Trp).

D. Short-lived vs long-lived species—The remaining plasma chemistry after the plasma is switched off

It remained questionable, which contribution from long-lived reactive species can be expected for the above-described

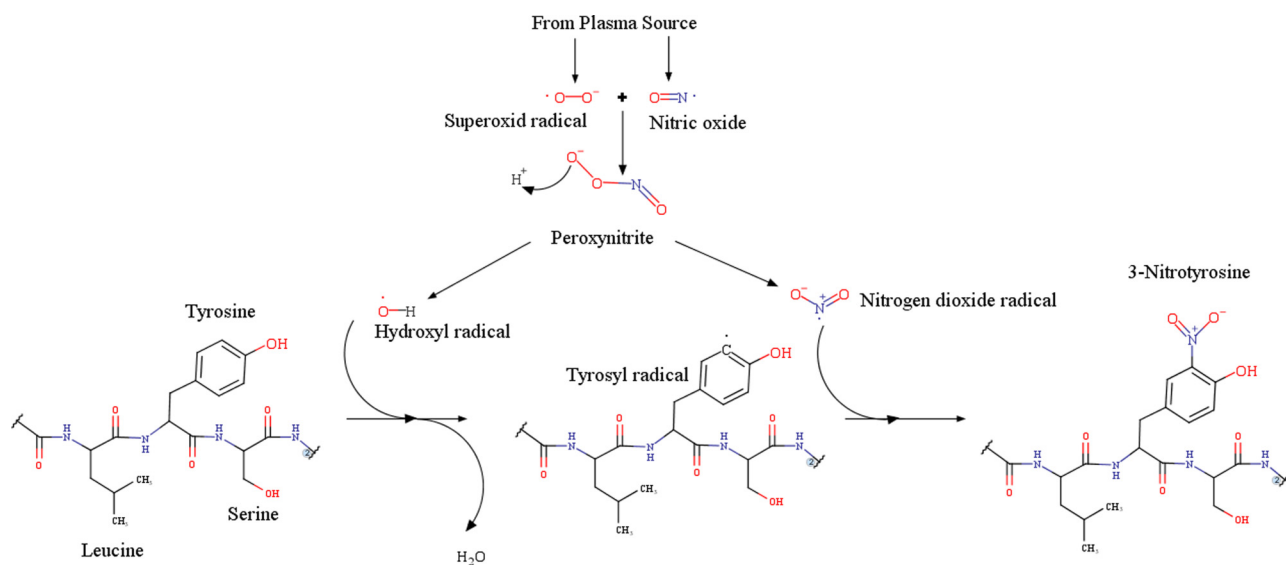


FIG. 8. Suggested reaction mechanism for the production of 3-nitrotyrosine in peptide 1, showing the structure of tyrosine and the two neighboring amino acids leucine and serine. Peroxynitrite is formed from the superoxide radical and nitric oxide and decomposes into an OH- and NO_2 -radical. In a first intermediate step, a tyrosyl radical is formed, which is then attacked by the nitrogen dioxide radical to form nitrotyrosine in a second step. Adapted from Ref. 67.

modifications. Hydrogen peroxide, nitrate, or ozone are formed to a varying degree during the treatment.³⁸ The medium-lived OCl^- chemistry preserves the short-lived atomic oxygen and requires to be considered likewise. Therefore, the peptides were exposed to CAP in two orthogonal approaches: the peptides were present either during the discharge was ignited (direct treatment) or were added to the liquid after the discharge had been switched off (indirect treatment). A significant difference between direct and indirect treatment regimens was observed for the two plasma sources [Figs. 10(a) and 10(b)], predominantly inflicted by the hypochlorite chemistry [Figs. 10(c) and 10(d)]. Amino acids sensitive to OCl-driven chlorination (Tyr, Lys) or carbonylation (Ser, Trp) were major targets of the indirect COST-Jet treatment. The co-occurrence of the two modifications strongly suggests that the hypochlorite ion is an active agent for both cases. In contrast, kINPen favored modifications generated during direct treatments, driven by the chemical impact of hydroxyl radicals, atomic oxygen, or singlet oxygen (Cys, Trp, Tyr). Therefore, nitration and the ring cleavages that occur only in direct treatments emphasize the role of the short-lived singlet oxygen and NO_2 radicals.⁷²

Perpetuating investigations on the role of the environment during the impact of plasma-derived ROS, the modification of peptides dissolved in water or a buffered, chloride ions containing system (PBS) was compared. In addition to the discussed hypochlorite chemistry, PBS favored reactions that benefit from higher pH such as the oxidation of thiol groups and aminations. Direct oxidations by gas phase species (atomic oxygen, singlet oxygen) decrease in PBS since the abundant chloride ions depress species density at the boundary layer significantly. Therefore, the number of ring cleavages at Trp is reduced in PBS. Reactions, which accelerate at low pH, e.g., nitrations, were found in water predominantly.

E. The chemical environment influences the modification pattern of an amino acid in the peptide chain

The role of the chemical environment of a given amino acid in the peptide chain determined by its position and neighboring amino acids is considered. To exemplify the situation, the nitration of tyrosine is considered (+44.98 Da; +N + 2O-H). While mostly observed for the kINPen (Ar, Ar/ N_2/O_2), its appearance fluctuated for the different tyrosine residues present in the library (see Fig. S4 in the supplementary material). Clearly, the sequence and the spatial structure of the peptides are relevant: in peptide 3 ($\text{NH}_2\text{-CHAGRYFVPW-COOH}$) and peptide 8 ($\text{NH}_2\text{-RYVFDEASIL-COOH}$), phenylalanine (Phe) is in close neighborhood to the modified tyrosine. The weakly reactive Phe has a large aromatic ring, interfering either by reducing access to the tyrosine moiety by steric hindrance, or by reducing the reactivity of the tyrosine's aromatic ring via hydrogen bonds or charge-transfer complexes.⁷³ In contrast, the tyrosine moieties of peptide 1 ($\text{NH}_2\text{-AWQDHGLYSK-COOH}$) and 6 ($\text{NH}_2\text{-IGYKALEVCH-COOH}$) do not have amino acids with bulkier or aromatic side chains nearby and can, therefore, be nitrated unhindered (Fig. 11). A similar observation has been made for complete proteins.⁷⁴ A second example is the chlorination (+33.96 Da, +Cl-H) (Fig. S2 in the supplementary material). Comparing all peptides in the library, the tyrosine in peptide 6 showed the highest sensitivity to chlorination. A possible explanation is that tyrosine is the exclusive target for oxidative chlorination in this peptide. The only other aromatic structure in the peptide is the imidazole ring of histidine, but this is located far from the targeted tyrosine and not prone for oxidative chlorination. Besides the ϵ -amino groups of lysine

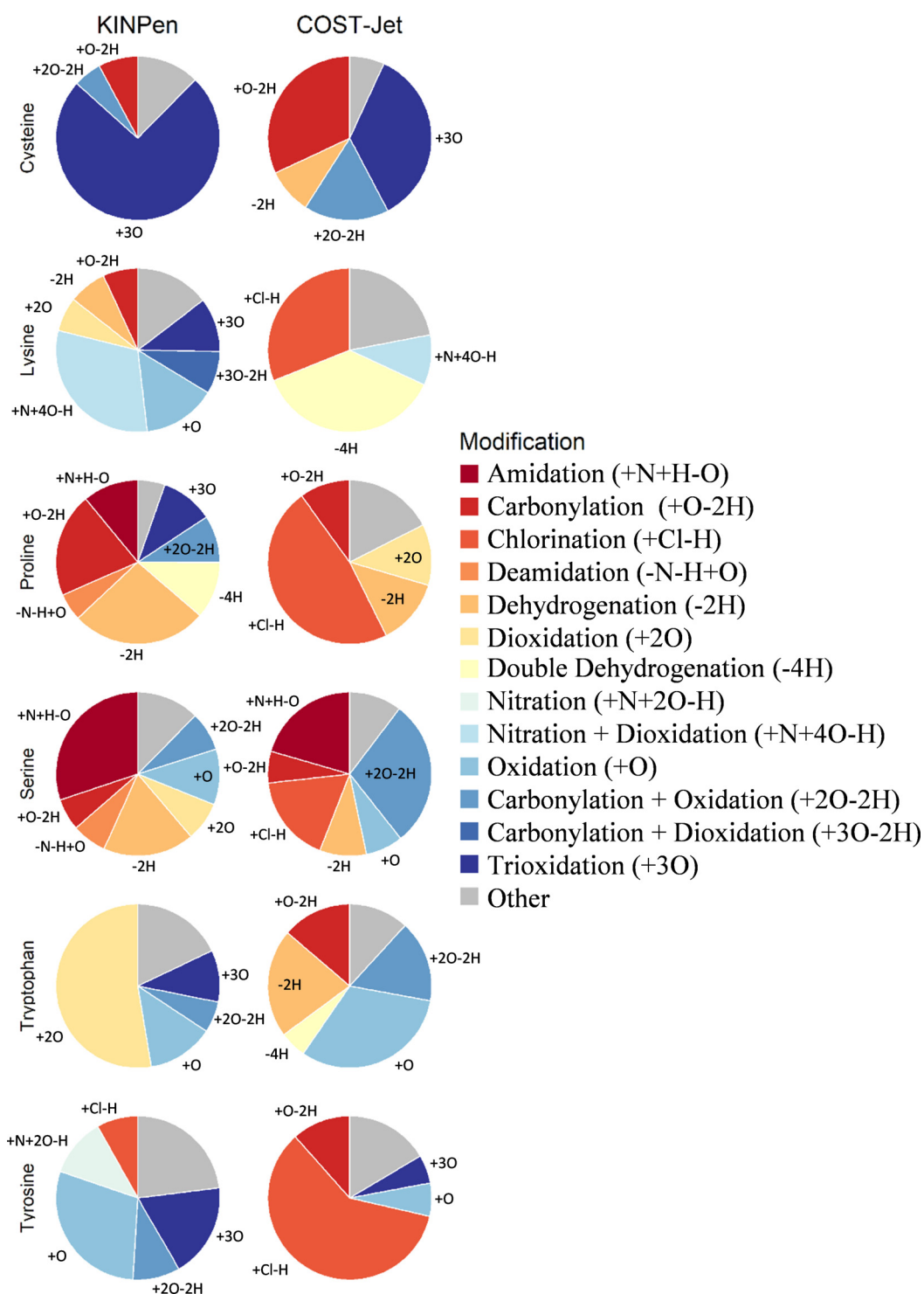


FIG. 9. Relative distribution of the most frequently identified modifications at the amino acids Cys, Lys, Pro, Ser, Trp, and Tyr after kINPen (left column) or COST-Jet treatments (right column). Treatment variations were not distinguished to reduce complexity. Shown are those modifications that contribute with at least 5% to the total amount. All remaining modifications are shown as "other."

within the peptide chain, the amino groups at the N-terminus of all peptides were chlorinated in appropriate conditions. The α -amino groups incorporated in the peptide chain as part of the peptide bond are not attacked. Cysteine is among the most frequently modified amino acids in the set and shows distinct differences in type and frequency of modifications (Fig. S5 in the supplementary material). The amino acid occurs at different positions in the peptides 2 (NH₂-MFCEPITRNV-COOH), 3 (NH₂-CHAGRYFVPW-COOH), 6 (NH₂-IGYKALEVCH-COOH), 7 (NH₂-TKHNQCPWMG-COOH), and 9 (NH₂-NLMPCTQHAT-COOH). It is worth mentioning that the cysteine in peptides 3 and 6 both have histidine as a neighboring amino acid and in peptides 7

and 9, proline is next to the cysteine. However, the modifications at cysteine in peptides 3 and 6 differ significantly.

While mono-/di-/trioxidation was found on the cysteine in peptide 6 in most treatment conditions, this is not the case for the cysteine in peptide 3. Here, cysteine is located at the N-terminus, while it is close to the C-terminal in peptide 6. Potentially, the local pH, which modulates the thiol group reactivity drastically, differs. The pKa value of the thiol group may range between pKa = 3.5 and 10, spanning several log-steps.⁷⁵ A high degree of dissociation aligns with a reaction probability. Yet, the isoelectric points (pI) of peptides 3 (pI = 8.23) and 6 (pI = 6.74) do not suggest a higher probability of cysteine oxidation in peptide 6. However, peptide 3

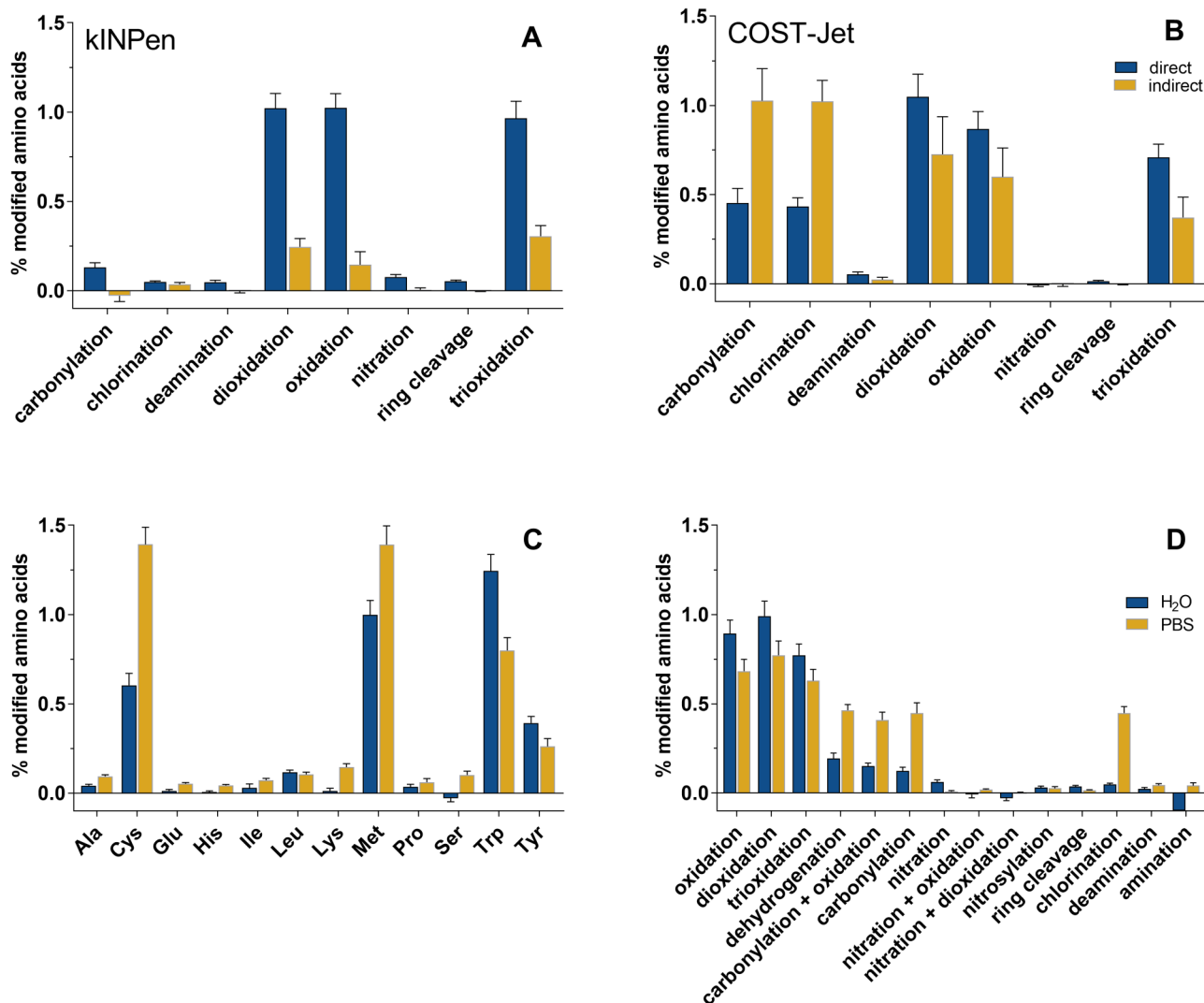


FIG. 10. The impact of timing: figures (a) (kINPen) and (b) (COST-Jet) compare the occurrence of plasma-driven modification after a direct treatment (peptide present in solution during plasma ignited, blue bars) or indirect treatment (yellow bars, peptide added to a plasma-treated solution after discharge was switched off). Impact of pH and chloride ion availability on target amino acids (c) and occurrence of modifications (d) indicate a strong role of atomic oxygen driven hypochlorite and are the basis of the strong impact of the COST-jet in indirect plasma treatment (PBS, phosphate buffered saline, pH 7.4).

has a C-terminally located tryptophan, which is an excellent scavenger for the plasma-generated species. It was shown that tryptophan reacts with a rate constant of $3.2 \times 10^7 \text{ M}^{-1} \text{ s}^{-1}$ ⁷⁶ with singlet oxygen ($^1\text{O}_2$), which is the fastest compared to other amino acids. In addition, since Trp is hydrophobic and the N-terminus protonated, the peptide adopts a protecting inward position of cysteine at the highly reactive interface toward the liquid bulk. Positively charged amino acids stabilize the resulting thiolate anion and contribute to the lower pKa, in parallel increasing the thiol group reactivity of the cysteine.⁷⁷ A similar observation was made for the cysteine residues the peptides 7 and 9. Redox-signaling proteins, e.g., peroxiredoxins, exploit this diversity in reactivity.⁵⁶ In addition, there is increasing evidence that oxidative modifications are in crosstalk with other regulatory post-translational modifications, controlling cells performance.⁵¹

F. Relationship of modifications, amino acids, and treatment conditions

Using statistical tools, the relationship between the plasma source, the mode of treatment, the treatment time, and the solvent

system was analyzed [Figs. 12(a) and 12(b)]. The best correlation between the targeted amino acids or observed modifications and the conditions under test was found for the mode of treatment (direct vs indirect). Corroborating, the solvent system (water or PBS) had a strong impact on the target. Both indicators point toward short-lived reactive species including the atomic oxygen-derived hypochlorite as major ROS/RNS. Of note, the treatment time exerted a very limited impact compared to the other parameters. This indicates to some degree the technical limitations of the adopted approach of PSM counting to quantify the observed modifications. It even more emphasizes the relevance of interface reactions, where the full amount of gas phase reactive species is present at any given time point during the treatment process. Whether a depletion of the boundary layer by fast gas phase species–target molecule reactions might be of relevance, leading to an increasing inefficacy of the treatment with longer treatment time, might be debatable.

A boundary layer depletion was observed for hypochlorite formation, and cysteine or glutathione thiol group oxidation.^{28,33,39,62} Experiments segregating the target peptides and the boundary layer yielded to a different pattern of modifications, indicating again that

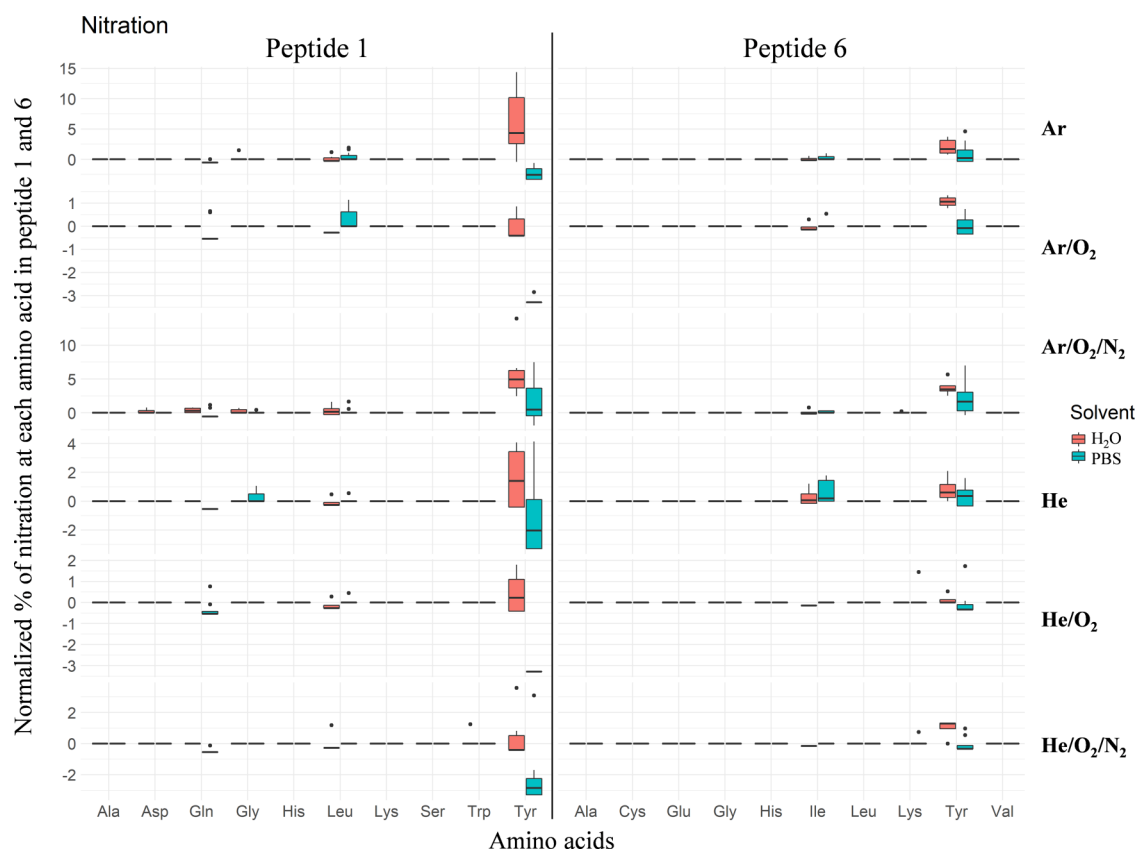


FIG. 11. Overview of every identified nitration in peptides 1 and 6. Divided according to the peptides in which the nitration was identified, and according to the different plasma treatment conditions. The percentage value of the nitrations both in water (orange) and PBS (green) are given and normalized to the amount of nitration found for the corresponding untreated peptide.

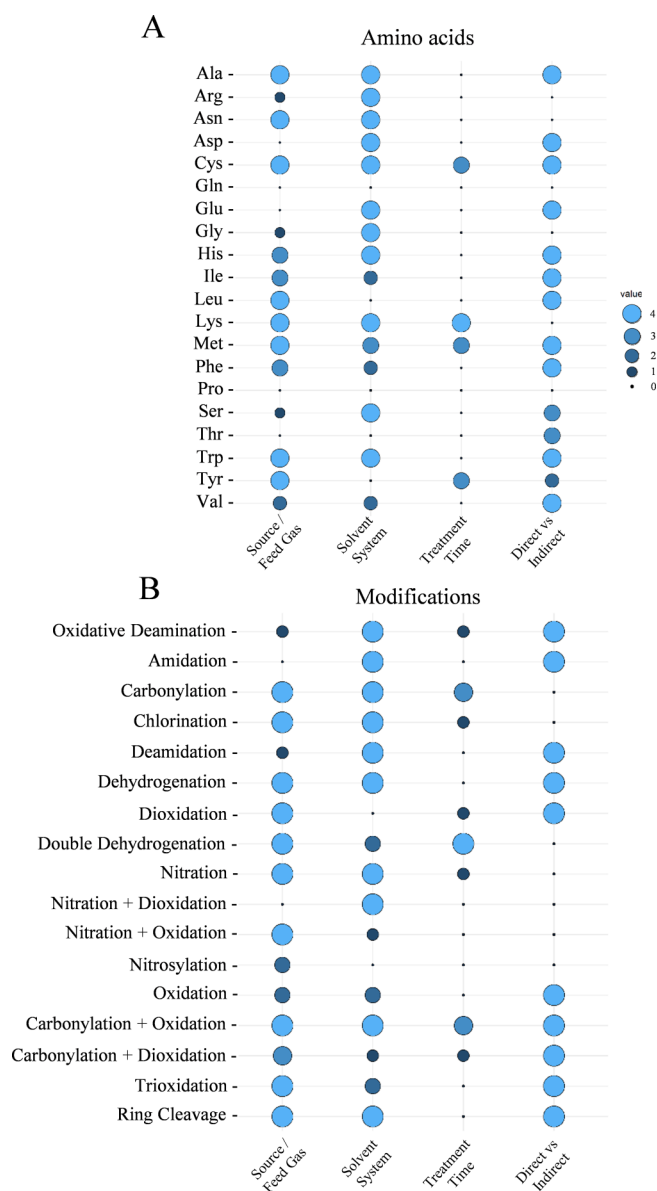


FIG. 12. Using ANOVA-test calculated dependencies of amino acids (a) and modifications (b) related to the gas composition of the plasma, solvent, treatment time, and treatment conditions (direct or indirect). Significance levels: "4" $p \leq 0.001$; "3" $p \leq 0.01$; "2" $p \leq 0.05$; and "1" $p \leq 0.1$.

interface reactions are dominant for all conditions where either atomic oxygen is irrelevant or chloride ions are not present. For future studies, it seems to be worth extending the investigated solvent systems, since the dominant role of chloride ions depends according to the literature on their concentration, modulating the hypochlorite formation. In addition, the presence of scavengers common to complex biological systems influences the modification pattern. Pilot experiments indicated a fundamental impact of free

histidine on the modification pattern. In the human skin, urocanic acid, a catabolite of histidine, may serve the same function.⁷⁸

IV. SUMMARY AND CONCLUSIONS

This work focused on the detection of covalent modifications introduced by reactive oxygen and nitrogen species from cold physical plasmas in a model peptide library. Major targets were the amino acids cysteine, methionine, tyrosine, and tryptophan bearing additional oxygen, nitrogen, or chlorine atoms forming additional hydroxyl, oxo, nitro, or chloro groups. The type of the modification and their extent depend on the CAP source, treatment conditions, the environment of the peptide or protein, and the local chemical environment of each amino acid. Dominant short-lived reactive species were atomic oxygen, singlet oxygen, and to a lesser extent hydroxyl radicals. The formation of hypochlorite and peroxyxynitrite showed a significant contribution to peptide modification. Long-lived species like hydrogen peroxide, nitrite, or nitrate were irrelevant. The cleavage of histidine and tryptophan pointed on singlet oxygen, a major product of the Ar-driven kINPen. Atomic oxygen, a major product of He/O₂ discharges (COST-Jet), left a significant mark via chlorination when favored by conditions.

Most of the newly introduced groups are identical or equivalent to the enzymatically introduced post-translational modifications (oxPTMs) in physiologic protein processing or cell signaling. They are stable enough to withstand sample preparation and mass spectrometry analysis, suggesting that such *de novo* introduced peptide or protein modifications occur *in vitro* and *in vivo* after a CAP treatment and may subsequently modulate local signaling or protein functionality. Reports on the impact of myeloperoxidase-derived products on the fibrous matrix protein fibronectin emphasize this notion,^{61,79} underlining the unique potential of CAP to interfere with biological processes via the modification of biomolecules.

SUPPLEMENTARY MATERIAL

In the [supplementary material](#), a complete overview of all oxidation (Fig. S1) and chlorination events (Fig. S2) for all peptides in the library is shown. The modifications are normalized and divided between the different peptides, gas compositions, and treatment conditions (Fig. S1) or the solvent system (Fig. S2). Figure S3 shows the impact of the different treatment times (15 and 60 s) for nine different amino acids (S3A) and ten different modifications (S3B). Figure S4 gives a similar overview, like Fig. S1, for all modifications identified at cysteine in the five peptides that contained this amino acid. Finally, Table S1 displays the peptide sequence (single letter amino acid code) for the whole library together with the corresponding molar mass and the calculated isoelectric point.

ACKNOWLEDGMENTS

Funding from the German Federal Ministry of Education and Research (Grant No. 03Z22DN11 to S.B. and 03Z22DN12 to K.W.) supported this work. The authors thank Niklas Lengner for laboratory assistance.

DATA AVAILABILITY

The data that support the findings of this study are available from the corresponding author upon reasonable request.

REFERENCES

- ¹G. L. Semenza, *Physiology* **19**, 176 (2004).
- ²P. H. Maxwell, M. S. Wiesener, G.-W. Chang, S. C. Clifford, E. C. Vaux, M. E. Cockman, C. C. Wykoff, C. W. Pugh, E. R. Maher, and P. J. Ratcliffe, *Nature* **399**, 271 (1999).
- ³A. L. Santos and A. B. Lindner, *Oxid. Med. Cell. Longev.* **2017**, 5716409 (2017).
- ⁴T. M. Karve and A. K. Cheema, *J. Amino Acids* **2011**, 207691 (2011).
- ⁵M. Audagnotto and M. Dal Peraro, *Comput. Struct. Biotechnol. J.* **15**, 307 (2017).
- ⁶G. Burnett and E. P. Kennedy, *J. Biol. Chem.* **211**, 969 (1954).
- ⁷M. K. Tarrant and P. A. Cole, *Annu. Rev. Biochem.* **78**, 797 (2009).
- ⁸A. Schmidt, S. Bekeschus, K. Jarick, S. Hasse, T. von Woedtke, and K. Wende, *Oxid. Med. Cell. Longev.* **2019**, 7017363 (2019).
- ⁹C. Waszczak, S. Akter, S. Jacques, J. Huang, J. Messens, and F. Van Breusegem, *J. Exp. Bot.* **66**, 2923 (2015).
- ¹⁰B. J. Ryan, A. Nissim, and P. G. Winyard, *Redox Biol.* **2**, 715 (2014).
- ¹¹G. A. Figtree, C.-C. Liu, S. Bibert, E. J. Hamilton, A. Garcia, C. N. White, K. K. M. Chia, F. Cornelius, K. Geering, and H. H. Rasmussen, *Circ. Res.* **105**, 185 (2009).
- ¹²H. H. Rasmussen, E. J. Hamilton, C.-C. Liu, and G. A. Figtree, *TCM* **20**, 85 (2010).
- ¹³Z. Cai and L. J. Yan, *J. Biochem. Pharmacol. Res.* **1**, 15 (2013).
- ¹⁴B. S. Berlett and E. R. Stadtman, *J. Biol. Chem.* **272**, 20313 (1997).
- ¹⁵H. Sies, *Stress: Physiology, Biochemistry, and Pathology* (Elsevier, 2019), p. 153.
- ¹⁶H. Sies, *Redox Biol.* **11**, 613 (2017).
- ¹⁷G. Melino, F. Bernassola, R. A. Knight, M. T. Corasaniti, G. Nisticò, and A. Finazzi-Agrò, *Nature* **388**, 432 (1997).
- ¹⁸A. V. Zamaraev, G. S. Kopeina, E. A. Prokhorova, B. Zhivotovsky, and I. N. Lavrik, *Trends Cell Biol.* **27**, 322 (2017).
- ¹⁹J. Zha, S. Weiler, K. J. Oh, M. C. Wei, and S. J. Korsmeyer, *Science* **290**, 1761 (2000).
- ²⁰J. Ehlbeck, U. Schnabel, M. Polak, J. Winter, Th. von Woedtke, R. Brandenburg, T. von dem Hagen, and K.-D. Weltmann, *J. Phys. D: Appl. Phys.* **44**, 013002 (2010).
- ²¹R. Foest, E. Kindel, H. Lange, A. Ohl, M. Stieber, and K.-D. Weltmann, *Contrib. Plasma Phys.* **47**, 119 (2007).
- ²²K.-D. Weltmann and T. von Woedtke, *Plasma Phys. Control. Fusion* **59**, 014031 (2017).
- ²³B. Stratmann, T.-C. Costea, C. Nolte, J. Hiller, J. Schmidt, J. Reindel, K. Masur, W. Motz, J. Timm, W. Kerner, and D. Tschoepe, *JAMA Netw. Open* **3**, e2010411 (2020).
- ²⁴S. Mitra, L. N. Nguyen, M. Akter, G. Park, E. H. Choi, and N. K. Kaushik, *Cancers (Basel)* **11**, 1030 (2019).
- ²⁵M. Khalili, L. Daniels, A. Lin, F. C. Krebs, A. E. Snook, S. Bekeschus, W. B. Bownel, and V. Miller, *J. Phys. D: Appl. Phys.* **52**, 423001 (2019).
- ²⁶L. Lin, Z. Hou, X. Yao, Y. Liu, J. R. Sirigiri, T. Lee, and M. Keidar, *Phys. Plasmas* **27**, 063501 (2020).
- ²⁷H.-R. Metelmann, C. Seebauer, V. Miller, A. Fridman, G. Bauer, D. B. Graves, J.-M. Povesle, R. Rutkowski, M. Schuster, S. Bekeschus, K. Wende, K. Masur, S. Hasse, T. Gerling, M. Hori, H. Tanaka, E. Ha Choi, K.-D. Weltmann, P. H. Metelmann, D. D. Von Hoff, and T. v. Woedtke, *Clin. Plasma Med.* **9**, 6 (2018).
- ²⁸G. Bruno, T. Heusler, J.-W. Lackmann, T. von Woedtke, K.-D. Weltmann, and K. Wende, *Clin. Plasma Med.* **14**, 100083 (2019).
- ²⁹J. W. Lackmann, G. Bruno, H. Jablonowski, F. Kogelheide, B. Offerhaus, J. Held, V. Schulz-von der Gathen, K. Stapelmann, T. von Woedtke, and K. Wende, *PLoS One* **14**, e0216606 (2019).
- ³⁰K. Wende, G. Bruno, M. Lalk, K.-D. Weltmann, T. von Woedtke, S. Bekeschus, and J.-W. Lackmann, *RSC Adv.* **10**, 11598 (2020).
- ³¹S. Bekeschus, K. Wende, M. M. Hefny, K. Rödder, H. Jablonowski, A. Schmidt, T. V. Woedtke, K.-D. Weltmann, and J. Benedikt, *Sci. Rep.* **7**, 2791 (2017).
- ³²J. Benedikt, M. Mokhtar Hefny, A. Shaw, B. R. Buckley, F. Iza, S. Schakermann, and J. E. Bandow, *Phys. Chem. Chem. Phys.* **20**, 12037 (2018).
- ³³K. Wende, P. Williams, J. Dalluge, W. V. Gaens, H. Aboubakr, J. Bischof, T. von Woedtke, S. M. Goyal, K.-D. Weltmann, A. Bogaerts, K. Masur, and P. J. Bruggeman, *Biointerphases* **10**, 029518 (2015).
- ³⁴V. S. K. Kondeti, C. Q. Phan, K. Wende, H. Jablonowski, U. Gangal, J. L. Granick, R. C. Hunter, and P. J. Bruggeman, *Free Radic. Biol. Med.* **124**, 275 (2018).
- ³⁵H. Jablonowski, J. Santos Sousa, K.-D. Weltmann, K. Wende, and S. Reuter, *Sci. Rep.* **8**, 12195 (2018).
- ³⁶E. Takai, T. Kitamura, J. Kuwabara, S. Ikawa, S. Yoshizawa, K. Shiraki, H. Kawasaki, R. Arakawa, and K. Kitano, *J. Phys. D: Appl. Phys.* **47**, 285403 (2014).
- ³⁷C. C. W. Verlact, W. Van Boxem, D. Dewaele, F. Lemiere, F. Sobott, J. Benedikt, E. C. Neyts, and A. Bogaerts, *J. Phys. Chem. C* **121**, 5787 (2017).
- ³⁸S. Wenske, J.-W. Lackmann, S. Bekeschus, K.-D. Weltmann, T. von Woedtke, and K. Wende, *Biointerphases* **15**, 061008 (2020).
- ³⁹C. Klinkhammer, C. Verlact, D. Smilowicz, F. Kogelheide, A. Bogaerts, N. Metzler-Nolte, K. Stapelmann, M. Havenith, and J.-W. Lackmann, *Sci. Rep.* **7**, 13828 (2017).
- ⁴⁰J.-W. Lackmann, S. Baldus, E. Steinborn, E. Edengeiser, F. Kogelheide, S. Langklotz, S. Schneider, L. I. O. Leichert, J. Benedikt, P. Awakowicz, and J. E. Bandow, *J. Phys. D: Appl. Phys.* **48**, 494003 (2015).
- ⁴¹J. Golda, J. Held, B. Redeker, M. Konkowski, P. Beijer, A. Sobota, G. Kroesen, N. S. J. Braithwaite, S. Reuter, M. M. Turner, T. Gans, D. O'Connell, and V. Schulz-von der Gathen, *J. Phys. D: Appl. Phys.* **49**, 084003 (2016).
- ⁴²S. Reuter, T. von Woedtke, and K.-D. Weltmann, *J. Phys. D: Appl. Phys.* **51**, 233001 (2018).
- ⁴³M. Bern, Y. J. Kil, and C. Becker, *Curr. Protoc. Bioinformatics* **20**, 13.20.1–13.20.14 (2012).
- ⁴⁴O. Pagel, S. Loroeh, A. Sickmann, and R. P. Zahedi, *Expert Rev. Proteomics* **12**, 235 (2015).
- ⁴⁵R. C. Team (2020).
- ⁴⁶H. Wickham, M. Averick, J. Bryan, W. Chang, L. McGowan, R. François, G. Grolemond, A. Hayes, L. Henry, J. Hester, M. Kuhn, T. Pedersen, E. Miller, S. Bache, K. Müller, J. Ooms, D. Robinson, D. Seidel, V. Spinu, K. Takahashi, D. Vaughan, C. Wilke, K. Woo, and H. Yutani, *J. Open Source Softw.* **4**, 1686 (2019).
- ⁴⁷K. Geumsoo, J. W. Stephen, and L. L. Rodney, *Biochim. Biophys. Acta Gen. Subj.* **1840**, 901 (2014).
- ⁴⁸D. Adrian and W. Jeannette, *Biochim. Biophys. Acta Proteins Proteom.* **1844**, 1367 (2014).
- ⁴⁹G. E. Ronsein, M. C. B. Oliveira, S. Miyamoto, M. H. G. Medeiros, and P. Di Mascio, *Chem. Res. Toxicol.* **21**, 1271 (2008).
- ⁵⁰G. Ferrer-Sueta, N. Campolo, M. Trujillo, S. Bartesaghi, S. Carballal, N. Romero, B. Alvarez, and R. Radi, *Chem. Rev.* **118**, 1338 (2018).
- ⁵¹T. H. Truong and K. S. Carroll, *Crit. Rev. Biochem. Mol. Biol.* **48**, 332 (2013).
- ⁵²C. L. Hawkins and M. J. Davies, *Biochim. Biophys. Acta* **1504**, 196 (2001).
- ⁵³F. Collin, *Int. J. Mol. Sci.* **20**, 2407 (2019).
- ⁵⁴R. Atkinson, *Int. J. Chem. Kinet.* **29**, 99 (1997).
- ⁵⁵R. G. Quiller, T. A. Baker, X. Deng, M. E. Colling, B. K. Min, and C. M. Friend, *J. Chem. Phys.* **129**, 064702 (2008).
- ⁵⁶J. Jeong, Y. Kim, J. Kyung Seong, and K.-J. Lee, *Proteomics* **12**, 1452 (2012).
- ⁵⁷A. M. Lietz and M. J. Kushner, *J. Phys. D: Appl. Phys.* **49**, 425204 (2016).
- ⁵⁸R. Biondi, Y. Xia, R. Rossi, N. Paolucci, G. Ambrosio, and J. L. Zweier, *Anal. Biochem.* **290**, 138 (2001).

- ⁵⁹J. Sanchez and T. N. Myers, *Kirk-Othmer Encyclopedia of Chemical Technology* (Wiley, 2000).
- ⁶⁰C. L. Hawkins and M. J. Davies, *Biochem. J.* **332**, 617 (1998).
- ⁶¹T. Nybo, S. Dieterich, L. F. Gamon, C. Y. Chuang, A. Hammer, G. Hoefler, E. Malle, A. Rogowska-Wrzesinska, and M. J. Davies, *Redox Biol.* **20**, 496 (2019).
- ⁶²V. Jirásek and P. Lukeš, *Plasma Sources Sci. Technol.* **28**, 035015 (2019).
- ⁶³W. V. Gaens, S. Iseni, A. Schmidt-Bleker, K.-D. Weltmann, S. Reuter, and A. Bogaerts, *New J. Phys.* **17**, 033003 (2015).
- ⁶⁴H. Xu, C. Chen, D. X. Liu, W. T. Wang, W. J. Xia, Z. J. Liu, L. Guo, and M. G. Kong, *Plasma Sci. Technol.* **21**, 115502 (2019).
- ⁶⁵A. Schmidt-Bleker, R. Bansemer, S. Reuter, and K.-D. Weltmann, *Plasma Processes Polym.* **13**, 1120 (2016).
- ⁶⁶A. N. Onyango, *Oxid. Med. Cell. Longev.* **2016**, 2398573 (2016).
- ⁶⁷H. Gunaydin and K. N. Houk, *Chem. Res. Toxicol.* **22**, 894 (2009).
- ⁶⁸C. Breen, R. Pal, M. R. J. Elsegood, S. J. Teat, F. Iza, K. Wende, B. R. Buckley, and S. J. Butler, *Chem. Sci.* **11**, 3164 (2020).
- ⁶⁹P. Lukes, E. Dolezalova, I. Sisrova, and M. Clupek, *Plasma Sources Sci. Technol.* **23**, 015019 (2014).
- ⁷⁰F. Girard, V. Badets, S. Blanc, K. Gazeli, L. Marlin, L. Authier, P. Svarnas, N. Sojic, F. Clement, and S. Arbault, *RSC Adv.* **6**, 78457 (2016).
- ⁷¹J. Al-Nu'airat, B. Z. Dlugogorski, X. Gao, N. Zeinali, J. Skut, P. R. Westmoreland, I. Oluwoye, and M. Altarawneh, *Phys. Chem. Chem. Phys.* **21**, 171 (2018).
- ⁷²G. Bruno, S. Wenske, J.-W. Lackmann, M. Lalk, T. von Woedtke, and K. Wende, *Biomolecules* **10**, 1687 (2020).
- ⁷³S. Y. Reece, J. Stubbe, and D. G. Nocera, *Biochim. Biophys. Acta* **1706**, 232 (2005).
- ⁷⁴R. Radi, *Acc. Chem. Res.* **46**, 550 (2013).
- ⁷⁵Z. R. Gan and W. W. Wells, *J. Biol. Chem.* **262**, 6704 (1987).
- ⁷⁶A. Michaeli and J. Feitelson, *Photochem. Photobiol.* **59**, 284 (1994).
- ⁷⁷H. S. Chung, S.-B. Wang, V. Venkatraman, C. I. Murray, and J. E. Van Eyk, *Circ. Res.* **112**, 382 (2013).
- ⁷⁸N. K. Gibbs and M. Norval, *J. Invest. Dermatol.* **131**, 14 (2011).
- ⁷⁹S. Vanichkitrungruang, C. Y. Chuang, C. L. Hawkins, A. Hammer, G. Hoefler, E. Malle, and M. J. Davies, *Free Radic. Biol. Med.* **136**, 118 (2019).

Article A3

Singlet Oxygen-Induced Phospholipase A2 Inhibition: a Major Role for Interfacial Tryptophan Dioxidation

Z. Nasri, S. Memari, S. Wenske, R. Clemen, U. Martens, M. Delcea, S. Bekeschus, K.-D. Weltmann, T. von Woedtke and K. Wende. *Chem. Eur. J.*, 27 (59), 14702, 2021.

© 2021 The Authors

Singlet-Oxygen-Induced Phospholipase A₂ Inhibition: A Major Role for Interfacial Tryptophan Dioxidation

Zahra Nasri,^{*[a]} Seyedali Memari,^[a, b] Sebastian Wenske,^[a] Ramona Clemen,^[a] Ulrike Martens,^[c, d] Mihaela Delcea,^[c, d] Sander Bekeschus,^[a] Klaus-Dieter Weltmann,^[a] Thomas von Woedtke,^[a, e] and Kristian Wende^{*[a]}

Abstract: Several studies have revealed that various diseases such as cancer have been associated with elevated phospholipase A₂ (PLA₂) activity. Therefore, the regulation of PLA₂ catalytic activity is undoubtedly vital. In this study, effective inactivation of PLA₂ due to reactive species produced from cold physical plasma as a source to model oxidative stress is reported. We found singlet oxygen to be the most relevant active agent in PLA₂ inhibition. A more detailed analysis of the plasma-treated PLA₂ identified tryptophan 128 as a hot spot, rich in double oxidation. The

significant dioxidation of this interfacial tryptophan resulted in an N-formylkynurenine product via the oxidative opening of the tryptophan indole ring. Molecular dynamics simulation indicated that the efficient interactions between the tryptophan residue and phospholipids are eliminated following tryptophan dioxidation. As interfacial tryptophan residues are predominantly involved in the attaching of membrane enzymes to the bilayers, tryptophan dioxidation and indole ring opening leads to the loss of essential interactions for enzyme binding and, consequently, enzyme inactivation.

Introduction

Phospholipase A₂ (PLA₂) is a group of membrane proteins that specifically cleaves the acyl ester bond at the *sn*-2 position of glycerophospholipids, releasing fatty acids and

lysophospholipids.^[1] The mammalian genome encodes more than 30 PLA₂ isoforms or related enzymes. The PLA₂ superfamily has three primary classification: secretory PLA₂ (sPLA₂), cytosolic PLA₂ (cPLA₂), and Ca²⁺-independent PLA₂ (iPLA₂). The activity of PLA₂ isoforms leads to the release of a mixture of bioactive lipids or lipid mediators. Lysophosphatidic acid (LPA) is one such bioactive phospholipid produced by the enzymatic action of PLA₂. It has been found to induce many cancer hallmarks, including cellular processes such as proliferation, growth, survival, migration, invasion, and angiogenesis promotion.^[2] PLA₂ overexpression is not only associated with numerous cancers,^[3] but also with inflammation in pathological processes such as asthma or allergy.^[4] Moreover, increased PLA₂ activity has been reported in autoimmune disorders,^[5] schizophrenia,^[6] autism,^[7] and bipolar disorders.^[8] Therefore, elevated PLA₂ activity may play a role in the aforementioned disease states, and the regulation of its activity is of great interest. Several PLA₂ inhibitors have been developed so far: Nevertheless, there has been no reported clinical successes to date and no treatments have reached the market.^[9] Hence, novel strategies for the effective and safe inhibition of PLA₂ are highly desirable.

Two regions are known to be involved in the PLA₂ activity; first, the interface site responsible for the enzyme binding to the membrane and the catalytic site.^[10] Accordingly, the lack of efficient binding to the lipid membrane leads to a reduction of enzymatic activity. Interfacial bindings are formed primarily by hydrophobic amino acids, of which tryptophan plays a significant role.^[11] Leslie et al. reported that the association of the catalytic domain of human cPLA₂ with the membrane is mediated in part by a tryptophan residue located at the membrane-exposed face of the enzyme.^[12] Mutation of this tryptophan residue significantly reduced the membrane association of the enzyme.^[13] It is also known that tryptophan plays

[a] Dr. Z. Nasri, S. Memari, S. Wenske, R. Clemen, Dr. S. Bekeschus, Prof. K.-D. Weltmann, Prof. T. von Woedtke, Dr. K. Wende
Center for Innovation Competence (ZIK) plasmatis
Leibniz Institute for Plasma Science and Technology (INP)
Felix-Hausdorff-Straße 2, 17489, Greifswald, Germany
E-mail: zahra.nasri@inp-greifswald.de
kristian.wende@inp-greifswald.de

[b] S. Memari
Institute of Anatomy and Cell Biology
University Medicine Greifswald
Friedrich-Loeffler-Straße 23c, Greifswald, 17487, Germany

[c] Dr. U. Martens, Prof. M. Delcea
Institute of Biochemistry
University of Greifswald
Felix-Hausdorff-Straße 4, Greifswald, 17489, Germany

[d] Dr. U. Martens, Prof. M. Delcea
Center for Innovation Competence (ZIK) HIKE (Humoral Immune Reactions
in Cardiovascular Diseases)
University of Greifswald, Greifswald
Fleischmannstraße 42, 17489, Germany

[e] Prof. T. von Woedtke
Institute for Hygiene and Environmental Medicine
University Medicine Greifswald, Greifswald
Walther-Rathenau-Straße 49 A, 17489, Germany

Supporting information for this article is available on the WWW under <https://doi.org/10.1002/chem.202102306>

© 2021 The Authors. Chemistry - A European Journal published by Wiley-VCH GmbH. This is an open access article under the terms of the Creative Commons Attribution Non-Commercial License, which permits use, distribution and reproduction in any medium, provided the original work is properly cited and is not used for commercial purposes.

an essential role in the interfacial binding and activity of other PLA₂ isoforms.^[14] Han et al. reported that tryptophan 31 in the binding surface of human group V PLA₂ was essential for membrane penetration of the enzyme.^[15] Hence, a mutation of tryptophan 31 reduced enzyme activity 7-fold.^[16] Notably, Beers et al. reported that the addition of only a single tryptophan to the membrane binding surface of human group IIA significantly enhanced the enzyme activity.^[17] PLA₂ enzymes which contain the tryptophan residue in the interfacial binding surface are reported to display the highest activity toward neutral phospholipid substrates.^[18] Gaspar et al. found that the non-steroidal anti-inflammatory drugs (NSAIDs) inhibit PLA₂ activity due to the disturbance of the enzyme binding efficiency to the membrane, possibly by shielding the tryptophan residues of the enzyme.^[19] Based on that, we considered the destruction of the tryptophan-lipid interactions beneficial for the enzyme inhibition.

It is reported that the indole ring of the tryptophan has efficient interactions with the membrane's interfacial region.^[20] We aimed to determine if the cleavage of the indole ring leads to the loss of effective enzyme-membrane binding. Tryptophan oxidation has been shown to be responsible for the opening of the indole ring.^[21] To this end, cold physical plasma (CPP) was used as a source of reactive oxygen and nitrogen species (RONS) for tryptophan oxidation. CPP is a promising medical tool, which has been widely studied in different fields of medicine, such as cancer cell treatment, blood coagulation, wound healing, and skin disease treatment.^[22] CPP is a body-temperature ionized gas produced at atmospheric pressure by applying energy to neutral gases.^[23] CPP produces a mixture of active agents, including free charged particles, radicals, RONS, UV radiation, and electromagnetic fields.^[24] It is assumed that plasma generated RONS, such as hydrogen peroxide (H₂O₂), ozone (O₃), hydroxyl radical (*OH), superoxide (*O₂⁻), singlet oxygen (¹O₂), atomic oxygen (O), peroxyxynitrite (ONOO⁻), and nitric oxide (*NO) are the critical elements in the above mentioned medical applications of CPPs.^[25]

Herein, we report the effective inhibition of bee venom PLA₂ by direct plasma treatment. The choice of enzyme was based on the existence of a tryptophan residue on its interfacial region. Supported lipid bilayers (SLBs) were prepared on the surface of a gold electrode, and the activity of the wild-type and plasma-treated enzymes to cleave the SLBs was monitored by electrochemical techniques. Moreover, a detailed analysis of the effect of plasma-produced RONS on the enzyme peptide chain was performed using high-resolution liquid chromatography-tandem mass spectrometry (HR-LC-MS). Finally, the impact of tryptophan oxidation on the enzyme-lipid interactions was identified by molecular dynamics (MD) simulation and molecular docking studies.

Results and Discussion

Electrochemical studies to access the activity of PLA₂

To study the PLA₂ activity to cleave the lipids, lipid bilayers from phosphoethanolamine (PE) and phosphatidylserine (PS) with ratio of PE:PS (70%:30%) were transferred onto the gold electrode surface by Langmuir-Blodgett and Langmuir-Schaefer deposition techniques. Optimum deposition pressure was assessed at 38 mN m⁻¹, where significant changes in the plot of surface pressure as a function of area per lipid molecule (π -A isotherm) were observed. It is possible to decrease the bilayer thickness by lowering the deposition pressure. As a result, thicker bilayers will be transferred at higher deposition pressures.^[26]

Electrochemical measurements were performed to confirm the successful transfer of the lipid bilayer to the electrode surface. As shown in Figure 1, the cyclic voltammogram (CV) and differential pulse voltammogram (DPV) of [Fe(CN)₆]^{3-/4-} as the redox probe, in the case of gold supported lipid bilayer had no significant peak current. This indicated that the gold electrode surface was covered with the lipid bilayer and the barrier properties of the transferred lipid bilayer were blocking the probe's access to the electrode surface. The enzymatic activity of PLA₂ to cleave the lipid bilayer was studied by injecting 10⁻⁴ mg mL⁻¹ of the enzyme into the electrochemical cell containing the gold supported lipid bilayer working electrode. It is reported that the bee venom PLA₂ molecule is Ca²⁺ dependent and highly basic (pI = 10.5 ± 1.0), which its

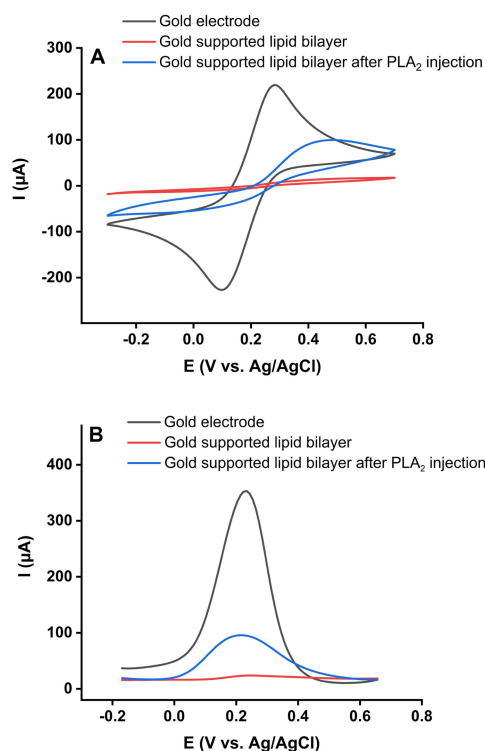


Figure 1. CVs (A) and DPVs (B) of the gold electrode, and gold supported lipid bilayer electrodes before and after injection of PLA₂ enzyme.

optimal activity occurs at alkaline pH.^[27] Based on that, measurements were performed in Tris buffer (pH 8.9) containing 5 mM CaCl₂.

The ability of the enzyme to hydrolyze the phospholipids damaged the lipid bilayer. It led to the gold electrode surface being more accessible for the redox probe, facilitating electron transfer between the probe and the electrode. As a result, the observed increase in the current and area of the DPV and CV peaks of [Fe(CN)₆]^{3-/4-} (Figure 1) after two hours was related to PLA₂ activity.

Balashov et al. have visualized the degradation of lipid bilayer due to the action of PLA₂ by atomic force microscopy. They found that hydrolysis of the lipid bilayer is initiated at specific regions where traces of structural bilayer defects or holes are distinguished or depressions in the bilayer have been identified. After PLA₂ injection, the existing structural defects were enlarged, and new holes appeared.^[28]

The changes in lipid bilayer permeability after injection of PLA₂ to the electrochemical cell were calculated based on Equation (1).

$$\% \text{ Changes in permeability} = [(A_1 - A_2)/A_3] \times 100 \quad (1)$$

A₁, A₂ and, A₃ were the area of the DPV curves of 10 mM [Fe(CN)₆]^{3-/4-} for gold supported lipid bilayer after two hours of PLA₂ injection, gold supported lipid bilayer, and gold electrode, respectively.

The effect of plasma treatment on the activity of the PLA₂ enzyme was investigated (Figure 2). A solution of 60 s Ar plasma-treated PLA₂ was added to the electrochemical cell containing a gold supported lipid bilayer working electrode. Interestingly, we found that lipid bilayer permeability changes were negligible (Figure 2A), which illustrated that the plasma-treated enzyme was no longer able to hydrolyze the phospholipids. To better understand the plasma-mediated enzyme inhibition, Tris buffer (pH 7.4) was exposed to Ar plasma, and the PLA₂ enzyme was added immediately after. The results of which demonstrated that this 'indirectly'-treated enzyme cleaved the lipid bilayer to increase its permeability: as such, indirect plasma treatment could not inhibit the enzyme activity. We concluded that short-lived reactive species from plasma were responsible for the observed enzyme inhibition, and the responsible agents for enzyme inactivation were lost in indirect treatment. Accordingly, the concentrations of deposited reactive species during 60 s Ar plasma treatment were quantified (Figure S2). We found •OH and ¹O₂ as short-lived and H₂O₂, nitrite (NO₂⁻), and nitrate (NO₃⁻) as long-lived plasma-produced reactive species in our measurement. Further experiments were conducted by adding a similar amount of identified long-lived reactive species to the PLA₂ solution. The obtained results are shown in Figure 2A, which indicated that none of these species were able to inactivate the enzyme.

¹O₂ was one of the short-lived reactive species found only within direct plasma treatment (Figure S2) and is reported to be related to the anti-tumor effects of CPP.^[29] Bauer et al. introduced 2 mM of histidine as a standard concentration of ¹O₂ scavenger.^[30] To assess the effect of ¹O₂, histidine was added to

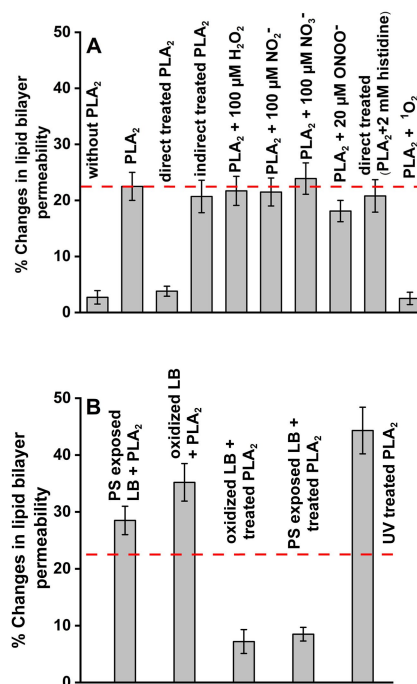


Figure 2. The changes in the PE: PS (70%: 30%) lipid bilayer (LB) permeability after incubation of bilayer with PLA₂ enzyme for 2 h (A). The changes in the lipid bilayer permeability after incubation of PE: PS lipid bilayers with different physical properties with PLA₂ for 2 h (B). The dashed red line indicated the activity of wild-type PLA₂ to cleave PE: PS (70%: 30%) lipid bilayer.

the PLA₂ solution during direct plasma treatment. It was found that in the presence of histidine, the direct plasma-induced abrogation was abolished. This suggested ¹O₂ to be the responsible agent for the enzyme inactivation. To verify the role of ¹O₂ in enzyme inhibition, a solution of PLA₂ in D₂O was irradiated in the presence of 10 μM of rose bengal as photosensitizer with continuous oxygenation. Then, the appropriate amount of the irradiated enzyme was injected in the electrochemical cell containing gold supported lipid bilayer to have 10⁻⁴ mg mL⁻¹ PLA₂. After two hours, the changes in the permeability of the lipid bilayer were monitored. We found that the irradiated enzyme was inactivated and was not able to cleave the phospholipids. The control experiment was repeated similarly by mixing PLA₂ and rose bengal in D₂O without irradiation. In the control experiment, the enzyme was able to cleave the bilayer and increase the permeability. These results confirm our suggestion that ¹O₂ is involved in the inactivation of the enzyme by plasma treatment. Moreover, the effect of substrate physical properties on the PLA₂ activity was investigated and is shown in Figure 2B. The obtained results indicated that wild-type PLA₂ had a higher activity for cleaving oxidized and PS exposed lipid bilayers (PE: PS (50%: 50%)) due to the altered structure of the membrane, which facilitated adsorption and access of the PLA₂ to the sn-2 ester bond of the phospholipids.^[31] However, cleavage of the oxidized and PS exposed membranes by treated PLA₂ was sluggish. Furthermore, the impact of UV radiation from the plasma on the

activity of PLA₂ was investigated. The enzyme was treated in a chamber with an MgF₂ window to eliminate the effects of plasma-generated RONS and ensure only UV radiation can affect the enzyme. As shown in Figure 2B, the UV radiation increases the enzyme activity of lipid cleavage and as such is unlikely to be an influential factor in enzyme inhibition.

Dynamic light scattering (DLS) and circular dichroism (CD)-spectroscopy measurements

DLS was performed to analyze possible enzyme degradation or aggregation by investigating any changes in size and heterogeneity of the enzyme after plasma treatment. Comparing the correlograms of PLA₂, there were no significant changes in the light scatter decay time (Figure 3A) and the total area under the curve (AUC) (Figure 3B) for the enzyme after plasma treatment. The high polydispersity index (wild-type=0.85, plasma-treated=0.87) suggested a significant level of heterogeneity that did not change following plasma treatment. Additionally, the size of the enzyme before and after plasma treatment was measured as 4.97±0.85 nm (wild-type) and 4.58±0.72 nm (plasma-treated) (Figure 3C), which revealed no notable changes in diameter after plasma treatment. Collectively, these findings suggest no enzyme degradation or aggregation as a result of plasma treatment.

Consequently, we performed CD-spectroscopy analyses to track the changes in the secondary structure of the enzyme that may appear after plasma treatment. For this purpose, the CD spectra of the PLA₂ enzyme before and after plasma treatment with the Tris buffer spectrum used as the control measurement were recorded. As is shown in Figure 3D, the enzyme α -helix is depicted in the CD-spectra without considerable changes. Assuming a constant enzyme concentration in both measurements, no significant differences appeared in the enzyme's secondary structure after plasma treatment.

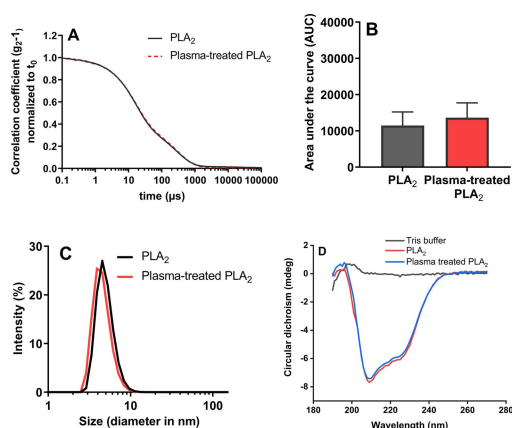


Figure 3. Correlation coefficient (A), AUC (B), and the size (C) of untreated and plasma-treated PLA₂ in Tris buffer (pH 7.4) measured by DLS ($n=3$), and CD spectra of Tris buffer (pH 7.4) and PLA₂ enzyme before and after plasma treatment (D) ($n=2$).

HR-LC-MS analysis

The inactivation of the plasma-treated PLA₂ prompted us to analyze the oxidative modifications of the enzyme induced by RONS using HR-LC-MS. The coverage of the protein sequence was more than 90% before filtering the peptide spectrum matches with Byonic and delta mod score and 75% after filtering. The comparison of the chromatograms revealed that cysteine and methionine, as very reactive amino acids,^[21e,32] did not show significant oxidative modifications after plasma treatment. However, tryptophan 128 at the exterior of the enzyme appeared as a hot spot. A detailed view of the RONS-induced oxidative modification sites found in the amino acid sequence of the enzyme after plasma treatment and the relative amount of each modification compared to the total number of modifications is shown in Figure 4. Obviously, among all modifications, tryptophan 128 dioxidation constituted more than 25% of all the identified modifications. This number indicated the high susceptibility of tryptophan to dioxidation, possibly due to the oxidation by ¹O₂ produced from plasma. The origin of other detected plasma-induced modifications of amino acids was studied extensively.^[33]

Dioxidation of tryptophan resulted in the formation of different products.^[34] Li et al. have studied the chemical basis of tryptophan oxidation using an Ar plasma jet.^[35] In addressing this issue, they fully characterized each tryptophan-derived product using LC-MS². They demonstrated that the plasma-induced oxidation of tryptophan gave rise to a mixture of hydroxyl derivatives and hydroperoxides, which were decom-

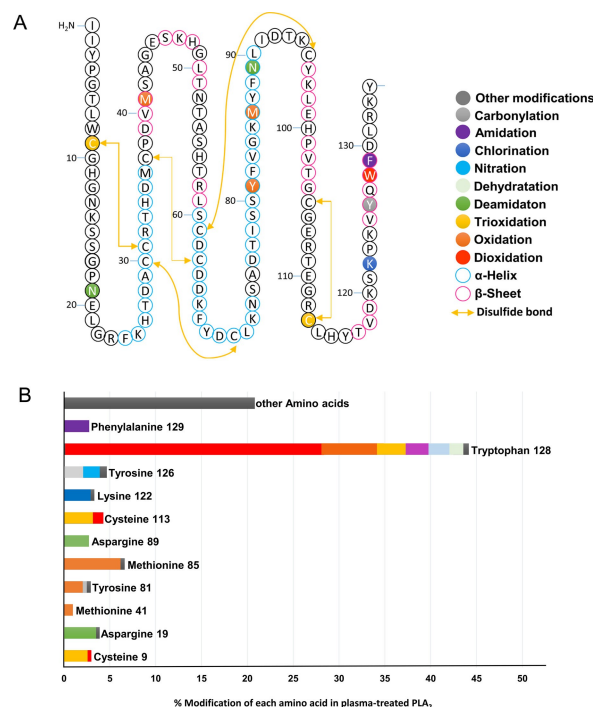


Figure 4. The complete amino acid sequence of PLA₂ with the specific location of each identified RONS-induced modification (A), and the relative amount of each amino acid modification in plasma-treated PLA₂ compared to the total number of modifications (B).

posed into N-formylkynurenine (NFK) under physiological conditions. Furthermore, they proposed a mechanism for the tryptophan reaction with the plasma-generated RONS, which introduced NFK as the final product of tryptophan oxidation by the Ar plasma jet. Moreover, Ronsein et al. have studied the mechanism of tryptophan oxidation by $^1\text{O}_2$.^[21b] They characterized two cis- and trans-tryptophan hydroperoxide (WOOH) isomers as the major tryptophan oxidation products. They have shown that WOOHs were highly unstable and rapidly decomposed under heating or basification, leading to the formation of NFK. A similar mechanism was proposed by Gracanin et al. for tryptophan oxidation to NFK.^[36] As plasma is a body-temperature ionized gas, and the treatment was done at slightly basic solutions (pH 7.4) and based on the UV absorption spectra (Figure S5), we assigned NFK as the major product of tryptophan dioxidation and the main oxidative product in the plasma-treated PLA₂ sequence.

The oxidation of tryptophan to NFK in proteins has been known. Kuroda et al. found that inactivation of lysozyme occurred only when one specific tryptophan residue was oxidized to NFK.^[37] It was the first evidence that oxidation of a particular tryptophan residue can impair enzyme activity. They reported this oxidative inactivation is accompanied by the loss of the ability of lysozyme to form an enzyme-substrate complex. Moreover, tryptophan dioxidation to NFK has been detected in a variety of other proteins, including mitochondrial ATP synthase,^[38] photosystem II subunits,^[39] apolipoprotein B-100,^[40] myoglobin,^[41] aconitase-2 (mitochondria),^[42] frataxin,^[43] troponin I and actin.^[44] Furthermore, Kasson et al. introduced NFK as a new marker identify ROS generation sites in photosystem II and other proteins.^[45]

It is known that the interactions of the tryptophan indole ring with biomembranes are highly remarkable in their solvation.^[20,46] As a result, tryptophan dioxidation and the indole ring-opening can prevent membrane proteins from efficiently anchoring into the lipid bilayer, which leads to enzyme inactivation. To prove our hypothesis, MD simulation and molecular docking were done to measure the interactions between wild-type PLA₂ containing tryptophan 128 residue and plasma-treated PLA₂ with the NFK group and a PE lipid.

MD simulation

To further highlight that tryptophan dioxidation and NFK formation had no effect on the size and structure of the enzyme, but only altered the interactions with phospholipids, MD simulation was applied. For this purpose, structures and the surface electrostatic potentials indicating the positively and negatively charged regions for the wild-type and plasma-treated PLA₂ were generated with PyMol and APBS and are compared in Figure 5. As is shown, there were no significant changes in the enzyme's structure and size after plasma treatment; especially in the active site of the enzyme, supports the finding of the obtained DLS and CD-spectroscopy experimental data. The most apparent structural change was observed in the region where tryptophan 128, tyrosine 126, and

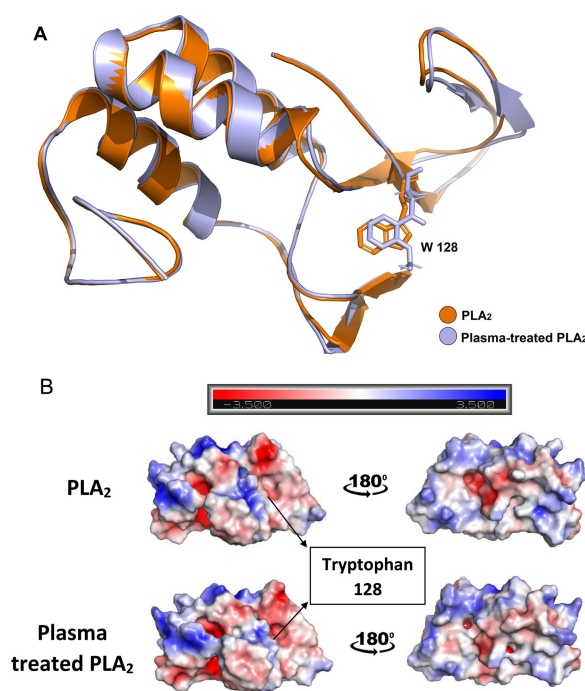


Figure 5. Structural alignments (A) and surface electrostatic potentials (blue for positively charged, red for negatively charged), before and after rotation by 180° about the vertical axis (B) for wild-type and plasma-treated PLA₂.

phenylalanine 129 were modified. Moreover, root-mean-square-deviation (RMSD) for untreated against plasma-treated PLA₂ was calculated as 0.585. This small RMSD suggests only partial differences between the structure of enzyme before and after plasma treatment.

As mentioned, tryptophan plays an essential role in the binding of membrane enzymes. In this regard, FTMap^[47] was performed to identify if tryptophan 128 could be a hotspot for different ligands. It was found that tryptophan 128 is able to establish hydrogen bonds with 2.46% ligands (Figure S6), which was a significant percentage for the outer region of the enzyme active site. Hydrogen bonds and electrostatic- π interactions are essential for indole solvation, and these interactions are responsible for tryptophan's role in anchoring proteins into the membrane.^[46] As a result, any changes in the indole ring structure due to plasma treatment could affect tryptophan's ability to bond with the membrane. As such, molecular docking was performed to simulate the interactions between PE lipid and wild-type or plasma-treated PLA₂ with tryptophan or NFK residues, respectively.

The molecular docking results indicate that PE lipids can establish two groups of hydrogen bonding via its carbonyl groups with tryptophan 128 of wild-type PLA₂. The first hydrogen bonding was between the lipid carbonyl group and NH₂ of tryptophan 128, which had an angle of 14.5 degrees to the x-axis, and 143.8 degrees to the y-axis at a distance of 3.0 Å. The other hydrogen bond formation was between the N atom of the tryptophan 128 indole ring and the second carbonyl group of PE, with an angle of 17.9 degrees to the x-axis and 116.8

degrees to the y-axis at a distance of 2.8 Å (Figure 6A and B). After plasma treatment and dioxidation of tryptophan, these hydrogen bond and the other electrostatic- π interactions of tryptophan 128 with phospholipid were eliminated (Figure 6C and D). Dioxidation of tryptophan and opening of the indole ring decreased the total interactions between the phospholipid and the enzyme. The enzyme's affinity for ligand binding was calculated as $-4.3 \text{ kcal mol}^{-1}$ (docking score) for PLA₂, which was reduced to $-3.4 \text{ kcal mol}^{-1}$ after plasma treatment. The molecular docking results indicated that in the case of plasma-treated PLA₂, the absence of sufficient interactions between the enzyme and lipid membrane prevented enzyme localization in the lipid bilayer, which resulted in the inactivation of the enzyme.

Kubiak et al. studied the products of bovine eye lens protein gB-crystallin (GCS) oxidation by MD modeling.^[48] They induced mutations at tryptophan residues converting them into NFK. According to quantum chemical calculations, they found the rearrangement of the charge distribution in the tryptophan moiety after its oxidation to NFK is localized in the opened indole ring. They demonstrated the increased local electric dipole moment of the NFK residue decreased the hydrophobicity of the molecule. Furthermore, they reported the NFK residue significantly more polar than tryptophan. Thus, under favorable conditions, new hydrogen bonds with water were created. They presented a snapshot from the GCS and NFK trajectories, showing that NFK penetrated the water further than tryptophan. Considering their results, oxidation of tryptophan to NFK was decreasing the lipophilicity of the treated enzyme. Thus, the plasma-treated enzyme had less affinity to form hydrogen bonds with phospholipids, leading to the loss of efficient interactions between the enzyme and phospholipids and enzyme inactivation. This could represent a novel treatment strategy for many diseases that involve PLA₂ over-expression.

Conclusion

In this study, we demonstrated that the plasma-produced ¹O₂ led to the efficient inactivation of the PLA₂ enzyme, which is highly desirable due to its increased activity in many diseases. We verified that the dioxidation of interfacial tryptophan 128 residue to NFK led to the decay of functional interactions between the enzyme and phospholipid, preventing the enzyme from anchoring in the membrane and consequently inhibited the enzyme efficiently. The introduced inhibition mechanism is not limited to the PLA₂ enzyme, but can be extended to those proteins in which interfacial tryptophan plays a role in their membrane anchoring and functionality. Influenza virus haemagglutinin,^[49] Ebola virus matrix protein,^[50] multidrug resistance protein 1,^[51] and Escherichia coli α -Hemolysin^[52] are only a few examples in which tryptophan residues are known to be required for their stabilizing and proper function in cells. This study deepens our knowledge of the structure-function relationship of the PLA₂ enzyme and introduces the possibility of using this inactivation strategy based on pro-oxidant

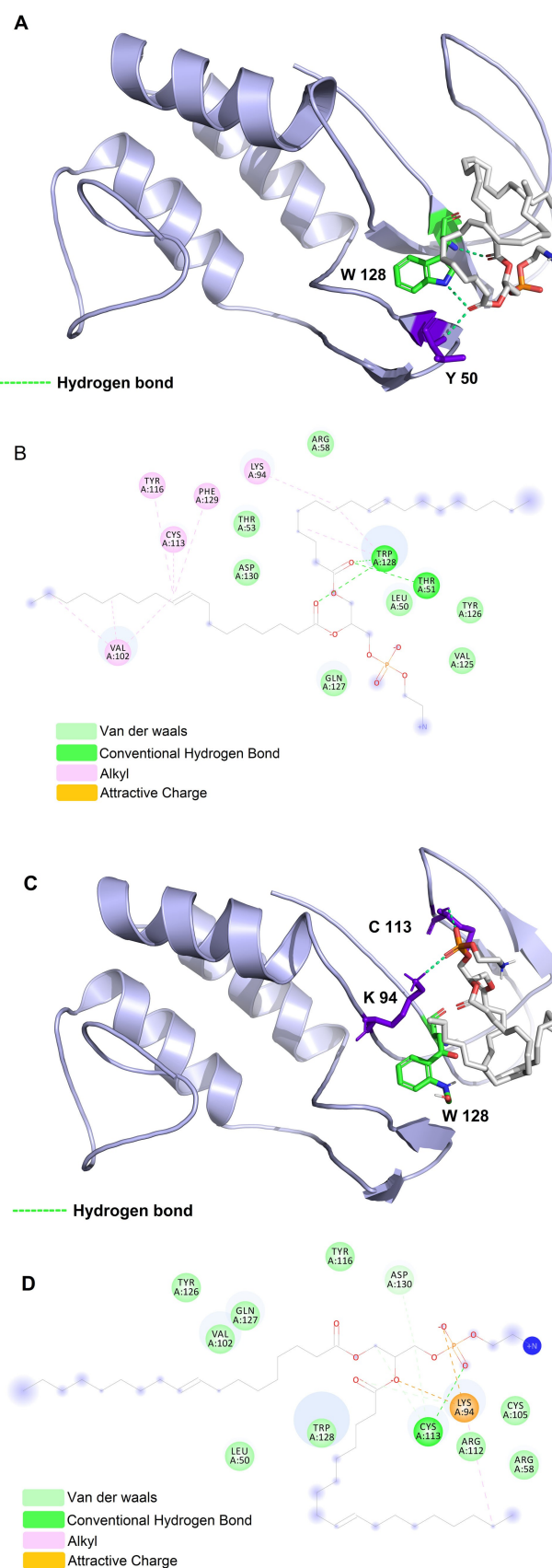


Figure 6. 3D and 2D interactions of PLA₂ and PE lipid before (A and B) and after (C and D) plasma treatment. Abbreviations for amino acids: W: tryptophan, Y: tyrosine, C: cysteine, K: lysine.

therapies for all the proteins in which tryptophan has a role in their membrane anchoring and functionality.

Experimental Section

Reagents

1,2-dioleoyl-sn-glycero-3-phosphoethanolamine (18:1 ($\Delta 9$ -Cis) PE (DOPE)) and 1,2-dioleoyl-sn-glycero-3-phospho-L-serine (sodium salt) (18:1 PS (DOPS)) were from Avanti Polar Lipids and purchased from Otto Nordwald (Otto Nordwald GmbH, Germany) and used without further purification. Chloroform and ethanol were HPLC grade from Carl Roth (Carl Roth GmbH+Co. KG, Germany). Methanol (99.95%) was from Th. Geyer (Th. Geyer GmbH & Co. KG, Germany). Phospholipase A₂ from honey bee venom (Apis mellifera, UniProt P00630), rose bengal, potassium hexacyanoferrate(II) trihydrate, potassium hexacyanoferrate(III), and hydrogen peroxide (30% w/w) were purchased from Sigma-Aldrich (Sigma-Aldrich Chemie GmbH, Germany). Peroxynitrite was from Merck (Merck Chemicals GmbH, Germany). Water used for cleaning and measurements was purified with ultrapure MilliQ water (Milli-Q® Merck KGaA, Germany). All other reagents were of analytical grade and used without further purification.

Preparation of gold supported lipid bilayer

To prepare the gold-supported lipid bilayers, Langmuir-Blodgett (LB) and Langmuir-Schaefer (LS) deposition techniques were applied for the transfer of the first and second lipid monolayers onto the Au(111) (arrandee metal GmbH+Co. KG, Germany) substrates, respectively. For this purpose, surface pressure-area isotherms were recorded using a Langmuir trough (KSV NIMA, LOT-QuantumDesign GmbH, Germany). The Au (111) substrate was flame-annealed and cleaned in piranha solution (3:1 mixture of concentrated sulfuric acid and 30% hydrogen peroxide solution) before being transferred into the trough.^[53] A sufficient quantity of 1 mg mL⁻¹ lipid solution was dispersed onto the surface of the water subphase in a dropwise manner. The lipid solvent was allowed to evaporate for 15 min, and then the barriers were closed to obtain the target pressure of 38 mNm⁻¹. The Au substrate was raised vertically through the monolayer film at a speed of 2 mm min⁻¹, while the pressure was maintained at the target pressure and then dried in argon for 30 min. A transfer ratio of 1.0 ± 0.1 was accepted as a successful transfer of the lipid to the substrate. To transfer the second monolayer, the Langmuir-Schaeffer (horizontal dip) was performed at a speed of 0.5 mm min⁻¹. The Au substrate-supported lipid bilayer was placed immediately into the electrochemical cell.

Electrochemical measurements

Electrochemical measurements were carried out using a potentiostat AUTOLAB PGSTAT302 N (Deutsche METROHM GmbH & Co. KG, Germany) electrochemical system. All experiments were performed in a three-electrode system consisting of a leakless Ag/AgCl miniature reference electrode and a platinum wire auxiliary electrode (eDAQ Europe, Poland), and a gold substrate supported lipid bilayer as the working electrode. DPVs and CVs were recorded in a solution of 10 mM [Fe(CN)₆]^{3-/4-} in Tris buffer [0.010 M Tris (pH 8.9), 0.150 M NaCl, 0.005 M CaCl₂].

CPP treatment

The kINPen09 (Neoplas tools GmbH, Germany) was used as a well-characterized plasma source^[54] running at 1.1 W and a frequency of 1 MHz. Argon was used as feed gas at a flux of 3.0 standard liters per minute (slm). Volumes of 750 μ l of PLA₂ enzyme in Tris buffer [0.010 M Tris (pH 7.4), 0.150 M NaCl, 0.005 M CaCl₂] were treated with the kINPen at a distance of 9 mm between the jet nozzle and the sample surface for 60 seconds.

Singlet oxygen generation

Samples of 0.01 mg mL⁻¹ PLA₂ enzyme in D₂O were irradiated for 30 minutes in the presence of 10 μ M of rose bengal as photosensitizer with PL201 compact laser module 520 nm wavelength (Thorlabs GmbH, Germany) with continuous oxygenation.

DLS measurements

Samples of untreated and plasma-treated PLA₂ (1 mg mL⁻¹) in Tris buffer (pH 7.4) were loaded in low-volume disposal cuvettes (ZEN0040). Spectra were recorded using a ZS90 dynamic light scattering device (Malvern Instruments, UK) equipped with a helium-neon laser light source (632 nm). The samples were measured at 25 °C, with an equilibration time of 120 seconds. Attenuator was set to 9, backscatter angled detection was performed at 173° with a scattering collection angle of 147.7°. Measurement was performed once in three technical replicates, with a measurement duration of 25.2 sec (1.68 sec per run) for each replicate. Data were evaluated with ZS XPLORER Software 1.3.0.140 and GraphPad prism 9.0.2.

CD-spectroscopy

Circular dichroism data were monitored with a Chirascan CD spectrometer (Applied Photophysics, UK) combined with a temperature controller (Quantum Northwest, USA). Each measurement was done with samples in a concentration of 25 μ g mL⁻¹ diluted in Tris buffer (pH 7.4) and loaded in 5 mm-pathlength cuvettes (Hellma Analytics, Germany). CD spectra were recorded at 25 °C in the range of 190 to 270 nm with a bandwidth of 1.0 nm, a scanning time of 1.5 s per point, and five repetitions. All spectra were blank corrected and repeated at least two times.

HR-LC-MS measurements and data analysis

The PLA₂ samples were heated for 10 min to 95 °C. After cooling down to room temperature, the protein was digested with trypsin with an enzyme to protein ratio of 1:25 for 2 h at 37 °C. After digestion, the peptides were ready for measurement by HR-LC-MS. The peptides were analyzed on an Orbitrap Exploris 480 mass spectrometer (Thermo Scientific, Germany) coupled to an UltiMate 3000 RSLCnano UHPLC system (Thermo Scientific, Germany). Peptides were loaded on a trap column (Acclaim PepMap100 C18 material, 5 μ M 0.1 × 20 mm, Thermo Fisher) with a flow rate of 5 μ L per minute for 6 minutes. The loaded peptides were resolved at 300 nL min⁻¹ flow rate using a linear gradient of 4 to 45% solvent B (0.1% acetic acid in 95% acetonitrile) over 42 minutes on an analytical column (150 mm × 75 μ m, 2.0 μ m particle size, Thermo Fisher Scientific). Attached was an EASY-Spray ion source operated at 1.9 kV voltage, and the temperature was 250 °C, with a stainless steel emitter.

Mass spectrometry analysis was carried out with the peptide application mode peptide and in a data-dependent manner with a

full scan range of 350 to 1200 m/z with top N where N was set to 15 most abundant ions. Both MS and ddMS² were measured using an Orbitrap mass analyzer. Full MS scans were measured with a resolution of 120,000 at 200 m/z. Precursor ions were fragmented using fixed normalized higher-energy collisional dissociation (HCD) collision of 30% and detected at a mass resolution of 15,000 at m/z 200. Normalized Automatic gain control (AGC) target for full MS was set to 300% (3e6 ions), and for MS² was set to standard with an automatic maximum ion injection time for full MS and 50 ms for ddMS². Dynamic exclusion was set to 30 seconds, and singly charged ions were excluded. The raw data analysis to identify the peptides and the oxidative modifications was performed with the Proteome Discoverer 2.4.1.15 software (Thermo Fisher Scientific) using Byonic (Protein Metrics)^[55] Version 3.8 as a plug-in tool. The peptide spectrum matches were filtered via Byonic score of 250 and delta mod score of 5. A list of expected oxidative modifications was used to screen and detect the modified peptides in Byonic (Table S2) can be found in the supplemented information of the paper.

MD simulation

MD simulation and molecular docking were applied to investigate the structure of PLA₂ and the interactions between tryptophan 128 residue of wild-type and plasma-treated PLA₂ and PE lipid. MD simulation was performed with GROMACS^[56] program package (version 5.0) OPLS-AA/L all-atom force field. The coordinate file of PLA₂ was obtained from the protein data bank (PDB ID: 1POC). The structure of PLA₂ was placed in the simulation box, and the box type was defined as a cube with a size of 5.5 nm. The box was filled with water molecules (the SPC water model) surrounding PLA₂, sodium ions were added to the system. Afterward, the energy of the system was minimized. Eventually, a 100 ps equilibration run was performed employing the NVT ensemble (i.e., a system with a constant number of particles N, volume V and temperature T). Finally, a 100 ns production run was accomplished using NPT dynamics (i.e., a system with a constant number of particles N, pressure P, and temperature T). The reference pressure was set to 1 bar. The calculated values were not identical for wild-type and plasma-treated PLA₂, and the treated enzyme showed less stability.

Molecular docking was performed by AutoDock Vina.^[57] The model mentioned above was used as the target, and PE was obtained from PubChem^[58] web server as the ligand. For docking, tryptophan 128 was chosen as the center of the grid box. According to affinity (kcal mol⁻¹) and root-mean-square-deviation, which were given by AutoDock Vina, the best model for wild-type PLA₂ was selected. The interactions between untreated PLA₂ and PE ligand were analyzed using AutoDockTools-1.5.6 and Discovery Studio.^[59] First, all the modifications detected by HR-LC-MS were applied to the wild-type PLA₂ using Avogadro^[60] software. Afterward, energy minimization was performed to optimize the modified structure using the steepest descent algorithm. After that, according to the study done by Kubiak et al.,^[48] angles and distances were investigated for tryptophan. Finally, the mentioned experiments were repeated to study the effect of modifications on the structure and interactions of treated PLA₂. Subsequently, the best model for the plasma-treated PLA₂ was selected, and by PyMOL,^[61] the structures of wild-type and plasma-treated PLA₂ were compared.

Acknowledgements

The authors are grateful to Johanna Striesow for the mass analysis of lipid samples and Dr. Nicholas McKitterick for

proofreading the article. We also thank Lukas Schulig for valuable comments on molecular dynamics simulation. This work is funded by the German Federal Ministry of Education and Research (BMBF) (grant numbers 03Z22DN12 and 03Z22Di1). Open Access funding enabled and organized by Projekt DEAL.

Conflict of Interest

The authors declare no conflict of interest.

Keywords: cold physical plasma · enzyme inhibition · plasma chemistry · protein modifications · reactive oxygen and nitrogen species

- [1] E. A. Dennis, J. Cao, Y. H. Hsu, V. Magriotti, G. Kokotos, *Chem. Rev.* **2011**, *111*, 6130–6185.
- [2] E. Gendaszewska-Darmach, *Acta Biochim. Pol.* **2008**, *55*, 227–240.
- [3] a) J. Chen, L. Ye, Y. Sun, Y. Takada, *Med. Chem.* **2017**, *13*, 606–615; b) Z. Peng, Y. Chang, J. Fan, W. Ji, C. Su, *Cancer Lett.* **2021**, *497*, 165–177.
- [4] a) S. A. Knowliden, S. E. Hillman, T. J. Chapman, R. Patil, D. D. Miller, G. Tigyi, S. N. Georas, *Am. J. Respir. Cell Mol. Biol.* **2016**, *54*, 402–409; b) S. J. Kim, H. G. Moon, G. Y. Park, *Biochim. Biophys. Acta Mol. Cell Biol. Lipids* **2020**, *1865*, 8; c) N. G. Jendzjowsky, A. Roy, N. O. Barioni, M. M. Kelly, F. H. Y. Green, C. N. Wyatt, R. L. Pye, L. Tenorio-Lopes, R. J. A. Wilson, *Nat. Commun.* **2018**, *9*, 15.
- [5] a) A. Trotter, E. Anstadt, R. B. Clark, F. Nichols, A. Dwivedi, K. Aung, J. L. Cervantes, *Mult. Scler. Relat. Disord.* **2019**, *27*, 206–213; b) J. Soubhye, P. van Antwerpen, F. Dufresne, *Curr. Med. Chem.* **2018**, *25*, 2418–2447; c) N. C. Stoddard, J. Chun, *Biomol. Ther.* **2015**, *23*, 1–11.
- [6] a) R. Junqueira, Q. Cordeiro, I. Meira-Lima, W. F. Gattaz, H. Vallada, *Psychiatr. Genet.* **2004**, *14*, 157–160; b) S. Smesny, D. Kinder, I. Willhardt, T. Rosburg, A. Lasch, G. Berger, H. Sauer, *Biol. Psychiatry* **2005**, *57*, 399–405; c) X. Meng, C. Kou, Q. Yu, J. Shi, Y. Yu, *Psychiatry Res.* **2010**, *175*, 186–187; d) C. Y. Xu, X. H. Yang, L. Y. Sun, T. Q. Yang, C. Q. Cai, P. Wang, J. Jiang, Y. Qing, X. W. Hu, D. D. Wang, P. K. Wang, G. P. Cui, J. Zhang, Y. Li, J. Feng, C. X. Liu, C. L. Wan, *Psychiatry Res.* **2019**, *273*, 782–787.
- [7] H. Qasem, L. Al-Ayadhi, H. Al Dera, A. El-Ansary, *Lipids Health Dis.* **2017**, *16*.
- [8] a) I. Meira-Lima, D. Jardim, R. Junqueira, E. Ikenaga, H. Vallada, *Bipolar Disord.* **2003**, *5*, 295–299; b) M. V. Zanetti, R. Machado-Vieira, H. P. G. Joaquin, T. M. Chaim, M. H. Serpa, R. T. de Sousa, W. F. Gattaz, G. F. Busatto, L. L. Talib, *Biol. Psychiatry* **2016**, *79*, 2665–2675.
- [9] a) A. Nikolaou, M. G. Kokotou, S. Vasilikaki, G. Kokotos, *Biochim. Biophys. Acta Mol. Cell Biol. Lipids* **2019**, *1864*, 941–956; b) Q. Z. Zhang, R. H. Fang, W. W. Gao, L. F. Zhang, *Angew. Chem. Int. Ed.* **2020**, *6*.
- [10] A. S. Alekseeva, P. E. Volynsky, N. A. Krylov, V. P. Chernikov, E. L. Vodovozova, I. A. Boldyrev, *Biochim. Biophys. Acta Biomembr.* **2021**, *1863*, 10.
- [11] A. J. de Jesus, T. W. Allen, *Biochim. Biophys. Acta* **2013**, *1828*, 864–876.
- [12] C. C. Leslie, *J. Lipid Res.* **2015**, *56*, 1386–1402.
- [13] J. H. Evans, C. C. Leslie, *J. Biol. Chem.* **2004**, *279*, 6005–6016.
- [14] M. Gelb, W. Cho, D. Wilton, *Curr. Opin. Struct. Biol.* **1999**, *9*, 428–432.
- [15] S. K. Han, K. P. Kim, R. Koduri, L. Bittova, N. M. Munoz, A. R. Leff, D. C. Wilton, M. H. Gelb, W. Cho, *J. Biol. Chem.* **1999**, *274*, 11881–11888.
- [16] R. V. Stahelin, W. Cho, *Biochemistry* **2001**, *40*, 4672–4678.
- [17] S. A. Beers, A. G. Buckland, N. Giles, M. H. Gelb, D. C. Wilton, *Biochemistry* **2003**, *42*, 7326–7338.
- [18] a) S. Bezzine, J. G. Bollinger, A. G. Singer, S. L. Veatch, S. L. Keller, M. H. Gelb, *J. Biol. Chem.* **2002**, *277*, 48523–48534; b) O. G. Berg, M. H. Gelb, M.-D. Tsai, M. K. Jain, *Chem. Rev.* **2001**, *101*, 2613–2654.
- [19] D. Gaspar, M. Lucio, S. Rocha, J. Lima, S. Reis, *Chem. Phys. Lipids* **2011**, *164*, 292–299.
- [20] a) A. N. Ridder, S. Morein, J. G. Stam, A. Kuhn, B. de Kruijff, J. A. Killian, *Biochemistry* **2000**, *39*, 6521–6528; b) H. C. Gaede, W. M. Yau, K. Gawrisch, *J. Phys. Chem. B* **2005**, *109*, 13014–13023; c) K. E. Norman, H. Nymeyer, *Biophys. J.* **2006**, *91*, 2046–2054.

- [21] a) M. J. Davies, *Biochem. Biophys. Res. Commun.* **2003**, *305*, 761–770; b) G. E. Ronsein, M. C. B. Oliveira, S. Miyamoto, M. H. G. Medeiros, P. Di Mascio, *Chem. Res. Toxicol.* **2008**, *21*, 1271–1283; c) G. E. Ronsein, M. C. de Oliveira, M. H. de Medeiros, P. Di Mascio, *J. Am. Soc. Mass Spectrom.* **2009**, *20*, 188–197; d) J. E. Plowman, S. Deb-Choudhury, A. J. Grosvenor, J. M. Dyer, *Photochem. Photobiol. Sci.* **2013**, *12*, 1960–1967; e) G. Uchida, Y. Mino, T. Suzuki, J. I. Ikeda, T. Suzuki, K. Takenaka, Y. Setsuhara, *Sci. Rep.* **2019**, *9*, 6625.
- [22] a) M. L. Semmler, S. Bekeschus, M. Schafer, T. Bernhardt, T. Fischer, K. Witzke, C. Seebauer, H. Rebl, E. Grambow, B. Vollmar, J. B. Nebe, H. R. Metelmann, T. V. Woedtke, S. Emmert, L. Boeckmann, *Cancers* **2020**, *12*; b) S. Bekeschus, J. Brüggemeier, C. Hackbarth, T. von Woedtke, L.-I. Partecke, J. van der Linde, *Clin. Plasma Med.* **2017**, *7–8*, 58–65; c) O. Assadian, K. J. Ousey, G. Daeschlein, A. Kramer, C. Parker, J. Tanner, D. J. Leaper, *Int. Wound J.* **2019**, *16*, 103–111; d) T. Bernhardt, M. L. Semmler, M. Schäfer, S. Bekeschus, S. Emmert, L. Boeckmann, *Oxidative Medicine and Cellular Longevity* **2019**, *2019*, 3873928.
- [23] K. D. Weltmann, T. von Woedtke, *Plasma Phys. Controlled Fusion* **2017**, *59*, 014031.
- [24] a) T. von Woedtke, A. Schmidt, S. Bekeschus, K. Wende, K. D. Weltmann, *In vivo* **2019**, *33*, 1011–1026; b) A. Privat-Maldonado, A. Schmidt, A. Lin, K. D. Weltmann, K. Wende, A. Bogaerts, S. Bekeschus, *Oxid. Med. Cell. Longevity* **2019**, *2019*, 9062098.
- [25] a) D. Yan, J. H. Sherman, M. Keidar, *Oncotarget* **2016**; b) M. Keidar, *Phys. Plasmas* **2018**, *25*, 083504; c) X. Lu, M. Keidar, M. Laroussi, E. Choi, E. J. Szili, K. Ostrikov, *Mat. Sci. Eng. R.* **2019**, *138*, 36–59.
- [26] A. V. Hughes, S. J. Roser, M. Gerstenberg, A. Goldar, B. Stidder, R. Feidenhans'l, J. Bradshaw, *Langmuir* **2002**, *18*, 8161–8171.
- [27] R. A. Shipolini, G. L. Callewaert, R. C. Cottrell, S. Doonan, C. A. Vernon, B. E. Banks, *Eur. J. Biochem.* **1971**, *20*, 459–468.
- [28] K. Balashev, N. John DiNardo, T. H. Callisen, A. Svendsen, T. Bjornholm, *Biochim. Biophys. Acta* **2007**, *1768*, 90–99.
- [29] a) G. Bauer, D. B. Graves, *Plasma Processes Polym.* **2016**, *13*, 1157–1178; b) G. Bauer, *Anti-Cancer Agents Med. Chem.* **2018**, *18*, 784–804; c) G. Bauer, *IEEE Trans. Radiat. Plasma Med. Sci.* **2018**, *2*, 87–98.
- [30] G. Bauer, D. Sersenová, D. B. Graves, Z. Machala, *Sci. Rep.* **2019**, *9*, 14210.
- [31] a) J. J. van den Berg, J. A. Op den Kamp, B. H. Lubin, F. A. Kuypers, *Biochemistry* **1993**, *32*, 4962–4967; b) E. Gibbons, J. Nelson, L. Anderson, K. Brewer, S. Melchor, A. M. Judd, J. D. Bell, *Biochim. Biophys. Acta* **2013**, *1828*, 670–676.
- [32] a) G. Bruno, T. Heusler, J.-W. Lackmann, T. von Woedtke, K.-D. Weltmann, K. Wende, *Clin. Plasma Med.* **2019**, *14*, 100083; b) S. Wenske, J.-W. Lackmann, S. Bekeschus, K.-D. Weltmann, T. von Woedtke, K. Wende, *Biointerphases* **2020**, *15*.
- [33] a) E. Takai, T. Kitamura, J. Kuwabara, S. Ikawa, S. Yoshizawa, K. Shiraki, H. Kawasaki, R. Arakawa, K. Kitano, *J. Phys. D* **2014**, *47*, 285403; b) S. Wenske, J. W. Lackmann, L. M. Busch, S. Bekeschus, T. von Woedtke, K. Wende, *J. Appl. Phys.* **2021**, *129*; c) S. Wenske, J. W. Lackmann, S. Bekeschus, K. D. Weltmann, T. von Woedtke, K. Wende, *Biointerphases* **2020**, *15*, 061008; d) S. Jiang, L. Carroll, L. M. Rasmussen, M. J. Davies, *Redox Biol.* **2021**, *38*, 101822; e) S. Jiang, L. Carroll, M. Mariotti, P. Häggglund, M. J. Davies, *Redox Biol.* **2021**, *41*, 101874.
- [34] P. Di Mascio, G. R. Martinez, S. Miyamoto, G. E. Ronsein, M. H. G. Medeiros, J. Cadet, *Chem. Rev.* **2019**, *119*, 2043–2086.
- [35] X. Y. Li, Z. Q. Feng, S. C. Pu, Y. Yang, X. M. Shi, Z. Xu, *Plasma Chem. Plasma Process.* **2018**, *38*, 919–936.
- [36] M. Gracanic, C. L. Hawkins, D. I. Pattison, M. J. Davies, *Free Radical Biol. Med.* **2009**, *47*, 92–102.
- [37] M. Kuroda, F. Sakiyama, K. Narita, *J. Biochem.* **1975**, *78*, 641–651.
- [38] S. Rexroth, A. Poetsch, M. Rogner, A. Hamann, A. Werner, H. D. Osiewacz, E. R. Schafer, H. Seelert, N. A. Dencher, *Biochim. Biophys. Acta* **2012**, *1817*, 381–387.
- [39] a) T. M. Dreaden, J. Chen, S. Rexroth, B. A. Barry, *J. Biol. Chem.* **2011**, *286*, 22632–22641; b) T. M. D. Kasson, S. Rexroth, B. A. Barry, *PLoS One* **2012**, *7*; c) S. Rinalducci, N. Campostrini, P. Antonioli, P. G. Righetti, P. Roepstorff, L. Zolla, *J. Proteome Res.* **2005**, *4*, 2327–2337.
- [40] A. Gießauf, B. van Wickern, T. Simat, H. Steinhart, H. Esterbauer, *FEBS Lett.* **1996**, *389*, 136–140.
- [41] M. Ehrenshaft, S. O. Silva, I. Perdivara, P. Bilski, R. H. Sik, C. F. Chignell, K. B. Tomer, R. P. Mason, *Free Radical Biol. Med.* **2009**, *46*, 1260–1266.
- [42] C. Hunzinger, W. Wozny, G. P. Schwall, S. Poznanovic, W. Stegmann, H. Zengerling, R. Schoepf, K. Groebe, M. A. Cahill, H. D. Osiewacz, N. Jagemann, M. Bloch, N. A. Dencher, F. Krause, A. Schratzenholz, *J. Proteome Res.* **2006**, *5*, 625–633.
- [43] A. R. Correia, S. Y. Ow, P. C. Wright, C. M. Gomes, *Biochem. Biophys. Res. Commun.* **2009**, *390*, 1007–1011.
- [44] M. Fedorova, T. Todorovsky, N. Kuleva, R. Hoffmann, *Proteomics* **2010**, *10*, 2692–2700.
- [45] T. M. D. Kasson, B. A. Barry, *Photosynth. Res.* **2012**, *114*, 97–110.
- [46] A. J. Johnston, Y. R. Zhang, S. Busch, L. C. Pardo, S. Imberti, S. E. McLain, *J. Phys. Chem. B* **2015**, *119*, 5979–5987.
- [47] D. Kozakov, L. E. Grove, D. R. Hall, T. Bohnuud, S. E. Mottarella, L. Luo, B. Xia, D. Beglov, S. Vajda, *Nat. Protoc.* **2015**, *10*, 733–755.
- [48] K. Kubiak, M. Kowalska, W. Nowak, *J. Mol. Struct.: THEOCHEM* **2003**, *630*, 315–325.
- [49] N. Ogata, *J. Gen. Virol.* **2012**, *93*, 2558–2563.
- [50] K. A. Johnson, R. Pokhrel, M. R. Budicini, B. S. Gerstman, P. P. Chapagain, R. V. Stahelin, *Pathogens* **2020**, *9*, 402.
- [51] K. Ito, S. L. Olsen, W. Qiu, R. G. Deeley, S. P. Cole, *J. Biol. Chem.* **2001**, *276*, 15616–15624.
- [52] L. O. Reid, A. H. Thomas, V. Herlax, M. L. Dantola, *Biochemistry* **2020**, *59*, 4213–4224.
- [53] E. Madrid, S. L. Horswell, *J. Electroanal. Chem.* **2018**, *819*, 338–346.
- [54] a) S. Reuter, T. von Woedtke, K. D. Weltmann, *J. Phys. D* **2018**, *51*; b) M. S. Mann, R. Tiede, K. Gavenis, G. Daeschlein, R. Bussiahn, K.-D. Weltmann, S. Emmert, T. v. Woedtke, R. Ahmed, *Clin. Plasma Med.* **2016**, *4*, 35–45.
- [55] M. Bern, Y. J. Kil, C. Becker, *Curr. Protoc. Bioinformatics* **2012**, *Chapter 13*, Unit13 20.
- [56] D. Van Der Spoel, E. Lindahl, B. Hess, G. Groenhof, A. E. Mark, H. J. Berendsen, *J. Comput. Chem.* **2005**, *26*, 1701–1718.
- [57] O. Trott, A. J. Olson, *J. Comput. Chem.* **2010**, *31*, 455–461.
- [58] S. Kim, J. Chen, T. Cheng, A. Gindulyte, J. He, S. He, Q. Li, B. A. Shoemaker, P. A. Thiessen, B. Yu, L. Zaslavsky, J. Zhang, E. E. Bolton, *Nucleic Acids Res.* **2019**, *47*, D1102–D1109.
- [59] D. S. Biovia, Vol. 936, Biovia, Dassault Systèmes, San Diego, CA, USA, **2017**.
- [60] M. D. Hanwell, D. E. Curtis, D. C. Lonie, T. Vandermeersch, E. Zurek, G. R. Hutchison, *J. Cheminf.* **2012**, *4*, 17.
- [61] W. L. DeLano, in *CCP4 Newsletter on protein crystallography*, Vol. 40, **2002**, pp. 82–92.

Manuscript received: June 26, 2021
Accepted manuscript online: August 10, 2021
Version of record online: September 15, 2021

Article A4




On the Liquid Chemistry of the Reactive Nitrogen Species Peroxynitrite and Nitrogen Dioxide Generated by Physical Plasmas

G. Bruno, [S. Wenske](#), J.-W. Lackmann, M. Lalk, T. von Woedtke, and K. Wende. *Biomolecules*, 10 (12), 1687, 2020.

© 2020 by the authors

Article

On the Liquid Chemistry of the Reactive Nitrogen Species Peroxynitrite and Nitrogen Dioxide Generated by Physical Plasmas

Giuliana Bruno ¹, Sebastian Wenske ¹, Jan-Wilm Lackmann ², Michael Lalk ³ ,
Thomas von Woedtke ⁴  and Kristian Wende ^{1,*} 

¹ Centre for Innovation Competence (ZIK) Plasmatis, Leibniz Institute for Plasma Science and Technology (INP Greifswald), 17489 Greifswald, Germany; giuliana.bruno@inp-greifswald.de (G.B.); sebastian.wenske@inp-greifswald.de (S.W.)

² Cluster of Excellence Cellular Stress Responses in Aging-Associated Diseases, University of Cologne, 50931 Cologne, Germany; jan-wilm.lackmann@uni-koeln.de

³ Institute of Biochemistry, University of Greifswald, 17487 Greifswald, Germany; lalk@uni-greifswald.de

⁴ Leibniz Institute for Plasma Science and Technology, 17489 Greifswald, Germany; woedtke@inp-greifswald.de

* Correspondence: kristian.wende@inp-greifswald.de

Received: 9 November 2020; Accepted: 9 December 2020; Published: 16 December 2020



Abstract: Cold physical plasmas modulate cellular redox signaling processes, leading to the evolution of a number of clinical applications in recent years. They are a source of small reactive species, including reactive nitrogen species (RNS). Wound healing is a major application and, as its physiology involves RNS signaling, a correlation between clinical effectiveness and the activity of plasma-derived RNS seems evident. To investigate the type and reactivity of plasma-derived RNS in aqueous systems, a model with tyrosine as a tracer was utilized. By high-resolution mass spectrometry, 26 different tyrosine derivatives including the physiologic nitrotyrosine were identified. The product pattern was distinctive in terms of plasma parameters, especially gas phase composition. By scavenger experiments and isotopic labelling, gaseous nitric dioxide radicals and liquid phase peroxynitrite ions were determined as dominant RNS. The presence of water molecules in the active plasma favored the generation of peroxynitrite. A pilot study, identifying RNS driven post-translational modifications of proteins in healing human wounds after the treatment with cold plasma (kINPen), demonstrated the presence of in vitro determined chemical pathways. The plasma-driven nitration and nitrosylation of tyrosine allows the conclusion that covalent modification of biomolecules by RNS contributes to the clinically observed impact of cold plasmas.

Keywords: cold physical plasmas; kINPen; redox signaling; reactive nitrogen species; nitrosative stress; oxidative post-translational modifications

1. Introduction

Reactive nitrogen and oxygen species (RNS/ROS) are unstable compounds prone to react rapidly with cellular molecules. In biological systems, they may be involved in redox signaling pathways (e.g., oxygen sensing, muscles and vascular physiology, immune defense, inflammatory processes) [1], mostly by covalently changing the structure of biomolecules such as lipids and proteins [2–5]. When their homeostasis is impaired, they become markers or drivers of pathological conditions like cancer progression as well as metabolic and neurodegenerative diseases. While some species are constantly formed as by-products of cell metabolism, others are generated for dedicated purposes (second messengers, oxidative burst) [4,6–9]. Well-known endogenous radicals are hydroxyl

radicals ($\cdot\text{OH}$); superoxide anion (O_2^-); nitric oxygen radicals ($\cdot\text{NO}$); nitric dioxide radicals ($\cdot\text{NO}_2$); and other reactive species like singlet oxygen ($^1\text{O}_2$), hydrogen peroxide (H_2O_2), peroxyxynitrite (ONOO^-), dinitrogen trioxide (N_2O_3), and the nitrite ion (NO_2^-). The dual role of ROS and RNS is exploited by various strategies aiming to control or modulate redox-signaling pathways [10–13]. Among these, cold plasma discharges, ionized gases with complex physical and chemistry properties, are being investigated [14,15]. Most prominent components are small reactive species, many of which are also endogenously generated. A large number of gas plasma sources with different gas phase chemistry have been developed [16,17]. One of the best-characterized plasma sources is the kINPen, approved as certified medical tool in the medical version (kINPen MED) [18], currently applied in research (cancer immunology) and in clinics (wound care, skin-related diseases) [19–24]. To the current knowledge, by tuning central parameters of the discharge including working gas composition, distance, or power, the variation of the resulting plasma chemistry is responsible for the observed biological and biochemical effects [25–29]. In addition to direct signaling events triggered by long-lived reactive species like H_2O_2 , e.g., via peroxiredoxins, plasma-derived short-lived reactive species can covalently modify biomolecules in model systems [26,30–35]. It remains to be clarified whether extracellularly modified molecules yield to intracellular physiological consequences or if only changes in cellular structures (e.g., cell membrane proteins) are relevant.

Gas plasmas can be tuned to create high levels of oxygen species, such as singlet oxygen $^1\text{O}_2$; atomic oxygen $\cdot\text{O}$; ozone O_3 ; and, to a lesser extent, hydrogen peroxide H_2O_2 and hydroxyl radicals $\cdot\text{OH}$. These conditions are applied for disinfection or cancer regression [36–40]. In contrast, other conditions foster an N_2 -driven chemistry, yielding species like $\cdot\text{NO}$, $\cdot\text{NO}_2$, N_3O_5 , HNO_2 , and HNO_3 [41,42]. The nitrogen species are assumed to play a role in bactericidal [43,44] and virucidal effects [45], as well as cell stimulation, e.g., in wound healing [11,46–52]. In contrast, data on their transport, solubilization, or production in liquids, as well as their impact on biological systems, are limited. While the long-lived species nitrite and nitrate can be easily accessed by the Griess assay or the ion chromatography and are almost inevitably observed for plasma discharges, both ions are in physiologic conditions not reactive enough to contribute significantly to the effects seen after plasma treatments. Nitration [28,53,54] and nitrosylation [35] of biomolecules have been observed, indicating the presence (and activity) of more reactive species at least under certain conditions. Potential candidates are, e.g., $\cdot\text{NO}_2$, N_2O_3 , and ONOO^- . The presence of peroxyxynitrite [43,54] and peroxyxynitrate [55] has been reported for liquid systems under acidic conditions ($\text{pH} < 4.5$), as well as in alkaline conditions ($\text{pH} 12$) in the case of peroxyxynitrite [56], while information on neutral environments is missing. However, using an peroxyxynitrite sensitive europium probe, intracellular peroxyxynitrite was recently detected in human cell lines following a plasma treatment [57]. Natural sources of RNS are enzymes of the nitric oxide synthase (NOS) complex, generating $\cdot\text{NO}$. This RNS can react with O_2 yielding oxidized RNS such as $\cdot\text{NO}_2$ and N_3O_5 , or with superoxide anion radicals produced by mitochondria, NADPH-oxidases, or xanthine oxidase, forming peroxyxynitrite [58]. Because of the capability of reactive nitrogen species to modify biological structures and to modulate signaling pathway, e.g., via acting as a second messenger like nitric oxide, a significant contribution of RNS can be expected [59].

Tyrosine is a key amino acid reactive towards RNS and protein tyrosines are significant targets in biological environments [60–62]. The principal roles of tyrosine are the formation of hydrophobic cores in proteins, as well as the transduction of signals via phosphorylation events. In this, tyrosine has a superior relevance compared with serine or threonine because of the high specificity of some protein kinases [63]. The presence of the aromatic hydroxyl group also allows the reaction with non-protein structures, in contrast to phenylalanine. Therefore, modifications of the tyrosine substructure yield a gain or loss of function of proteins and subsequently alter signaling pathways or immunological responses [61,64]. Protein nitration also acts as a signal for negative feedback regulation, leading to ubiquitination and protein degradation [65,66]. Some studies suggest the involvement of tyrosine nitration in the pathogenesis or as marker of nitro-oxidative stress [65,67–69]. Nitric oxide and its oxidation products are also involved in wound healing processes, although the mechanisms are

still under investigation [70,71]. For example, tyrosine nitration occurring on metalloproteinase-13 (MMP-13) promoted its release by endothelial cells, triggering a faster cell migration, angiogenesis, and wound healing [67]. In the same way, it was shown that protein tyrosine nitration by exogenous ·NO donors inhibited the degranulation processes in mast cell lines [72]. The release of exogenous ·NO is a possible strategy to stimulate skin healing [73], potentially beneficial in diabetic patients, where the increased hyperglycemia leads to decreased ·NO bioavailability and delays the wound healing process [74]. The effectiveness of cold plasmas was shown in the treatment of wounds in both diabetic and normal subjects, as well as in wound models [22,23,75,76]. The responsible species are not completely known, but recent observations emphasized the role of the local cell stimulation over wound bed disinfection—suggesting that reactive nitrogen species may be involved. Therefore, this work intends to further investigate the N₂-driven biochemistry induced by the kINPen plasma source, aiming to define the principal formed bioactive reactive species and their mechanisms of action. To reach this aim, tyrosine was chosen as a tracer molecule and modifications occurring as a result of the impact of plasma-derived reactive nitrogen species were identified and quantified via high-resolution mass spectrometry. Finally, the ability of kINPen plasmas in modulating the RNS-mediated pathways in complex models was tested. Overall, a significant impact of nitrosating and nitrosylating agents, assumingly peroxynitrite, was observed, leading to a covalent chemical modification of sensitive target structures. Given this result, functional consequences will arise in both pro- and eukaryotic cells, highlighting a possible key mechanism in promoting wound healing, modulation of cancer immunology, and antimicrobial effects.

2. Materials and Methods

2.1. Sample Preparation

2.1.1. Model Solutions

L-tyrosine (Merck KGaA, Darmstadt, Germany) solutions with a concentration of 0.3 and 30 mM were prepared in 5 mM ammonium formate buffer pH 7.4 (Merck KGaA, Darmstadt, Germany) fresh and kept on ice until use. The singlet oxygen and superoxide scavenger ergothioneine (Enzo Life Sciences GmbH, Lörrach, Germany) and the nitric oxide scavenger cPTIO (Lot. PK822, Dojindo Molecular Technologies, Kumamoto, Japan) were dissolved in double distilled water to create a 10× stock solution with 3 mM concentration [77–79].

2.1.2. Wound Exudates

Wound exudates were obtained from seven diabetic patients with chronic wounds of the Klinikum Kalsburg, Germany according to an existent ethics approval. After removal of the wound bandage material, the patient wound was rinsed with sterile natural saline followed by blotting with a dry gauze. Afterwards, Copan eSwab samples (Mast Diagnostica GmbH, Reinfeld, Germany) were taken in a circular, inside-out motion across the treated wound surface, and rotated during sampling. Samples were placed in 1000 µL of serum-free Roswell Park Memorial Institute (RPMI) 1640 medium (Thermo Scientific, Rockford, IL, USA). Subsequently, wounds were plasma treated (see Section 2.2), rinsed again, and sampled as before using eSwabs. The swabs were vortexed for the maximal elution of wound exudates into the medium, and the supernatant was centrifuged at 4500 rpm for 5 min and sterile-filtered (0.22 µm). All swabs and supernatants were kept at −80 °C until further use.

2.2. Cold Plasma Treatments and Incubation with Control Oxidants

For the model solutions, the kINPen09 (neoplas tools GmbH, Greifswald, Germany) with a shielding device was used as a source of reactive species, as shown in Figure 1. Briefly, 750 µL of tyrosine solutions was treated in 24-well plates at a distance of 9 mm for 30 or 180 seconds. Argon (±1% of molecular gas admixture, Air Liquide, Paris, France) served as working gas using 3

standard liters per minute (slm). Admixtures were 1% oxygen, 1% nitrogen, or a mix of both (0.7% N₂ and 0.3% O₂, Air Liquide, Paris, France). For some treatments, isotopically labelled working gas admixtures (¹⁵N₂, or ¹⁸O₂, Merck KGaA, Darmstadt, Germany) or solvent (water, H₂¹⁸O, Merck KGaA, Darmstadt, Germany) were used. The plasma effluent was shielded against the ambient air by a gas shielding of 5 slm nitrogen. For some treatments, the working gas was enriched with water (320 ppm) by guiding 1% of the total flow through a gas wash bottle containing double distilled water [41,80,81]. Chronic wounds were treated in the Klinikum Karlsburg using the kINPen MED (neoplas tools GmbH, Greifswald, Germany) under standard medical conditions (30 s per 1 cm² of wound area and 5 slm of Argon (Air Liquide, Paris, France), without a shielding device.

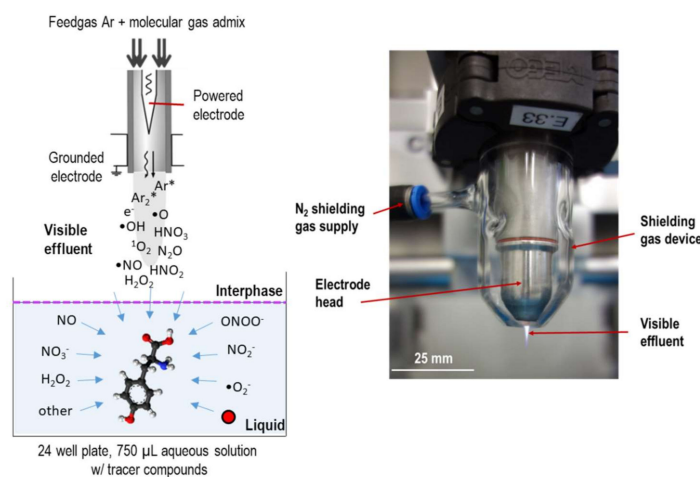


Figure 1. Schematic layout of treatment of tyrosine model solutions (left), and kINPen device w/gas shield installed (right).

Buffered solutions (pH 7.4) of tyrosine 0.3 mM were incubated for 2 min at room temperature under constant mixing with equimolar amounts of control oxidants (300 µM). Those were (1) peroxyntirite (Merck KGaA, Darmstadt, Germany) at pH 14; (2) peroxyntirite at pH 6.4, yielding 30% peroxyntirous acid dissociation in nitric dioxide radicals and hydroxyl radicals [54,82,83]; (3) the nitric oxide donor DEA NONOate (Biomol GmbH, Hamburg, Germany); (4) nitrite and nitrate (Merck KGaA, Darmstadt, Germany); (5) hydrogen peroxide (Merck KGaA, Darmstadt, Germany); and (6) mixed solutions of nitrite, nitrate, and hydrogen peroxide. For solutions (5) and (6), 300 µM of each control oxidant was included. After reaction, samples were put on ice and immediately subjected to mass spectrometry analysis. An overview of all the plasma treatment conditions (working gases and treated solutions) and of the solutions incubated with control oxidants is shown in Figure 2.

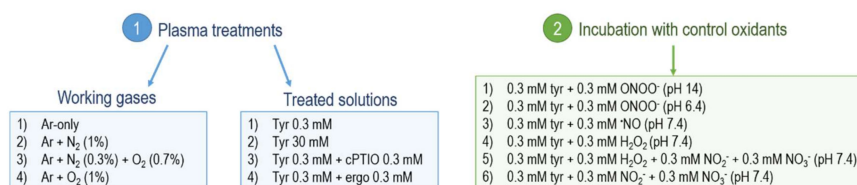


Figure 2. Overview of the solutions treated with plasmas (1) and incubated with control oxidants (2). Here, 3 slm of every working gas applied, together with 5 slm N₂ shielding gas. Prepared solutions were buffered with 5 mM ammonium formiate. Tyrosine (Tyr); ergothioneine (ergo).

2.3. Cold Plasma-Induced Modifications of Tyrosine

2.3.1. Qualitative Screening via Direct Infusion High-Resolution Mass Spectrometry

All samples were analyzed by high-resolution mass spectrometry using a TripleTOF 5600 (AB Sciex GmbH, Darmstadt, Germany). Samples were diluted 1:1 with acetonitrile/0.1% formic acid to stimulate ionization and to facilitate evaporation and injected using a syringe pump (50 μ L/min). Ionization was achieved by positive mode electro spray ionization with the following settings: +5.5 kV probe voltage, 300 °C, +30 V declustering potential, 40 psi curtain gas, 20 psi gas 1, and 25 psi gas 2 (Turbo Ion Source). Concentrated sample solutions (30 mM) were diluted 1:100 before injection. All spectra were acquired in the m/z range from 40 to 600 m/z . After a first qualitative scan of the produced compounds, their structures were elucidated by acquisition in tandem mass spectrometry (MS^2 spectra) and collisional energies for optimal fragmentation were tuned for each compound of interest.

2.3.2. HPLC- MS^2 Quantitation of Tyrosine and 3-Nitrotyrosine

Considering their relevance, L-tyrosine and 3-nitro-L-tyrosine (Merck KGaA, Darmstadt, Germany) were absolutely quantified by coupling a chromatographic separation (Infinity II 1290, Agilent Technologies, Berlin, Germany) to the mass spectrometry detection (qTRAP 5500, AB Sciex GmbH, Darmstadt, Germany). A hydrophilic liquid chromatography (HILIC) strategy was adopted, using a 2.1 mm \times 5 mm Acquity Amide VanGuard Pre-column followed by a 2.1 mm \times 100 mm Acquity Amide Column (both 130 Å pore size, 1.7 μ m particle size, Waters Corporation, Berlin, Germany). For the separation, eluent A (85% acetonitrile, 0.15% of formic acid, and 10 mM ammonium formate) and eluent B (HPLC water, 0.15% formic acid, and 10 mM ammonium formate; pH 3), were used. A linear gradient at a flow rate of 800 μ L/min was applied (time, B): 0 min, 99%; 4 min, 92%; 4.1 min, 99%; 5 min, 99%. After a 1:5 dilution in buffer A, 20 μ L of sample was injected. Ionization was achieved in positive mode, using the following parameters: +5.5 kV probe voltage at 150 °C, +100 V declustering potential, 35 psi curtain gas, 25 psi gas 1, and 30 psi gas 2. Compounds of interest were quantified by multiple reaction monitoring. The transitions and collisional energies (CEs) were tuned differently for each compound: tyrosine 182 \rightarrow 136 m/z (quantitative), CE 18 V and 165 m/z (qualitative), CE 10 V. Nitro-tyrosine 227 \rightarrow 181 m/z (quantitative) and 158 m/z (qualitative), both CE 10 V. For the quantification, external calibration curves were generated.

2.3.3. Data Analysis and Visualization

All experiments were performed three times each with technical duplicates. Statistical analysis was performed using GraphPad Prism 7. The MarvinSketch software (version 18.8.0) was used to identify the exact molecular weight and the formula of each compound, as well as to predict the reactivity of tyrosine and control oxidants in different pH. The spectra produced through direct infusion high-resolution mass spectrometry were calibrated and analyzed with PeakView (version 1.2.0.3, AB Sciex GmbH, Darmstadt, Germany). The peak areas of each observed derivative were normalized on the peak area of the control (untreated tyrosine), giving a relative estimate of the conversion. For treatments involving isotopes, the measurement data were corrected according to [36], taking into account the natural distribution of isotopes and the purity grade.

2.4. Characterization of Plasma-Induced Protein Modifications in Wound Exudates

Proteins were precipitated by incubating with 80% ice-cold acetone (Carl Roth GmbH, Karlsruhe, Germany) overnight. The pellets were washed twice and dissolved in 100 μ L resuspension buffer (10 mM Tris/HCl with 1 mM EDTA, pH 8, all Merck KGaA, Darmstadt, Germany). Protein concentrations were determined by Bradford assay following the vendor's high sensitivity protocol (Roti-Nanoquant, Roth, Germany). Single dimension electrophoresis was achieved by loading 60 μ g of each sample onto 10% precast protein gels (Bio-Rad Laboratories, Hercules, CA, USA), followed by in-gel digestion [30].

Briefly, gel slices were dried and incubated for 5 min with 50 μ L of 10 mM tris(2-carboxyethyl)phosphine (Merck KGaA, Darmstadt, Germany) at 60 °C followed by an incubation with 50 μ L of 50 mM iodoacetamide to alkylate reduced thiols at room temperature (RT) for 30 min (Merck KGaA, Darmstadt, Germany). After brief drying, 2.5 μ g trypsin (sequencing grade, Promega GmbH, Mannheim, Germany) was added and samples were incubated at 37 °C for 16 h. Peptides were eluted into ultra-pure water by ultra-sonication for 30 min. The peptides were further purified using Pierce C18 tips (Thermo Fisher Scientific, Hennigsdorf, Germany) following the included protocol for peptide purification and desalting. Eluted peptides were subjected to nanoLC/HRMS. An UltiMate 3000 nanoLC (Dionex Corp., Sunnyvale, CA, USA) was coupled to a QExactive mass spectrometer using electrospray ionisation (both Thermo Fisher Scientific, Hennigsdorf, Germany). Sample aliquots of 1 μ g were loaded onto an Acclaim PepMap 100 precolumn (2 cm \times 100 μ m, 5 μ m particle size, 100 Å pore size) for 6 min at 5 μ L/min flow followed by separation on a PepMap RSLC column (25 cm \times 75 μ m, 2 μ m particle size, 100 Å pore size). The following gradient was used at 200 nl/min: 2% to 35% in 6 min, to 50% B in 15 min, to 90% B in 15 min, keeping at 90% for 15 min, and equilibration at 2% B for 20 min (A: H₂O + 0.1% acetic acid, B: acetonitrile + 0.1% acetic acid, both Merck KGaA, Darmstadt, Germany). Each sample was injected twice. The QExactive was run in Top10 DDA mode with a dynamic exclusion of 30 s. MS1 spectra were acquired with a resolution of 70,000, whereas MS2 spectra were acquired in 17,500 resolution. Raw data files were analyzed with the Proteome Discoverer 2.2 (Thermo Fisher Scientific, Hennigsdorf, Germany) software. At least two unique peptides had to be identified with a maximal mass divergence of 5 ppm (MS1) and 0.02 Da (MS2) for the corresponding protein to be accepted. A maximum false discovery rate (FDR) of 5% was accepted for the datasets. Afterwards, abundances were normalized on individual trypsin intensities and resulting relative intensities taken for label free quantification using two-fold cut offs. In a second step, samples were analyzed using the Byonic (Protein Metrics Version 3.6) plug-in for Proteome Discoverer. Here, a list of oxidative chemical modifications was identified using a machine-learning algorithm with a database, which was previously acquired using model peptides [84]. For normalization, the peptide spectrum matches with a modification were counted and divided by the total number of peptide spectrum matches in each of the samples. The modifications found with Byonic were filtered and scored to separate nonsense peptide spectrum matches from those correctly identified.

3. Results and Discussion

3.1. Tyrosine Modification Induced by Plasma-Generated Reactive Oxygen and Nitrogen Species

Tyrosine solutions were treated by cold plasma with varying parameters or incubated with control oxidants. The generated products were identified via the accurate monoisotopic mass and on the tandem-MS level identifying molecule substructures. All the identified structures are listed in Table 1, independently from the condition in which they were produced. According to [33,34], where tyrosine solutions have been treated with plasma sources operated with air or helium as ionized gases, structures 2, 3, 10, and 22 were also identified in the current work using kINPen plasmas. Besides, more than 20 other types of functionalization were observed. The dominant modifications observed were all localized on the aromatic ring: hydroxylations, nitrosylations, nitrations, and a combination of different groups (up to four groups). Here, the addition of a functional group via electrophilic substitutions is stabilized by resonance effects [85,86]. To a lesser extent, the dimerization of tyrosine to dityrosine and the functionalization of this structure with other groups were also detected. While hydroxylations were mostly driven by oxygen species, the presence of N-containing functional groups indicated an active RNS chemistry. This was partially shown previously using cysteine as tracer, yielding S-nitroso-cysteine [30].

Table 1. Overview of modifications introduced in the tyrosine (Y) structure by tuning kINPen cold plasmas. * Assignment of a group letter in relation to the results obtained from the experiment performed in the presence of scavengers (details in Paragraph 3.5, Figure S4). The areas of compounds scavenged in the same way were summed up to generate six groups (from a to f).

Functional Group(s) on Tyrosine	Formula	[M+H] ⁺	Compound Code	Group Letter *
None	C ₉ H ₁₁ NO ₃	182.081725	1	-
1 × OH	C ₉ H ₁₁ NO ₄	198.0766	2	-
2 × OH	C ₉ H ₁₁ NO ₅	214.071525	3	-
3 × OH	C ₉ H ₁₁ NO ₆	230.066425	4	-
4 × OH	C ₉ H ₁₁ NO ₇	246.061425	5	-
1 × NO	C ₉ H ₁₀ N ₂ O ₄	211.071925	6	e
2 × NO	C ₉ H ₉ N ₃ O ₅	240.062025	7	a, d
3 × NO	C ₉ H ₈ N ₄ O ₆	269.052225	8	b, d
4 × NO	C ₉ H ₇ N ₅ O ₇	298.042325	9	b, d
1 × NO ₂ + 1 × OH, 1 × NO	C ₉ H ₁₀ N ₂ O ₅	227.066825	10	c, e
2 × NO ₂ + 2 × OH, 2 × NO	C ₉ H ₉ N ₃ O ₇	272.051825	11	b, e
3 × NO ₂	C ₉ H ₈ N ₄ O ₉	317.036925	12	b, e
4 × NO ₂	C ₉ H ₇ N ₅ O ₁₁	362.022025	13	b, e
1 × Y	C ₁₈ H ₂₀ N ₂ O ₆	361.139925	14	-
1 × Y, 1 × OH	C ₁₈ H ₂₀ N ₂ O ₇	377.134925	15	-
1 × Y, 2 × OH	C ₁₈ H ₂₀ N ₂ O ₈	393.129825	16	-
1 × Y, 3 × OH	C ₁₈ H ₂₀ N ₂ O ₉	409.124725	17	-
1 × Y, 1 × NO	C ₁₈ H ₁₉ N ₃ O ₇	390.130125	18	c, d
1 × Y, 1 × NO ₂ + 1 × Y, 1 × OH, 1 × NO	C ₁₈ H ₁₉ N ₃ O ₈	406.125025	19	e
1 × OH, 2 × NO	C ₉ H ₉ N ₃ O ₆	256.056925	20	a, f
1 × OH, 3 × NO	C ₉ H ₈ N ₄ O ₇	285.047125	21	b, f
1 × OH, 1 × NO ₂ + 2 × OH, 1 × NO	C ₉ H ₁₀ N ₂ O ₆	243.061725	22	c, f
2 × OH, 1 × NO ₂ + 3 × OH, 1 × NO	C ₉ H ₁₀ N ₂ O ₇	259.056625	23	f
3 × OH, 1 × NO ₂	C ₉ H ₁₀ N ₂ O ₈	275.051525	24	f
1 × OH, 2 × NO ₂	C ₉ H ₉ N ₃ O ₈	288.046825	25	f
2 × OH, 2 × NO ₂	C ₉ H ₉ N ₃ O ₉	304.041725	26	a, f
1 × OH, 3 × NO ₂	C ₉ H ₈ N ₄ O ₁₀	333.031825	27	f

However, the detected amounts were low, suggesting that cysteine is not an optimal target for the intended downstream analysis technique. The number and amount of identified N-containing modifications of tyrosine show a good suitability to study the RNS output of cold plasma discharges. An overview of oxidative modifications induced on tyrosine by different reactive species, possibly also formed by kINPen plasmas, is shown in Figure 3. When considering a radical-driven reaction mechanism, the first step for tyrosine derivatization is the formation of tyrosyl radicals by different one-electron oxidants ($\cdot\text{NO}_2$, $\cdot\text{OH}$). $\cdot\text{NO}_2$ is a candidate species able to form tyrosyl radicals via a slow reaction ($k = 3.2 \times 10^5 \text{ M}^{-1} \text{ s}^{-1}$), while hydroxyl radicals react at rates $\geq 1 \times 10^9 \text{ M}^{-1} \text{ s}^{-1}$. Consequential further direct reactions of tyrosyl radicals with tyrosine yield dityrosine ($k = 2.3 \times 10^8 \text{ M}^{-1} \text{ s}^{-1}$); those with $\cdot\text{NO}$ yield nitrosotyrosine ($k = 1.0 \times 10^9 \text{ M}^{-1} \text{ s}^{-1}$); those with $\cdot\text{NO}_2$ yield nitrotyrosine ($k = 3.0 \times 10^9 \text{ M}^{-1} \text{ s}^{-1}$); and those with $\cdot\text{O}_2^-$ yield tyrosine hydroxyquinone ($k = 1.5 \times 10^9 \text{ M}^{-1} \text{ s}^{-1}$) (only on free tyrosines). This last product rapidly loses O_2 from the structure to reform tyrosine [59,65,87]. After the formation of those derivatives, a further addition of groups led by reactive species was assumed. The conversion of NO-tyrosine to NO₂-tyrosine can occur in oxidative conditions firstly by formation of an iminoxyl radical ($\cdot\text{NO}$ -tyrosine) and, further,

oxygen addition. This two one-electron oxidation step process is a slow one, promoted by the presence of metals, which are not included in the used liquid model. In contrast, a direct reaction with $\cdot\text{OH}$ (and possibly $\cdot\text{O}$) leads to the formation of tyrosine hydroxyl radicals ($\cdot\text{OH}$ -tyrosine) ($k = 1.2 \times 10^{10} \text{ M}^{-1} \text{ s}^{-1}$), which rapidly lose an electron to become OH-tyrosine [65].

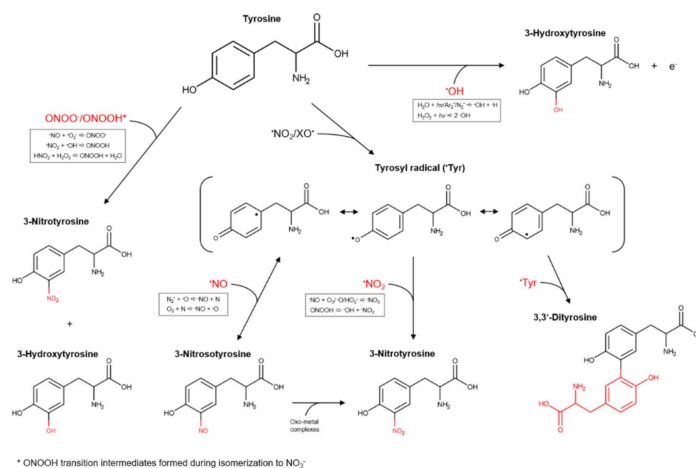


Figure 3. Formation pathways of tyrosine derivatives considering a neutral pH. The hypothesized possible responsible species generated by kINPen plasmas and the reactions leading to their origin are highlighted in the box [15,65,81,88,89].

A non-radical mechanism driven by peroxyntrous acid and peroxyntrite has also been proposed by [88], leading to tyrosine hydroxylation and nitration by formation of ONOOH transition intermediates during the H^+ driven isomerization of peroxyntrous acid to NO_3^- and H^+ . Indeed, the energy and the rate for the isomerization (18 kcal mol^{-1} and 1.3 s^{-1} , respectively) are equivalent to those necessary to achieve the nitration or hydroxylation of aromatic compounds, occurring independently from their concentrations. At very low pH (<2.5), the formation of nitril anion (NO_2^+) by peroxyntrous acid or peroxyntrite heterolysis could occur and lead to tyrosine nitration [89]. However, this mechanism can be excluded in our system, because of the controlled pH at 7.4.

3.2. Gas Composition: A Crucial Parameter to Regulate the NO_x Generation

Tyrosine solutions were treated using different working gas compositions and treatment times, yielding various products. While tyrosine and 3-nitrotyrosine were absolutely quantified by a multiple reaction monitoring approach (Figure 4), all other tyrosine derivatives were relatively quantified (Figure 5—dry working gas, Figure 6—humidified working gas).

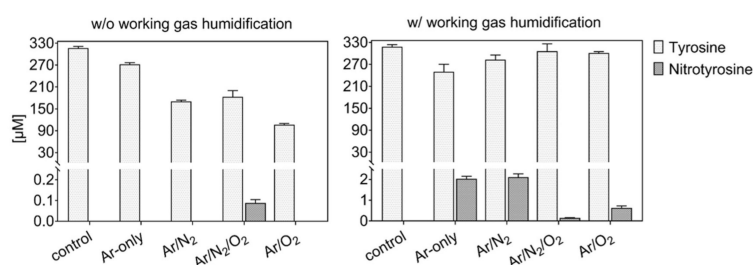


Figure 4. Tyrosine consumption and 3-nitrotyrosine formation by plasma-derived reactive oxygen species (ROS). The presence of water in the working gas reduced gas phase oxidation of reactive nitrogen species (RNS) and yielded higher activity of RNS in the liquid (3 min, 0.3 mM tyrosine in 5 mM ammonium formate, pH 7.4). Plasma is formed from dry (left) or humid (320 ppm H_2O , right) working gas.

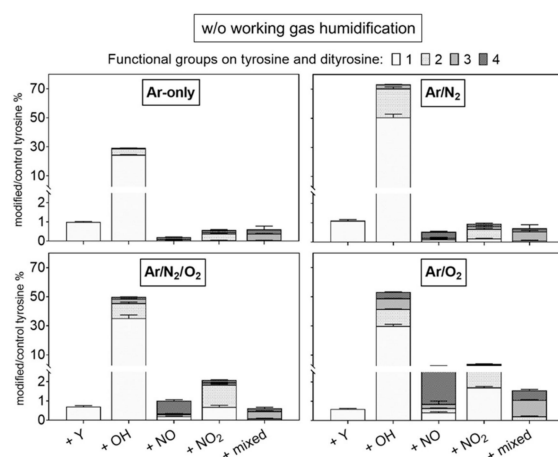


Figure 5. Modifications of tyrosine observed after plasma treatment using dry working gas are dominated by hydroxylation. Multiple nitrations/nitrosylations were observed predominantly when O_2 was present in the working gas. Labels: +Y (tyrosyl, +180.066 Da), +OH (hydroxyl, +15.9949 Da), +NO (nitroso, +28.9902 Da), and +NO₂ (nitro, +44.9851 Da). Up to four groups were observed per molecule (indicated by light to dark grey). The introduction of diverse groups is represented as “mixed” (Compounds 20 to 27, Table 1). Treatment time 3 min, 0.3 mM tyrosine in 5 mM ammonium formate, pH 7.4. Relative compound intensities are given (tyrosine ~4445 counts in control).

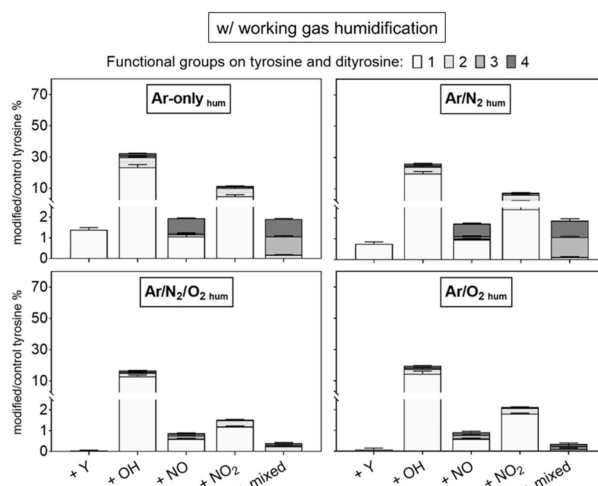


Figure 6. Modifications of tyrosine observed after plasma treatment using humidified working gas show a substantial introduction of one nitroso or nitro group. Labels: +Y (tyrosyl, +180.066 Da), +OH (hydroxyl, +15.9949 Da), +NO (nitroso, +28.9902 Da), and +NO₂ (nitro, +44.9851 Da). Up to four groups were observed per molecule (indicated by light to dark grey). The introduction of diverse groups is represented as “mixed” (Compounds 20 to 27, Table 1). Treatment time 3 min, 0.3 mM tyrosine in 5 mM ammonium formate, pH 7.4. Relative compound intensities are given (tyrosine ~4445 counts in control).

The highest tyrosine consumption (68%) was observed for a discharge regime rich in short-lived ROS (dry Ar/ O_2) [25]. In contrast, hydrogen peroxide rich conditions (dry Ar) [81] yielded only 14% tyrosine conversion.

Using admixtures of molecular gases, more than 50% of tyrosine was converted into hydroxytyrosine. Target water ionization, homolysis, or photolysis is promoted by excited states of Ar₂ or N₂ (excimers), as well as from radical reactions [36,90]. The direct reaction with those species (or for excimers, with their radiation) leads to the predominant formation in water of $\cdot OH$ and $\cdot H$ [91–93], which would react directly with tyrosine to form hydroxytyrosine. The higher OH-tyrosine production

in conditions with Ar/N₂ (up to 70% converted tyrosine) confirmed the synergistic action on the target of Ar₂ and N₂ excimers [15]. In contrast, in conditions including oxygen, gaseous radicals (e.g., $\cdot\text{O}$) are predominantly formed, and could be responsible for tyrosine hydroxylation (up to 4 $-\text{OH}$ groups) via direct reaction with tyrosine or via water dissociation and $\cdot\text{OH}$ formation in liquid [94,95]. In the presence of both N₂ and O₂ in the working gas, a substantial consumption of tyrosine was observed ($\approx 5\%$), alongside the detection of only small amounts of 3-nitrotyrosine in dry conditions (Figure 4).

Accordingly, the formation of primary or secondary nitrosative NO_x species can be assumed for this condition, corroborating previous results determining S-nitrosocysteine formation. Here, the presence of $\cdot\text{NO}$ in the liquid did not yield in S-nitrosylation, and $\cdot\text{NO}$ oxidation products (e.g., ONOO⁻, N₂O₃) were assumed to be of relevance. Considering the strong accumulation of nitrate in this discharge condition, an end product that can derive from the decomposition of peroxyxynitrite, ONOO⁻ could be responsible for both S-nitrosylation and nitrotyrosine formation [96]. The incorporation of two $-\text{NO}_2$ (%) and four $-\text{NO}$ (up to 5%) groups was detected in major amounts in admixtures including oxygen (Figure 5), confirming an active nitrogen chemistry in the liquid also using shielding N₂ as a source [42,97]. Considering quantitative data, an isobaric structure for nitrotyrosine (e.g., hydroxy-nitrosotyrosine, see Table 1) was detected in conditions with oxygen only as admix. Previous simulation studies showed the highest gas phase formation of $\cdot\text{NO}_2$ ($\sim 8 \times 10^{13} \text{ cm}^{-3}$) and N₂O ($\sim 5 \times 10^{12} \text{ cm}^{-3}$) using dry working gases (N₂ shielded) containing 1 % N₂/O₂ with O₂ in less than 50%. Those species decreased by increasing the O₂ %, with the increase of highly oxidized species, such as O₃ ($\sim 1.5 \times 10^{15} \text{ cm}^{-3}$) and N₂O₅ ($\sim 3 \times 10^{13} \text{ cm}^{-3}$) [81]. Considering the higher production of nitrotyrosine in conditions with 1:1 N₂/O₂ admixtures (Figure 4), $\cdot\text{NO}_2$ could be a direct nitrating agent of tyrosyl radicals in the target. However, it must be considered that only a minimal amount of $\cdot\text{NO}_2$ would be able to diffuse from the gas phase into the bulk of the liquid, owing to its low solubility in water ($H^{\text{CP}} = 3.4 \times 10^{-2} \text{ Pa}^{-1}$) [98]. Most likely, a direct nitration due to gaseous $\cdot\text{NO}_2$ could occur at the interface. These limitations could justify the overall low production of nitrotyrosine.

Alternatively, the production of other nitrating agents that have $\cdot\text{NO}_2$ as precursor can be considered. The reaction between $\cdot\text{NO}_2$ and water molecules generates HNO₂, which is highly soluble [35]. However, at a pH of 7.4, the nitrous acid cannot be considered as a nitrating agent. $\cdot\text{NO}_2$ could form N₂O₃, a nitrating agent, by reaction with $\cdot\text{NO}$, which is present in gas and liquid phase [81]. However, because of the low solubility of N₂O₃ ($H^{\text{CP}} = 6.0 \times 10^{-1} \text{ Pa}^{-1}$) [98], its penetration to the target is unlikely. With that, the well soluble peroxyxynitrite could be a prominent candidate for the effective nitrating species, acting on tyrosine via dissociation in $\cdot\text{NO}_2$ [65], or transition intermediates of peroxyxynitrous acid formed during its isomerization in nitrate [99]. ONOOH/ONOO⁻ production is promoted by reaction of gaseous $\cdot\text{NO}$ and $\cdot\text{O}_2^-$ [81], but considering $\cdot\text{NO}_2$ as major gaseous precursor, interface/bulk reactions of $\cdot\text{NO}_2$ (gas) with $\cdot\text{OH}$ (in liquid) or HNO₂ with H₂O₂ (in liquid) are possible formation pathways [99–101]. The production in liquid of H₂O₂ and $\cdot\text{OH}$ by water dissociation/ionization driven by radicals and vacuum UV radiation was shown previously [36,90]. The formation of peroxyxynitrite by the reaction of HNO₂ with H₂O₂ is favored by low pH (<4), which may be achieved in the gas–liquid interface [99,101] and not in the liquid bulk (Figure S1) [102].

As shown in Figures 4 and 6, the addition of humidity in the working gas reduced the general tyrosine oxidation in conditions containing oxygen, increasing drastically in Ar and Ar/N₂ the production of nitrotyrosine (up to 2 μM), nitrosotyrosine (one and four $-\text{NO}$ groups, 2%), mixed modifications (2%), and multiple nitration events (two $-\text{NO}_2$ groups, 8%). Conditions with Ar-only in the working gas became slightly more oxidative (25% oxidized tyrosine) than dry conditions. In contrast, tyrosine oxidation was lower than in dry conditions with molecular admixtures (7% and 5% for Ar/O₂ and Ar/N₂/O₂, respectively), as well as the production of tyrosine derivatives (Figure 6).

This can be explained by the interaction of water molecules in the effluent with gaseous species formed using Ar/O₂ and Ar/N₂/O₂ (e.g., $\cdot\text{O}$, $^1\text{O}_2$, $\cdot\text{NO}_2$). In parallel, it was shown that this interaction, mostly with Ar₂^{*} and $\cdot\text{O}$, generated $\cdot\text{OH}$, $\cdot\text{H}$, and $\cdot\text{O}_2^-$ in the effluent area, which partially diffuse into the target, forming high amounts of H₂O₂ by recombination of $\cdot\text{OH}$ [40,103]. In the gas phase of

humidified kINPen plasmas with low O₂%, a boost of gaseous nitrogen chemistry was also detected, with higher production of HNO₃ (~4 × 10¹³ cm⁻³) and ·NO (~6 × 10¹³ cm⁻³), rather than ·NO₂, the formation of which depended on O₂% densities [41].

Considering the 10-times higher production of nitrotyrosine in humid conditions with Ar-only or Ar/N₂ than in conditions with Ar/O₂ and Ar/N₂/O₂, a higher formation of nitrogen species in liquid is key. Rather than a direct impact of gaseous ·NO₂, the formation of peroxyxynitrite via different pathways is facilitated. The reaction of gaseous or dissolved ·NO with ·O₂⁻ at the interface or in the bulk of the liquid is a substantial pathway. Additionally, the high amounts of HNO₃ in the gas phase favor an attack of ·OH, forming ·NO₃, which is an unstable species generating H₂O₂ and ·NO₂ in contact with water. Alternatively, ·NO₂ could form HNO₂ by reacting with water molecules. The subsequent reaction with H₂O₂ yielding ONOOH is not favored at the pH of 7.4, precluding this as a major reaction route [102]. At the interface, ·NO₂ could form peroxyxynitrite by the reaction with ·OH radicals. Table 2 shows an overview of the major modifications induced on tyrosine during plasma treatment, together with the related plasma-derived species in the gas phase and the proposed reactions occurring in liquid to form the attacking species.

Table 2. Overview of the most relevant tyrosine derivatives observed in solution, potentially related plasma-derived species [41,81,97], and proposed reactions occurring in the liquid [15,81,99–101].

	Added Functional Groups on Tyrosine	Plasma Components in the Gas Phase	Proposed Reactions in Liquid
Ar-only	1 × OH	Ar ₂ [*] , VUV	H ₂ O → ·H + ·OH
Ar + N₂	1–2 × OH	Ar ₂ [*] , VUV	H ₂ O + <i>hν</i> → ·H + ·OH
Ar + N₂ + O₂	1–2 × OH; 1, 4 × NO; 1–2 × NO ₂	·NO _{2(g)} , ·O _(g)	·O + H ₂ O → ·OH + ·OH ·NO ₂ + ·OH → ONOOH
Ar + O₂	1–4 × OH; 1, 4 × NO; 1–2 × NO ₂ ; mixed	·NO _{2(g)} , ·O _(g) , O _{3(g)} N ₂ O _{5(g)}	·O + H ₂ O → ·OH + ·OH ·NO ₂ + ·OH → ONOOH
Ar-only hum	1 × OH; 1, 4 × NO; 1–2 × NO ₂ ; mixed	·NO _(g) , HNO _{3(g)} , H ₂ O _{2(aq)} , ·O ₂ ⁻ _(aq) , ·OH _(aq)	·NO + ·O ₂ ⁻ → ONOOH HNO ₂ + H ₂ O ₂ → ONOOH
Ar + N₂ hum	1 × OH; 1, 4 × NO; 1–2 × NO ₂ ; mixed	·NO _(g) , HNO _{3(g)} , H ₂ O _{2(aq)} , ·O ₂ ⁻ _(aq) , ·OH _(aq)	·NO + ·O ₂ ⁻ → ONOOH HNO ₂ + H ₂ O ₂ → ONOOH
Ar + N₂ + O₂ hum	1 × OH; 1 × NO; 1 × NO ₂	·NO _{2(g)} , N ₂ O _{5(g)} , H ₂ O _{2(aq)} , ·O ₂ ⁻ _(aq) , ·OH _(aq)	·NO ₂ + ·OH → ONOOH HNO ₂ + H ₂ O ₂ → ONOOH
Ar + O₂ hum	1 × OH; 1 × NO; 1 × NO ₂	·NO _{2(g)} , N ₂ O _{5(g)} , H ₂ O _{2(aq)} , ·O ₂ ⁻ _(aq) , ·OH _(aq)	·NO ₂ + ·OH → ONOOH HNO ₂ + H ₂ O ₂ → ONOOH

3.3. Tyrosine Modification Induced by Control Oxidants

Incubations with control oxidants (NO donor, NO₂⁻/NO₃⁻, H₂O₂/NO₂⁻/NO₃⁻) were performed at neutral pH (7.4). Peroxyxynitrite was tested at two different pH (pH 14 and 6.4) [83,84]. The observed tyrosine derivatives are shown in Figure 7 (quantitative) and 8 (qualitative). Peroxyxynitrite was most efficient in modifying tyrosine (46% and 37% at pH 14 and 6.4, respectively). In particular, nitrotyrosine (~10 μM) was formed (Figure 7). The substantial functionalization observed for ONOO⁻ at near neutral pH is due to the protonation of the ion, yielding instable peroxyxynitrous acid (ONOOH, 58.7% considering pK_a = 6.8). This rapidly isomerizes into NO₃⁻ and H⁺, and dissociates in ·OH and ·NO₂ (30% yield) [62,66,70]. The incorporation of up to four –NO₂ groups in the tyrosine structure emphasized the favored formation of ·NO₂ by peroxyxynitrite dissociation. In addition, the single nitration of tyrosine could be induced by the indirect reaction of ONOOH via the formation of a transition intermediate generated in the isomerization of ONOOH to NO₃⁻ [88]. According to [88,89], the hydroxylation was stronger at lower pH because of the formation of a peroxyxynitrous acid intermediate that facilitates the cleavage of the ions O–O bond.

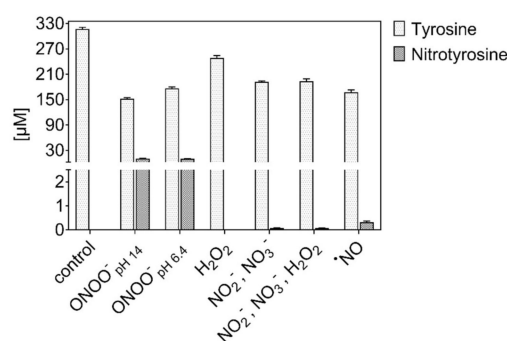


Figure 7. Tyrosine consumption and 3-nitrotyrosine formation by control oxidants. Peroxynitrite efficiently introduced a nitro group, but independently from pH (3 min incubation of 0.3 mM tyrosine in 5 mM ammonium formate, pH 7.4, 300 μM of each control oxidant).

However, at pH 14, a similar nitration yield was observed. According to [99], different products generated during ONOO⁻ homolysis ($\cdot\text{NO}$ and $\cdot\text{O}_2^-$) and decomposition (O_2 and NO_2^-) could be involved in the direct or indirect functionalization of biomolecules, including the peroxyntiric anion (O_2NOO^-). The functionalization of tyrosine via non-radical processes was confirmed, also inducing a higher incorporation of up to four different functional groups into the tyrosine moiety (+2 -OH groups, two and four mixed groups) (Figure 8). Incubations with any other compound (mix) yielded very low amounts of nitrotyrosine (<0.5 μM), and only the $\cdot\text{NO}$ donor could induce nitroso-groups on tyrosine, confirming a direct reaction with the aromatic ring (Figure 8) [65]. The low formation of nitrosotyrosine indicates the low reactivity of $\cdot\text{NO}$ itself with the ring and a limited oxidation of $\cdot\text{NO}$ to nitrite ions' respective nitrous acid. A partial oxidation to $\cdot\text{NO}_2$ in the presence of O_2 could justify the formation of nitrotyrosine.

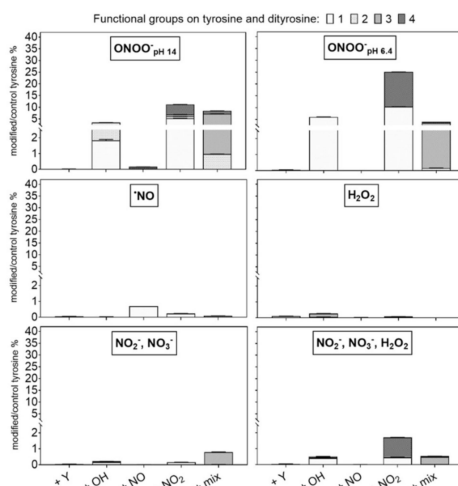


Figure 8. Modifications of tyrosine observed after treatment using control oxidants. Peroxynitrite was most efficient, with higher pH boosting the introduction of multiple groups. Labels: +Y (tyrosyl, +180.066 Da), +OH (hydroxyl, +15.9949 Da), +NO (nitroso, +28.9902 Da), and +NO₂ (nitro, +44.9851 Da). Up to four groups were observed per molecule (indicated by light to dark grey). The introduction of diverse groups is represented as “mixed” (Compounds 20 to 27, Table 1). Treatment time 3 min, 0.3 mM tyrosine in 5 mM ammonium formate, pH 7.4, direct infusion high-resolution mass spectrometry (MS). Relative compound intensities are given (tyrosine ~4948 counts in control).

By the incubation with H₂O₂, only 11% of the tyrosine was consumed, and yielded hydroxylated products. When nitrite and nitrate ions were available at the same time, a few nitrations were observed. Of note, no nitrosylation occurred, indicating that peroxyntirite, formed from H₂O₂ and NO₂⁻,

was responsible. However, because of the pH of 7.4 in the experiment, this reaction was not favored. Likewise, the pH in the plasma treatment never reached below pH 7, even after 10 min of treatment (Figure S1 in SI), excluding a substantial formation of peroxyxynitrite in the bulk. When nitrite/nitrate were the sole available compounds, no modification of tyrosine occurs. The apparent consumption of tyrosine in conditions with a high sodium content was overestimated as a result of the formation of tyrosine salts that evaded detection in the applied experimental conditions.

3.4. Both Gas Phase- and Liquid Phase-Derived Species Contribute to Tyrosine Modification

To investigate the role of solvent-derived reactive species, higher concentrated solutions of tyrosine (30 mM) were treated. The identified products were similar to the more diluted solutions (see Figure S2/dry working gas and Figure S3/humidified working gas for a complete overview). While the total number of oxidized molecules increased, the conversion was proportionally lower and indicated a limitation of the produced ROS/RNS in liquid. In conditions with Ar-only, Ar/N₂, and Ar/O₂, a conversion of 3.2×10^{18} , 3.0×10^{18} , and 5.0×10^{18} molecules per second occurred respectively (Figure 9). This corresponds to a total of 24%, 22%, and 36% tyrosine conversion in derivatives. In comparison, treatments of 0.3 mM tyrosine solutions yielded a conversion rate of 1.8×10^{16} , 6.6×10^{16} , and 9.5×10^{16} molecules per second, corresponding to 12.8% (Ar-only), 45% (Ar/N₂), and 66% (Ar/O₂) converted tyrosine, respectively. On average, the conversion in concentrated tyrosine solutions was a factor of ≈ 50 fold higher than in diluted solutions, while their concentration was 100-fold higher. This would suggest that, using these working gases and a high tyrosine concentration, the amount of induced modifications was reduced as a result of limited production/action of species in liquid. In parallel, gaseous species were still effective on the target.

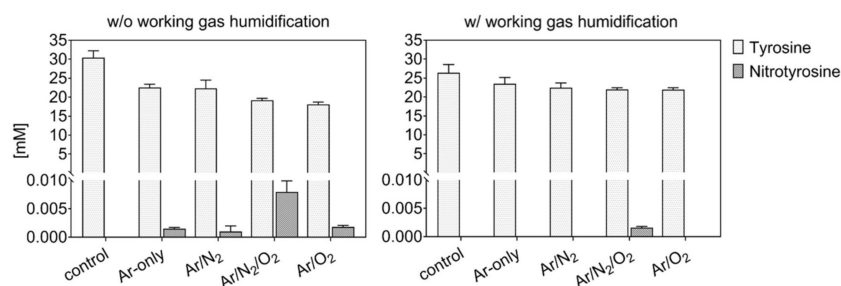


Figure 9. Tyrosine consumption and 3-nitrotyrosine formation by plasma-derived ROS in concentrated tyrosine solutions. The activity of peroxyxynitrite (humid conditions) is quenched in favor of nitrogen dioxide (dry conditions). Three minutes, 30 mM tyrosine in 5 mM ammonium formate, pH 7.4. Plasma is formed from dry (left) or humid (320 ppm H₂O, right) working gas.

In contrast, conditions with both N₂ and O₂ in the dry working gas led to an identical proportional formation of nitrotyrosine (0.026% of converted tyrosine) for both concentrations. In this case, the high amounts of generated $\cdot\text{NO}_2$ in the gas phase could directly modify tyrosine molecules at the interface or in the underlying water layers of both high and low concentrated solutions. The apparent reaction probability remained constant, indicating that the interface occupation by the tyrosine molecules did not change with the concentration or that a corresponding decay reaction (e.g., formation of hydroxytyrosine from nitrotyrosine) increased proportionally.

The role of gaseous $\cdot\text{NO}_2$ in forming nitrotyrosine was determined using heavy isotopes (¹⁵N₂ or ¹⁸O₂, or H₂¹⁸O). Almost 80% ¹⁸O and 100% ¹⁵N originated from the gas phase (Figure 10), confirming the direct nitration of tyrosine by $\cdot\text{NO}_2$, rather than other species (e.g., peroxyxynitrite) originating from liquid chemistry.

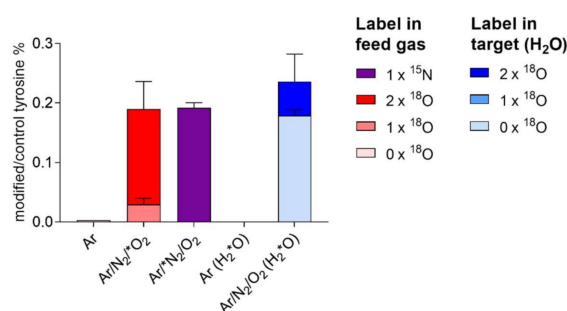


Figure 10. Nitrotyrosine formed from plasma treatment of tyrosine incorporates predominantly gas phase-derived atoms (100% N, \approx 80% O). Here, 20% of oxygen atoms are introduced from the solvent (water), indicating a role for water-derived OH radicals (for details, see text). Dry argon working gas contained $^{18}\text{O}_2$ and $^{15}\text{N}_2$. In independent experiments, tyrosine was dissolved in labelled water (H_2^{18}O). Measurements performed via direct infusion mass spectrometry in triplicates.

By introducing humidity in the working gas, the oxidation of tyrosine, as well as the production of nitrotyrosine (Figure 9) and other tyrosine derivatives, such as dityrosine and nitrosotyrosine (Figure S3), were drastically reduced in relation to dry conditions (Figure S2). This suggests that, in humidified conditions, relevant species act and/or are formed in the bulk of the liquid. It was observed that, for working gases with $<0.5\ \text{O}_2\%$, the presence of water molecules induced mostly the formation of species such as HNO_3 and $\cdot\text{NO}$, along with water-derived species H_2O_2 , $\cdot\text{OH}$, $\cdot\text{H}$, and $\text{O}_2^{\cdot-}$, rather than highly oxidized gaseous species, such as N_2O_5 , O_3 , and $\cdot\text{NO}_2$ [41]. When treating 0.3 mM tyrosine solutions with humid plasmas, nitrotyrosine was detected in a 10-fold higher amount than for the respective dry discharges. Considering that high concentrated solutions limited the formation/action of reactive species in liquid, gaseous species formed in humidified working gases ($<0.5\ \text{O}_2\%$) acted only in the bulk liquid or most likely as precursors of other nitrating species (e.g., peroxyxynitrite) formed in liquid.

3.5. Identification of Plasma-Derived Reactive Nitrogen Species

In presence of the $\cdot\text{NO}$ scavenger cPTIO or the peroxyxynitrite scavenger ergothioneine, the formation of N-containing tyrosine derivatives was differential.

A general overview of all identified compounds containing nitrogen is given in Figure S4, while Figure 11 shows quantitative data achieved by quantitative mass spectrometry (HILIC-MRM) for nitrotyrosine. As shown in Figure 11, in conditions with humidified working gases, the production of nitrotyrosine was almost abolished in the presence of cPTIO or ergothioneine. Further, almost all other N-containing tyrosine derivatives were inhibited (Figure S4). These results are in good agreement with the hypothesis that the addition of humidity to the working gas favors the production of peroxyxynitrite, predominantly originating by the reaction of $\cdot\text{NO}$ with $\text{O}_2^{\cdot-}$ derived by water dissociation. The conversion of HNO_3 in $\cdot\text{NO}_2$ in liquid and its further reaction with $\cdot\text{OH}$ could still be an additional route for peroxyxynitrite formation.

The formation and activity of reactive nitrogen species in liquids could not be excluded for dry working gases (Figure S4). Indeed, the formation of some compounds that bear nitroso-groups was prevented only by cPTIO ($<0.5\%$ in $\text{Ar}/\text{N}_2/\text{O}_2$, Figure S4a), indicating a role for a direct or indirect role of $\cdot\text{NO}$, reformed in the liquid phase from gaseous $\cdot\text{NO}_2$ [81]. Furthermore, almost 2.5% of tyrosine was converted in conditions with dry $\text{Ar}/\text{N}_2/\text{O}_2$ in derivatives scavenged by ergothioneine (Figure S4b,c). These data confirm the formation and chemical activity of peroxyxynitrite in dry working gas conditions. Finally, conditions with dry working gases produced the maximal amount of nitrogen-containing derivatives in the presence of gas admixtures (3% oxidized tyrosine). Their formation was due paramount to the direct action of gaseous $\cdot\text{NO}_2$ and, to a lesser extent, to a reformation of nitrosative species in the liquid (e.g., H^+/NO_2^- , ONOO^-). For humidified working gas, an increase of

nitrogen-containing derivatives was evident, provided when no oxygen was added (>14% oxidized tyrosine). Here, the nitrosative peroxyxynitrite is formed in liquid (Figure S4).

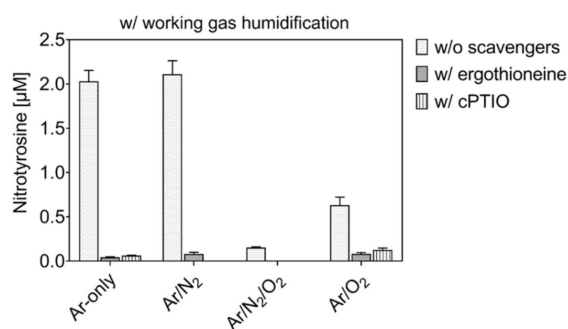


Figure 11. Nitrotyrosine formation by plasma treatment is prevented in the presence of scavengers. Three minute treatment, 0.3 mM tyrosine in 5 mM ammonium formate, pH 7.4, with and without ergothioneine or cPTIO, using Ar ± 1% N₂/O₂ as humidified working gas and N₂ as shielding gas.

However, non-specific reactions must be considered. It was reported that the NO scavenger cPTIO partially reacts with ·NO₂ [78], while ergothioneine is able to scavenge ¹O₂ and ·OH [79,104]. No discriminative derivatives produced by the reaction of scavengers with control oxidants could be identified in this work.

3.6. Plasma Induces Oxidative and Nitrosative Protein Modifications in Wounds

In order to verify that nitrosative modifications are introduced in vivo as well, the wound proteome of human patients before and after plasma treatment was analyzed. A special emphasis was given to modifications at the tyrosine moiety.

Overall, 330 proteins have been identified and were searched for oxidative post-translational modifications (PTMs). PTMs were detected at 80 proteins; 27 of these were modified at tyrosine moieties (Table 3). An increase of 63% (oxidation), 44% (nitration), and 69% (nitrosylation) compared with the control was observed (Figure 12). Target proteins were highly abundant blood plasma and blood cell components (transferrin, albumin, hemoglobin, and so on), or belonged to the wound bed/wound margins (keratins, fibronectin). The modified tyrosine residues were located at the protein surface or otherwise exposed structures. As samples were taken immediately after treatment, regular physiologic reactions were unlikely and the increase of modifications was attributed directly to the impact of plasma-derived reactive species. The oxidation of tyrosine and cysteine residues in blood plasma proteins was already observed for inflammatory levels of hypochlorous acid [105]. Target proteins were, among others, complement C3 and apolipoprotein A-I, and albumin was affected in this study as well. Cold plasma-derived atomic oxygen forms hypochlorite anions upon reaction with chloride ions locally, which subsequently serves as oxidants yielding di-tyrosine, hydroxylations, and chlorinations (rare). The introduction of nitro and nitroso groups into tyrosine occurs by local formation of peroxyxynitrite and NO₂ radicals, which are only effective at or close to the treated surface. Yielding a higher reactivity of the tyrosine's phenolic hydroxyl group, significant effects on the regulation of cell migration, angiogenesis, and mast cell degranulation [67,72] were described for physiologic conditions (nitric oxide pathway). The proportional strong oxidation/nitration of haptoglobin, a protein protective against hemoglobin related oxidative stress, and of bulky structural proteins like fibronectin and keratins, confirms a significant presence of reactive species from the plasma discharge and the proteins' roles as scavenger molecules.

Table 3. Twenty seven proteins were identified from wound exudates carrying oxidative modifications on tyrosine (oxidation/+15.99 Da, nitrosylation/+28.99 Da, nitration/+44.99 Da). The total number of proteins found with modification was 80 out of 308 proteins identified. Blood-derived proteins dominate the list. Modifications occur predominantly at the protein surface.

Uniprot Identifier	Abbreviated Protein Name	Protein Name	Modified Tyrosine Residue (Bold Denotes Significant Site)
P02768	ALBU	Albumin	Y54 , Y172, Y174, Y287 , Y377 , Y425, Y356, Y365 , Y521
P01009	A1AT	Alpha-1-antitrypsin	Y184
P01023	A2MG	Alpha-2-macroglobulin	Y544, Y818, Y1152, Y1264
O43299	AP5Z1	AP-5 complex subunit zeta-1	Y344
P02647	APOA1	Apolipoprotein A-I	Y124, Y190
P00915	CAH1	Carbonic anhydrase 1	Y21
P00450	CERU	Ceruloplasmin	Y55, Y539
P01024	CO3	Complement C3	Y139, Y1447, Y1620
P0C0L4	CO4A	Complement C4-A	Y1612
P02751	FINC	Fibronectin	Y841, Y2362
P00738	HPT	Haptoglobin	Y224, Y242 , Y280 , Y386, Y389
P69905	HBA	Hemoglobin subunit alpha	Y25 , Y43
P68871	HBB	Hemoglobin subunit beta	Y36 , Y131
P02042	HBD	Hemoglobin subunit delta	Y36, Y131
P01876	IGHA1	Immunoglobulin heavy constant alpha 1	Y276
P01857	IGHG1	Immunoglobulin heavy constant gamma 1	Y161 , Y319
Q14624	ITI4	Inter-alpha-trypsin inhibitor heavy chain H4	Y157
P13645	K1C10	Keratin, type I cytoskeletal 10	Y172, Y325
P02533	K1C14	Keratin, type I cytoskeletal 14	Y46
P35527	K1C9	Keratin, type I cytoskeletal 9	Y330, Y345
P04264	K2C1	Keratin, type II cytoskeletal 1	Y266, Y295, Y358, Y373
Q7Z794	K2C1B	Keratin, type II cytoskeletal 1b	Y361
P35908	K22E	Keratin, type II cytoskeletal 2	Y563, Y589
P02788	TRFL	Lactotransferrin	Y211 , Y545
P32119	PRDX2	Peroxiredoxin-2	Y126
P00747	PLMN	Plasminogen	Y66
P02787	TRFE	Serotransferrin	Y114, Y333, Y533

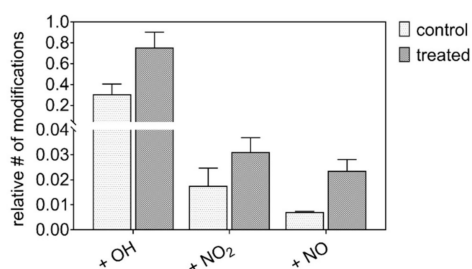


Figure 12. Cold plasma induced post-translational modifications in the proteome of wound exudates of diabetic patients. Proteome analysis performed via nanoLC-MS, with the detection of mass shifts corresponding to the introduced functional group (OH = 15.9949 Da; NO = 28.9902 Da, NO₂ = 44.9851 Da), according to [80].

The introduction of nitro groups into proteins by plasma-derived species suggests at least a contributing role in the observed crosstalk to cellular redox signaling pathways involved in acute and chronic wound healing, well in line with a recent study that emphasized the role of target cell stimulation over anti-microbial effects [22]. The results of this study suggest that the clinical effectivity of cold plasmas would benefit from a switch from the current condition (argon only) to argon/N₂/O₂ as a working gas to increase the impact of the plasma-derived RNS on biomolecules and subsequent signaling events.

4. Summary and Conclusions

This work studied the liquid chemistry of argon plasmas generated by the kINPen, with a special focus on reactive nitrogen species. Assuming that the liquid chemistry is the bridge between the gaseous plasma and biological systems, we looked for the impact of nitrogen species on the model biomolecule tyrosine. Using a mass spectrometry driven approach, 26 different compounds were identified. Their respective pattern was exploited to determine the dominant reactive species formed in the gas or in/at the liquid phase.

Nitration reactions were significant for dry Ar/O₂/N₂ plasma. Gaseous $\cdot\text{NO}_2$ was found to be responsible for a direct nitration of tyrosine at the gas–liquid interface. Additionally, it is involved in the formation of peroxyntirite and nitric oxide radicals. While the relevance of nitric oxide for the product formation was limited, peroxyntirite contributed to a substantial extent. When water molecules were present in the working gas, its role was further emphasized owing to a higher peroxyntirite formation via additional pathway; that is, the reaction of gaseous nitric oxide with superoxide anion radicals and the reaction of hydrogen peroxide and nitrous acid/nitrite at the gas–liquid interface. In conditions with a high prevalence of ROS (e.g., dry Ar/O₂), the impact of RNS was minimized. Here, stable species like N₂O₅ that do not penetrate the interface evolve from $\cdot\text{NO}_2$ in the gas phase and the formation of peroxyntirite decreases. Because of the high activity of ROS at the interface and the liquid bulk, potentially formed nitrated/nitrosylated tyrosine products are eliminated in favor of hydroxylated compounds. Finally, the introduction of nitroso and nitro groups into proteins in vivo by cold plasma treatments was confirmed in human diabetes 2-related chronic wounds. The tyrosine moiety was particularly attacked, allowing for changes in the protein functionality. This suggests a contribution of plasma-derived RNS via covalent changes to the observed efficacy in wound healing.

In conclusion, this work verified the controllability of kINPen plasmas to achieve a relevant production of reactive nitrogen species (Figure 13). The dissolved or at the interface generated species, especially $\cdot\text{NO}_2$ and ONOO[−], led to nitrosative reactions on biomolecules, in both complex and model conditions. A relevant contribution to the observed biomedical effects of plasmas must be assumed.

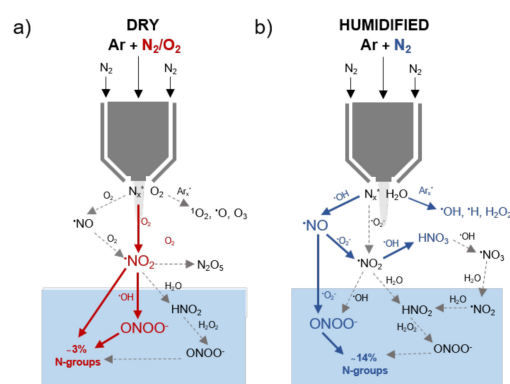


Figure 13. Suggested chemical pathways for the production of bioactive RNS species in plasma treated tyrosine solutions in dry (a) and humidified (b) conditions. Represented species were previously detected for the kINPen [41,82,100], except for peroxyntirite. Pathway confirmed in liquids (compact lines) by use of scavengers or isotope labels.

Supplementary Materials: The following are available online at <http://www.mdpi.com/2218-273X/10/12/1687/s1>, Figure S1: pH measurements performed after 30, 180 and 600 seconds plasma treatment of 0.3 mM tyrosine solutions (in 5 mM ammonium formate) using different working gas admixtures ($\text{Ar} \pm 1\% \text{N}_2/\text{O}_2$); Figure S2: Modifications of tyrosine observed after plasma treatment using dry working gas of high concentrated tyrosine solutions; Figure S3: Modifications of tyrosine observed after plasma treatment using dry working gas of high concentrated tyrosine solutions; Figure S4: Modifications of tyrosine observed after plasma treatment using dry and humidified working gases of normal tyrosine solutions and in presence of scavengers.

Author Contributions: Conceptualization, G.B. and K.W.; methodology, G.B., K.W., and S.W./J.-W.L. (proteome and PTMs analysis); formal analysis, G.B. and S.W./J.-W.L. (proteome and PTMs analysis); investigation, G.B.; data curation, G.B.; writing—original draft preparation, G.B. and S.W. (proteome and PTMs analysis); writing—review and editing, G.B., K.W., M.L. and T.v.W.; visualization, G.B. All authors have read and agreed to the published version of the manuscript.

Funding: This research and the article processing charges were funded by the German Federal Ministry of Education and Research (grant number 03Z22DN12 to K.W.).

Conflicts of Interest: The authors declare no conflict of interest.

References

1. Alfadda, A.A.; Sallam, R.M. Reactive oxygen species in health and disease. *J. Biomed. Biotechnol.* **2012**, *2012*, 936486. [[CrossRef](#)] [[PubMed](#)]
2. Parvez, S.; Long, M.J.C.; Poganik, J.R.; Aye, Y. Redox Signaling by Reactive Electrophiles and Oxidants. *Chem. Rev.* **2018**, *118*, 8798–8888. [[CrossRef](#)] [[PubMed](#)]
3. Törnvall, U. Pinpointing oxidative modifications in proteins—Recent advances in analytical methods. *Anal. Methods* **2010**, *2*. [[CrossRef](#)]
4. Sies, H.; Berndt, C.; Jones, D.P. Oxidative Stress. *Annu. Rev. Biochem.* **2017**, *86*, 715–748. [[CrossRef](#)] [[PubMed](#)]
5. Cai, Z.; Yan, L.J. Protein Oxidative Modifications: Beneficial Roles in Disease and Health. *J. Biochem. Pharmacol. Res.* **2013**, *1*, 15–26. [[PubMed](#)]
6. Halliwell, B. Free Radicals and Other Reactive Species in Disease. In *Encyclopedia of Life Sciences*; John Wiley & Sons, Ltd.: Hoboken, NJ, USA, 2005.
7. Winterbourn, C.C. Reconciling the chemistry and biology of reactive oxygen species. *Nat. Chem. Biol.* **2008**, *4*, 278–286. [[CrossRef](#)]
8. Adams, L.; Franco, M.C.; Estevez, A.G. Reactive nitrogen species in cellular signaling. *Exp. Biol. Med.* **2015**, *240*, 711–717. [[CrossRef](#)]
9. Hancock, J.T.; Desikan, R.; Neill, S.J. Role of reactive oxygen species in cell signalling pathways. *Biochem. Soc. Trans.* **2001**, *29 Pt 2*, 345–350. [[CrossRef](#)]
10. von Woedtke, T.; Schmidt, A.; Bekeschus, S.; Wende, K.; Weltmann, K.D. Plasma Medicine: A Field of Applied Redox Biology. *In Vivo* **2019**, *33*, 1011–1026. [[CrossRef](#)]
11. Privat-Maldonado, A.; Schmidt, A.; Lin, A.; Weltmann, K.D.; Wende, K.; Bogaerts, A.; Bekeschus, S. ROS from Physical Plasmas: Redox Chemistry for Biomedical Therapy. *Oxid. Med. Cell. Longev.* **2019**, *2019*, 9062098. [[CrossRef](#)]
12. Agostinis, P.; Berg, K.; Cengel, K.A.; Foster, T.H.; Girotti, A.W.; Gollnick, S.O.; Hahn, S.M.; Hamblin, M.R.; Juzeniene, A.; Kessel, D.; et al. Photodynamic therapy of cancer: An update. *CA Cancer J. Clin.* **2011**, *61*, 250–281. [[CrossRef](#)] [[PubMed](#)]
13. Vozenin, M.C.; Hendry, J.H.; Limoli, C.L. Biological Benefits of Ultra-high Dose Rate FLASH Radiotherapy: Sleeping Beauty Awoken. *Clin. Oncol. (R. Coll. Radiol.)* **2019**, *31*, 407–415. [[CrossRef](#)] [[PubMed](#)]
14. Adamovich, I.; Baalrud, S.D.; Bogaerts, A.; Bruggeman, P.J.; Cappelli, M.; Colombo, V.; Czarnetzki, U.; Ebert, U.; Eden, J.G.; Favia, P.; et al. The 2017 Plasma Roadmap: Low temperature plasma science and technology. *J. Phys. D Appl. Phys.* **2017**, *50*, 323001. [[CrossRef](#)]
15. Bruggeman, P.J.; Kushner, M.J.; Locke, B.R.; Gardeniers, J.G.E.; Graham, W.G.; Graves, D.B.; Hofman-Caris, R.C.H.M.; Maric, D.; Reid, J.P.; Ceriani, E.; et al. Plasma-liquid interactions: A review and roadmap. *Plasma Sources Sci. Technol.* **2016**, *25*, 053002. [[CrossRef](#)]
16. Laroussi, M.; Lu, X.; Keidar, M. Perspective: The physics, diagnostics, and applications of atmospheric pressure low temperature plasma sources used in plasma medicine. *J. Appl. Phys.* **2017**, *122*, 020901. [[CrossRef](#)]

17. Park, G.Y.; Park, S.J.; Choi, M.Y.; Koo, I.G.; Byun, J.H.; Hong, J.W.; Sim, J.Y.; Collins, G.J.; Lee, J.K. Atmospheric-pressure plasma sources for biomedical applications. *Plasma Sources Sci. Technol.* **2012**, *21*, 043001. [[CrossRef](#)]
18. Reuter, S.; von Woedtke, T.; Weltmann, K.D. The kINPen—a review on physics and chemistry of the atmospheric pressure plasma jet and its applications. *J. Phys. D Appl. Phys.* **2018**, *51*. [[CrossRef](#)]
19. Semmler, M.L.; Bekeschus, S.; Schafer, M.; Bernhardt, T.; Fischer, T.; Witzke, K.; Seebauer, C.; Rebl, H.; Grambow, E.; Vollmar, B.; et al. Molecular Mechanisms of the Efficacy of Cold Atmospheric Pressure Plasma (CAP) in Cancer Treatment. *Cancers* **2020**, *12*, 269. [[CrossRef](#)]
20. Pasqual-Melo, G.; Sagwal, S.K.; Freund, E.; Gandhirajan, R.K.; Frey, B.; von Woedtke, T.; Gaipf, U.; Bekeschus, S. Combination of Gas Plasma and Radiotherapy Has Immunostimulatory Potential and Additive Toxicity in Murine Melanoma Cells in Vitro. *Int. J. Mol. Sci.* **2020**, *21*, 1379. [[CrossRef](#)]
21. Lin, A.; Gorbanev, Y.; De Backer, J.; Van Loenhout, J.; Van Boxem, W.; Lemiere, F.; Cos, P.; Dewilde, S.; Smits, E.; Bogaerts, A. Non-Thermal Plasma as a Unique Delivery System of Short-Lived Reactive Oxygen and Nitrogen Species for Immunogenic Cell Death in Melanoma Cells. *Adv. Sci.* **2019**, *6*, 1802062. [[CrossRef](#)]
22. Stratmann, B.; Costea, T.C.; Nolte, C.; Hiller, J.; Schmidt, J.; Reindel, J.; Masur, K.; Motz, W.; Timm, J.; Kerner, W.; et al. Effect of Cold Atmospheric Plasma Therapy vs. Standard Therapy Placebo on Wound Healing in Patients With Diabetic Foot Ulcers: A Randomized Clinical Trial. *JAMA Netw. Open* **2020**, *3*, e2010411. [[CrossRef](#)] [[PubMed](#)]
23. Schmidt, A.; Bekeschus, S. Redox for Repair: Cold Physical Plasmas and Nrf2 Signaling Promoting Wound Healing. *Antioxidants* **2018**, *7*, 146. [[CrossRef](#)] [[PubMed](#)]
24. Preissner, S.; Kastner, I.; Schutte, E.; Hartwig, S.; Schmidt-Westhausen, A.M.; Paris, S.; Preissner, R.; Hertel, M. Adjuvant antifungal therapy using tissue tolerable plasma on oral mucosa and removable dentures in oral candidiasis patients: A randomised double-blinded split-mouth pilot study. *Mycoses* **2016**, *59*, 467–475. [[CrossRef](#)] [[PubMed](#)]
25. Jablonowski, H.; Santos Sousa, J.; Weltmann, K.D.; Wende, K.; Reuter, S. Quantification of the ozone and singlet delta oxygen produced in gas and liquid phases by a non-thermal atmospheric plasma with relevance for medical treatment. *Sci. Rep.* **2018**, *8*, 12195. [[CrossRef](#)] [[PubMed](#)]
26. Bruno, G.; Heusler, T.; Lackmann, J.-W.; von Woedtke, T.; Weltmann, K.-D.; Wende, K. Cold physical plasma-induced oxidation of cysteine yields reactive sulfur species (RSS). *Clin. Plasma Med.* **2019**, *14*, 100083. [[CrossRef](#)]
27. Wende, K.; von Woedtke, T.; Weltmann, K.D.; Bekeschus, S. Chemistry and biochemistry of cold physical plasma derived reactive species in liquids. *Biol. Chem.* **2018**, *400*, 19–38. [[CrossRef](#)] [[PubMed](#)]
28. Wende, K.; Williams, P.; Dalluge, J.; Gaens, W.V.; Aboubakr, H.; Bischof, J.; von Woedtke, T.; Goyal, S.M.; Weltmann, K.D.; Bogaerts, A.; et al. Identification of the biologically active liquid chemistry induced by a nonthermal atmospheric pressure plasma jet. *Biointerphases* **2015**, *10*, 029518. [[CrossRef](#)]
29. Jablonowski, H.; von Woedtke, T. Research on plasma medicine-relevant plasma–liquid interaction: What happened in the past five years? *Clin. Plasma Med.* **2015**, *3*, 42–52. [[CrossRef](#)]
30. Lackmann, J.-W.; Bruno, G.; Jablonowski, H.; Kogelheide, F.; Offerhaus, B.; Held, J.; Schulz-von der Gathen, V.; Stapelmann, K.; von Woedtke, T.; Wende, K. Nitrosylation vs. oxidation—How to modulate cold physical plasmas for biological applications. *PLoS ONE* **2019**, *14*, e0216606. [[CrossRef](#)]
31. Lackmann, J.W.; Baldus, S.; Steinborn, E.; Edengeiser, E.; Kogelheide, F.; Langklotz, S.; Schneider, S.; Leichert, L.I.O.; Benedikt, J.; Awakowicz, P.; et al. A dielectric barrier discharge terminally inactivates RNase A by oxidizing sulfur-containing amino acids and breaking structural disulfide bonds. *J. Phys. D Appl. Phys.* **2015**, *48*, 494003. [[CrossRef](#)]
32. Striesow, J.; Lackmann, J.W.; Ni, Z.; Wenske, S.; Weltmann, K.D.; Fedorova, M.; von Woedtke, T.; Wende, K. Oxidative modification of skin lipids by cold atmospheric plasma (CAP): A standardizable approach using RP-LC/MS(2) and DI-ESI/MS(2). *Chem. Phys. Lipids* **2020**, *226*, 104786. [[CrossRef](#)] [[PubMed](#)]
33. Lackmann, J.W.; Bandow, J.E. Inactivation of microbes and macromolecules by atmospheric-pressure plasma jets. *Appl. Microbiol. Biotechnol.* **2014**, *98*, 6205–6213. [[CrossRef](#)] [[PubMed](#)]
34. Zhou, R.; Zhou, R.; Zhuang, J.; Zong, Z.; Zhang, X.; Liu, D.; Bazaka, K.; Ostrikov, K. Interaction of Atmospheric-Pressure Air Microplasmas with Amino Acids as Fundamental Processes in Aqueous Solution. *PLoS ONE* **2016**, *11*, e0155584. [[CrossRef](#)] [[PubMed](#)]

35. Takai, E.; Kitamura, T.; Kuwabara, J.; Ikawa, S.; Yoshizawa, S.; Shiraki, K.; Kawasaki, H.; Arakawa, R.; Kitano, K. Chemical modification of amino acids by atmospheric-pressure cold plasma in aqueous solution. *J. Phys. D Appl. Phys.* **2014**, *47*, 285403. [[CrossRef](#)]
36. Wende, K.; Bruno, G.; Lalk, M.; Weltmann, K.-D.; von Woedtke, T.; Bekeschus, S.; Lackmann, J.-W. On a heavy path—Determining cold plasma-derived short-lived species chemistry using isotopic labelling. *RSC Adv.* **2020**, *10*, 11598–11607. [[CrossRef](#)]
37. Benedikt, J.; Mokhtar Hefny, M.; Shaw, A.; Buckley, B.R.; Iza, F.; Schakermann, S.; Bandow, J.E. The fate of plasma-generated oxygen atoms in aqueous solutions: Non-equilibrium atmospheric pressure plasmas as an efficient source of atomic O(aq). *Phys. Chem. Chem. Phys.* **2018**, *20*, 12037–12042. [[CrossRef](#)]
38. Bekeschus, S.; Wende, K.; Hefny, M.M.; Rodder, K.; Jablonowski, H.; Schmidt, A.; Woedtke, T.V.; Weltmann, K.D.; Benedikt, J. Oxygen atoms are critical in rendering THP-1 leukaemia cells susceptible to cold physical plasma-induced apoptosis. *Sci. Rep.* **2017**, *7*, 2791. [[CrossRef](#)]
39. Winter, J.; Tresp, H.; Hammer, M.U.; Iseni, S.; Kupsch, S.; Schmidt-Bleker, A.; Wende, K.; Dunnbier, M.; Masur, K.; Weltmann, K.D.; et al. Tracking plasma generated H₂O₂ from gas into liquid phase and revealing its dominant impact on human skin cells. *J. Phys. D Appl. Phys.* **2014**, *47*. [[CrossRef](#)]
40. Reuter, S.; Winter, J.; Iseni, S.; Schmidt-Bleker, A.; Dunnbier, M.; Masur, K.; Wende, K.; Weltmann, K.D. The Influence of Feed Gas Humidity Versus Ambient Humidity on Atmospheric Pressure Plasma Jet-Effluent Chemistry and Skin Cell Viability. *IEEE Trans. Plasma Sci.* **2015**, *43*, 3185–3192. [[CrossRef](#)]
41. Schmidt-Bleker, A.; Bansemer, R.; Reuter, S.; Weltmann, K.-D. How to produce an NO_x- instead of Ox-based chemistry with a cold atmospheric plasma jet. *Plasma Process Polym.* **2016**, *13*, 1120–1127. [[CrossRef](#)]
42. Schmidt-Bleker, A.; Winter, J.; Bosel, A.; Reuter, S.; Weltmann, K.D. On the plasma chemistry of a cold atmospheric argon plasma jet with shielding gas device. *Plasma Sources Sci. Technol.* **2016**, *25*, 015005. [[CrossRef](#)]
43. Zhou, R.; Zhou, R.; Prasad, K.; Fang, Z.; Speight, R.; Bazaka, K.; Ostrikov, K. Cold atmospheric plasma activated water as a prospective disinfectant: The crucial role of peroxyxynitrite. *Green Chem.* **2018**, *20*, 5276–5284. [[CrossRef](#)]
44. Naïtali, M.; Herry, J.-M.; Hnatiuc, E.; Kamgang, G.; Brisset, J.-L. Kinetics and Bacterial Inactivation Induced by Peroxyxynitrite in Electric Discharges in Air. *Plasma Chem. Plasma Process.* **2012**, *32*, 675–692. [[CrossRef](#)]
45. Yamashiro, R.; Misawa, T.; Sakudo, A. Key role of singlet oxygen and peroxyxynitrite in viral RNA damage during virucidal effect of plasma torch on feline calicivirus. *Sci. Rep.* **2018**, *8*, 17947. [[CrossRef](#)]
46. Ulrich, C.; Kluschke, F.; Patzelt, A.; Vandersee, S.; Czaika, V.A.; Richter, H.; Bob, A.; von Hutten, J.; Painsi, C.; Hugel, R.; et al. Clinical use of cold atmospheric pressure argon plasma in chronic leg ulcers: A pilot study. *J. Wound Care* **2015**, *24*, 196–203. [[CrossRef](#)]
47. Emmert, S.; Brehmer, F.; Haenßle, H.; Helmke, A.; Mertens, N.; Ahmed, R.; Simon, D.; Wandke, D.; Maus-Friedrichs, W.; Daeschlein, G.; et al. Atmospheric pressure plasma in dermatology: Ulcus treatment and much more. *Clin. Plasma Med.* **2013**, *1*, 24–29. [[CrossRef](#)]
48. van Gils, C.A.J.; Hofmann, S.; Boekema, B.K.H.L.; Brandenburg, R.; Bruggeman, P.J. Mechanisms of bacterial inactivation in the liquid phase induced by a remote RF cold atmospheric pressure plasma jet. *J. Phys. D Appl. Phys.* **2013**, *46*, 175203. [[CrossRef](#)]
49. Bekeschus, S.; Freund, E.; Spadola, C.; Privat-Maldonado, A.; Hackbarth, C.; Bogaerts, A.; Schmidt, A.; Wende, K.; Weltmann, K.D.; von Woedtke, T.; et al. Risk Assessment of kINPen Plasma Treatment of Four Human Pancreatic Cancer Cell Lines with Respect to Metastasis. *Cancers* **2019**, *11*, 1237. [[CrossRef](#)]
50. Bekeschus, S.; von Woedtke, T.; Weltmann, K.-D.; Metelmann, H.-R. Plasma, Cancer, Immunity. *Clin. Plasma Med.* **2018**, *9*, 13–14. [[CrossRef](#)]
51. Bekeschus, S.; Favia, P.; Robert, E.; von Woedtke, T. White paper on plasma for medicine and hygiene: Future in plasma health sciences. *Plasma Process Polym.* **2019**, *16*, 1800033. [[CrossRef](#)]
52. Shekhter, A.B.; Pekshev, A.V.; Vagapov, A.B.; Butenko, A.V.; Fayzullin, A.L.; Rudenko, T.G.; Sharapov, N.A.; Serejnikova, N.B.; Vasilets, V.N. Dose-dependent effect of plasma-chemical NO-containing gas flow on wound healing. An experimental study. *Clin. Plasma Med.* **2020**, 19–20. [[CrossRef](#)]
53. Bekeschus, S.; Kolata, J.; Winterbourn, C.; Kramer, A.; Turner, R.; Weltmann, K.D.; Broker, B.; Masur, K. Hydrogen peroxide: A central player in physical plasma-induced oxidative stress in human blood cells. *Free Radic. Res.* **2014**, *48*, 542–549. [[CrossRef](#)] [[PubMed](#)]

54. Lukes, P.; Dolezalova, E.; Sisrova, I.; Clupek, M. Aqueous-phase chemistry and bactericidal effects from an air discharge plasma in contact with water: Evidence for the formation of peroxyxynitrite through a pseudo-second-order post-discharge reaction of H₂O₂ and HNO₂. *Plasma Sources Sci. Technol.* **2014**, *23*, 015019. [[CrossRef](#)]
55. Ikawa, S.; Tani, A.; Nakashima, Y.; Kitano, K. Physicochemical properties of bactericidal plasma-treated water. *J. Phys. D Appl. Phys.* **2016**, *49*, 425401. [[CrossRef](#)]
56. Girard, F.; Badets, V.; Blanc, S.; Gazeli, K.; Marlin, L.; Authier, L.; Svarnas, P.; Sojic, N.; Clement, F.; Arbault, S. Formation of reactive nitrogen species including peroxyxynitrite in physiological buffer exposed to cold atmospheric plasma. *RSC Adv.* **2016**, *6*, 78457–78467. [[CrossRef](#)]
57. Breen, C.; Pal, R.; Elsegood, M.R.J.; Teat, S.J.; Iza, F.; Wende, K.; Buckley, B.R.; Butler, S.J. Time-resolved luminescence detection of peroxyxynitrite using a reactivity-based lanthanide probe. *Chem. Sci.* **2020**, *11*, 3164–3170. [[CrossRef](#)]
58. Calcerrada, P.; Peluffo, G.; Radi, R. Nitric oxide-derived oxidants with a focus on peroxyxynitrite: Molecular targets, cellular responses and therapeutic implications. *Curr. Pharm. Des.* **2011**, *17*, 3905–3932. [[CrossRef](#)]
59. Mikkelsen, R.B.; Wardman, P. Biological chemistry of reactive oxygen and nitrogen and radiation-induced signal transduction mechanisms. *Oncogene* **2003**, *22*, 5734–5754. [[CrossRef](#)]
60. Paulsen, C.E.; Carroll, K.S. Cysteine-mediated redox signaling: Chemistry, biology, and tools for discovery. *Chem. Rev.* **2013**, *113*, 4633–4679. [[CrossRef](#)]
61. Bartesaghi, S.; Radi, R. Fundamentals on the biochemistry of peroxyxynitrite and protein tyrosine nitration. *Redox Biol.* **2018**, *14*, 618–625. [[CrossRef](#)]
62. Ischiropoulos, H. Biological selectivity and functional aspects of protein tyrosine nitration. *Biochem. Biophys. Res. Commun.* **2003**, *305*, 776–783. [[CrossRef](#)]
63. Betts, M.J.; Russell, R.B. Amino-Acid Properties and Consequences of Substitutions. In *Bioinformatics for Geneticists*; John Wiley & Sons, Ltd.: Hoboken, NJ, USA, 2007; pp. 311–342.
64. Bartesaghi, S.; Peluffo, G.; Zhang, H.; Joseph, J.; Kalyanaraman, B.; Radi, R. Tyrosine nitration, dimerization, and hydroxylation by peroxyxynitrite in membranes as studied by the hydrophobic probe N-t-BOC-l-tyrosine tert-butyl ester. *Methods Enzymol.* **2008**, *441*, 217–236. [[CrossRef](#)] [[PubMed](#)]
65. Ferrer-Sueta, G.; Campolo, N.; Trujillo, M.; Bartesaghi, S.; Carballal, S.; Romero, N.; Alvarez, B.; Radi, R. Biochemistry of Peroxyxynitrite and Protein Tyrosine Nitration. *Chem. Rev.* **2018**, *118*, 1338–1408. [[CrossRef](#)] [[PubMed](#)]
66. Rubbo, H.; Radi, R. Protein and lipid nitration: Role in redox signaling and injury. *Biochim. Biophys. Acta* **2008**, *1780*, 1318–1324. [[CrossRef](#)] [[PubMed](#)]
67. Lizarbe, T.R.; Garcia-Rama, C.; Tarin, C.; Saura, M.; Calvo, E.; Lopez, J.A.; Lopez-Otin, C.; Folgueras, A.R.; Lamas, S.; Zaragoza, C. Nitric oxide elicits functional MMP-13 protein-tyrosine nitration during wound repair. *FASEB J.* **2008**, *22*, 3207–3215. [[CrossRef](#)] [[PubMed](#)]
68. Yakovlev, V.A.; Bayden, A.S.; Graves, P.R.; Kellogg, G.E.; Mikkelsen, R.B. Nitration of the tumor suppressor protein p53 at tyrosine 327 promotes p53 oligomerization and activation. *Biochemistry* **2010**, *49*, 5331–5339. [[CrossRef](#)] [[PubMed](#)]
69. Carballal, S.; Bartesaghi, S.; Radi, R. Kinetic and mechanistic considerations to assess the biological fate of peroxyxynitrite. *Biochim. Biophys. Acta* **2014**, *1840*, 768–780. [[CrossRef](#)]
70. Abaffy, P.; Tomankova, S.; Naraine, R.; Kubista, M.; Sindelka, R. The role of nitric oxide during embryonic wound healing. *BMC Genom.* **2019**, *20*, 815. [[CrossRef](#)]
71. Kitano, T.; Yamada, H.; Kida, M.; Okada, Y.; Saika, S.; Yoshida, M. Impaired Healing of a Cutaneous Wound in an Inducible Nitric Oxide Synthase-Knockout Mouse. *Dermatol. Res. Pract.* **2017**, *2017*, 2184040. [[CrossRef](#)]
72. Sekar, Y.; Moon, T.C.; Slupsky, C.M.; Befus, A.D. Protein tyrosine nitration of aldolase in mast cells: A plausible pathway in nitric oxide-mediated regulation of mast cell function. *J. Immunol.* **2010**, *185*, 578–587. [[CrossRef](#)]
73. Masters, K.S.; Leibovich, S.J.; Belem, P.; West, J.L.; Poole-Warren, L.A. Effects of nitric oxide releasing poly(vinyl alcohol) hydrogel dressings on dermal wound healing in diabetic mice. *Wound Repair Regen.* **2002**, *10*, 286–294. [[CrossRef](#)] [[PubMed](#)]
74. Luo, J.D.; Chen, A.F. Nitric oxide: A newly discovered function on wound healing. *Acta Pharmacol. Sin.* **2005**, *26*, 259–264. [[CrossRef](#)] [[PubMed](#)]

75. Hartwig, S.; Doll, C.; Voss, J.O.; Hertel, M.; Preissner, S.; Raguse, J.D. Treatment of Wound Healing Disorders of Radial Forearm Free Flap Donor Sites Using Cold Atmospheric Plasma: A Proof of Concept. *J. Oral Maxillofac. Surg.* **2017**, *75*, 429–435. [[CrossRef](#)] [[PubMed](#)]
76. Shome, D.; von Woedtke, T.; Riedel, K.; Masur, K. The HIPPO Transducer YAP and Its Targets CTGF and Cyr61 Drive a Paracrine Signalling in Cold Atmospheric Plasma-Mediated Wound Healing. *Oxid. Med. Cell. Longev.* **2020**, *2020*, 4910280. [[CrossRef](#)]
77. Aruoma, O.I.; Whiteman, M.; England, T.G.; Halliwell, B. Antioxidant action of ergothioneine: Assessment of its ability to scavenge peroxynitrite. *Biochem. Biophys. Res. Commun.* **1997**, *231*, 389–391. [[CrossRef](#)]
78. Goldstein, S.; Russo, A.; Samuni, A. Reactions of PTIO and carboxy-PTIO with *NO, *NO₂, and O₂*. *J. Biol. Chem.* **2003**, *278*, 50949–50955. [[CrossRef](#)]
79. Franzoni, F.; Colognato, R.; Galetta, F.; Laurenza, I.; Barsotti, M.; Di Stefano, R.; Bocchetti, R.; Regoli, F.; Carpi, A.; Balbarini, A.; et al. An in vitro study on the free radical scavenging capacity of ergothioneine: Comparison with reduced glutathione, uric acid and trolox. *Biomed. Pharmacother.* **2006**, *60*, 453–457. [[CrossRef](#)]
80. Winter, J.; Wende, K.; Masur, K.; Iseni, S.; Dunnbier, M.; Hammer, M.U.; Tresp, H.; Weltmann, K.D.; Reuter, S. Feed gas humidity: A vital parameter affecting a cold atmospheric-pressure plasma jet and plasma-treated human skin cells. *J. Phys. D Appl. Phys.* **2013**, *46*. [[CrossRef](#)]
81. Jablonowski, H.; Schmidt-Bleker, A.; Weltmann, K.D.; von Woedtke, T.; Wende, K. Non-touching plasma-liquid interaction—Where is aqueous nitric oxide generated? *Phys. Chem. Chem. Phys.* **2018**, *20*, 25387–25398. [[CrossRef](#)]
82. Beckman, J.S.; Beckman, T.W.; Chen, J.; Marshall, P.A.; Freeman, B.A. Apparent hydroxyl radical production by peroxynitrite: Implications for endothelial injury from nitric oxide and superoxide. *Proc. Natl. Acad. Sci. USA* **1990**, *87*, 1620–1624. [[CrossRef](#)]
83. Squadrito, G.L.; Pryor, W.A. Oxidative chemistry of nitric oxide: The roles of superoxide, peroxynitrite, and carbon dioxide. *Free Radic. Biol. Med.* **1998**, *25*, 392–403. [[CrossRef](#)]
84. Wenske, S.; Lackmann, J.-W.; Bekeschus, S.; Weltmann, K.-D.; von Woedtke, T.; Wende, K. Nonenzymatic post-translational modifications in peptides by cold plasma-derived reactive oxygen and nitrogen species. *Biointerphases* **2020**, *15*. [[CrossRef](#)] [[PubMed](#)]
85. Radi, R. Protein tyrosine nitration: Biochemical mechanisms and structural basis of functional effects. *Acc. Chem. Res.* **2013**, *46*, 550–559. [[CrossRef](#)] [[PubMed](#)]
86. Bent, D.V.; Hayon, E. Excited state chemistry of aromatic amino acids and related peptides. I. Tyrosine. *J. Am. Chem. Soc.* **1975**, *97*, 2599–2606. [[CrossRef](#)]
87. Winterbourn, C.C.; Parsons-Mair, H.N.; Gebicki, S.; Gebicki, J.M.; Davies, M.J. Requirements for superoxide-dependent tyrosine hydroperoxide formation in peptides. *Biochem. J.* **2004**, *381*, 241–248. [[CrossRef](#)]
88. Koppenol, W.H.; Moreno, J.J.; Pryor, W.A.; Ischiropoulos, H.; Beckman, J.S. Peroxynitrite, a cloaked oxidant formed by nitric oxide and superoxide. *Chem. Res. Toxicol.* **1992**, *5*, 834–842. [[CrossRef](#)]
89. Ramezani, M.S.; Padmaja, S.; Koppenol, W.H. Nitration and hydroxylation of phenolic compounds by peroxynitrite. *Chem. Res. Toxicol.* **1996**, *9*, 232–240. [[CrossRef](#)]
90. Jablonowski, H.; Bussiahn, R.; Hammer, M.U.; Weltmann, K.D.; von Woedtke, T.; Reuter, S. Impact of plasma jet vacuum ultraviolet radiation on reactive oxygen species generation in bio-relevant liquids. *Phys. Plasmas* **2015**, *22*, 122008. [[CrossRef](#)]
91. Snyder, H.L.; Smtih, B.T.; Parr, T.P.; Martin, R.M. Dissociative Excitation of Water by Metastable Argon. *Chem. Phys.* **1982**, *65*, 397–406. [[CrossRef](#)]
92. Zvereva, G.N. Using vacuum ultraviolet radiation to obtain highly reactive radicals. *J. Opt. Technol.* **2012**, *79*, 477–483. [[CrossRef](#)]
93. Attri, P.; Kim, Y.H.; Park, D.H.; Park, J.H.; Hong, Y.J.; Uhm, H.S.; Kim, K.N.; Fridman, A.; Choi, E.H. Generation mechanism of hydroxyl radical species and its lifetime prediction during the plasma-initiated ultraviolet (UV) photolysis. *Sci. Rep.* **2015**, *5*, 9332. [[CrossRef](#)] [[PubMed](#)]
94. Plowman, J.E.; Deb-Choudhury, S.; Grosvenor, A.J.; Dyer, J.M. Protein oxidation: Identification and utilisation of molecular markers to differentiate singlet oxygen and hydroxyl radical-mediated oxidative pathways. *Photochem. Photobiol. Sci.* **2013**, *12*, 1960–1967. [[CrossRef](#)] [[PubMed](#)]

95. Wang, Z.C.; Li, Y.K.; He, S.G.; Bierbaum, V.M. Reactivity of amino acid anions with nitrogen and oxygen atoms. *Phys. Chem. Chem. Phys.* **2018**, *20*, 4990–4996. [[CrossRef](#)] [[PubMed](#)]
96. Conte, M.L.; Carroll, K.S. The chemistry of thiol oxidation and detection. In *Oxidative Stress and Redox Regulation*; Springer: Berlin/Heidelberg, Germany, 2013; pp. 1–42.
97. Schmidt-Bleker, A.; Winter, J.; Iseni, S.; Dunnbier, M.; Weltmann, K.D.; Reuter, S. Reactive species output of a plasma jet with a shielding gas device-combination of FTIR absorption spectroscopy and gas phase modelling. *J. Phys. D Appl. Phys.* **2014**, *47*, 145201. [[CrossRef](#)]
98. Sander, R. *Compilation of Henry's Law Constants for Inorganic and Organic Species of Potential Importance in Environmental Chemistry*; Max-Planck Institute of Chemistry, Air Chemistry Department: Mainz, Germany, 1999.
99. Koppenol, W.H.; Bounds, P.L.; Nauser, T.; Kissner, R.; Ruegger, H. Peroxynitrous acid: Controversy and consensus surrounding an enigmatic oxidant. *Dalton Trans.* **2012**, *41*, 13779–13787. [[CrossRef](#)]
100. Shilov, V.P.; Fedoseev, A.M. Role of peroxynitrite in oxidation of f-element ions in HNO₃ solutions. *Radiochemistry* **2013**, *55*, 366–368. [[CrossRef](#)]
101. Lobachev, V.L.; Rudakov, E.S. The chemistry of peroxynitrite. Reaction mechanisms and kinetics. *Usp. Khim.* **2006**, *75*, 422–444. [[CrossRef](#)]
102. Robinson, K.M.; Beckman, J.S. Synthesis of peroxynitrite from nitrite and hydrogen peroxide. *Methods Enzymol.* **2005**, *396*, 207–214. [[CrossRef](#)]
103. Gorbanev, Y.; O'Connell, D.; Chechik, V. Non-Thermal Plasma in Contact with Water: The Origin of Species. *Chemistry (Easton)* **2016**, *22*, 3496–3505. [[CrossRef](#)]
104. Stoffels, C.; Oumari, M.; Perrou, A.; Termath, A.; Schlundt, W.; Schmalz, H.G.; Schafer, M.; Wewer, V.; Metzger, S.; Schomig, E.; et al. Ergothioneine stands out from hercynine in the reaction with singlet oxygen: Resistance to glutathione and TRIS in the generation of specific products indicates high reactivity. *Free Radic. Biol. Med.* **2017**, *113*, 385–394. [[CrossRef](#)]
105. Colombo, G.; Clerici, M.; Altomare, A.; Rusconi, F.; Giustarini, D.; Portinaro, N.; Garavaglia, M.L.; Rossi, R.; Dalle-Donne, I.; Milzani, A. Thiol oxidation and di-tyrosine formation in human plasma proteins induced by inflammatory concentrations of hypochlorous acid. *J. Proteom.* **2017**, *152*, 22–32. [[CrossRef](#)] [[PubMed](#)]

Publisher's Note: MDPI stays neutral with regard to jurisdictional claims in published maps and institutional affiliations.



© 2020 by the authors. Licensee MDPI, Basel, Switzerland. This article is an open access article distributed under the terms and conditions of the Creative Commons Attribution (CC BY) license (<http://creativecommons.org/licenses/by/4.0/>).

Article A5

Radiation driven chemistry in biomolecules – is (V)UV involved in the bioactivity of argon jet plasmas?

G. Bruno, [S. Wenske](#), H. Mahdikia, T. Gerling, T. von Woedtke, and K. Wende. *Frontiers in Physics*, 9, 759005, 2021.

© 2021 The Authors



Radiation Driven Chemistry in Biomolecules—Is (V)UV Involved in the Bioactivity of Argon Jet Plasmas?

G. Bruno^{1,2}, S. Wenske¹, H. Mahdikia³, T. Gerling¹, T. von Woedtke^{3,4} and K. Wende^{1*}

¹ZIK Plasmatis, Leibniz Institute for Plasma Science and Technology (INP), Greifswald, Germany, ²Metabolomics Facility, Berlin Institute of Health (BIH) at Max Delbrück Center for Molecular Medicine, Berlin, Germany, ³Leibniz Institute for Plasma Science and Technology (INP), Greifswald, Germany, ⁴Institute for Hygiene and Environmental Medicine, University Medicine Greifswald, Greifswald, Germany

OPEN ACCESS

Edited by:

Vladimir I. Kolobov,
CFD Research Corporation,
United States

Reviewed by:

Anna Khlyustova,
Institute of Solution Chemistry (RAS),
Russia
Zdenko Machala,
Comenius University, Slovakia

*Correspondence:

K. Wende
kristian.wende@inp-greifswald.de

Specialty section:

This article was submitted to
Plasma Physics,
a section of the journal
Frontiers in Physics

Received: 15 August 2021

Accepted: 09 November 2021

Published: 14 December 2021

Citation:

Bruno G, Wenske S, Mahdikia H,
Gerling T, von Woedtke T and
Wende K (2021) Radiation Driven
Chemistry in Biomolecules—Is (V)UV
Involved in the Bioactivity of Argon Jet
Plasmas?
Front. Phys. 9:759005.
doi: 10.3389/fphy.2021.759005

Cold physical plasmas, especially noble gas driven plasma jets, emit considerable amounts of ultraviolet radiation (UV). Given that a noble gas channel is present, even the energetic vacuum UV can reach the treated target. The relevance of UV radiation for antimicrobial effects is generally accepted. It remains to be clarified if this radiation is relevant for other biomedical application of plasmas, e.g., in wound care or cancer remediation. In this work, the role of (vacuum) ultraviolet radiation generated by the argon plasma jet kINPen for cysteine modifications was investigated in aqueous solutions and porcine skin. To differentiate the effects of photons of different wavelength and complete plasma discharge, a micro chamber equipped with a MgF₂, Suprasil, or Borosilicate glass window was used. In liquid phase, plasma-derived VUV radiation was effective and led to the formation of cysteine oxidation products and molecule breakdown products, yielding sulfite, sulfate, and hydrogen sulfide. At the boundary layer, the impact of VUV photons led to water molecule photolysis and formation of hydroxyl radicals and hydrogen peroxide. In addition, photolytic cleavage of the weak carbon-sulfur bond initiated the formation of sulfur oxy ions. In the intact skin model, protein thiol modification was rare even if a VUV transparent MgF₂ window was used. Presumably, the plasma-derived VUV radiation played a limited role since reactions at the boundary layer are less frequent and the dense biomolecules layers block it effectively, inhibiting significant penetration. This result further emphasizes the safety of physical plasmas in biomedical applications.

Keywords: cold physical plasma, redox signaling, porcine skin model, VUV radiation, tape stripping model, kINPen

1 INTRODUCTION

Emerging therapies for the treatment of chronic wounds and cancerous lesions involve the administration of exogenous reactive species directly delivered on the target (e.g., cold physical plasmas) [1–4]; or produced *in situ* by administration of specific drugs (e.g., nanoprodrugs) [5,6]. For example, the formation of singlet oxygen by irradiation (600–800 nm) of a photosensitizer, is the molecular mechanism behind the effectiveness of the photodynamic therapy in use for cancer regression [7]. Among the emerging therapies, cold physical plasmas are multi-function tools comprising of reactive species, ions, metastables, electrons, magnetic fields, and photons [8,9]. These, synergistically acting on the target, are effective in cancer regression [10–12]; and wound healing

[13–15]. Furthermore, the use of plasmas is considered in other fields, such as sterilization [16–18]; and dentistry [19–21].

While downstream effects have been detected [11,22], many are the open questions regarding the working mechanism of plasmas on biological target. Therefore, the variable production of plasma elements has been studied, with focus on reactive species, at date considered the predominant responsible of plasma effectiveness [23]. In particular, their amounts on the target can be regulated by tuning the plasma parameters (e.g., treatment duration, distance, working gases) [2,24], achieving bivalent aims such as promoting cell proliferation and migration in wound healing, or inducing cell death and apoptosis for cancer treatment and biological decontamination. Cold plasmas can be generated by a multitude of different designs, yielding differences in species output and biomedical impact [25]; [26].

One plasma source is the kINPen, an argon-driven jet which gas phase has been already well characterized. The production of primary reactive species such as excited states of argon (e.g., metastables, excimers) were observed in the effluent area (or gas phase). Those reactive species react with others gases (e.g., N_2 , O_2 , H_2) present in the surrounding atmosphere or in the core gas to generate secondary species, such as atomic oxygen ($\cdot O$), singlet oxygen (1O_2), ozone (O_3), hydroxyl radicals (OH), superoxide anions radicals (O_2^-), hydrogen peroxide (H_2O_2), nitric oxide radicals (NO_x), acids containing nitrogen (HNO_x). Finally, a tertiary chemistry is stimulated directly in the target. Using biochemical models, covalent modification of biomolecules were predicted and observed, especially in amino acids and proteins [27–30]; and lipids [31–33].

In the cellular environment, plasma-induced biomolecules modifications could be the responsible event for the deregulation of redox signaling pathways. Indeed, it was shown that kINPen plasmas led to an abnormal production/functioning of e.g., transcription factors (e.g., Nrf2 and p53), which modulates differentially gene expressions, cellular organization and apoptosis processes [15,34–36]. Together with reactive species, radiation generated by cold plasmas could cover important synergistic effects in stimulating these processes.

In kINPen plasmas, their relevance in inducing oxidative stress must be considered, since the emission region goes from the vacuum UV region (105 nm) (emitted by argon excimers) to the near infrared (1,000 nm) [9,37]. The ultraviolet radiation (100–400 nm) emitted by kinpen plasmas could have a synergistic role in their effectiveness, e.g., for antibacterial purposes as shown also for other plasma sources [38–41].

Radiation can be generally classified in ionizing (10–125 nm), which have short wavelength, high frequency and energy, and non-ionizing (>125 nm), which oppositely are longer wavelengths with lower frequency and energy. Therefore, even if measured in low levels [42,43], vacuum UV radiation (100–200 nm) emitted by argon metastable produced by kINPen plasmas could have enough energy to impact strongly on the biological matter, leading to DNA damage, protein denaturation and cell death. Indeed, it is well known that high levels of ionizing radiation can be harmful for the living matter, generally disrupting and damaging molecular structures (e.g.,

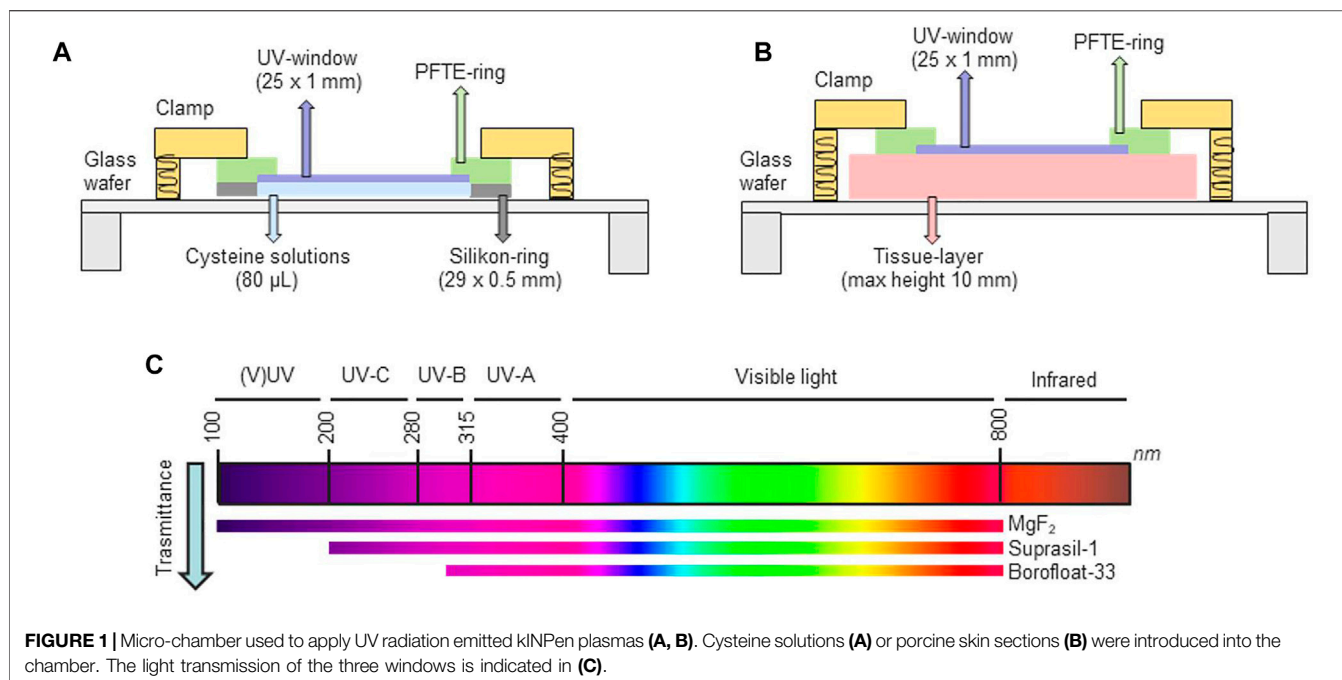
lipids, proteins, nucleic acids, carbohydrates) [44–48]. However, in relation to the quantity and time of exposure, UV radiation (mostly UV-C and UV-B, 200–315 nm) can also increase the general oxidative stress, induce indirectly or directly structural changes in biomolecules, and consequentially modulate redox signaling pathways [49,50]. The mechanism of action of radiation is still under clarification in biology, but generally they can generate biomolecules modifications by being directly absorbed (e.g., amino acids cysteine, tyrosine, tryptophan), or by stimulating sensitizing compounds (e.g., exogenous or endogenous). In both cases, excited forms will be generated, which starts photo-oxidation reactions. Indeed, radicals can be formed by hydrogen abstraction or one electron oxidation (Type I mechanism) and reactive species can be formed by energy transfer to molecular oxygen, which forms singlet oxygen (Type II mechanism) [50,51]. Generally, an increased release of reactive species from mitochondria was measured after radiation exposure, as well as the activation of a calcium dependent NOS-1 with increase of peroxynitrite levels. The chain reaction induced by photo-oxidation can be harmful in long and intense exposure, but for short and not severe exposure a transitory effect was observed, leading to a cytoprotective response mediated by MAPK1/2 activation [51]. The UV and vacuum UV light produced by different plasma sources has been considered as essential elements for the antimicrobial activity [38–41,52,53].

In this work, the role of ultraviolet radiation generated by the argon plasma jet kINPen for cysteine modifications was investigated. Cysteine is easily oxidized, and served to investigate plasma chemistry in liquids before [24,54–56]. Modifications occurring on cysteine in aqueous solutions or porcine epithelium were identified via mass spectrometry and major derivatives were quantified using it coupled to high-pressure liquid chromatography. To isolate the effects of photons from complete plasma discharge, a micro chamber equipped with VUV, UV-C, and UV-A windows was used. Alongside, optical emission spectrometry and aqueous chemistry was applied to characterize reactive species formation in the gas and liquid phase. A significant contribution of plasma derived UV radiation on cysteine chemistry was observed if water molecules were present.

2 MATERIALS AND METHODS

2.1 Sample Preparation

Crystalline cysteine (Sigma Aldrich) was solubilized in double distilled water (ddH_2O) to a final concentration of 2 mM on a daily basis. For short-term storage, blue ice was used to avoid pH value distortions during freeze-thawing cycles [57]. After respective plasma or irradiation treatments, solutions were immediately subjected to high-resolution mass spectrometry, multiple reaction monitoring mass spectrometry, or ion chromatography. Fresh porcine ears were received from Landmetzgerei Urich (Bad Koenig, Germany) on blue ice, serving as a well-accepted replacement model for human skin [58]. The ears were washed carefully, shaved, and the superficial



corneocyte layer was removed with a single CorneoFix strip (Courage and Khazaka electronic GmbH, Cologne, Germany) to increase homogeneity. Plasma treatment was performed in selected clean and homogenous areas of a 2 cm × 2 cm dimension.

2.2 Plasma Treatments

The kINPen, an argon-driven (99.999%, Air Liquide) dielectric barrier plasma jet with a flow rate of 3 standard liters per minute (slm) served as plasma source. If desired, the working gas was modified by 1% admixture of molecular oxygen (99.998, Air Liquide). Its central electrode is powered by an alternating current with a sinusoidal waveform, 2–6 kV peak–peak voltage, and a frequency of around 1 MHz. The outer electrode is insulated by a ceramic tube. The dissipated electrical power is around 1.1 W. For most experiments, a gas curtain created by a nozzle and 5 slm nitrogen (99.999%, Air Liquide) shielded the effluent from the ambient air. For details about the design and working principle of the jet, refer to Reuter and colleagues [9] and citations therein. To investigate the plasma-derived products and emitted radiation by optical emission spectroscopy, the plasma jet was positioned on axis at a distance of 9 mm to the front of a spectrometer (AvaSpec-2048; Avantes, Germany) allowing the observation of both UV and VIS/NIR range (195–980 nm) with a spectral resolution of 0.7 nm. For the VUV spectral measurements, a single grating monochromator (Acton VM-502, grating 1200 g/mm) was used. This system was set to a spectral resolution of 0.2 nm and the spectral range of 100–200 nm was observed. Furthermore, the system was under low pressure (2.2×10^{-6} mbar) and connected via an MgF₂ window for VUV transmissions down to 100 nm. The kINPen was placed at 9 mm distance in front of the MgF₂ window.

The distance between the nozzle and the target was kept at 9 mm. Targets were either 750 μL aqueous solution in a 24 well-plate, fresh porcine skin prepared as described in 2.1, or a 25 mm diameter radiation chamber. The chamber could be equipped with windows that transmit different parts of the VUV/UV radiation and was filled with 80 μL solution forming a 500 μm thick layer or sections of porcine skin (Figure 1A,B). After treatments (20 s–180 s) samples were submitted to reactive species analysis (Section 2.3). Liquids containing the tracer molecule cysteine were also analyzed via liquid chromatography coupled to mass spectrometry for the detection of oxidative modifications (Section 2.4). The first 3 layers of treated porcine skin tissues were sampled using three consecutive CorneoFix strips that were immediately deposited in a protein solubilization buffer and subjected to shotgun proteomics (as described in Section 2.5). Each experiment was performed in triplicate.

2.3 OH and H₂O₂ Quantification via Colorimetric Assays in Liquids

For the quantification of plasma-generated, short-lived ROS (hydroxyl radicals, atomic oxygen) solution of 5 mM terephthalic acid in 25 mM phosphate buffer, pH 7.4 was used despite the limited selectivity [59]. The reaction yield to the fluorescent compound 2-hydroxyterephthalic acid (HTPA) that could be quantified at 318 nm excitation and 426 nm emission using an external calibration curve. Hydrogen peroxide deposited in treated liquids was determined using the ferrous oxidation–xylenol orange (FOX) assay according to the manufacturer's protocol (Thermo Scientific, Dreieich, Germany). The reaction yield to a purple product, which absorbance at 595 nm was

measured in a spectrophotometer (Tecan M200 multi-plate reader, Männedorf, Switzerland).

2.4 Characterization of Plasma-Induced Sulfur Chemistry in Liquids

2.4.1 Cysteine Derivatives.

Cysteine, cystine, cysteine sulfonic acid, cysteine sulfinic acid, alanine, cysteine-S-sulfonate were quantified by coupling a chromatographic separation (Agilent 1,290 Infinity II, Waldbronn, Germany) to targeted mass spectrometry (Q-Trap 5500, Sciex, Darmstadt, Germany). Analytes were separated on a 2.1 mm × 100 mm Acquity Amide Column with 130 Å pore size and 1.7 μm particle size and a corresponding VanGuard precolumn (Waters, Manchester, England) at a column temperature of 35°C. Mobile phase A consisted of 10 mM ammonium formate in water plus 0.15% formic acid while B consisted of 10 mM ammonium formate in acetonitrile plus 0.15% formic acid. The flow rate was 0.8 ml/min. A linear gradient was applied (0.0 min–99% B; 4.0 min–85% B; 7.0 min–30% B; 7.1 min–99% B; 9.0 min–99% B). Prior to injection, samples were diluted 1:5 in mobile phase B. Compounds were determined via multiple reaction monitoring in positive mode. The electrospray (ESI) source parameters were the following: curtain gas 35 psi, gas 1 20 psi, gas 2 25 psi, temperature 150°C, 5.5 kV probe voltage, 50 V declustering potential. The transitions and the correspondent collisional energies (CE) used for each compounds were for cysteine 122 → 76 m/z, CE 20; cystine 241 → 152 m/z, CE 10; cysteine sulfinic acid 154 → 74 m/z, CE 20; cysteine sulfonic acid 170 → 124 m/z, CE 10; cysteine-S-sulfonate 202 → 120 m/z, CE 10; alanine 90.1 → 44.1 m/z, CE 8. External calibration curves allowed the absolute quantification of the listed compounds in plasma-treated or irradiated samples.

2.4.2 Hydrogen Sulfide.

To quantify the formation of hydrogen sulfide (H₂S) from cysteine, the monobromobimane (mBB) assay was optimized [60]. A solution of 100 mM MBB in acetonitrile was freshly prepared. First, 25 μL of analyte solutions was mixed with 2 μL MBB and 65 μL of 100 mM phosphate buffer at pH 7.8. After vigorous mixing, samples were incubated at 37°C for 10, 30, or 60 min using a thermomixer, yielding sulfodibimane (SDB) in the presence of H₂S. The reaction was stopped by adding 5 μL formic acid 50% and cleared by centrifugation. SDB was quantified by targeted mass spectrometry. Analytes were separated on a 2.1 × 50 mm Zorbax RRHD Eclipse Plus C18 column (Waters, 95 Å pore size, 1.8 μm particle size) and corresponding guard column. Mobile phases were water (A; Th. Geyer, Renningen, Germany) and acetonitrile (B; *ibid.*). A linear gradient was applied (0 min–5% B; 2.1 min–40% B; 5 min–40% B; 5.1 min–98% B; 6 min–98% B; 6.1 min–5% B; 8 min–5% B). The flow rate was of 0.8 ml/min. Atmospheric pressure chemical ionization (APCI) was applied with the following source parameters: curtain gas 20 psi, gas 1 50 psi, temperature 500°C, 3 kV needle current, 100 V declustering potential, 32 V collision energy. The transitions used

for the analyzed compounds were for MBB 272 → 193 m/z; SDB 415.1 → 193.3 m/z.

2.4.3 Sulfite and Sulfate.

Ion chromatography (ICS-5000, Dionex Corp., Sunnyvale, United States) was used for the quantification of sulfite (SO₃⁻) and sulfate (SO₄⁻) anions. These were separated on a IonPac[®] AS23 pre-column (2 × 50 mm) coupled to an IonPac[®] AS23 anion exchange column (2 × 250 mm, Thermo Fisher Scientific Inc., Waltham, United States). Isocratic separation was achieved using a carbonate buffer (4.5 mM Na₂CO₃/0.8 mM NaHCO₃) and the flow rate of 0.25 ml/min.

2.5 Investigation of Protein Modifications in Tissues

2.5.1 Protein sample preparation.

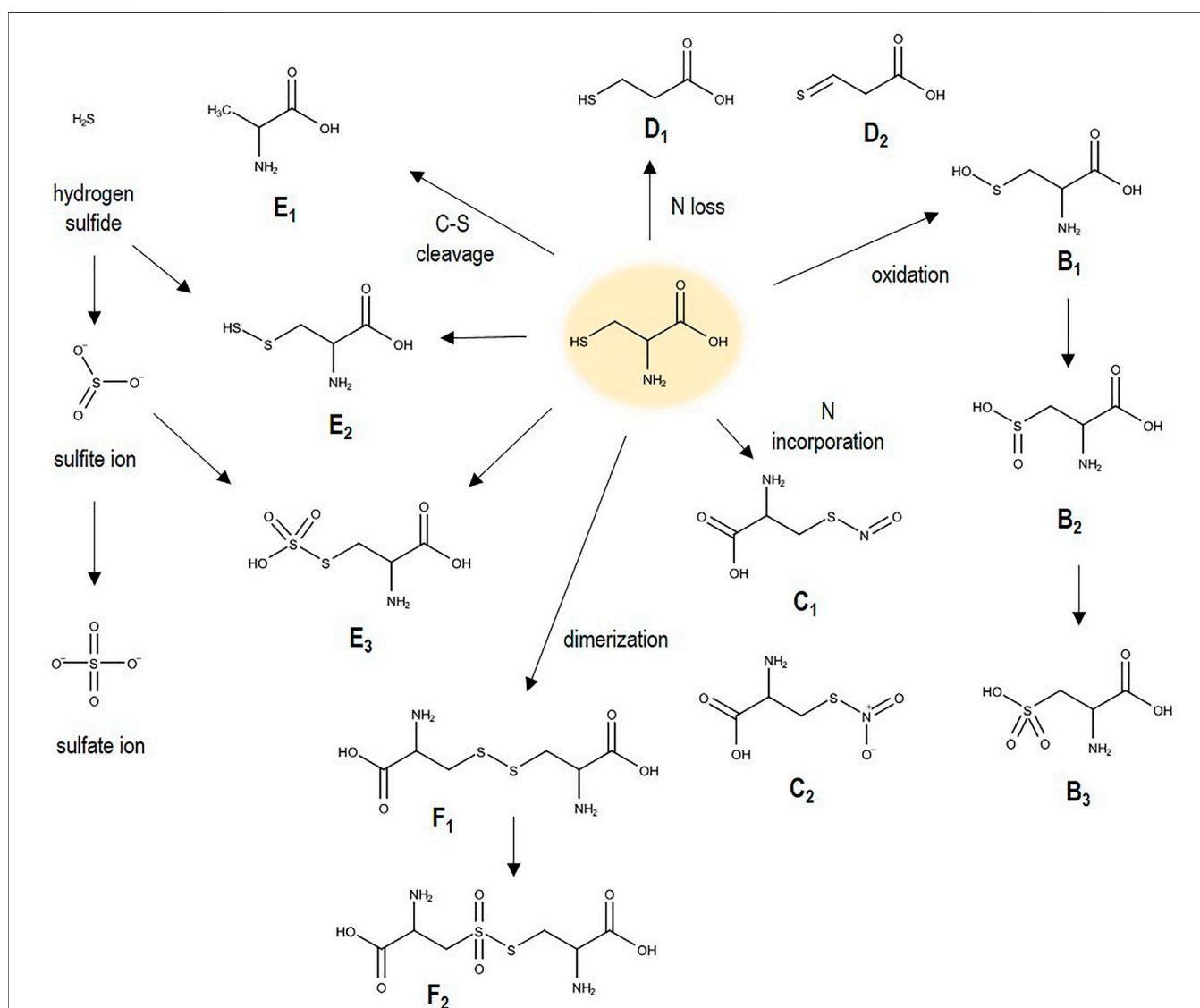
After sampling via tape stripping controls and plasma treated porcine skin layers, proteins were solubilized by introducing the tape strip in 500 μL of SDS-based lysis buffer (5% SDS, 50 mM TEAB pH 7.55) and by vortexing the vials for 2 min at room temperature. A S-Trap midi spin column digestion protocol from ProtiFi was applied according to the manufacturers protocol. The solutions were sonicated to disrupt cells, dissolve proteins, and shear DNA and clarified by centrifugation at 4000g for 10 min at 4°C. The supernatant was transferred to a clean vial. The reduction and alkylation of sulfhydryl groups was performed by incubating respectively with 5 mM tris(2-carboxyethyl) phosphine (TCEP, 55°C, 15 min) and subsequently with 20 mM methyl methanethiosulfonate (MMTS) at RT for 10 min. The reaction was stopped by adding 12% phosphoric acid. Next, 300 μL S-Trap buffer (90% methanol, 100 mM TEAB, pH 7.1) was added, and samples were transferred to the spin column. After centrifugation (2 min × 4000 g), the column was washed with 300 μL S-Trap buffer three times. Protein digestion was achieved in column by adding 1:25 wt:wt sequencing grade trypsin (Promega, Madison, United States) in 50 mM TEAB and incubating for 1 hour at 47°C. In this case, the columns were sealed with a lid to avoid solution evaporation. Finally, peptides were eluted with 500 μL of acetonitrile containing 0.2% formic acid. The solutions were dried using a SpeedVac and resuspended in 10 μL of water containing 0.1% formic acid before nanoLC-MS analysis.

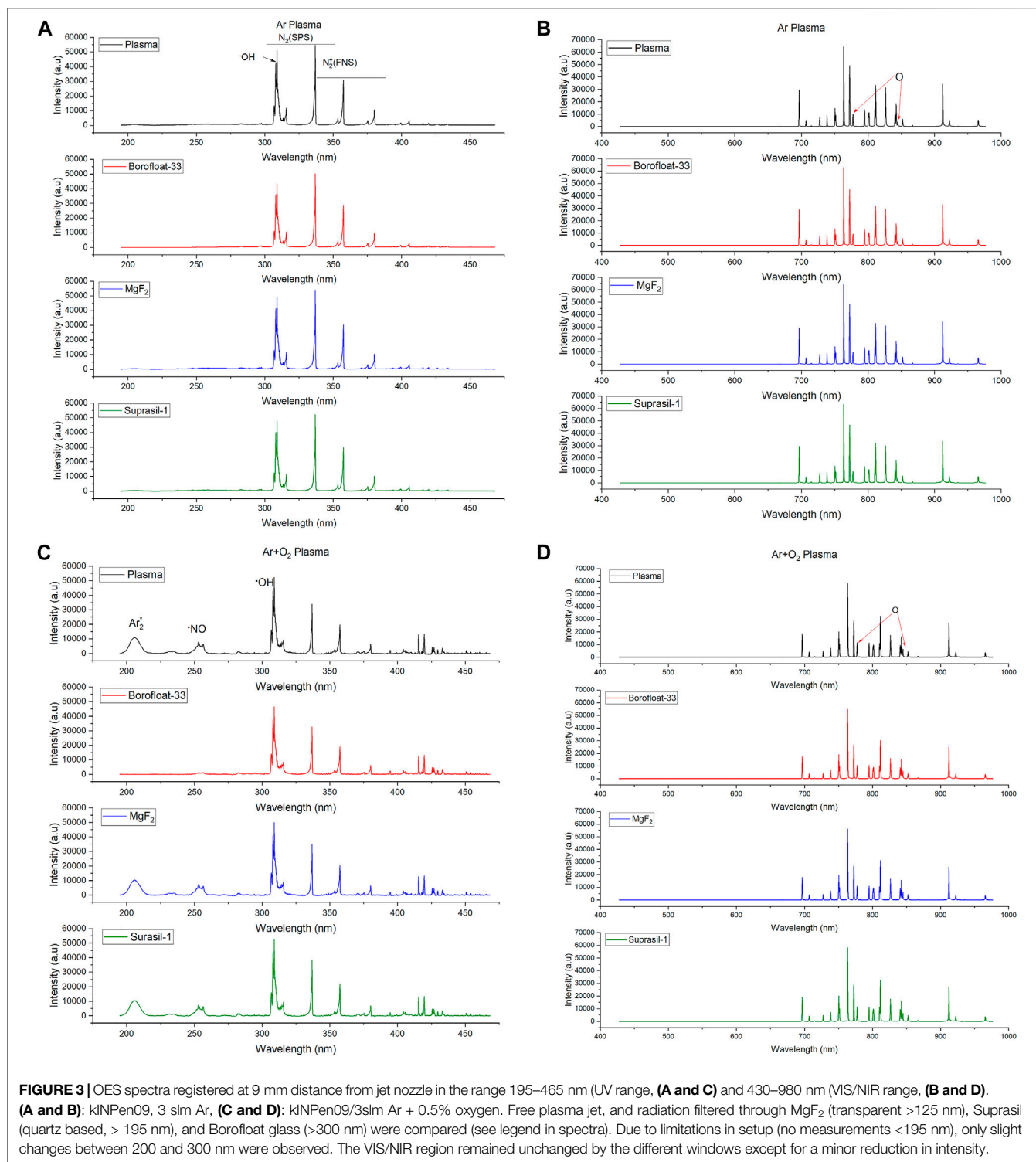
2.5.2 LC-MS analysis.

The proteomes and the oxidative modifications occurring in porcine skin layers after treatments were analyzed by nanoflow liquid chromatography, using an UltiMate 300 RSLCnano coupled to a QExactive Hybrid-Quadrupol-Orbitrap from Thermo Fisher Scientific, Dreieich/Germany. The technical details of the separation and detection are described in Wenske et al., 2021. Raw data were analyzed with the Proteome Discoverer 2.4 (Thermo Fischer Scientific) and the Byonic 3.6.0 node (Protein Metrics) for searching protein modifications. A list of 15 modifications previously identified for gas plasma treatments of thiol moieties was used to reduce

TABLE 1 | Analyzed thiols oxidative modifications occurring in the proteome of plasma treated porcine skin samples.

Mass shift (Da)	Composition	Modification	Acronym	Label
-2.02	-2H	Dehydrogenation	Didehydro	A
+15.99	+O	Oxidation	Oxidation	B ₁
+21.98	+2O	Dioxidation	Dioxidation	B ₂
+47.98	+3O	Trioxidation	Trioxidation	B ₃
+28.99	+N + O -H	Nitrosylation	Nitrosyl	C1
+44.98	+N +2O -H	Nitration	Nitro + O	C2
-15.01	-N -H	Deamination	-NH	D1
-17.03	-N -3H	Deamination + Dehydrogenation	-NH3	D2
-31.97	-S	Sulphur loss	-S (alanine)	E ₁
+31.97	+S	Sulphur addition	+S	E ₂
+79.96	+S +3O	Sulfonylation	+SO3	E ₃
+119.00	+S +3C +5H + N +2O	Cysteine addition	+S2R	F ₁
+150.99	+S +3C +5H + N +4O	Cysteine addition + Dioxidation	+S2O4R	F ₂

**FIGURE 2** | Cysteine oxidation and cleavage products (see Tables 1, 2). When incorporated into a protein, the carboxyl and amino group are incorporated in the peptide bond.



calculation times (**Table 1**) [24,55]. A maximum of three modifications per peptide was set, and to ensure result validity, only peptides with a Byonic score >250 and a Delta Mod score of >5 were accepted for downstream data analysis. A normalization on the total peptides containing cysteine was performed, yielding a percentage of modified thiols on the

total proteome. Furthermore, the oxidative modifications found in controls were subtracted as background from all other samples and data are shown as difference from the control. One-way ANOVA statistical test was performed in order to detect significant modifications, allowing a comparison between different conditions.

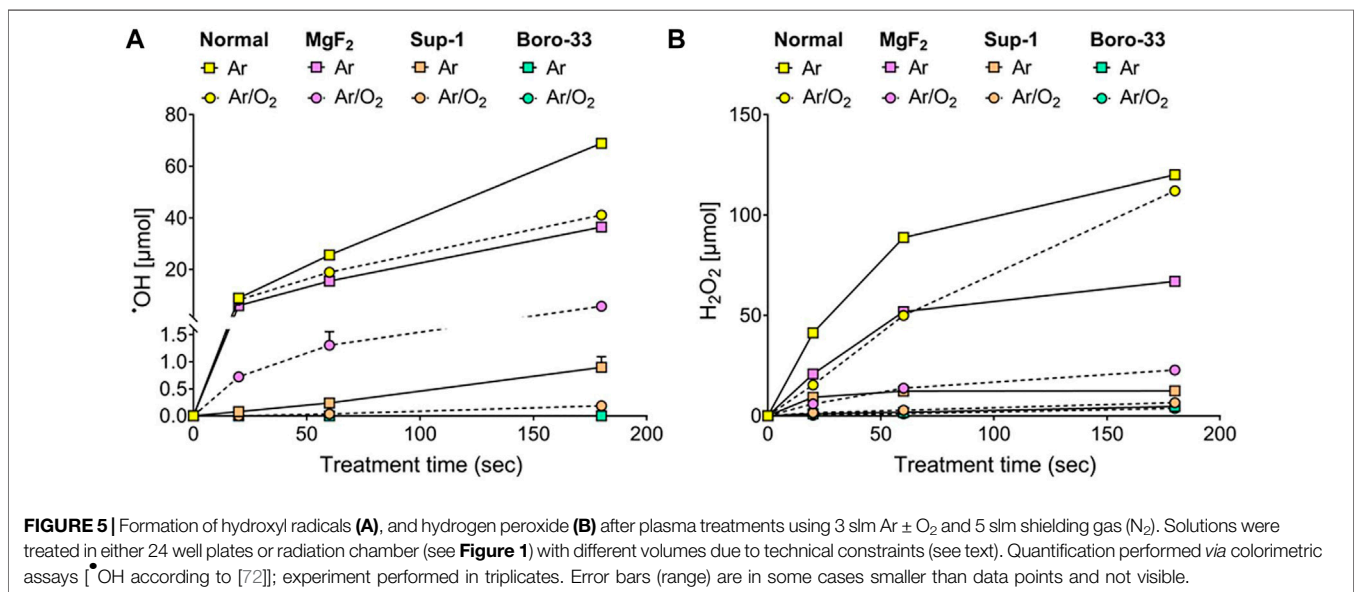
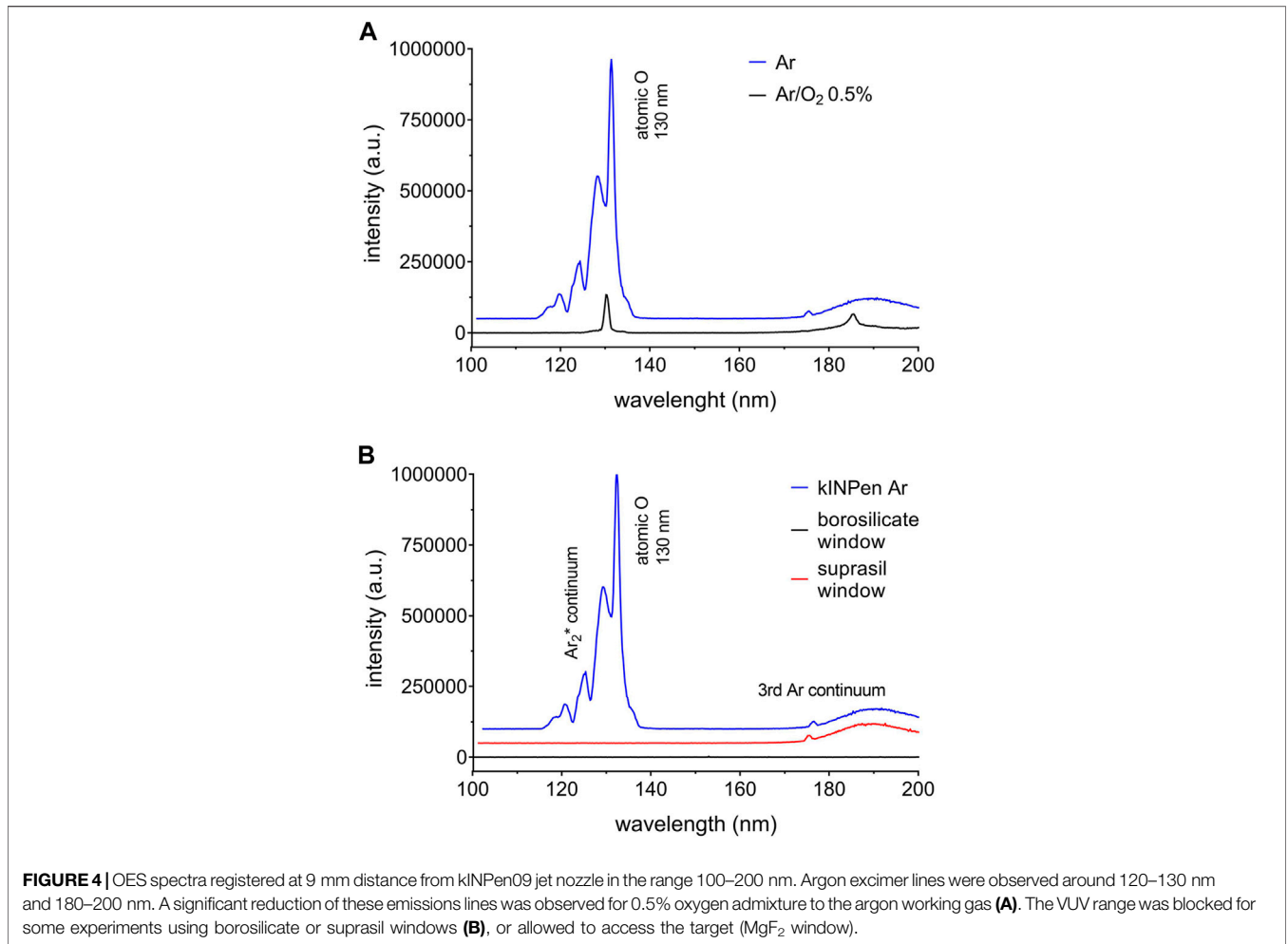
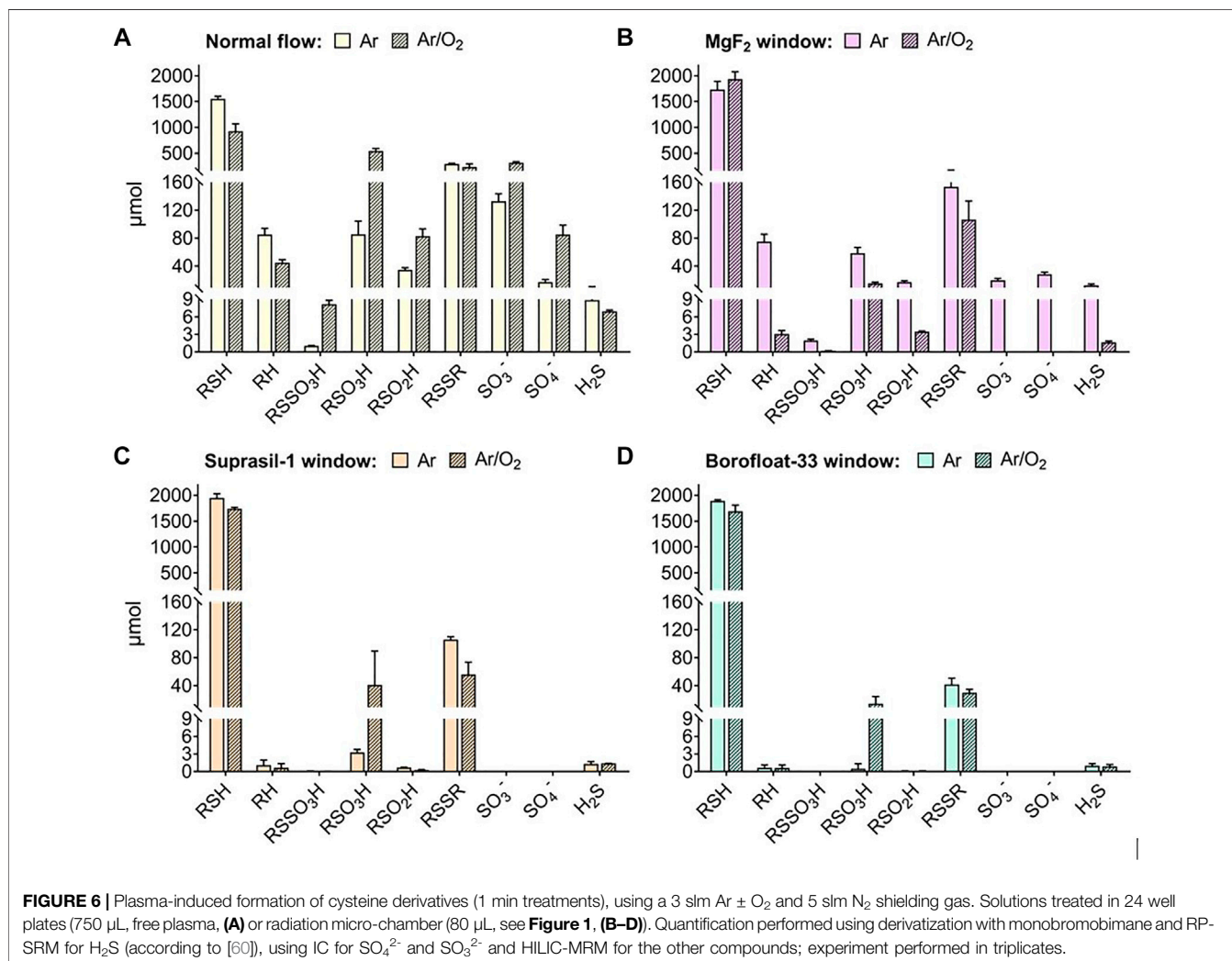


TABLE 2 | Analyzed cysteine derivatives, acronyms, formulas, quantification method and responsible plasma element.

Name	Acronym	Hill notation	Analysis	Plasma element
Cysteine	RSH	$C_3H_6NO_2S$	HILIC-MRM	None
Cystine	RSSR	$C_6H_{12}N_2O_4S_2$	HILIC-MRM	Radicals
Alanine	RH	$C_3H_7NO_2$	HILIC-MRM	(V)UV
Sulfonic acid	RSO_3H	$C_3H_7NO_5S$	HILIC-MRM	OH , 1O_2 , O
Sulfinic acid	RSO_2H	$C_3H_7NO_4S$	HILIC-MRM	OH , 1O_2 , O
S-sulfonate	$RSSO_3H$	$C_3H_7NO_5S_2$	HILIC-MRM	OH , O (indirect)
Sulfite	SO_3^-	O_3S	IC	(M)UV, OH , 1O_2 , O
Sulfate	SO_4^-	O_4S	IC	(M)UV, OH , 1O_2 , O
Hydrogen sulfide	H_2S	H_2S	MBB, RP-MRM	(M)UV



3 RESULTS AND DISCUSSION

3.1 Fingerprinting the kINPen Plasma Radiation

The kINPen spectra of emission goes from the vacuum UV (100 nm) to the near infrared (1,000 nm) [61]. The intensity of the UV irradiation was determined to be around 100 μ J cm⁻².

Optical emission spectroscopy was performed in order to characterize the emission spectra of the applied plasma treatment conditions (**Figure 1**). In this case, the emission spectra were measured applying the three different windows filtering various radiation ranges (**Figure 2**). Additionally, the vacuum UV range was recorded using a vacuum setup (**Figure 3**) [9,37]. In pure argon, emission lines from impurities of $\bullet OH$ and

N_2 were measured between 300 and 350 nm, and small atomic oxygen lines at 777 and 844 nm. The infrared region was dominated by argon emission lines, while between the range 400–700 nm no emission was observed. In the vacuum UV region (<195 nm), a dominant continuum centered at 126 nm can be measured for argon excimer (Ar_2^*), which includes also small absorption lines from ozone and O_2 . The modulation of working or shielding gases, induced changes in the emission spectra, e.g., the addition of molecular oxygen in the working gas leads to a reduction of Ar_2^* emission lines and increase those oxygen-based [9,37]; (Figure 2). The presence of molecular O_2 in the working gas interfered with the gas phase chemistry and UV emission of various species, such as $\bullet OH$, N, $\bullet NO$, and Ar_2^* . Suprasil and Borofloat-33 scavenged the emission of argon excimers, while in the range between 195 and 465 more subtle changes were observed, reflecting the characteristics of normal glass (Figure 2). Particularly in conditions with pure argon, which are certified for medical applications with kINPen MED, the role of vacuum UV radiation was dominant (Figure 3). As discussed previously, this event could be due to the lower formation of gaseous reactive species and therefore less reactions of argon metastable and excimers with surrounding gases to form further species, e.g., ozone, atomic oxygen, singlet oxygen, etc. [9,37]; (Figures 2, 4).

3.2 Vacuum UV as Source of Water-Derived $\bullet OH$ and H_2O_2 Production

The formation of $\bullet OH$ and H_2O_2 in water was compared using full plasma treatments (3 slm Ar and Ar + 1% O_2) and treatments using windows filtering different radiation ranges (Figure 5). The dissociation of water yielding OH radicals was favored in full argon plasma treatments and when VUV radiation was admitted (MgF_2 -window). For short treatments only small differences in $\bullet OH$ production was observed, but enlarging with treatment time. Full argon plasma produced around 30 μmol of $\bullet OH$ more than Ar plasma/ MgF_2 -window. It may be argued that either OH radicals from the gas phase contributed here or atomic oxygen generated from impurities. A recent report showed the sensitivity of terephthalic acid to this reactive short-lived species. Also liquid dynamic effects increasing the contact area between emitted radiation and target in contrast to the static treatments performed in the micro-chamber can contribute. Upon addition of molecular oxygen to the working gas, a decrease in $\bullet OH$ and H_2O_2 production was observed, especially when the MgF_2 -window was used, blocking interphase chemistry. In the near-complete absence of VUV radiation from the argon excimers, water dissociation did not occur. Corroborating this observation, almost no OH/ H_2O_2 formation was sparked by the longer UV ranges (UV-C and B and UV-A, respectively Suprasil-1 and Borofloat 33). Therefore, oxygen-base emission lines (atomic oxygen in NIR, ozone and O_2 in VUV), which increases in presence of molecular oxygen in the working gas, did not led to water dissociation. However, their potential direct impact on cysteine structures was investigated [55]. Overall, being highly energetic, VUV radiation emitted by Ar_2^* were able to induce water ionization, in contrast to the other UV ranges.

Therefore, the direct and indirect (e.g., water-derived species production) impact of VUV radiation resulted as predominant responsible of the effects induced on the liquid target. In the presence of oxygen in the gas phase, species derived from interphase chemistry and/or chemistry in liquid bulk are dominant, while VUV radiation is eliminated (Figure 3A).

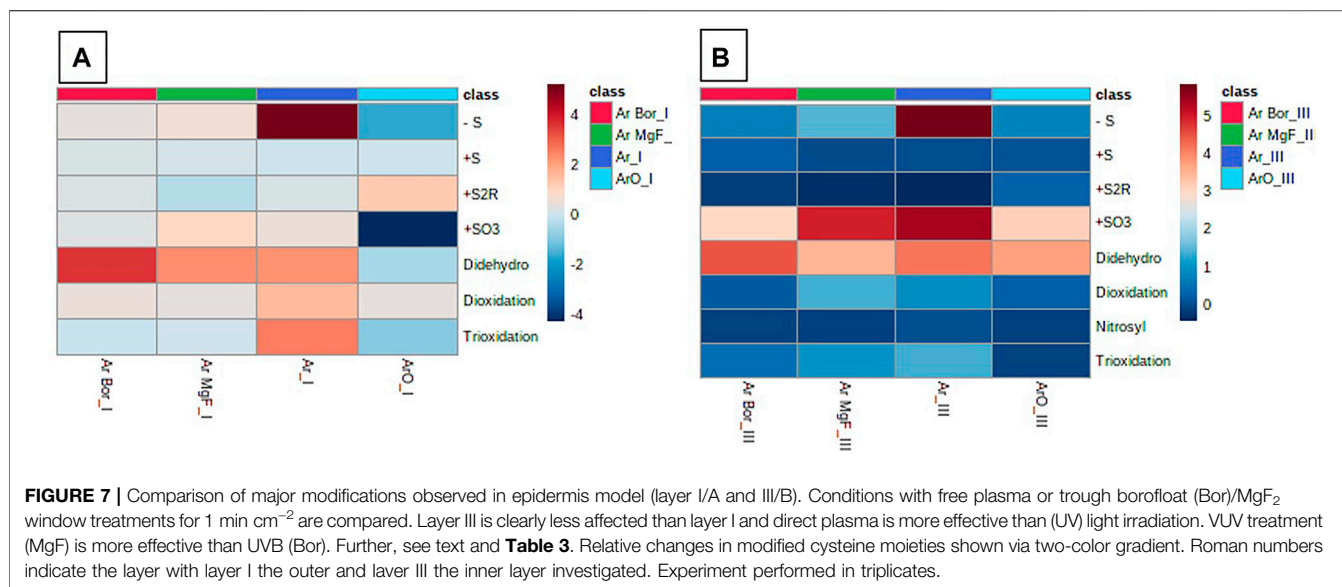
3.2 Direct and Liquid-Mediated Effects of Radiation on Cysteine Solutions

The impact of full plasma treatments and plasma-generated UV/VIS/NIR light on cysteine molecules is shown in Figure 6. Table 2 shows the structures, the quantification methods, and the major plasma components involved in the generation of each cysteine derivative. As discussed, argon plasma conditions stimulated predominantly pathways in liquid via impact of VUV radiation emitted by argon excimers, leading to $\bullet OH$ and H_2O_2 production. The same experiments were performed with cysteine containing solutions. The formation of products that derive from the loss of the thiol group in cysteine (alanine, cysteine-S-sulfonate, sulfite ions, sulfate ions, and hydrogen sulfide) was almost identical in treatments with full argon plasmas and filtered VUV radiation of argon plasmas (MgF_2). In contrast, these products almost disappeared when VUV-impermeable oxygen was introduced to the working gas and gas-liquid phase chemistry was blocked by an MgF_2 -window. This confirmed the key role of VUV radiation, leading to a cleavage of the carbon-sulfur bond [63], that was not observed by using other windows/radiation ranges. The energy of this bond is 272 $kJ mol^{-1}$, weaker than other bonds in cysteine or water (H-O 465 $kJ mol^{-1}$, C-C 347 $kJ mol^{-1}$, S-H 347 $kJ mol^{-1}$). The energy of the impinging UV photons of the argon excimer lines is much higher, 949 $kJ mol^{-1}$ (126 nm), allowing the cleavage of all bonds present in the target, including the oxygen-hydrogen bond in water molecules. Accordingly, it might be argued that OH radical formation is the first step ultimately yielding in thiol moiety abstraction. However, the presence of hydrogen sulfide (H_2S) clearly indicates that a direct cleavage of the C-S bond contributes significantly or is even dominant considering the weaker bond energy compared to the H-O bond. Interestingly, no indications of a C-C bond breakage in cysteine, leading e.g. to the formation formic acid, was observed. Summarizing, conditions with pure argon showed a significant contribution of the VUV radiation, stimulating i) the production of OH radicals, and ii) C-S bond breakages. Under VUV radiation, derivatives such as cystine and cysteine acids were also produced in consistent amounts in relation to full argon plasmas. The origin of the oxygen incorporated in structures such as sulfite, sulfate, cysteine acids and S-sulfonate, in this case, are water-derived species [55].

As previously discussed, due to the controlled pH (7.2), only low amounts of thiolate were available to react with H_2O_2 since the pKa of the cysteine thiol group is 8.18—allowing less than 5% deprotonation. Therefore, a minimal role in thiol oxidation could be attributed to hydrogen peroxide. Furthermore, a two-step reaction would be needed to form cystine: a first reaction of H_2O_2 with thiolate, with formation of cysteine sulfenic acid, and a second reaction of RSOH with another thiolate [63]; [64]. More

TABLE 3 | Cysteine focused protein modifications observed in porcine epidermis model (ANOVA and Post-hoc analysis Fisher's LSD, p-value and FDR ≤ 0.05).

	$p < 0.05$ (n)	Type of modification
Overall	5	sulphur loss (-S), Trioxidation, Sulfenylation (+SO ₃), Cysteine addition (+S ₂ R), Didehydrogenation (didehydro)
Layer I	5	Sulphur loss (-S), Trioxidation, Sulfenylation (+SO ₃), Cysteine addition (+S ₂ R), Didehydrogenation (didehydro)
Layer II	3	Cysteine addition (+S ₂ R), Nitrosylation (nitrosyl), Sulphur loss (-S)
Layer III	3	Sulphur loss (-S), Cysteine addition (+S ₂ R), Trioxidation
Ar/O ₂ plasma	5	Nitrosylation (nitrosyl), Sulphur loss (-S), Sulfenylation (+SO ₃), Trioxidation, Didehydrogenation (didehydro)
Ar plasma	4	Cysteine addition (+S ₂ R), Sulfenylation (+SO ₃), Didehydrogenation (didehydro), Sulphur loss (-S)
Ar MgF ₂ window	1	Nitrosylation (nitrosyl)
Ar Borofloat window	1	Cysteine addition (+S ₂ R)



likely, the reaction of $\bullet\text{OH}$ with cysteine generates cystine by first formation of thiyl radicals ($\text{RS}\bullet$), which rapidly recombine to form cystine. The formation of cysteinyl radicals was detected using BMPO/EPR spectroscopy earlier [54].

The reaction of $\text{RS}\bullet$ with $\bullet\text{OH}$ would lead to cysteine sulfenic acid, which immediately is oxidized into sulfinic and further to sulfonic acid by $\bullet\text{OH}$ or H_2O_2 [65–67]. The production of S-sulfonate (RSSO_3H), in absence of atomic oxygen, could be promoted by first cysteine oxidation by two $\bullet\text{OH}$, with following C-S breakage promoted by VUV and final incorporation of another oxygen. Sulfite can be generated by cut of the C-S bond in cysteine sulfonic acids, or most likely, cysteine S-sulfonate (S-S bond dissociation energy $414.6 \text{ kJ mol}^{-1}$) [68]. Supplementary experiments have been performed by treating cysteine sulfonic acid in the radiation chamber, as shown in the supplementary material (**Supplementary Figure S1**). Despite the high concentration of the reference compound cysteine sulfonic acid, only small amounts of sulfite and sulfate ions are formed, indicating that the majority of C-S bond cleavages takes place at the cysteine or cystine level. With that, most sulfite and sulfate ions were generated by the oxidation of H_2S . This pathway is favored in the presence of reactive oxygen species produced by the cleavage water molecules (e.g. H_2O_2 , $\bullet\text{OH}$). Clearly, a number

of chemical pathways were active in liquids under the influence of vacuum UV radiation, in contrast to radiation $>195 \text{ nm}$ (UV-C).

The cysteine products generated by UV-C (Suprasil) or UVB/UVA (Borofloat) were clearly different. In these cases, almost no production of the water-derived species $\text{OH}/\text{H}_2\text{O}_2$ (**Figure 5**) and cysteine derivatives generated by C-S bond cleavage (SO_4^{2-} , SO_3^{2-} , alanine/RH; **Figure 6**) were observed.

The formation of cystine via hydrogen abstraction in cysteine (type I photo-oxidation mechanisms) and $\text{RS}\bullet$ recombination [50,51]; was observed independent from the window, but with lower extent when vacuum UV is blocked (Borofloat/Suprasil). The production of sulfonic acid (RSO_3H , **Figure 6**) was measured in conditions with oxygen in the working gas, suggesting the potential role of radiation emitted in the near infrared and depending by the presence of O_2 . The origin of oxygen incorporated by sulfonic acid, in this case, could be due to the reaction of thiyl radical with water, generating $\bullet\text{OH}$ by hydrogen abstraction. Even though the radiation emitted in these ranges are not ionizing, due to the lower energy, it was shown that also the UV radiation $>200 \text{ nm}$ can induce oxidative stress in cellular compartments in relation to the exposure time, with increase in the cellular production of reactive species [49,50].

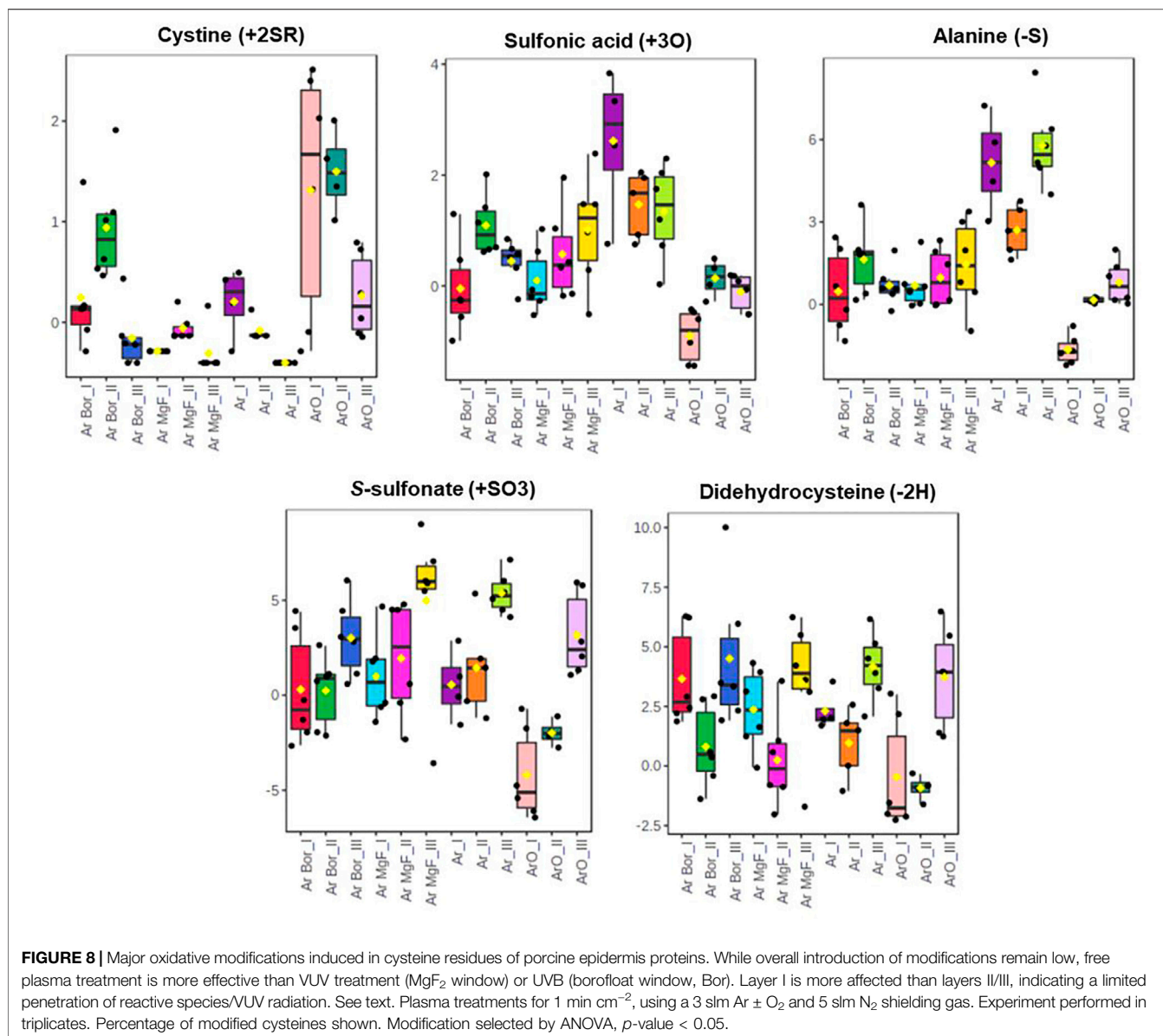


FIGURE 8 | Major oxidative modifications induced in cysteine residues of porcine epidermis proteins. While overall introduction of modifications remain low, free plasma treatment is more effective than VUV treatment (MgF₂ window) or UVB (borofloat window, Bor). Layer I is more affected than layers II/III, indicating a limited penetration of reactive species/VUV radiation. See text. Plasma treatments for 1 min cm⁻², using a 3 slm Ar ± O₂ and 5 slm N₂ shielding gas. Experiment performed in triplicates. Percentage of modified cysteines shown. Modification selected by ANOVA, *p*-value < 0.05.

3.3 Plasma Radiation Impact on Epidermal Protein Structures

The analysis of the oxidative modifications of cysteine belonging to the porcine epidermal proteome was performed via tape stripping assay in combination with high-resolution mass spectrometry. The oxidation was monitored in the first three stratum corneum layers of the porcine epidermis, reflecting a penetration depth of 5–7 μm. **Table 3** and **Figure 7** give an overview of the detected modifications, while **Figure 8** shows a quantitative comparison of the most relevant oxidative modifications. Unstable oxidative modifications, such as S-nitrosylation, may have been underestimated. According to proteomics standard procedures, thiols were reduced and alkylated during sample workup. Some losses to the plasma chemistry on protein thiols (e.g., sulfenic acids,

S-nitrosylation) cannot be excluded although stable modifications (e.g., cysteine sulfonic acid, cysteine-S-sulfonate) were retained. Overall, five types of modifications were found to be introduced into the epidermal proteins with a statistical significance. These are the apparent replacement of cysteine by alanine (sulphur loss), the formation of cysteine sulfonic acid (trioxidation), the formation of cysteine-S-sulfonate (sulfonylation), the formation of a disulfide with other cysteine moieties (+S₂R), and the loss of two hydrogen atoms forming an unsaturated cysteine molecule (didehydrogenation) (**Table 3**). Alongside depth in the epidermis, the intensity and number of detected modifications decrease (**Figure 7**). The impact of plasma-derived UV or VUV light was lower than expected from the *in vitro* experiments (**Table 3**). Only nitrosylation was found to be significantly elevated by MgF₂ filtered kINPen irradiation, pointing at a limited role of (V)UV photons *in vivo*.

The conversion of cysteine in cysteine S-sulfonate (+SO₃) and dehydrogenated cysteine (-2H) (**Figure 8**), was promoted especially in the third skin epidermis layer, regardless of the applied treatment condition. The results indicate that protein modifications result from complex dynamics and are not corresponding to the action of only one plasma components produced in specific conditions.

Some modifications appear in special conditions only. For example, the conversion of cysteine into cystine was observed in treatment with Ar/O₂ full plasmas, with a maximum in the first layer and a progressive decrease in the second and third. In this condition, the effluent contains significant amounts of singlet oxygen and atomic oxygen, especially at short distances from the nozzle. Atomic oxygen is able to form thyl radicals by hydrogen abstraction to the protein cysteines, which rapidly may recombine forming a disulfide bond. This event causes conformational changes of the protein, alongside a potential gain or loss of function. The oxidation of cysteine into sulfonic acid by the incorporation of three oxygen atoms, and the breakage of the C-S bond with conversion of cysteine to alanine were events observed predominantly in treatments with full argon plasma in the first layer of the skin. When using windows, even in case of the VUV-transmitting MgF₂ and more prominent in suprasil and Borofloat-33 windows, only few such modifications were detected. This indicates that the VUV radiation, although most prominent in Ar plasma, does in soft targets not contribute in the same manner to biomolecule modification than in liquid targets. In this case, the direct impact of argon metastables and other gas phase species and the subsequent formation of secondary reactive species is more prominent. This is in line with a report investigating the oxidation of human skin lipids that showed a limited impact of the argon plasma on lipid side chain oxidation in the absence of water [33]. Obviously, the highly energetic VUV radiation is unable to penetrate deeper into layers of biomolecules such as the model described here or the sebum lipids, limiting its ability to contribute significantly to the plasma chemistry *in situ*.

4 CONCLUSION

In aqueous targets (**Sections 3.2, 3.3**), plasma-derived VUV radiation is an effective component in plasma-liquid chemistry. The liquid phase acts as compartment amplifying the plasma chemistry by the *de novo* formation of secondary water-derived reactive species (e.g., hydroxyl radicals, hydrogen peroxide) at the gas-liquid interphase, that subsequently allow the modification of sensitive targets such as thiol moieties. In contrast, in complex targets like the intact skin the plasma-derived VUV radiation is blocked effectively by the dense biomolecules layers and plays a limited role only. While this might be disappointing from the scientific

viewpoint it emphasizes the safety of physical plasmas which has been a significant concern for years. Corroborating a number of reports proofing the safety [69]; [70]; [71], our results further support the safe application of physical plasmas. Even in humid wounds where resident water molecules allow the formation of secondary species by the UV radiation increasing the effectiveness of plasma while the protein layer in the wound bed protects the local tissue.

Proteomics Data

The proteomics data connected to this paper have been uploaded to the ProteomeXchange servers under the project name “Gas plasma and (V)UV impact on porcine epidermis using a tape strip assay approach” (Project accession: PXD028915, username: reviewer_pxd028915@ebi.ac.uk/Password: OPKS8hii).

DATA AVAILABILITY STATEMENT

The datasets presented in this study can be found in online repositories. The names of the repository/repositories and accession number(s) can be found below: ProteomeXchange with accession PXD028915.

AUTHOR CONTRIBUTIONS

GB, KW, and TvW devised the experiments, wrote an corrected the manuscript HM and TG performed OES measurements and discussed the data GB, SW, and KW performed mass spectrometry analysis and discussed the data/incorporated it into the manuscript.

FUNDING

Funding from the German Federal Ministry of Education and Research (grant number 03Z22DN12 to KW) supported this work.

ACKNOWLEDGMENTS

The authors like to thank Steffen Franke for contributing the VUV spectrometer setup.

SUPPLEMENTARY MATERIAL

The Supplementary Material for this article can be found online at: <https://www.frontiersin.org/articles/10.3389/fphy.2021.759005/full#supplementary-material>

REFERENCES

- Weltmann K-D, Von Woedtke T Plasma Medicine-Current State of Research and Medical Application. *Plasma Phys Control Fusion* (2017) 59:014031–41. doi:10.1088/0741-3335/59/1/014031
- Khlyustova A, Labay C, Machala Z, Ginebra M-P, Canal C Important Parameters in Plasma Jets for the Production of RONS in Liquids for Plasma Medicine: A Brief Review. *Front Chem Sci Eng* (2019) 13:238–52. doi:10.1007/s11705-019-1801-8
- Von Woedtke T, Schmidt A, Bekeschus S, Wende K, Weltmann K-D Plasma Medicine: A Field of Applied Redox Biology. *In Vivo* (2019) 33:1011–26. doi:10.21873/invivo.11570
- Stratmann B, Costea T-C, Nolte C, Hiller J, Schmidt J, Reindel J, et al. Effect of Cold Atmospheric Plasma Therapy vs Standard Therapy Placebo on Wound Healing in Patients with Diabetic Foot Ulcers. *JAMA Netw Open* (2020) 3:e2010411. doi:10.1001/jamanetworkopen.2020.10411
- Zhang W, Hu X, Shen Q, Xing D Mitochondria-specific Drug Release and Reactive Oxygen Species Burst Induced by Polyprodrug Nanoreactors Can Enhance Chemotherapy. *Nat Commun* (2019) 10:1704. doi:10.1038/s41467-019-09566-3
- Tang ZM, Liu YY, Ni DL, Zhou JJ, Zhang M, Zhao PR, et al. Biodegradable Nanopodrugs: "Delivering" ROS to Cancer Cells for Molecular Dynamic Therapy. *Adv Mater* (2020) 32:e1904011. doi:10.1002/adma.201904011
- Agostinis P, Berg K, Cengel KA, Foster TH, Girotti AW, Gollnick SO, et al. Photodynamic Therapy of Cancer: an Update. *CA: A Cancer J Clinicians* (2011) 61:250–81. doi:10.3322/caac.20114
- Graves DB Mechanisms of Plasma Medicine: Coupling Plasma Physics, Biochemistry, and Biology. *IEEE Trans Radiat Plasma Med Sci* (2017) 1: 281–92. doi:10.1109/trpms.2017.2710880
- Reuter S, Von Woedtke T, Weltmann KD The kINPen-A Review on Physics and Chemistry of the Atmospheric Pressure Plasma Jet and its Applications. *J Phys D-Applied Phys* (2018) 51. doi:10.1088/1361-6463/aab3ad
- Gay-Mimbrera J, García MC, Isla-Tejera B, Rodero-Serrano A, García-Nieto AV, Ruano J Clinical and Biological Principles of Cold Atmospheric Plasma Application in Skin Cancer. *Adv Ther* (2016) 33:894–909. doi:10.1007/s12325-016-0338-1
- Liedtke KR, Bekeschus S, Kaeding A, Hackbarth C, Kuehn J-P, Heidecke C-D, et al. Non-thermal Plasma-Treated Solution Demonstrates Antitumor Activity against Pancreatic Cancer Cells *In Vitro* and *In Vivo*. *Sci Rep* (2017) 7:8319. doi:10.1038/s41598-017-08560-3
- Liedtke KR, Freund E, Hackbarth C, Heidecke C-D, Partecke L-I, Bekeschus S A Myeloid and Lymphoid Infiltrate in Murine Pancreatic Tumors Exposed to Plasma-Treated Medium. *Clin Plasma Med* (2018) 11:10–7. doi:10.1016/j.cpm.2018.07.001
- Bekeschus S, Schmidt A, Weltmann K-D, Von Woedtke T The Plasma Jet kINPen - A Powerful Tool for Wound Healing. *Clin Plasma Med* (2016) 4: 19–28. doi:10.1016/j.cpm.2016.01.001
- Bernhardt T, Semmler ML, Schäfer M, Bekeschus S, Emmert S, Boeckmann L. Plasma Medicine: Applications of Cold Atmospheric Pressure Plasma in Dermatology. *Oxid Med Cel Longev* (2019) 2019:3873928. doi:10.1155/2019/3873928
- Schmidt A, Von Woedtke T, Vollmar B, Hasse S, Bekeschus S Nrf2 Signaling and Inflammation Are Key Events in Physical Plasma-Spurred Wound Healing. *Theranostics* (2019) 9:1066–84. doi:10.7150/thno.29754
- Lackmann J-W, Bandow JE Inactivation of Microbes and Macromolecules by Atmospheric-Pressure Plasma Jets. *Appl Microbiol Biotechnol* (2014) 98: 6205–13. doi:10.1007/s00253-014-5781-9
- Jablonowski H, Hänsch MAC, Dünnbier M, Wende K, Hammer MU, Weltmann K-D, et al. Plasma Jet's Shielding Gas Impact on Bacterial Inactivation. *Biointerphases* (2015) 10:029506. doi:10.1116/1.4916533
- Matthes R, Jablonowski L, Koban I, Quade A, Hübner N-O, Schlueter R, et al. *In Vitro* treatment of *Candida Albicans* Biofilms on Denture Base Material with Volume Dielectric Barrier Discharge Plasma (VDBD) Compared with Common Chemical Antiseptics. *Clin Oral Invest* (2015) 19:2319–26. doi:10.1007/s00784-015-1463-y
- Duske K, Koban I, Kindel E, Schröder K, Nebe B, Holtfreter B, et al. Atmospheric Plasma Enhances Wettability and Cell Spreading on Dental Implant Metals. *J Clin Periodontol* (2012) 39:400–7. doi:10.1111/j.1600-051x.2012.01853.x
- Jablonowski L, Koban I, Berg MH, Kindel E, Duske K, Schröder K, et al. Elimination of *E. Faecalis* by a New Non-Thermal Atmospheric Pressure Plasma Handheld Device for Endodontic Treatment. A Preliminary Investigation. *Plasma Process. Polym* (2013) 10:499–505. doi:10.1002/ppap.201200156
- Duske K, Jablonowski L, Koban I, Matthes R, Holtfreter B, Sckell A, et al. Cold Atmospheric Plasma in Combination with Mechanical Treatment Improves Osteoblast Growth on Biofilm Covered Titanium Discs. *Biomaterials* (2015) 52:327–34. doi:10.1016/j.biomaterials.2015.02.035
- Hartwig S, Doll C, Voss JO, Hertel M, Preissner S, Raguse JD Treatment of Wound Healing Disorders of Radial Forearm Free Flap Donor Sites Using Cold Atmospheric Plasma: A Proof of Concept. *J Oral Maxillofac Surg* (2017) 75:429–35. doi:10.1016/j.joms.2016.08.011
- Bruggeman PJ, Kushner MJ, Locke BR, Gardeniers JGE, Graham WG, Graves DB, et al. Plasma-liquid Interactions: a Review and Roadmap. *Plasma Sourc Sci. Technol.* (2016) 25:053002. doi:10.1088/0963-0252/25/5/053002
- Bruno G, Heusler T, Lackmann J-W, Von Woedtke T, Weltmann K-D, Wende K Cold Physical Plasma-Induced Oxidation of Cysteine Yields Reactive Sulfur Species (RSS). *Clin Plasma Med* (2019) 14:100083. doi:10.1016/j.cpm.2019.100083
- Brandenburg R Dielectric Barrier Discharges: Progress on Plasma Sources and on the Understanding of Regimes and Single Filaments. *Plasma Sourc Sci. Technol.* (2017) 26:053001. doi:10.1088/1361-6595/aa6426
- Bruggeman PJ, Iza F, Brandenburg R Foundations of Atmospheric Pressure Non-equilibrium Plasmas. *Plasma Sourc Sci. Technol.* (2017) 26:123002. doi:10.1088/1361-6595/aa97af
- Takai E, Kitamura T, Kuwabara J, Ikawa S, Yoshizawa S, Shiraki K, et al. Chemical Modification of Amino Acids by Atmospheric-Pressure Cold Plasma in Aqueous Solution. *J Phys D: Appl Phys* (2014) 47:285403. doi:10.1088/0022-3727/47/28/285403
- Lackmann JW, Baldus S, Steinborn E, Edengeiser E, Kogelheide F, Langklotz S, et al. A Dielectric Barrier Discharge Terminally Inactivates RNase A by Oxidizing Sulfur-Containing Amino Acids and Breaking Structural Disulfide Bonds. *J Phys D-Applied Phys* (2015) 48. doi:10.1088/0022-3727/48/49/494003
- Verlact CCW, Van Boxem W, Dewaele D, Lemière F, Sobott F, Benedikt J, et al. Mechanisms of Peptide Oxidation by Hydroxyl Radicals: Insight at the Molecular Scale. *J Phys Chem C* (2017) 121:5787–99. doi:10.1021/acs.jpcc.6b12278
- Nasri Z, Memari S, Wenske S, Clemens R, Martens U, Delcea M, et al. Singlet Oxygen-Induced Phospholipase A2 Inhibition: a Major Role for Interfacial Tryptophan Dioxidation. *Eur Chem J* (2021) 27(59):14702–10. doi:10.1002/chem.202102306
- Maheux S, Frache G, Thomann JS, Clément F, Penny C, Belmonte T, et al. Small Unilamellar Liposomes as a Membrane Model for Cell Inactivation by Cold Atmospheric Plasma Treatment. *J Phys D: Appl Phys* (2016) 49:344001. doi:10.1088/0022-3727/49/34/344001
- Yusupov M, Wende K, Kupsch S, Neyts EC, Reuter S, Bogaerts A Effect of Head Group and Lipid Tail Oxidation in the Cell Membrane Revealed through Integrated Simulations and Experiments. *Sci Rep* (2017) 7:5761. doi:10.1038/s41598-017-06412-8
- Striesow J, Lackmann J-W, Ni Z, Wenske S, Weltmann K-D, Fedorova M, et al. Oxidative Modification of Skin Lipids by Cold Atmospheric Plasma (CAP): A Standardizable Approach Using RP-LC/MS2 and DI-ESI/MS2. *Chem Phys Lipids* (2020) 226:104786. doi:10.1016/j.chemphyslip.2019.104786
- Schmidt A, Bekeschus S Redox for Repair: Cold Physical Plasmas and Nrf2 Signaling Promoting Wound Healing. *Antioxidants (Basel)* (2018) 7. doi:10.3390/antiox7100146
- Muzumdar S, Hiebert H, Haertel E, Ben-Yehuda Greenwald M, Bloch W, Werner S, et al. Nrf2-Mediated Expansion of Piloosebaceous Cells Accelerates Cutaneous Wound Healing. *Am J Pathol* (2019) 189:568–79. doi:10.1016/j.ajpath.2018.11.017
- Schmidt A, Bekeschus S, Jarick K, Hasse S, Von Woedtke T, Wende K. Cold Physical Plasma Modulates P53 and Mitogen-Activated Protein Kinase Signaling in Keratinocytes. *Oxid Med Cel Longev* (2019) 2019:7017363. doi:10.1155/2019/7017363

37. Jablonowski H, Bussiahn R, Hammer MU, Weltmann K-D, Von Woedtke T, Reuter S Impact of Plasma Jet Vacuum Ultraviolet Radiation on Reactive Oxygen Species Generation in Bio-Relevant Liquids. *Phys Plasmas* (2015) 22:122008. doi:10.1063/1.4934989
38. Laroussi M, Dobbs FC, Wei Z, Doblin MA, Ball LG, Moreira KR, et al. Decontamination of Water by Excimer UV Radiation. *IEEE Trans Plasma Sci* (2002) 30:1501–3. doi:10.1109/tps.2002.804208
39. Brandenburg R, Lange H, Von Woedtke T, Stieber M, Kindel E, Ehlbeck J, et al. Antimicrobial Effects of UV and VUV Radiation of Nonthermal Plasma Jets. *IEEE Trans Plasma Sci* (2009) 37:877–83. doi:10.1109/tps.2009.2019657
40. Schneider S, Lackmann J-W, Ellerweg D, Denis B, Narberhaus F, Bandow JE, et al. The Role of VUV Radiation in the Inactivation of Bacteria with an Atmospheric Pressure Plasma Jet. *Plasma Process. Polym* (2012) 9:561–8. doi:10.1002/ppap.201100102
41. Judé F, Wattiaux G, Merbahi N, Mansour M, Castanié-Cornet MP The Antibacterial Activity of a Microwave Argon Plasma Jet at Atmospheric Pressure Relies Mainly on UV-C Radiations. *J Phys D: Appl Phys* (2014) 47:405201. doi:10.1088/0022-3727/47/40/405201
42. Lange H, Foest R, Schafer J, Weltmann K-D Vacuum UV Radiation of a Plasma Jet Operated with Rare Gases at Atmospheric Pressure. *IEEE Trans Plasma Sci* (2009) 37:859–65. doi:10.1109/tps.2009.2019982
43. Bahre H, Lange H, Schulz-Von Der Gathen V, Foest R. Vacuum Ultraviolet (VUV) Emission of an Atmospheric Pressure Plasma Jet (M-APPJ) Operated in Helium-Oxygen Mixtures in Ambient Air. *Acta Technica* (2011) 56.
44. Yurkova I, Shadyro O, Kisel M, Brede O, Arnhold J Radiation-induced Free-Radical Transformation of Phospholipids: MALDI-TOF MS Study. *Chem Phys Lipids* (2004) 132:235–46. doi:10.1016/j.chemphyslip.2004.08.006
45. Corre I, Niaudet C, Paris F Plasma Membrane Signaling Induced by Ionizing Radiation. *Mutat Research/Reviews Mutat Res* (2010) 704:61–7. doi:10.1016/j.mrrev.2010.01.014
46. Rastogi RP, RichaKumar A, Kumar A, Tyagi MB, Sinha RP. Molecular Mechanisms of Ultraviolet Radiation-Induced DNA Damage and Repair. *J Nucleic Acids* (2010) 2010:592980. doi:10.4061/2010/592980
47. Islam MT Radiation Interactions with Biological Systems. *Int J Radiat Biol* (2017) 93:487–93. doi:10.1080/09553002.2017.1286050
48. Lalande M, Schwob L, Vizcaino V, Chirof F, Dugourd P, Schlathöler T, et al. Direct Radiation Effects on the Structure and Stability of Collagen and Other Proteins. *Chembiochem* (2019) 20:2972–80. doi:10.1002/chic.201900202
49. Mikkelsen RB, Wardman P Biological Chemistry of Reactive Oxygen and Nitrogen and Radiation-Induced Signal Transduction Mechanisms. *Oncogene* (2003) 22:5734–54. doi:10.1038/sj.onc.1206663
50. Pattison DJ, Davies MJ *Actions of Ultraviolet Light on Cellular Structures*. Birkhauser, Basel: EXS (2006). p. 131–57.
51. Pattison DJ, Rahmanto AS, Davies MJ Photo-oxidation of Proteins. *Photochem Photobiol Sci* (2012) 11:38–53. doi:10.1039/c1pp05164d
52. Von Woedtke T, Jülich W-D, Thal S, Diederich M, Stieber M, Kindel E Antimicrobial Efficacy and Potential Application of a Newly Developed Plasma-Based Ultraviolet Irradiation Facility. *J Hosp Infect* (2003) 55:204–11. doi:10.1016/s0195-6701(03)00290-1
53. Laroussi M, Leipold F Evaluation of the Roles of Reactive Species, Heat, and UV Radiation in the Inactivation of Bacterial Cells by Air Plasmas at Atmospheric Pressure. *Int J Mass Spectrom* (2004) 233:81–6. doi:10.1016/j.ijms.2003.11.016
54. Lackmann J-W, Bruno G, Jablonowski H, Kogelheide F, Offerhaus B, Held J, et al. Nitrosylation vs. Oxidation - How to Modulate Cold Physical Plasmas for Biological Applications. *PLoS One* (2019) 14:e0216606. doi:10.1371/journal.pone.0216606
55. Wende K, Bruno G, Lalk M, Weltmann K-D, Von Woedtke T, Bekeschus S, et al. On a Heavy Path - Determining Cold Plasma-Derived Short-Lived Species Chemistry Using Isotopic Labelling. *RSC Adv* (2020) 10:11598–607. doi:10.1039/c9ra08745a
56. Sremački I, Bruno G, Jablonowski H, Leys C, Nikiforov AY, Wende K Influence of Aerosol Injection on the Liquid Chemistry Induced by an RF Argon Plasma Jet. *Plasma Sources Sci. Technol.* (2021) 30(9). doi:10.1088/1361-6595/abe176
57. Pikal-Cleland KA, Cleland JL, Anchordoquy TJ, Carpenter JF. Effect of glycine on pH Changes and Protein Stability during Freeze-Thawing in Phosphate Buffer Systems. *J Pharm Sci* (2002) 91:1969–79. doi:10.1002/jps.10184
58. Jacobi U, Kaiser M, Toll R, Mangelsdorf S, Audring H, Otberg N, et al. Porcine Ear Skin: an *In Vitro* Model for Human Skin. *Skin Res Technol* (2007) 13:19–24. doi:10.1111/j.1600-0846.2006.00179.x
59. Myers B, Ranieri P, Smirnova T, Hewitt P, Peterson D, Quesada MH, et al. Measuring Plasma-Generated center Dot OH and O Atoms in Liquid Using EPR Spectroscopy and the Non-selectivity of the HTA Assay. *J Phys D-Applied Phys* (2021) 54. doi:10.1088/1361-6463/abd9a6
60. Shen X, Kolluru GK, Yuan S, Kevil CG Measurement of H2S *In Vivo* and *In Vitro* by the Monobromobimane Method. *Methods Enzymol* (2015) 554:31–45. doi:10.1016/bs.mie.2014.11.039
61. Foest R, Kindel E, Lange H, Ohl A, Stieber M, Weltmann K-D RF Capillary Jet - a Tool for Localized Surface Treatment. *Contrib Plasma Phys* (2008) 47:119–28. doi:10.1002/ctpp.200710017
62. Reuter S, Winter J, Schmidt-Bleker A, Schroeder D, Lange H, Knake N, et al. Atomic Oxygen in a Cold Argon Plasma Jet: TALIF Spectroscopy in Ambient Air with Modelling and Measurements of Ambient Species Diffusion. *Plasma Source Sci Tech* (2012) 21:024005.%&
63. Abedinzadeh Z, Gardes-Albert M, Ferradini C Kinetic Study of the Oxidation Mechanism of Glutathione by Hydrogen Peroxide in Neutral Aqueous Medium. *Can J Chem* (1989) 67:1247–55. doi:10.1139/v89-190
64. Luo D, Smith SW, Anderson BD Kinetics and Mechanism of the Reaction of Cysteine and Hydrogen Peroxide in Aqueous Solution. *J Pharm Sci* (2005) 94:304–16. doi:10.1002/jps.20253
65. Enescu M, Cardey B Mechanism of Cysteine Oxidation by a Hydroxyl Radical: a Theoretical Study. *Chem Eur J Chem Phys* (2006) 7:912–9. doi:10.1002/cphc.200500585
66. Gupta V, Carroll KS Sulfenic Acid Chemistry, Detection and Cellular Lifetime. *Biochim Biophys Acta (Bba) - Gen Subjects* (2014) 1840:847–75. doi:10.1016/j.bbagen.2013.05.040
67. Chauvin J-PR, Pratt DA On the Reactions of Thiols, Sulfenic Acids, and Sulfenic Acids with Hydrogen Peroxide. *Angew Chem Int Ed* (2017) 56:6255–9. doi:10.1002/anie.201610402
68. Stans MH *Bond Dissociation Energies in Simple Molecules*NIST Special Publication 1 %6, 58 %& (1970).
69. Wende K, Bekeschus S, Schmidt A, Jatsch L, Hasse S, Weltmann KD, et al. Risk Assessment of a Cold Argon Plasma Jet in Respect to its Mutagenicity. *Mutat Research/Genetic Toxicol Environ Mutagenesis* (2016) 798-799:48–54. doi:10.1016/j.mrgentox.2016.02.003
70. Schmidt A, Woedtke TV, Stenzel J, Lindner T, Polei S, Vollmar B, et al. One Year Follow-Up Risk Assessment in SKH-1 Mice and Wounds Treated with an Argon Plasma Jet. *Int J Mol Sci* (2017) 18. doi:10.3390/ijms18040868
71. Bekeschus S, Schmidt A, Kramer A, Metelmann H-R, Adler F, Von Woedtke T, et al. High Throughput Image Cytometry Micronucleus Assay to Investigate the Presence or Absence of Mutagenic Effects of Cold Physical Plasma. *Environ Mol Mutagen* (2018) 59:268–77. doi:10.1002/em.22172
72. Linxiang L, Abe Y, Nagasawa Y, Kudo R, Usui N, Imai K, et al. An HPLC Assay of Hydroxyl Radicals by the Hydroxylation Reaction of Terephthalic Acid. *Biomed Chromatogr* (2004) 18:470–4. doi:10.1002/bmc.339

Conflict of Interest: The authors declare that the research was conducted in the absence of any commercial or financial relationships that could be construed as a potential conflict of interest.

Publisher's Note: All claims expressed in this article are solely those of the authors and do not necessarily represent those of their affiliated organizations, or those of the publisher, the editors and the reviewers. Any product that may be evaluated in this article, or claim that may be made by its manufacturer, is not guaranteed or endorsed by the publisher.

Copyright © 2021 Bruno, Wenske, Mahdikia, Gerling, von Woedtke and Wende. This is an open-access article distributed under the terms of the Creative Commons Attribution License (CC BY). The use, distribution or reproduction in other forums is permitted, provided the original author(s) and the copyright owner(s) are credited and that the original publication in this journal is cited, in accordance with accepted academic practice. No use, distribution or reproduction is permitted which does not comply with these terms.

7. Eigenständigkeitserklärung

Hiermit erkläre ich, Sebastian Wenske, dass diese Arbeit bisher von mir weder an der Mathematisch-Naturwissenschaftlichen Fakultät der Universität Greifswald noch einer anderen wissenschaftlichen Einrichtung zum Zwecke der Promotion eingereicht wurde.

Ferner erkläre ich, dass ich diese Arbeit selbstständig verfasst und keine anderen als die darin angegebenen Hilfsmittel und Hilfen benutzt und keine Textabschnitte eines Dritten ohne Kennzeichnung übernommen habe.

Date

Sebastian Wenske

8. Curriculum Vitae

Sebastian Wenske

Geburtsdatum: 22. August 1989

Geburtsort: Neuruppin, Deutschland

Adresse: Senator-Caesar-Str. 10, 28213 Deutschland

Kontakt: sebastianwenske89@gmail.com

Berufserfahrungen

04.2016 – 05.2017 Universität Greifswald: Institut für Biochemie, Greifswald
Wissenschaftliche Hilfskraft

Ausbildung

03.2018 - 06.2021 Promotion an der Universität Greifswald

10.2015 - 02.2018 Master Studium Biochemie an der Universität Greifswald
Abschluss: Master of Science

10.2012 - 09.2015 Bachelor Studium Biochemie an der Universität Greifswald
Abschluss: Bachelor of Science

10.2010 - 09.2012 Bachelor Studium Physik an der Universität Rostock

08.2009 - 04.2010 Zivildienst in den Ruppiner Kliniken GmbH als OP Helfer

08.2002 - 07.2009 Karl-Friedrich-Schinkel-Gymnasium in Neuruppin
Abschluss: Allgemeine Hochschulreife

Date

Sebastian Wenske

9. List of Publications & Conference Contributions

Publications in Peer-Reviewed Journals

- G. Bruno, S. Wenske, J.-L. Lackmann, M. Lalk, T. von Woedtke, K. Wende. "On the liquid chemistry of the reactive nitrogen species peroxyxynitrite and nitrogen dioxide generated by physical plasmas". *Biomolecules*, 10 (12), 1687, 2020.
- S. Wenske, J.-W. Lackmann, S. Bekeschus, K.-D. Weltmann, T. von Woedtke and K. Wende. "Nonenzymatic post-translational modifications in peptides by cold plasma-derived reactive oxygen and nitrogen species". *Biointerphases*, 15 (6), 061008, 2020.
- M.-C. Sommer, M. Balazinski, R. Rataj, S. Wenske, J. F. Kolb and K. Zocher. "Assessment of Phycocyanin Extraction from *Cyanidium caldarium* by Spark Discharges, Compared to Freeze-Thaw Cycles, Sonication, and Pulsed Electric Fields". *Microorganisms*, 9, 1452, 2021
- S. Wenske, J.-W. Lackmann, L.-M. Busch, S. Bekeschus, T. von Woedtke and K. Wende. "Reactive species driven oxidative modifications of peptides—Tracing physical plasma liquid chemistry". *J. Appl. Phys.*, 129 (19), 193305, 2021.
- Z. Nasri, S. Memari, S. Wenske, R. Clemen, U. Martens, M. Delcea, S. Bekeschus, K.-D. Weltmann, T. von Woedtke and K. Wende. "Singlet Oxygen-Induced Phospholipase A2 Inhibition: a Major Role for Interfacial Tryptophan Dioxidation ". *Chem. Eur. J.*, 27 (59), 14702, 2021.
- J. Striesow, J.-W. Lackmann, Z. N. Ni, S. Wenske, K.-D. Weltmann, M. Fedorova, T. von Woedtke and K. Wende. "Oxidative modification of skin lipids by cold atmospheric plasma (CAP): A standardizable approach using RP-LC/MS² and DI-ESI/MS²". *Chem. Phys. Lipids*, 223, 104786, 2019.
- G. Bruno, S. Wenske, H. Mahdikia, T. Gerling, T. von Woedtke, and K. Wende. "Radiation driven chemistry in biomolecules – is (V)UV involved in the bioactivity of argon jet plasmas?". *Frontiers in Physics*, 9, 759005, 2021.

Contributions to Workshops and Conferences

Oral presentations

- S. Wenske, J.-L. Lackmann, T. von Woedtke, K.-D. Weltmann, K. Wende. "Oxidative PTMs in peptides and proteins – Identification strategies and physiological implications". *Baltic Redox Workshop*. Virtual Conference. September, 2020.
- S. Wenske, J.-L. Lackmann, T. von Woedtke, K. Wende. "Creation of a cold atmospheric plasma (CAP) generated post-translational modification (PTM) library of amino acids and investigation in artificial skin model system". *Plasma-Biomed-Workshop*. Neumünster, Germany. October, 2019.
- S. Wenske, J.-L. Lackmann, T. von Woedtke, K. Wende. "The investigation of posttranslational protein modifications (PTMs) in artificial skin after cold atmospheric plasma treatment". *8th Young Professionals Workshop on Plasma Medicine - Frontiers in Redox Biochemistry and Medicine (FiRBaM)*. Rostock, Germany. August, 2019.
- S. Wenske, J.-L. Lackmann, T. von Woedtke, K.-D. Weltmann, M. Lalk, K. Wende. "Mass spectrometry-based investigations of cold physical plasma-induced PTMs in peptides". *7th Young Professionals Workshop on Plasma Medicine - Frontiers in Redox Biochemistry and Medicine (FiRBaM)*. Rostock, Germany. September, 2018.

Poster presentations

- S. Wenske, J.-L. Lackmann, G. Bruno, S. Bekeschus, T. von Woedtke, K.-D. Weltmann, K. Wende. "MS-based investigations of cold physical plasma-induced PTMs in peptides". *22nd International Mass Spectrometry Conference (IMSC)*. Florence, Italy. August, 2018.
- S. Wenske, J.-L. Lackmann, T. von Woedtke, K.-D. Weltmann, K. Wende. "MS-based investigations of cold physical plasma-induced PTMs". *52nd Tagung der deutschen Gesellschaft für Massenspektrometrie (DGMS)*. Rostock, Deutschland. März, 2019.
- S. Wenske, J.-L. Lackmann, T. von Woedtke, K.-D. Weltmann, K. Wende. "MS-based investigations of cold physical plasma-induced PTMs". *Advances in the Study of Lipid and Protein Oxidation: From Methods to Targets*. Gent, Belgien. März, 2019.
- S. Wenske, J.-L. Lackmann, T. von Woedtke, K.-D. Weltmann, K. Wende. "MS-based investigations of cold physical plasma-induced PTMs". *XIII. Annual Congress of the European Proteomics Association: From Genes via Proteins and their Interactions to Functions*. Potsdam, Deutschland. März, 2019.
- S. Wenske, J.-L. Lackmann, T. von Woedtke, K.-D. Weltmann, K. Wende. "Mass spectrometry-based investigations of cold atmospheric plasma-induced PTMs in model peptides". *24th International Symposium on Plasma Chemistry (ISPC)*. Neapel, Italien. Juni, 2019.

- S. Wenske, J.-L. Lackmann, T. von Woedtke, K.-D. Weltmann, K. Wende. “Non-enzymatic oxidative post-translational modifications in peptides – Key to understand the functional consequences of cold atmospheric plasma (CAP)”. 18. *Human Proteome Organization World Congress (HuPo)*. Adelaide, Australien. September, 2019.
- S. Wenske, J.-L. Lackmann, K.-D. Weltmann, T. von Woedtke, K. Wende. “Non-enzymatic oxidative PTMs in peptides – Understanding the functional consequences of cold atmospheric plasma (CAP)”. *Next-Generation Protein Analysis and Detection (3rd edition)*. Gent, Belgien. November, 2019.
- S. Wenske, J.-L. Lackmann, T. von Woedtke, K.-D. Weltmann, K. Wende. “Oxidative PTMs in peptides – Understanding the physiological consequences of physical plasma”. 19. *Human Proteome Organization World Congress (HuPo)*. Stockholm, Schweden. Oktober, 2020 (online).

Date

Sebastian Wenske

Acknowledgements

Zuerst möchte ich gern meinem Betreuer am INP, Herrn Dr. Kristian Wende, dafür ganz herzlich danken, dass ich unter seiner Leitung meine Dissertation zu diesem spannenden Thema verfassen durfte. Dank der vielen fruchtbaren Diskussionen und hilfreichen Ideen zu den verschiedenen Bereichen der Arbeit, wurden mir die essenziellen Konzepte in der Wissenschaft, wie über den Tellerrand hinausschauen, um neues zu entdecken und gleichzeitig den Blick fürs Detail zu schärfen, sehr bewusst. Darüber hinaus möchte ich mich auch sehr bei Herrn Prof. Dr. Michael Lalk dafür bedanken, dass er sich dazu bereit erklärt hat diese Arbeit von Seiten der Universität Greifswald zu betreuen und zu leiten.

Meinen herzlichsten Dank möchte ich gern auch an Jan Lackmann, meinem Post-Doc Tandem Partner, ausrichten. Durch dich habe ich die Begeisterung für die komplexe Welt der Massenspektrometrie in Anwendung und Reparatur kennengelernt. Darüber hinaus hast du aber auch stets dafür gesorgt, dass ich nicht vergesse alles kritisch zu hinterfragen und nie den Blick für das Ganze zu verlieren. Nicht zuletzt wegen der unzähligen, nie ganz nüchternen Spieleabende, war die Arbeit mit dir zu jeder Zeit eine großartige Erfahrung.

Weiterhin möchte ich auch gern der ganzen Arbeitsgruppe ZIK-PFE danken. Zahra, Mehdi, Nicolas, Anna, Paul, Laura und Nick, vielen Dank für eine großartige Zeit mit vielen wertvollen Erfahrungen und noch mehr leckeren Kuchen. Natürlich möchte ich mich auch bei allen anderen Kollegen des INP bedanken die mich die Zeit über begleitet haben: Liane, Christina, Marie, Julia, Ramona, Deba, Sander und natürlich der ganzen Tischtennisgruppe.

Inbesondere möchte ich mich bei Johanna und Giuliana bedanken, welche mich auch dann im Büro ertragen haben, wenn ich mit Musik auf den Ohren zu laut war, oder aber Ihnen die Welt mit Rick und Morty erklären musste. Ich bin froh, dass der schlimmste Streit zwischen uns den Öffnungsgrad des Fensters betraf und ich bin auch sehr froh euch als Freunde gefunden zu haben. Dank euch war die Zeit im Labor und im Büro unfassbar Spaßig und durch die Gespräche mit euch ging mir doch das eine oder andere Mal dann ein Licht auf, welches vorher im verborgen blieb.

Bedanken möchte ich mich auch bei Tobi, der für mich stets in allen Zeiten ein offenes Ohr hatte und der über das Studium hinaus ein guter Freund für mich geworden ist.

Weiterhin möchte ich auch meiner ganzen Familie herzlich danken, dass Sie mich all die Jahre stets unterstützt und gefördert haben. Weil ich das machen durfte, was und wie ich es machen wollte, konnte ich meine Ziele erreichen. Ich bin und war mir sehr über diesen Umstand bewusst und bin euch dafür über alles dankbar.

Abschließend möchte ich mich bei meiner Verlobten und der großen Liebe meines Lebens bedanken. Giuliana, ich habe dich als durchsetzungsstarke und intelligente Kollegin kennen lernen dürfen und nun planen wir unsere gemeinsame Zukunft zusammen. Es ist absolut bemerkenswert und eine einzigartige Eigenschaft, dass du es schaffst, mich oft besser zu verstehen als ich mich selbst. Etwas poetisch würde ich zum Ausdruck bringen, dass mein Tag keine Sonne hätte und die Zeit erdrückend langsam verläuft ohne dich. Absolut nichts scheint unmöglich und wird wie durch Zauberhand leichter mit dir. Wenn ich jemanden in meinem Leben hätte finden sollen, dann habe ich das jetzt. Ich liebe dich und kann es nicht erwarten den Rest meines Lebens mit dir zu verbringen.